UNIVERSITY OF LIVERPOOL

Cancerous Inhibitor of Protein Phosphatase 2A (CIP2A) in Chronic Myeloid Leukaemia

Thesis submitted in accordance with the requirements of the University of Liverpool for the degree of Doctor in Philosophy by

Elizabeth McDonald

October 2015

Table of Contents

This thesis is dedicated to my family. Their unique brand of love and encouragement has helped me through these, the most challenging of years.

Acknowledgements

'So much of me, is made from what I learned from you...'

First and foremost to my mum, I say thank you for the nagging! Though I often call you a pain-in-the-bum, the push you gave was more help than you could ever know. Negotiating your way through the minefield of my PhD-dependent mood swings, taking the bus so I could rob your car instead and allowing my Bank-of-Mother debt to remain interest-free all this time…for all this I will be eternally grateful.

To my dad, the peacekeeper: no problem was ever too small for you, regardless of your own struggles. Thank you for always having the time and patience to listen to my (many!) rants. I hope to one day master your tactful way of telling me when I'm actually in the wrong! Thanks also to Ann, for topping up many a double vodka to help me to forget a bad day!

'You'll be with me, like a handprint on my heart...'

Thank you to my brother James, to Pam and of course to my beautiful niece, Amy. Our Wednesday meals have been the perfect counselling session! You have heard me moan for 4 years, yet never stopped being the listening ears I needed. Amy, you were without a doubt the highlight of these meals – always there to demand Auntie Liz's attention, have me climb into a ball pool or pester me into a fashion shoot, you never failed to put a smile back on my face; I love you.

'Because I knew you, I have been changed for good...'

To the girl who through these years has been more like a sister than a friend, there are no words that are good enough. Rach, getting through this PhD without you would have been impossible. You not only held me up through the bad times, but you held up the laptop bag/punch bag too! Dancing on tables, naps on the desks and sharing hangovers are just a few of the many memories of taking this crazy ride with you that I will cherish for years to come.

To Athina and Andrea, where to begin?! You two have been an unwavering support that has helped me through this entire experience. The perfect mix of friend, supervisor and lab mother figures…depending on what I was most in need of at the time! For the Costa breaks that allowed us all to vent on the extra hard days and for the patience you both had to share an office with me for so long, I thank you a thousand times over.

Thank you to those in the others in the Haematology Department. Support can be given in all sorts of ways, from tea breaks spent laughing with Alix, Ali, Gemma, Sophia and Elinor, to de-stressing badminton matches with Andrew and Tony. I thank everyone that offered help, advice or laughter. To Joe and Lakis, thank you for putting up with my tears and over-emotional meetings in the office – I could not have gotten to the end of this PhD without the emotional and intellectual support from you both.

'I'm through accepting limits, 'cause someone says they're so...'

I also want to thank my supervisor Professor Richard Clark and also Claire for the opportunity to experience this PhD. Richard, thank you for your patience throughout my write-up!

'The trouble with school is; they always try to teach the wrong lessons...'

I would not have arrived at the end of this journey as a (mostly!) sane individual without the awesome friends that have surrounded me throughout. Pub Fridays with darts, pool and questionable amounts of Britney Spears and Will Smith music, may well have fuelled my decent into alcoholism, but they were a necessity for PhD survival. Thanks to Holly, Ali, Alix, Peeney, Aine, Agnes, Harriet, Fiazia, Jo and Pika. Thanks also for never kicking me out of 23 Club, even though I refused to drink ale or whiskey; Ryan, Jack, Sully, Jamie, Andy and Liam. Special mention to Liam and Jamie, who never fussed when I practically lived in their flat! To Jack and Jess, thanks for taking me in so many times when I needed a friend and never tiring of my tears. Ryan, through the years of lab stress you never failed to make me giggle at your strangely tasty, yet ridiculous food combinations! Thank you for the cuddles and the memories.

To Alexia, Junnat, Becci and Maria – thank you for the (often nightly!) sessions in the Flute. You guys never failed to turn up to drink our troubles away, no matter how busy. The many nights of 'just one quick drink' helped more than I could have imagined. To Helen, my best friend of 23 years; thank you for listening without judgement whenever it was needed.

Finally, thank you to Rich and his family, who over the last months of thesis writing and viva prep stressing, have had nothing but words of encouragement. Rich thank you for your unwavering patience and love during the unexplainable tears and 3am phone calls…and for calming me down with snuggles and wine.

'It's time to trust my instincts, close my eyes and leap....'

Abstract: CIP2A in CML

Chronic myeloid leukaemia (CML) is a myeloproliferative disorder arising in a haematopoietic stem cell (HSC) and defined by the presence of BCR-ABL1, a deregulated tyrosine kinase that drives numerous oncogenic signalling pathways. Current CML therapies are tyrosine kinase inhibitors (TKIs) that target the constitutive action of BCR-ABL1. However, resistance to TKIs remains a concern for a substantial proportion of CML patients and thus investigating the mechanisms underlying poor clinical response is of great importance.

The tumour suppressor protein phosphatase 2A (PP2A) plays a crucial role in the inhibition of several critical oncogenic signalling pathways. Consequently, reports of aberrant PP2A activity in human malignancies are abundant. Cancerous inhibitor of PP2A (CIP2A) is an endogenous inhibitor of PP2A that is overexpressed in a plethora of tumours; CIP2A inhibits the dephosphorylation of the oncogenic transcription factor c-Myc by PP2A.

In CML, it was shown that high CIP2A protein expression at diagnosis was predictive of progression into blast crisis in imatinib-treated CML. This thesis aimed to determine if CIP2A retained its potential prognostic indicator status in CML treated with dasatinib or nilotinib. The molecular pathogenesis of the CIP2A/PP2A pathway within CML and the central role played by CIP2A is also investigated.

Molecular interactions of proteins have been known to greatly differ between transcript variants of the same gene. No *CIP2A* transcript variant has ever been reported. This thesis aimed to identify two *CIP2A* transcript variants previously undescribed *in vivo,* and analyse their differing expressions within a CML population.

Aberrant epigenetic regulation is an expanding area of interest; many genes have their expression altered via deregulated methylation, transcription factor binding and micro RNAs. This thesis focussed on the methylation of the *CIP2A* promoter in CML of varying disease phase and clinical outcome.

In summary, this thesis provides novel information about CIP2A in response to CML treatment, CIP2A protein interactions, *CIP2A* gene variations and epigenetic regulation. With more knowledge of this oncoprotein, its oncogenic mechanisms may in the future be specifically targeted and overcome.

Publications and Presentations

Publications and presentations of data from this thesis are as follows:

Publications

- 'Second generation tyrosine kinase inhibitors prevent disease progression in high-risk (high CIP2A) chronic myeloid leukaemia patients'
    - *Leukemia,* **29**(7): 1514-1523 (13 March 2015)

Presentations

- **Poster presentation:** 'The high rate of blast crisis in imatinib treated chronic myeloid leukaemia with high CIP2A levels is nullified by first line dasatinib or nilotinib.'
    - European Haematology Association (EHA) Annual Scientific Meeting
        - Amsterdam, 2012

Chapter 1: Introduction

1.1. CML: From Past to Present

In 1845, the earliest report of chronic myeloid leukaemia (CML) was described by Dr Hughes Bennett in his paper titled "Case of hypertrophy of the spleen and liver in which death took place from suppuration of the blood"(Bennet, 1845). Just 5 weeks later, Rudolf Virchow, another leading scientist of the time, also published a case of CML; he described the blood as "Weisses Blut" due to the abnormally high number of white blood cells he witnessed(Virchow, 1845). At the time, the disease was widely called 'leucocythaemia', a term coined by Bennett, meaning literally 'white cell blood'(Bennett, 1852). (Geary, 2000; Kampen, 2012; Piller, 2001)

Two years after his original CML publishing, Virchow documented 4 out of a further 9 leukaemic cases that (along with the original patients described by both himself and Bennett) also had distinct splenomegaly and granular appearance of the blood cells(Virchow, 1847). In identifying that his leukaemic patients had either granular or non-granular white blood cells, Virchow was the first to categorise two forms of chronic leukaemia depending on the tissue of origin; splenic and lymphatic(Virchow, 1849, 1856).

Another great pioneer in CML was Ernst Neumann. In 1868, Neumann noted the abnormal "dirty green-yellow" colour of the marrow of a deceased

leukaemia patient during an autopsy and 2 years later published his theory that the bone marrow was the site of blood cell production(Neumann, 1870). In 1878, after extensive studies into the cell types within the marrow, he added "myelogenous" leukaemia as an additional classification to Virchow's splenic and lymphatic(Neumann, 1869, 1878).

It is important to note that the discoveries discussed thus far predate cellular staining. The development of a triacid stain in 1879 by Paul Ehrlich meant that interior structures (such as the nucleus and cytoplasm) of blood cells could be clearly seen and thus the distinction of different blood cells began. Neumann's myelogenous form of leukaemia was now seen to closely resemble the splenic form described 20 years earlier by Virchow; lymphoid and myelogenous became the widely used terms and were the two firmly established forms of chronic leukaemia.

A major step forward in understanding CML biology came in 1960 when Peter Nowell and David Hungerford observed the abnormally small chromosome 22 of two CML patients; they named the altered chromosome the "Philadelphia chromosome"(Nowell & Hungerford, 1960). The astonishing detection of the Philadelphia chromosome was in fact the first chromosomal abnormality to be associated with any malignant disease. Originally it was believed that a partial chromosome deletion was the cause of the shortened chromosome 22, but thirteen years after the original observation Janet Rowley demonstrated that it had in fact translocated onto the long arm of chromosome 9 and that this is

accompanied by a reciprocal translocation of 9q to 22 (**Figure 1.2**)(J. D. Rowley, 1973). This was the first description of a balanced translocation in any human cancer (though interestingly its publication date is somewhat after the report of the t(15;17)(q22;q12) balanced translocation in acute promyelocytic leukaemia (APML) by the same group(J. Rowley et al., 1977)).

The next 25 years saw the identification of the genes involved in the translocation (*ABL1* and *BCR*) and the tyrosine kinase they encoded (BCR-ABL1). The detection of the *BCR-ABL1* fusion oncogene and the potential therapeutic target of its subsequent protein were critical discoveries in CML and have underpinned the revolution in the way in which the disease is now treated.

1.2. Early CML Treatment

In the years following Bennett's first reported case of CML there were a variety of treatments used to attempt to treat the disease though most only acted to alleviate some of the patient's symptoms (such as fever, anaemia and pain). The first widely used CML therapy was low dose-arsenic, an idea inspired by the use of Fowler's Solution (1% arsenic sulphide) in the 19thcentury for the treatment of fevers and headaches. Interestingly, the first report of its use in CML may have been by Arthur Conan Doyle (famed for Sherlock Holmes and other fiction); the article in the Lancet has his name misspelt(Cowan Doyle, 1882). Arsenic produced not only improvements in spleen size, leucocyte count and anaemia but also patients' spirits lifted when treated with arsenic and improvement could last for a period of some months.

Arsenic treatment was well established in CML until 1903 when it was replaced by radiotherapy following the development of the x-ray 8 years before. The apparent return to health of patients that occasionally lasted more than 12 months meant that 'remission' of CML (though it was not at the time called this) was first considered as a potential possibility. Nitrogen mustards (derivatives of First World War mustard gas) and (in 1953) busulphan were amongst those that followed, the latter of which had more success in treating CML. Superior results of busulphan compared to radiotherapy meant it became the main CML treatment for the next 35 years, until its replacement by hydroxyurea and later, interferon-α (IFN-α) from 1983.

In 1970, eradication of Philadelphia positive cells in CML was first reported in Seattle, following haematopoietic stem cell transplantation (HSCT). HSCT was in fact first performed on 5 patients suffering from irradiation poisoning in 1959 by Georges Mathé(Baccarani et al., 2006), who followed this with an announcement in 1963 that he had cured a leukaemic patient using this technique(Mathe, Amiel, Schwarzenberg, Cattan, & Schneider, 1963). With regards to CML treatment, allogeneic HSCT was originally limited to younger patients with suitable matching donors. Thus this was not an option for a large proportion of CML patients.

Nowadays, HSCT remains a legitimate treatment option due to the difficulty of treating patients who have progressed past the stable chronic phase of the disease; the effectiveness of modern-day tyrosine kinase inhibitors (TKIs) significantly drops for patients beginning treatment in advanced phases of the disease; just 11% and 8% of patients achieve a complete cytogenetic response (CCR) after beginning imatinib treatment in accelerated and blastic phases respectively(Sawyers et al., 2002; Talpaz et al., 2002). HSCT is now reserved for those with little alternative options available and remains the only curative therapy for CML patients.

In the early 1980s IFN-α was used as a treatment for CML and for the first time CCR and long-term survival were seen in a small subset of patients(Group, 1997); the correlation between CCR and extended survival highlighted the importance of this milestone in patient outcome(H. M. Kantarjian et al., 2003; H.

M. Kantarjian et al., 1995). Until the introduction of the TKI imatinib in the late 1990s (**Section 1.8.1**), IFN-α (sometimes in combination with cytarabine) remained the standard treatment for CML, unless the patient was young and had a suitable available donor for allogeneic HSCT.

1.3. CML Epidemiology

CML is rare in children, though it accounts for around 15% of all leukaemias in adults. Despite this high percentage, the mortality rate has been significantly decreased (<2-3% in the first year) since the development of imatinib and other TKIs. The annual incidence of CML is approximately 0.6-2 cases per 100 000 worldwide, with around 600 patients newly diagnosed in the UK each year. The chance of CML occurring increases with age(McNally, Rowland, Roman, & Cartwright, 1997), thus it is possible that these figures have been on the rise as average life expectancy increases(Rohrbacher & Hasford, 2009). The median age of diagnosis is generally reported as 45-55, though in some trials this is higher. CML occurs more commonly in men than women (though it is not understood why) with the ratio of men to women varying between 1.3:1 and 1.8:1(McNally et al., 1997; Phekoo, Richards, Moller, & Schey, 2006). It is important to remember that these figures come from countries where diagnostic techniques are readily available and thus reliable statistics can be taken. It is possible that results would alter or other variations may be masked by a lack of data from certain areas.

The only known risk factor that predisposes individuals to CML is ionising radiation, such as therapeutic irradiation used unwisely in the 1950s. There was also an increase in newly diagnosed CML cases roughly 8 years after the atomic bombing incidents of Hiroshima and Nagasaki(Ichimaru, Tomonaga, Amenomori, & Matsuo, 1991). No inherited, geographical, viral or chemical factors have been shown to correlate with CML.

1.4. Clinical Features of CML

Many CML patients are asymptomatic at diagnosis; it is apparent in blood samples taken for other reasons. If symptoms are indeed present these can include fever, night sweats, weight loss, symptoms of anaemia or abdominal/shoulder pain due to splenomegaly.

1.4.1. Diagnosis

Upon medical suspicion of CML three diagnostic tests are typically taken: a full blood count, a bone marrow aspirate for morphology and metaphase karyotyping and molecular analysis for *BCR-ABL1* (**Section 1.6.3**). Choice of treatment, determination of disease phase and risk stratifications (which also require assessment of splenomegaly) are dependent upon these results as well as the ability to monitor response in comparison to baseline data. The majority of patients present in chronic phase, and thus have a low or absent peripheral blood blast count, though immature myeloid cells such as myelocytes and promyelocytes are present.(M. W. Deininger, 2008a)

1.4.2. Monitoring Patient Response to Treatment

Following diagnosis, the examination of peripheral blood samples and/or bone marrow karyotyping are key in monitoring patient response to their given treatment protocol. Blood samples are analysed using quantitative real time reverse transcriptase polymerase chain reaction (qRT-PCR) (**Section 2.9.3**) for *BCR-ABL1* transcript levels. At diagnosis, a ratio of *BCR-ABL1* to total *ABL1* (or

other control gene) of 30% or more is typically seen; this ratio falls on successful treatment (**Section 1.7.1**).

Kinase domain mutations (**Section 1.9.1**) are a common mechanism of imatinib resistance and imatinib plasma trough levels have been shown to be an indicator of depth of response, thus both are considered in patient care(M. W. Deininger, 2008a).

1.5. CML Pathogenesis

CML is classically described as a triphasic disease, beginning in an indolent chronic phase (CP). Untreated CP has a variable duration (usually 3-5 years) and sees the accumulation of neutrophils and their immature precursors in the blood, bone marrow and extramedullary sites(Nowell & Hungerford, 1960). An accelerated phase (AP) can then, but not always, precede the final phase, blast crisis (BC). **Table 1.1** defines the three phases of CML, according to 2013 European Leukaemia Net (ELN) guidelines.

Table 1.1. Criteria for Classification of CML Phase by ELN 2013

	CHRONIC PHASE (CP)	ACCELERATED PHASE (AP)	BLAST CRISIS (BC)
ELN GUIDELINE CRITERIA	Blasts <15% or Blasts + promyelocytes <30% Basophils <20%	Blasts 15-29% or Blasts + promyelocytes >30% Basophils ≥20% Persistent thrombocytopenia (<100 x 10^9/L) unrelated to therapy Clonal chromosomal abnormalities in Ph+ cells	Blasts ≥30% Extramedullary blast cell proliferation (excepting spleen and liver)

The precise mechanism of progression from CP through to BC is unknown, though additional chromosomal mutations (e.g. additional Ph+ chromosome copies and p53 mutations(J. D. Rowley, 1973; Stuppia et al., 1977)) are often seen. The mass expansion of myeloid precursors (>30% blasts seen in the peripheral blood) is also a feature of BC, with little treatment options and a reduction in life expectancy to less than 3 months without treatment(Shet, Jahagirdar, & Verfaillie, 2002).

1.6. Molecular Pathogenesis of CML

CML is driven by a fusion oncogene *BCR-ABL1* encoding a constitutively active tyrosine kinase. Before delving into the mechanisms of action of this protein, we must understand the molecular structure and thus must discuss the genes involved in this fusion; *BCR* and *ABL1*.

1.6.1. Normal *BCR*

The understanding of normal breakpoint cluster region (BCR) protein is fairly limited in comparison to its fusion partner *c-ABL1* and their resultant oncogene. It is known to have serine/threonine kinase activity and span 1271 amino acids(Zhao, Ghaffari, Lodish, Malashkevich, & Kim, 2002). The main structural importance of *BCR* is the coiled coil domain ($BCR_{30\text{-}65}$), which is involved in the dimerisation with the 3' sequences of *ABL1*.

BCR consists of 23 exons, of which up to 19 are conserved in *BCR-ABL1*. Variation in BCR-ABL1 protein size is dependent upon the breakpoint location along the *BCR* gene; 210kDa is the most common length in CML. (Helgason, Karvela, & Holyoake, 2011)

1.6.2. Normal *ABL1*

The discovery of *v-ABL1* (*retroviral-ABL1*) from the Abelson leukaemia virus preceded that of *c-ABL1*, though when linked to BCR-ABL1 protein in CML, the

importance of this proto-oncogene was widely noted(Abelson & Rabstein, 1970). *c-ABL1* (*cellular Abl1*) is a 145kDa non-receptor tyrosine kinase with a range of implicated functions; these include cell migration, growth and survival amongst other things(Hantschel & Superti-Furga, 2004). In addition to CML, *c-ABL1* has been implicated in a variety of other haematological malignancies including acute myeloid leukaemia (AML), myeloproliferative neoplasms (MPN) and both B- and T-cell acute lymphoblastic leukaemia (ALL) via its fusion with other genes. (De Braekeleer et al., 2011)

Figure 1.1. Structure of *c-Abl1* and the oncogene *BCR-ABL1*. *c-Abl1* contains both actin- and DNA-binding domains, a proline rich region (PR), SH3, SH2 and kinase domains and a myristoylation modification signal (M). In *BCR-ABL1*, no myristoylation modification signal is present, since BCR is fused to the N-terminal of *c-Abl1*. Adapted from De Braekeleer *et al*, EJH 2011(De Braekeleer et al., 2011).

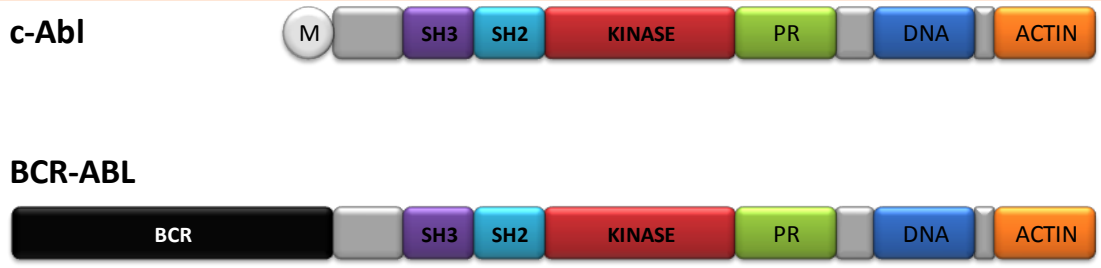

The structure of c-ABL1 plays much of a role in its own regulation. Of the three sarcoma (SRC) homology domains, Src homology domain 1 (SH1) carries the kinase function of c-ABL1. This produces positive signals for the array of pathways c-ABL1 is involved in, yet intramolecular folding, which occurs via the binding of SH3 to a single proline residue between SH2 and the kinase domain,

causes the autoinhibition of c-ABL1 kinase activity(Brasher, Roumiantsev, & Van Etten, 2001). In CML however, this self-regulation is disrupted by the fusion of BCR coiled-coil domain with the N-terminus of c-ABL1, thus the kinase activity of this new protein runs unchecked. Interestingly, SH2 and SH3 are also responsible for protein-protein interactions.(De Braekeleer et al., 2011; M. W. N. Deininger, Goldman, & Melo, 2000)

1.6.3. *BCR-ABL1*

The presence of *BCR-ABL1* is the hallmark of CML and a subset of ALL patients. This occurs when the *ABL1* gene from chromosome 9 is translocated to *BCR* on chromosome 22, where oncogenic fusion occurs. This encodes the oncoprotein BCR-ABL1. In CML, it is the resultant constitutively active ABL1 kinase activity of this protein that drives the leukaemia. Mechanisms of BCR-ABL1 mediated cell transformation include altered adhesion, activation of signalling cascades (e.g. mitogen-activated protein kinase (MAPK) and protein phosphatase 2A (PP2A) pathways) and diminished apoptosis (**Section 1.10**).(Quintás-Cardama & Cortes, 2009; Ellen Weisberg, Manley, Cowan-Jacob, Hochhaus, & Griffin, 2007)

Figure 1.2. The Philadelphia chromosome, created via the reciprocal translocation of chromosomes 9 and 22 at points q34 and q11 respectively. Adapted from The Molecular Oncology Report, 2007(Armand, 2007).

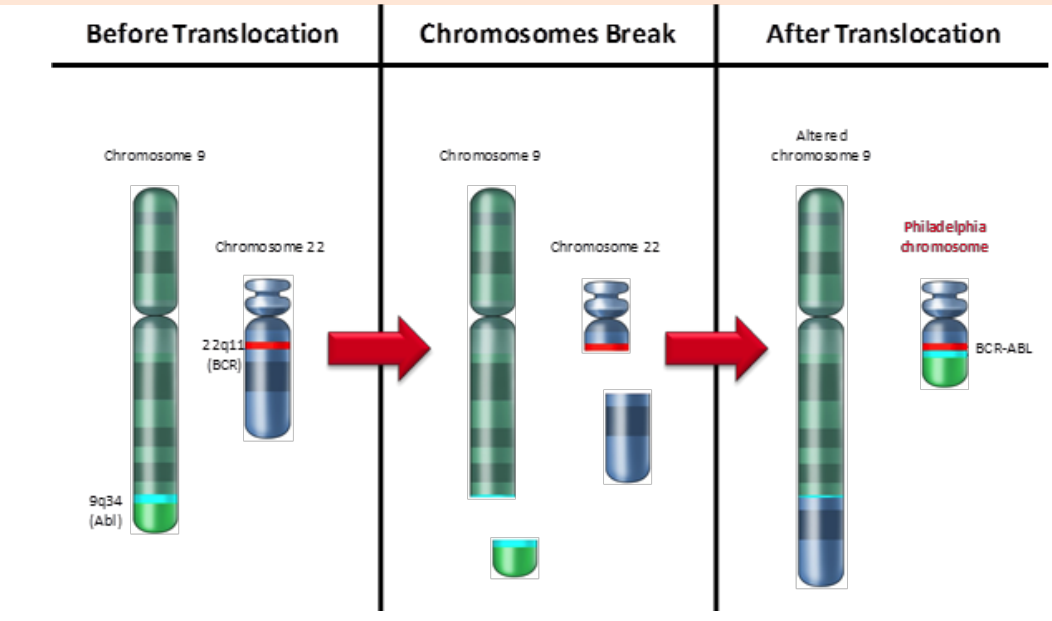

1.6.3.1. *BCR-ABL1* Transcript Types

Different *BCR-ABL1* transcripts of varying lengths have been identified in both CML and ALL. These occur due to alternative breakpoint sites within both *BCR* and *ABL1*. Rare variants such as *e13a3*(L.-G. Liu et al., 2003), *e14a3*(Burmeister & Reinhardt, 2008), *e6a2*(Dupont, Jourdan, & Chiesa, 2000; Hochhaus et al., 1996; Schultheis, Wang, Clark, & Melo, 2003), *e8a2*(Branford, Rudzki, & Hughes, 2000; Park et al., 2008) and *e18a2*(Wada et al., 1995) have been only occasionally described and thus here only the main isoforms reported will be discussed at length, namely *e1a2*, *e13a2*, *e14a2* and *e19a2*. (M. W. N. Deininger et al., 2000; Weerkamp et al., 2009)

Three *ABL1* break point locations upstream of exon 2 are shown on **Figure 1.3**; the more common location is between alternative exons 1a and 1b. Regardless of which breakpoint location (because of alternative splicing), all of these isoforms give rise to a *BCR-ABL1* gene with *BCR* fusion at *ABL1* exon2.

Three *BCR* regions are identified; major, minor and more recently, micro (*M-BCR*, *m-BCR* and *μ-BCR*, respectively). *M-BCR* encompasses exons 12-16, with 2 breakpoint sites; downstream of exon 13 which gives rise to an *e13a2* transcript, and downstream of exon 14 resulting in an *e14a2* transcript; both encode a 210kDa protein. The *m-BCR* breakpoint site occurs upstream of exon 2 and is responsible for *e1a2* (190kDa). The final *BCR-ABL1* transcript shown is *e19a2*(Haškovec et al., 1998), encoding a 230kDa protein, resulting from a *μ-BCR* breakpoint. (M. W. N. Deininger et al., 2000; Weerkamp et al., 2009)

Figure 1.3.Main *BCR-ABL1* fusion genes. The different *BCR-ABL1* transcripts shown are formed from alternative breakpoint sites of *BCR*; 2 sites within *M-BCR*, 1 in *m-BCR* and 1 in *μ-BCR*. These result in 4 different isoforms of *BCR-ABL1*, of 3 varying lengths.

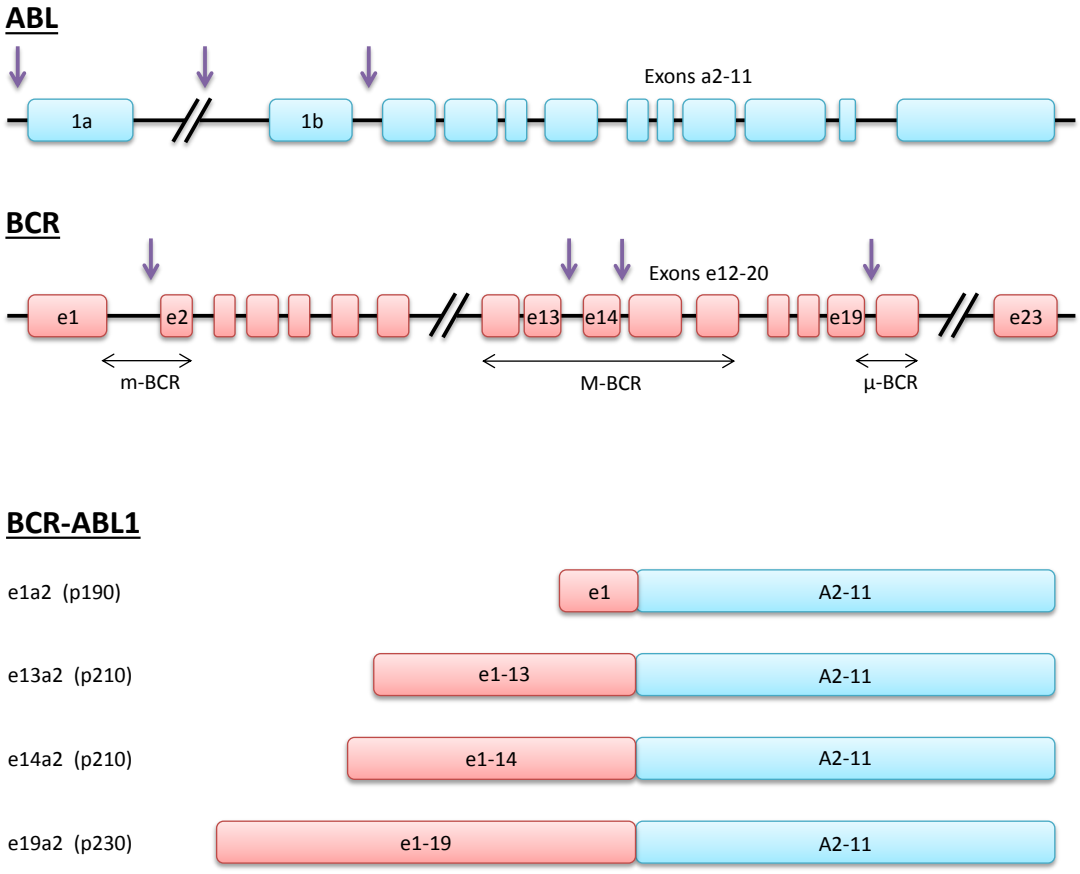

In CML, the most common *BCR-ABL1* transcripts are *e13a2* and *e14a2*, though in 2-3% of cases patients have isoform *e1a2*(Melo, 1996). Conversely, in Philadelphia-positive ALL the most common form of *BCR-ABL1* is *e1a2* with only a third of patients having splice forms resulting from the *M-BCR*. The rarest form, *e19a2* has been mostly identified in patients suffering from chronic neutrophilic leukaemia. (Advani & Pendergast, 2002; Kwong & Cheng, 1993; Pane et al., 1996)

1.7. CML Treatment

Following the original discovery of CML almost 170 years ago, several advances were made in its treatment that palliated the symptoms of the disease, but made little difference to its natural history. This changed in the early 1980s with the introduction of IFN-α, which prolonged median survival but was not curative. More recently, unlike previous treatments that were non-specific, TKIs target the driving force of CML; BCR-ABL1. TKI treatment mechanisms, resistance and clinical trial data are described in this section.

Figure 1.4. Relationship between leukaemic cell count, *BCR-ABL1* transcript level and CML patient response. Adapted from Baccarani M *et al* Blood 2006(Baccarani et al., 2006).

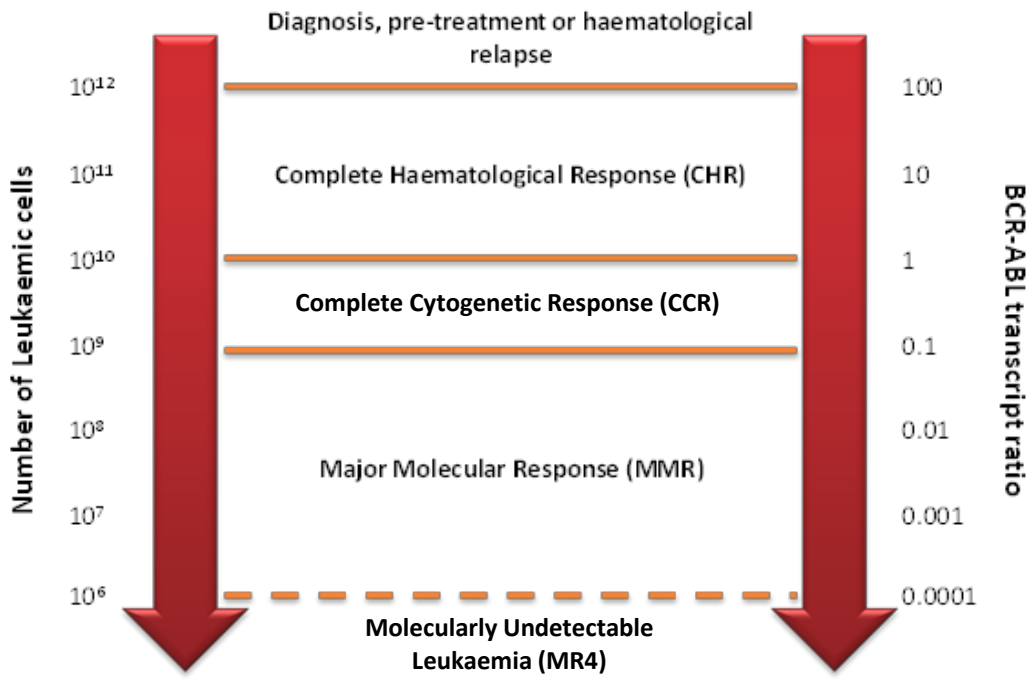

1.7.1. Definitions of Response

Certain clinical 'milestones' are used in CML to describe the level of treatment response that a patient achieves (**Figure 1.4**). These are dependent upon *BCR-ABL1* transcript ratio and the number of leukaemic cells present within the blood.

The International Scale

It should be noted here, that the International Scale (IS) is used to standardise the quantitative measurements of *BCR-ABL1* transcript across different laboratories(Timothy Hughes et al., 2006). As each laboratory can differ in their choice of regents and protocols, variation can occur due to numerous factors; different RNA preparation, laboratory instruments, enzymes, standard curve materials etc. The IS is therefore used to eliminate this variation and is imperative in facilitating collaborative, interlaboratory studies.

The IS was developed in 2005 and utilises the International Randomized Study of Interferon vs STI571 (IRIS) trial to determine fixed baseline and MMR values(T. Hughes et al., 2003). Each laboratory is given its own individual conversion factor based on the IS and this conversion is then applied to their study results, rendering all laboratory studies standardised to the IS and thus more easily comparable.

1.7.1.1. Definitions of Molecular Response

Complete Haematologic Response (CHR): Normalisation of the blood (WBCs <10 x 10^9/L, platelet count <450 x 10^9/L, <5% basophils and no immature granulocytes) and resolution of splenomegaly.

Complete Cytogenetic Response (CCR): No Philadelphia positive metaphases amongst at least 20 marrow metaphases. Several studies have shown that cytogenetically defined CCR is equivalent to a*BCR-ABL1/ABL1* ratio of ≤ 1%.

Major Molecular Response (MMR): *BCR-ABL1/ABL1* ratio of ≤ 0.1%.

Molecularly Remission at the 4-log level (MR4): No detectable *BCR-ABL1* transcripts in two consecutive blood samples of adequate sensitivity (>10^4), or a log 4 reduction in *BCR-ABL1/ABL1* transcript ratio (≤ 0.01%). N.B. This was formerly described by some as 'complete molecular response'.

1.7.1.2. Definitions of Clinical Response

The time taken to achieve CHR, CCR, MMR and MR4 is also important in monitoring CML patients; several clinical studies have shown that patients who achieve a response earlier are less likely to relapse and more likely to maintain their response. Therefore, patients have been categorised by the European Leukaemia Net (ELN) according to both the depth and rate of their response to first line treatment. Response definitions vary depending on duration of treatment; 3, 6 or 12 months and then at any time after. All response definitions used within this thesis are according to 2013 ELN guidelines. (Baccarani et al., 2013)

Optimal response:

- At 3 months: BCR-ABL1/ABL1 ratio ≤ 10% and/or Ph+ ≤ 35%.
- At 6 months: BCR-ABL1/ABL1 ratio ≤ 1% and/or Ph+ 0%.
- At 12 months: BCR-ABL1/ABL1 ratio ≤ 0.1%.
- Any time after: BCR-ABL1/ABL1 ratio ≤ 0.1%.

N.B. In such patients there is no indication that an alternative treatment may improve survival.

Warning/Suboptimal response:

- At 3 months: BCR-ABL1/ABL1 ratio > 10% and/or Ph+ ≤ 36-95%.
- At 6 months: BCR-ABL1/ABL1 ratio 1-10% and/or Ph+ 1-35%.
- At 12 months: BCR-ABL1/ABL1 ratio of > 0.1-1%.
- Any time after: CCA/Ph-.

N.B. In such patients, there is a possible substantial long-term benefit to the patient from continuing current treatment but less chance of achieving an optimal response. Patients may be considered for possible alternative therapy.

Treatment Failure:

- At 3 months: no CHR and/or Ph+ >95%.
- At 6 months: BCR-ABL1/ABL1 ratio > 10% and/or Ph+ >35%.
- At 12 months: BCR-ABL1/ABL1 ratio >1% and/or Ph+ >0.
- Any time after: loss of CHR, loss of CCR, loss of MMR (confirmed in 2 consecutive tests) development of additional chromosomal mutations or CCA/Ph+.

N.B. In such patients a positive patient outcome is highly unlikely and the patient should be transferred onto an alternative therapy where possible.

1.7.2. Definitions of Survival

Long-term treatment efficacies of large cohorts of CML patients are analysed according to overall, progression free and event free survival. The definitions of death, progression and events that are used in the analysis of each of these response groups are variable, but most studies use the following definitions of events for each of these parameters:

Overall Survival (OS): Death by any cause (CML or non-CML related).

Progression Free Survival (PFS): Death due to any cause, or progression into accelerated or blast phase.

Event Free Survival (EFS): Death by any cause (CML or non-CML related), progression into accelerated or blast phase, a loss of complete haematologic or cytogenetic response. Some, but not all, studies also include a failure to achieve a CCR by 12 months.

1.7.3. Definitions of TKI Resistance and Failure

Unfortunately, some patients can be resistant to certain (or in extreme cases all current) TKIs and may need to switch to a different treatment. Changes in treatment plan may also be due to adverse reactions to a drug that interfere with or jeopardise a patient's life. Resistance and intolerance definitions are as follows:

Primary Resistance: No treatment efficacy from the onset of TKI therapy. This can also be referred to as intrinsic resistance.

Secondary Resistance: Loss of an initial response to TKI treatment. This can also be referred to as acquired resistance and is considered a relapse.

TKI intolerance: Side effects to TKI treatment that lead to a switch in treatment, in spite of a low *BCR-ABL1* percentage.

In CML research, the definition of treatment failure can vary slightly from study to study. In this thesis treatment failure is defined as any of the following: death by CML; progression to advanced phases of CML; a change of treatment due to high *BCR-ABL1* percentage (i.e. primary/secondary resistance) or a change of treatment due to TKI intolerance (i.e. undesirable side effects).

1.8. Targeting BCR-ABL1 – The TKI Era

TKIs are now the standard therapy for CML, following the original development of imatinib and the subsequent introduction of the second generation TKIs (2G TKIs) dasatinib and nilotinib. All three of these drugs are now approved for frontline CML treatment and are based on the same mechanistic idea – blocking the kinase activity of BCR-ABL1 by drug binding within the catalytic site. Nilotinib (structurally based upon imatinib) and dasatinib (a more multi-targeted TKI) were developed following the realisation of imatinib resistance and the additional 2G TKI bosutinib has also shown promise. Controversy has recently surrounded the youngest of the TKIs, ponatinib, whose adverse events have unfortunately dampened the original excitement of its efficacy against the *BCR-ABL1* kinase domain (KD) mutation T315I. Mechanisms of action, clinical trial data and resistance of these TKIs are discussed forthwith.

Figure 1.5. Chemical structures of imatinib (Novartis), dasatinib (Bristol-Myers Squibb), nilotinib (Novartis), bosutinib (Pfizer) and ponatinib (Ariad). Figure taken from Santos, FP et al, 2011(Santos, Kantarjian, Quintás-Cardama, & Cortes, 2011).

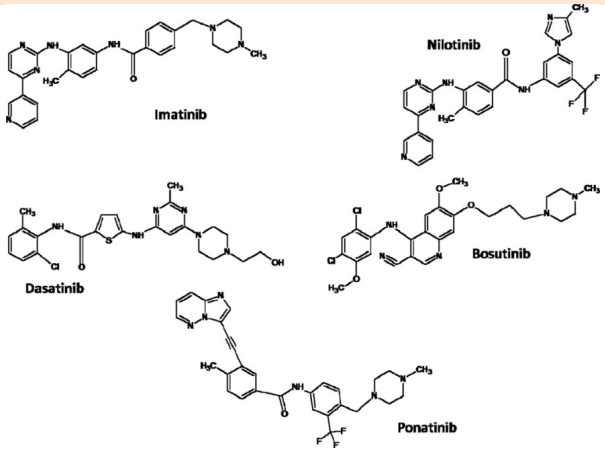

1.8.1. Imatinib

CML therapy was revolutionised by the arrival of imatinib (STI-571/Gleevec/Glivec), a site-specific treatment designed to target the tyrosine kinase activity of BCR-ABL1. This ATP-competitive molecule binds to the inactive form of BCR-ABL1 and blocks further substrate phosphorylation by the deregulated tyrosine kinase(Hassan, Sharma, & Warmuth, 2010). Early studies showed imatinib also inhibited platelet-derived growth factor receptor α/β (PDGFRα/β), inhibited proliferation and induced apoptosis in BCR-ABL1-positive cells(B.J Druker et al., 1996).

Figure 1.6. Imatinib: mechanism of action. In active CML, ATP binds to the catalytic site of BCR-ABL1. BCR-ABL1 transfers a phosphate group from ATP (subsequently releasing ADP) to a tyrosine residue on its substrate, leading to increased leukaemic activity. In the presence of imatinib, ATP binding and therefore further downstream tyrosine kinase activity is inhibited.

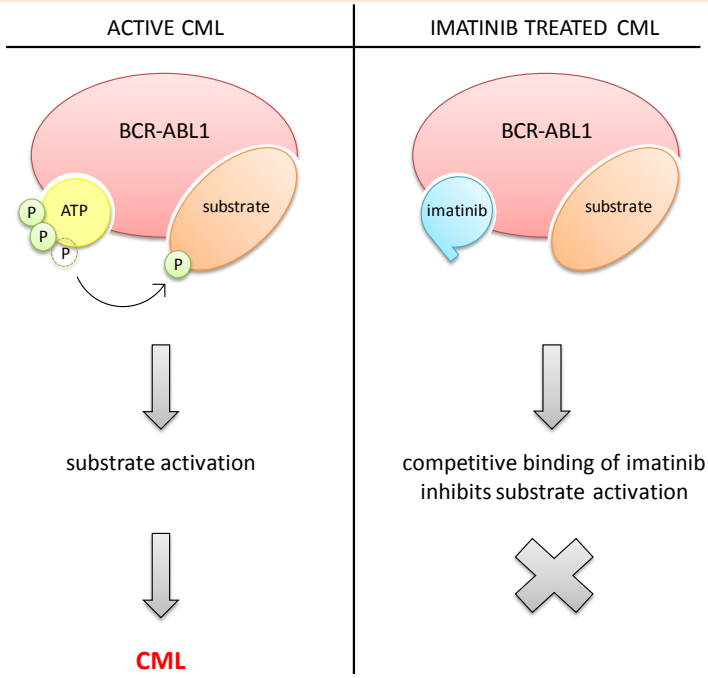

1.8.1.1. Phase I and II Imatinib Clinical Trials

The imatinib Phase I trial recruited 83 patients with IFN-α-resistant (70 patients) or intolerant (13 patients) CML and showed extremely promising results; 53/54 patients given ≥300mg/day achieved CHR, typically within 4 weeks and 13% of these achieved a CCR within approximately 12 weeks. (Brian J. Druker et al., 2001)

Phase II clinical trials were conducted on 3 separate cohorts of patients; CP-CML, AP-CML and BC-CML (532, 235 and 260 patients respectively). CHR and CCR rates of 88% and 30% were observed in CP-CML. A haematological response rate of 63% (CHR 28%) and 26% was observed in AP-CML and BC-CML respectively with a median duration of approximately 5-6 months. These incredible responses to imatinib in early phase studies saw its accelerated Food and Drug Administration (FDA) approval in May 2001. (Cohen et al., 2002)

1.8.1.2. Late Phase and Ongoing Imatinib Clinical Trials

In June 2000 the phase III trial IRIS (International Randomized Study of Interferon versus STI571) was initiated for patients with newly diagnosed CP-CML. The purpose of the study was to investigate the potentially superior efficacy of imatinib to IFN-α (in combination with low-dose cytarabine) in treatment naïve CML patients. Early results showed a dramatic difference in response rates of the two drugs; 95.3% compared to 55.5% CHR, and 73.8% compared to 8.5% CCR (imatinib vs IFN-α respectively)(O'Brien et al., 2003).

These superior results yielded by imatinib led to the majority of patients being switched from IFN-α (crossovers by 31st January 2002: 318/553 IFN-α to imatinib, compared to 11/553 imatinib to IFN-α). IRIS has thus become a long-term study of imatinib. (T. P. Hughes et al., 2010; O'Brien et al., 2003)

The most up to date IRIS trial data published are a 7 year patient follow-up. The study shows a CCR and MMR rate of 82% and 87% respectively in imatinib treated patients. However, 17% of those who achieved a CCR failed to maintain it. Only 6% of patients progressed in the first 36 months. This international trial also publishes data highlighting the importance of early molecular responses in long-term patient survival; 100% of patients who had achieved an MMR by 18 months remained progression-free at 7 years and the frequency of an event also decreased dramatically over time. (T. P. Hughes et al., 2010; O'Brien et al., 2003)

However, it is important to remember the strict limitations of patient criteria in clinical trials and thus other results may vary. Lucas *et al* investigated the reproducibility of the IRIS trial within a general population of 84 newly diagnosed CP-CML patients; 68 received imatinib 400mg/day as first line treatment. In the first 12 months, 1 patient lost a CHR, 2 were intolerant and 3 progressed into AP/BC. The remaining 62 patients were assessed and showed a 12 month CCR rate of 41%; of the patients who did not achieve a CCR at this time, 5 had progressed or lost a CHR. The overall CCR rates of assessable

patients at 12, 18 and 24 months follow-up were 41%, 49% and 51% respectively. (C. Lucas et al., 2008)

The differences in the data presented by Novartis and Lucas *et al* suggest care should be taken when extrapolating clinical trial data to assess a non-biased general population of patients.

1.8.2. Dasatinib

Dasatinib was the first of the 2G TKIs to be approved for imatinib-resistant CML and is now also approved for frontline therapy at a standard dose of 100mg/day in CP-CML or 140mg/day (or 70mg twice daily) in AP-CML and BC-CML. *In vitro* inhibition of wild type BCR-ABL1 by dasatinib was shown to be 325-fold greater than with imatinib. Additionally, dasatinib has shown excellent efficacy against almost all *BCR-ABL1* mutations of imatinib-resistant CML, with the exception of point mutation T315I(Thomas O'Hare et al., 2005)

Dasatinib is structurally unrelated to imatinib as it was originally developed to target SRC family kinases (SFKs). During initial testing it was discovered to also have extreme potency in BCR-ABL1 inhibition(J. Das et al., 2006). This dual SFK/ABL1 inhibitor has a variety of molecular targets and is the only first line TKI to bind both active and inactive forms of BCR-ABL1(Tokarski et al., 2006).

1.8.2.1. Phase I and II Dasatinib Clinical Trials

The dasatinib phase I dose escalation study included 84 patients (40, 11, 23 and 10 in CP, AP, BC and Ph+ ALL, respectively) resistant or intolerant to imatinib, assigned to a dose of 15-240mg per day, administered once or twice daily. Of those patients in CP, AP and BC a CHR/CCR was observed in 92/35, 45/18 and 35/26% of patients, respectively. In addition, dasatinib proved effective against all *ABL1* tyrosine KD mutations, with the exception of T315I. A twice-daily dose of 70mg was sufficient for constant BCR-ABL1 inhibition. (Talpaz et al., 2006)

Four different phase II dasatinib studies were launched following the success of the phase I trial. The trials, known as START studies (SRC-ABL1 Tyrosine Kinase Inhibition Activity Research Trial), were split according to CML phase; chronic (START-C), accelerated (START-A), myeloid blast crisis (START-B) and lymphoid blast crisis (START-L). In these four trials START-C, START-A, START-B and START-L, a CHR/CCR was achieved in 90/49, 45/32, 27/27 and 29/46% of patients respectively. (Santos et al., 2011)

1.8.2.2. Late Phase and Ongoing Dasatinib Clinical Trials

The phase III DASISION (Dasatinib Versus Imatinib Study In Treatment-naïve CML) trial recruited CP-CML patients who were randomly assigned to receive either imatinib (400mg once daily) or dasatinib (100mg once daily). The results are summarised in **Table 1.2**. (E. Jabbour et al., 2014)

Table 1.2. DASISION Study: 3 year follow-up.

	IMATINIB (400mg once daily)	**DASATINIB (100mg once daily)**
Patients (n)	258	258
OS (%)	99	98
PFS (%)	93	93
MMR (%)	55	69
MR4.5 (%)	12	22
Progression to AP/BC (%)	7	7

1.8.3. Nilotinib

Contrary to dasatinib, nilotinib is structurally similar to imatinib, with slight chemical modifications designed to bind more tightly to the BCR-ABL1 protein. This more topological fit allows greater efficacy over *BCR-ABL1* KD mutations and also gives a potency 20-fold more than that of imatinib(E Weisberg et al., 2006). Nilotinib binds to inactive BCR-ABL1 and is only completely ineffective against the T315I mutation; against all other mutations nilotinib shows some activity(M. W. Deininger, 2008b). Compared to imatinib, the specificity of nilotinib for BCR-ABL1 is increased; imatinib activity favours c-KIT and PDGFR over BCR-ABL, yet the reverse is seen in nilotinib. It is also the most lipophilic TKI, which can prove favourable in drug transport. (M. W. Deininger, 2008b)

1.8.3.1. Phase I and II Nilotinib Clinical Trials

A phase I dose escalation study included 119 imatinib-resistant Ph+ CML/ALL patients; 17/56/33 in CP-/AP-/BC respectively. Increasing doses of nilotinib were given; 50-1200mg once daily or 400/600mg twice daily. A CHR/CCR was achieved by 65/35, 46/14 and 6/6% of the CP, AP and BC patients, respectively. Impressively, 9 AP and 8 BC patients had their CML return to CP following nilotinib treatment. Nilotinib also showed activity against all *BCR-ABL1* mutations, except T315I. (H. Kantarjian et al., 2006; Santos et al., 2011)

In phase II trials, imatinib resistant/intolerant patients were split according to clinical phase (CP, AP and BC and Ph+ ALL). In CP, AP and BC groups, CHR/CCR

was achieved in 76/44, 30/19 and 25/0% respectively, showing promising results for nilotinib as a salvage therapy for imatinib failure. (Giles et al., 2008; H. M. Kantarjian et al., 2011; P le Coutre et al., 2012; Santos et al., 2011)

1.8.3.2. Late Phase and Ongoing Nilotinib Clinical Trials

The ENESTnd (Evaluating Nilotinib Efficacy and Safety in Clinical Trials Newly Diagnosed Patients) trial is a phase III comparison study of imatinib and nilotinib in treatment naïve CP-CML. Patients were randomly assigned to receive imatinib (400mg once daily), or nilotinib (300mg/400mg twice daily). Three year follow-up is summarised in **Table 1.3**. (Larson et al., 2012)

Table 1.3. ENESTnd Study: 3 year follow-up.

	IMATINIB (400mg once daily)	NILOTINIB (300mg twice daily)	NILOTINIB (400mg twice daily)
Patients (n)	283	282	281
OS (%)[a]	95.2	98.1	98.5
PFS (%)[b]	94.7	96.9	98.3
EFS (%)[b]	93.1	95.3	97.4
MMR (%)[b]	53	73	70
MR4 (%)[b]	26	50	44
Progression to AP/BC (%)[b]	95.2	99.3	98.7

[a] Overall Survival including only CML related deaths.

[b] Percentages are estimated by Kaplan–Meier analysis.

1.8.4. Other Current Treatments in CML

1.8.4.1. Bosutinib

Similarly to dasatinib, bosutinib is a dual SRC/ABL1 kinase inhibitor with greater activity against BCR-ABL1 compared to imatinib. However, its efficacy against PDGFRβ and c-KIT is much lower; IC50 370nM and 6000nM for PDGFRβ and c-KIT respectively.

In phase I/II studies, bosutinib was shown to be effective in CP-CML patients with imatinib resistance(Jorge E. Cortes et al., 2012) and also in patients who had subsequently failed dasatinib and/or nilotinib(Khoury et al., 2012). In imatinib resistant and multiple TKI resistant CML, a CHR/CCR was achieved by 86/41 and 73/24% of patients, with an optimal dose of 500mg once daily. Bosutinib also showed inhibitory activity against all *BCR-ABL1* mutations, except T315I.

The phase III BELA study (Bosutinib Efficacy and Safety in Newly Diagnosed Chronic Myeloid Leukaemia) compared the efficacy of imatinib (400mg once daily) and bosutinib (500mg once daily) in 502 treatment naïve CP-CML patients. The percentage of patients achieving a CCR within 12 months was similar for both imatinib (68%) and bosutinib (70%), but a higher percentage of bosutinib patients achieved an MMR at the time compared to imatinib (41% and 27%, respectively). Unfortunately, a high number of patients randomly assigned to receive bosutinib had a treatment discontinuation due to side

effects; 19% of bosutinib patients compared to 6% of imatinib patients. The most severe side effect with bosutinib was grade 3/4 diarrhoea, which was reported in 68% of patients. As this undesirable adverse effect is not commonly seen with the other 2G TKIs, this explains clinicians' reduced inclination to prescribe bosutinib to patients when dasatinib and nilotinib are readily available. (Jorge E. Cortes et al., 2011)

1.8.4.2. Ponatinib

Despite the availability of three clinically approved TKIs, the development of the T315I 'gatekeeper' mutation of *BCR-ABL1* has until recently been without a solution; ponatinib has been specifically designed to tackle this problem. The threonine to isoleucine single point mutation of T315I causes the disruption of the hydrogen bond usually made between the TKI and *BCR-ABL1* at T315. Additionally, the bulky nature of the isoleucine side chain can cause difficulties in TKI binding. Unlike all other currently available TKIs, ponatinib does not form a hydrogen bond at T315 and also has a long and flexible structure that can avoid the isoleucine side chain, thus ponatinib is the only TKI to have shown efficacy against T315I. (T O'Hare et al., 2009; Santos et al., 2011)

Phase I ponatinib trials observed a CHR in 95% and CCR in 53% of CP-CML patients. Moreover, of the 9 patients positive for T315I, 100% achieved a CHR and 89% a CCR. During the phase II PACE (Ponatinib Ph-positive acute lymphoblastic leukaemia [ALL] and CML Evaluation) trial, the percentage of CP,

AP and BC CML patients who achieved a CCR were 46, 24 and 18% respectively. Impressively, of the CP, AP and BC patients with T315I, a CCR was observed in 66, 33 and 21%. (J.E. Cortes et al., 2013)

Unfortunately, following the recognition of a high number of serious cardiovascular/peripheral arterial events in the PACE trial and phase III EPIC trial (which compared ponatinib and imatinib in newly diagnosed CP-CML), ponatinib was put under a partial temporary hold and EPIC was closed. However, due to the lack of any other treatment options for T315I positive CML patients, ponatinib remains approved in such cases where all other options are exhausted.

1.9. Mechanisms of TKI Resistance

The 7 year IRIS study follow-up suggests more than 1 in every 3 CML patients will need alternative treatment beyond imatinib at some point during their disease, with other studies suggesting this may be even higher in the general population. IRIS concludes a 41% resistance to first line imatinib therapy; 18% primary resistance, 17% secondary resistance and 6% progression. Resistance to 2G TKIs is an additional problem that is arising and often is based upon the promptness of clinical intervention following imatinib resistance. It follows therefore that finding a method of identifying which TKIs are the optimal treatment for an individual patient at diagnosis would be of immense benefit to CML clinical outcome.

Additionally, increasing chances of TKI resistance correlate with the phase of CML, progression rate and time to achieve an initial response. Therefore, understanding the mechanisms of this resistance is imperative if we wish to improve CML survival rates. The various, well documented mechanisms of TKI resistance in CML are separated into two distinct categories; *BCR-ABL1* dependent and independent.

1.9.1. BCR-ABL1 Dependent Resistance

***BCR-ABL1* Overexpression:** *BCR-ABL1* gene amplification and subsequent elevated protein levels are seen in a small proportion of imatinib-resistant patients. The duplication of *BCR-ABL1* has been reported in both resistant cell lines(Philipp le Coutre et al., 2000; Ellen Weisberg & Griffin, 2000) and CML patients(Gorre et al., 2001). This mechanism of imatinib resistance can be occasionally overcome by increasing concentrations of imatinib(Hochhaus & La Rosee, 2004), though is most frequently observed at progression to advanced disease.

Excess Active BCR-ABL1: Conventional thought is that BCR-ABL1 exists in equilibrium of both its inactive and active states. Imatinib and nilotinib bind only to the inactive form of BCR-ABL1. In its inactive conformation, the SH3 autoregulation (**Section 1.6.2**) remains intact; this is displaced when Tyr421 and subsequently Tyr242 of c-ABL1 (Tyr1127 of BCR-ABL1) are phosphorylated and a conformational change occurs. An excess of the active form of BCR-ABL1 (i.e. SH3 mutation or increased BCR-ABL1 phosphorylation) may therefore be attributed to some imatinib (and nilotinib) resistance. (Walz & Sattler, 2006)

***BCR-ABL1* Mutations:** KD mutations are the most common cause of secondary resistance in CML as they can alter the BCR-ABL1 active site so as to inhibit TKI binding. This mutation will therefore confer an advantage to the cells, which are then selected within the leukaemic cell population and thus a TKI-resistant

subclone is formed. Many mutations have been identified, some more common than others that affect TKI activity against BCR-ABL1. T315I is the only *BCR-ABL1* mutation that confers a resistance to all three clinically approved first line TKIs at a clinically achievable concentration. All other KD mutations have a TKI that has some efficacy against them. (Fava, Kantarjian, & Cortes, 2012)

1.9.2. *BCR-ABL1* Independent Resistance

TKI Influx/Efflux Variances: Transport of TKIs into and out of the cell is essential for its ability to function. As imatinib is highly lipophobic, its transport across the cell membrane is dependent upon transmembrane proteins, thus the expression of such vehicles are of great interest within imatinib resistance research. The main imatinib influx transporter is human organic cation transporter (hOCT1), which actively transports imatinib across the cell membrane and into the cell. High pre-treatment *hOCT1* expression levels correlate with a greater overall survival and PFS when compared to low *hOCT1(L Wang et al., 2008)*. Additionally, the M420del single nucleotide polymorphism (SNP) of *hOCT1* leads to a greater risk of imatinib failure, further highlighting the importance of high levels of an intact hOCT1 transporter in imatinib treatment(Athina Giannoudis et al., 2013). Dasatinib and nilotinib are favourable alternative therapies for these low *hOCT1* patients, as their influx is *hOCT1*-independent(Davies et al., 2009; Athina Giannoudis et al., 2008). Furthermore, efflux transporters in the ATP-binding cassette (ABC) family (e.g. *MDR1*) act to reduce intracellular imatinib concentration by transporting it back out into the surrounding plasma. Imatinib is a substrate for the ABCC3

transporter and elevated expression of ABCC3 (MRP3) correlated with imatinib failure. (A Giannoudis et al., 2014)

Pharmacokinetics: Differences in patient drug metabolism can impact treatment effectiveness. Varying levels of metabolising enzymes and/or inhibiting proteins such as α1-acid glycoprotein (AGP) that can reduce intracellular imatinib concentrations, have been shown to correlate with imatinib resistance. (Gambacorti-Passerini et al., 2000)

Compliance: Poor patient adherence to TKIs has been reported in a number of studies. One UK study in Hammersmith Hospital evaluated the drug compliance of 87 CML patients receiving imatinib for a median of 5 years, using a computerised pill bottle that recorded each opening of the bottle; 26% of patients were ≤90% compliant(Marin et al., 2010). The ADAGIO (Adherence Assessment with Glivec: Indicators and Outcomes) study used pill counting and found only 14.2% of patients to have taken their medication as prescribed; 71% took less than indicated and 14.8% took more(Noens et al., 2009). Both of these studies shown strong correlations between imatinib adherence and patient responses; a CCR was achieved in patients taking 90-93% of their prescription, while only a partial CR by those taking 74-77% of their imatinib(Noens et al., 2009). Additionally, the probability of achieving an MMR was only 28% in patients with a compliance of <90%, compared to 95% probability in patients taking >90% of their prescribed dose(Marin et al., 2010). It is clear from this that patient compliance is a critical determinant of disease response and though

other mechanisms of resistance may arise, TKI adherence should be taken into careful consideration. (E. J. Jabbour, Kantarjian, Eliasson, Megan Cornelison, & Marin, 2012)

Activation of BCR-ABL1 Independent Signalling Pathways: Alternative activation of signalling pathways that are downstream of BCR-ABL1 may alleviate the dependence upon BCR-ABL1 and thus confer resistance to TKIs that specifically target BCR-ABL1 activity. A variety of these have been reported, though this thesis focuses on the CIP2A/PP2A pathway, which will be discussed in **Section 1.15**.

1.9.3. TKI Toxicity

TKI toxicity is tightly linked with intolerance. Different TKIs have been shown to cause different side effects, which can result in the patient having to switch their course of treatment. Though it varies between trials, intolerance is generally defined as any nonhaematological toxicity with a severity grade of 3 or higher, or can also include prolonged grade 2 effects. Some adverse effects may not necessarily have an impact on whether or not the patient is able to continue TKI treatment, but may impact upon their quality of life and thus alternative therapies are considered.

Grade 3/4 neutropenia and anaemia are more common in imatinib treated patients than those treated with dasatinib(J. Cortes, Jones, & Kantarjian,

2010)or nilotinib(Saglio et al., 2010), as well as nausea and vomiting. However, for dasatinib, the rates of pleural effusion are higher than in patients treated with other TKIs and can cause discontinuation of treatment in some patients. As already described, bosutinib has a high incidence of severe diarrhoea that causes many patients to switch TKI treatment, and ponatinib patients have a high level of severe cardiovascular complications compared to all other TKIs.

1.10. BCR-ABL1 Signalling Pathways

The central role of BCR-ABL1 in CML is seen by its wide variety of interacting proteins. Its activation of oncogenic signalling pathways enhances CML progression via genomic instability, increased proliferation and haematopoietic stem cell (HSC) renewal and inhibition of apoptosis(Cilloni & Saglio, 2012; McCubrey et al., 2008; Sinclair, Latif, & Holyoake, 2013). Signalling cascades include (amongst others) the phosphatidylinositol-3-kinase (PI3K)/protein kinase B (AKT/PKB) pathway(Kharas & Fruman, 2005), MAPK pathways(McCubrey et al., 2007), janus-activated kinase 2 (JAK2)/signal transducer and activator of transcription 5A (STAT5) pathway(Steelman et al., 2000) and the CIP2A/PP2A pathway(C. M. Lucas et al., 2011). In this thesis I focus on the CIP2A/PP2A pathway (**Section 1.15**).

Figure 1.7. The main BCR-ABL1 signalling pathways in CML pathogenesis.

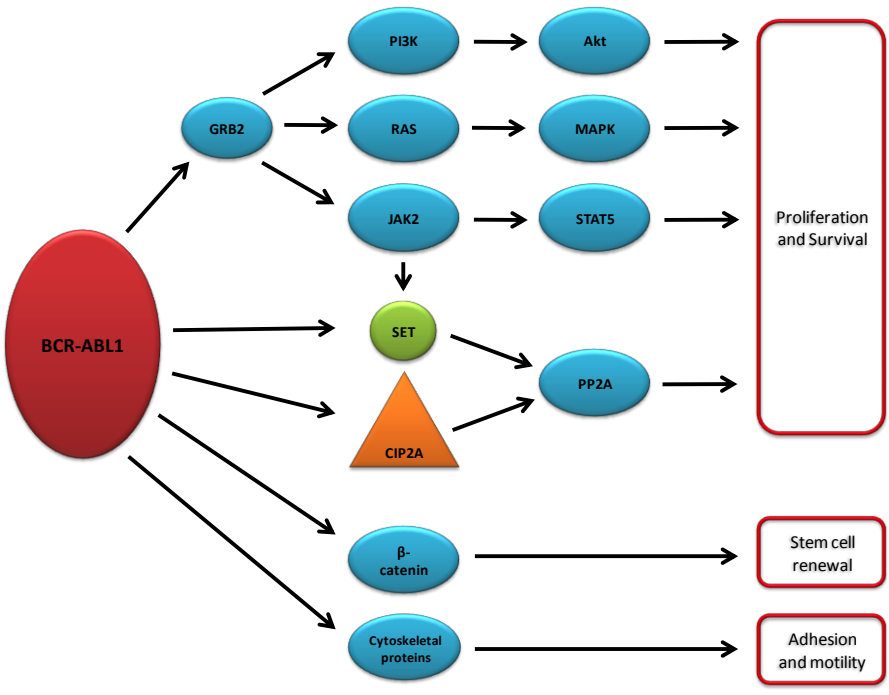

1.11. PP2A Overview

Cell signalling networks throughout the body rely heavily upon post-translational modifications to switch on/off regulatory molecules and maintain correct functionality. Reversible phosphorylation is one such mechanism that is responsible for the regulation of a diverse range of intracellular processes; protein phosphatases work in opposition to protein kinases, dephosphorylating molecules to regulate their activity.

One specific phosphatase – protein phosphatase 2A (PP2A) – accounts for over 90% of the serine/threonine phosphatase activity within the cell. PP2A acts to dephosphorylate proteins to inhibit oncogenic activity; it is involved in proliferation, survival, gene regulation, cytoskeletal organisation and protein synthesis. With such a wide variety of cellular implications it is no shock that PP2A inhibition has been implicated in several pathological conditions; cancer and Alzheimer's Disease are amongst the most studied, with PP2A often found to be underexpressed, inactivated or mutated. (H. Kantarjian et al., 2010; Saglio et al., 2010)

Regulation of PP2A's cellular activity is a key point in ongoing research. Its vast array of molecular targets in various subcellular components, as well as the many naturally occurring PP2A inhibitors (e.g. okadaic acid), highlight its importance in normal cellular homeostasis. Investigating PP2A and/or its various subunits as a therapeutic target may be of clinical benefit. It is

therefore important to thoroughly understand the mechanisms of interaction this holoenzyme has with other cellular proteins and the way in which this can be disrupted in malignant cells.

1.11.1. PP2A: Protein Structure

Cellular PP2A exists in one of two forms: a core heterodimer consisting of a structural subunit (A) and a catalytic subunit (C), or a heterotrimeric complex which also involves one of a wider variety of regulatory subunits (B). It is the association of this variable B subunit (along with other post-translational modifications) that determines the subcellular localisation of the trimeric complex and gives PP2A its distinct substrate specificity that is crucial for its regulatory role within the cell. (Ruediger, Ruiz, & Walter, 2011; Slupe, Merrill, & Strack, 2011)

Figure 1.8. Assembly of PP2A heterotrimeric protein, including various B subunit families and isoforms.

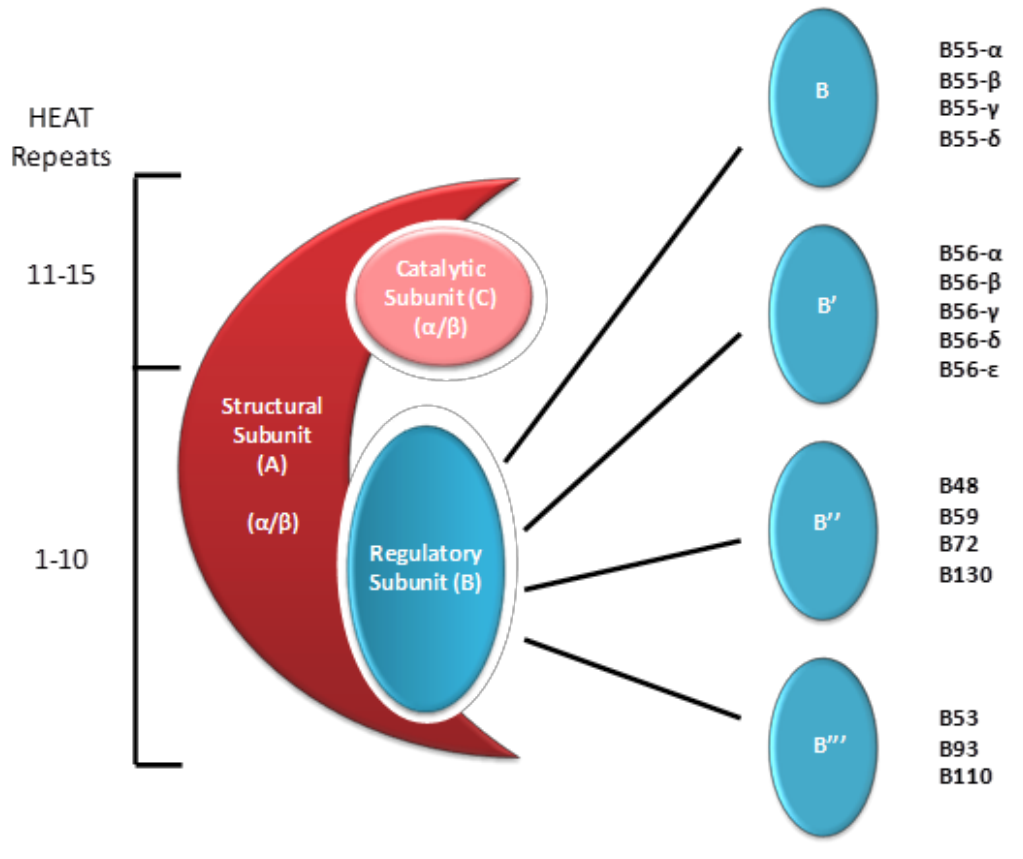

1.11.1.1. Structural Subunit (A)

The structural subunit plays a scaffold role in the assembly of the PP2A complex and can be in either α or β form (the α form being more prevalent). This 65kDa protein contains 15 HEAT repeats that form a horseshoe shape due their almost parallel stacking; repeats 11-15 are the recognition site for C and mutations within this site have been shown to block AC interaction. The association of the B subunit occurs at HEAT repeats 1-10. (Sablina & Hahn, 2007)

1.11.1.2. Catalytic Subunit (C)

The C subunit (also with an α/β form; α expression is 10-fold higher in humans) is typically 36kDa and is the main target of post-translational modifications within the core heterodimer. The most recognised of these modifications are phosphorylation of tyrosine 307 and threonine 304 which are associated with PP2A inactivation, and leucine 309 methylation, which has been shown to affect the binding of certain B subunits. (Seshacharyulu, Pandey, Datta, & Batra, 2013)

1.11.1.3. Regulatory Subunits (B)

In this ever-expanding subunit category there are currently four reported B subunit families; B, B', B'' and B'''. The association of these with the core dimer is tightly regulated and gives PP2A its selective targeting(Slupe et al., 2011). Each of these families contains up to five different reported isoforms, some with different splice variants; there is great inter-family conservation though little

similarity across families. The known B subunit families can be seen in **Figure 1.8**. (Seshacharyulu et al., 2013)

1.11.1.4. Inactive PP2A Holoenzyme Structures

Of interest, several catalytically inactive PP2A complexes have been reported; two such complexes are C subunit/α4 (IGBP1) and C subunit/A subunit/PP2A Methyl Esterase 1 (PME-1). Numerous tumours show increased expression of both α4 and PME-1, suggesting a bias towards the formation of inactive PP2A heterotrimers over the active tumour suppressor complexes. (Haesen, Sents, Lemaire, Hoorne, & Janssens, 2014)

1.11.2 PP2A Regulation and Modification

The differing B subunits, when combined with α and β isoforms of the structural and catalytic subunits, are thought to give rise to approximately 70 variations of the PP2A holoenzyme, thus highlighting the extraordinary substrate specificity of PP2A that is possible. Regulation of PP2A activity within the cell relies heavily on the proportions of specific PP2A heterotrimers formed.

PP2A expression is tightly regulated at the translational level via auto-phosphorylation in order to maintain constitutive tumour suppressor activity. Additionally, its catalytic activity is modified by leucine (L) methylation and tyrosine (Y) and threonine (T) phosphorylation. Methylation at L309 favours specific holoenzyme assembly, while phosphorylation at Y307 and T304 inactivates PP2A.

1.11.3. PP2A Inhibition in Human Malignancies

The vast implications of PP2A inhibition in cancer progression and cell transformation have been widely reported. Indeed, several studies have found that activation of the rat sarcoma (RAS) oncoprotein is not sufficient for the transformation of cells unless accompanied by the suppression of PP2A activity(Junttila et al., 2007). Deregulated signalling cascades involving PP2A inhibition are seen in many cancers; blocking PP2A holoenzyme assembly, phosphorylation and thereby inactivation of PP2A, and even the 'shielding' of proteins from PP2A binding and subsequent dephosphorylation are just some of the main mechanisms of inhibiting PP2A's tumour suppressor activity.

Papers reporting genetic alterations that consequently lead to impaired PP2A activity are also in abundance in cancer research(Colella et al., 2001; Van Hoof & Goris, 2004). Many of these refer to the impaired binding of mutated forms of *PP2A-Aα/β* to certain PP2A-B subunits, and thus an inability to form necessary PP2A multimeric complexes(Colella et al., 2001). Alteration of the A subunit has also resulted in downstream signalling alterations, such as increased AKT(Chen, Arroyo, Timmons, Possemato, & Hahn, 2005).

CML: With regards to PP2A in CML, its activity is significantly diminished at diagnosis in MNCs and also in HSCs. This has been shown via two mechanisms; BCR-ABL1-induced SET (**Section 1.12**)(AK Samanta, SN Chakraborty, Y Wang, & H Kantarjian, 2009; P Neviani et al., 2013; Paolo Neviani et al., 2005; Perrotti

& Neviani, 2006) expression and overexpression of CIP2A (**Section 1.14**)(C. M. Lucas et al., 2011). Along with the influence of c-Myc (**Section 1.13**), these PP2A inhibitors cause the increased phosphorylation and subsequent deactivation of PP2A. It is imperative to understand these PP2A inhibitors and their mechanisms of action if advances are to be made in the treatment of CML and other malignancies.

1.12. SET

SET nuclear proto-oncogene (SET) is a well-established endogenous inhibitor of PP2A that is known to be involved in a variety of human malignancies(Li, Makkinje, & Damuni, 1996). Three specific mechanisms of PP2A inhibition by SET have been reported; overexpression of SET, altered SET phosphorylation and altered endogenous ceramide (SET inhibitor) expression. Structural information of SET/PP2A binding has not been widely reported, though a region (residues 36-124) located close to the SET N-terminal is critical for PP2A inhibitory function.

CML: In CML, SET is overexpressed during blast crisis and directly correlates with a loss of PP2A activity. Additionally, SET knock down restores PP2A activity by decreasing the levels of the inactive pY307-PP2A(Paolo Neviani et al., 2005), indicating a causal role of PP2A inhibition by SET in CML BC. Interestingly, this PP2A inhibition by SET occurs only during BC and not during CP CML.

Other kinase signalling pathways such as MAPK and AKT were downregulated upon the decrease of SET, suggesting that BCR-ABL1-induced SET expression is one way of the leukaemic cell overcoming inhibition of other pathways. Stabilisation of SET by SET binding protein (SETBP1) is also reported to aid the inhibition of PP2A(Piazza et al., 2013), and JAK2 inhibition has been shown to

cause a decrease in the expression of SET and subsequent PP2A activity(AK Samanta et al., 2009).

Importantly, SET expression is inhibited by imatinib, leading to the restoration of PP2A activity(Perrotti & Neviani, 2006).

1.13. c-Myc Overview

One of the most studied proto-oncogenes is *c-Myc*. It is involved in such a diverse array of cellular functions, including proliferation, cell cycle regulation and metabolism, that its overexpression in a vast number of cancers is no surprise. It is estimated that 15% of human genes have c-Myc binding sites and thus the possibility to be affected by this pleiotropic transcription factor. (Fernandez et al., 2003; Zirong Li et al., 2003)

The over expression of c-Myc is seen in so many different cancer types it has been questioned whether c-Myc itself is the driving force behind the malignancies or if it is merely a consequence. It is overexpressed in approximately 70% of cancers including Burkitt's lymphoma, prostate and breast cancer, to name but a few.

CML: In CML, c-Myc is reported to be overexpressed at transformation to blast crisis. Additionally, in CP samples of patients destined to progress to BC, protein expression of both total c-Myc and its phosphorylated stabilised form c-Myc pS62 are elevated. The overexpression and stabilisation of c-Myc, increased CIP2A protein expression and increased BCR-ABL1 tyrosine kinase activity are all associated; these effects lead to a greater inhibition of PP2A activity.

1.13.1. c-Myc Post-Translational Regulation

Post-translational modification of c-Myc is responsible for both its stabilisation and degradation; phosphorylation sites at serine (S) 62 and threonine (T) 58 are involved in these mechanisms (**Figure 1.9**). The S62 phosphorylation of c-Myc by extracellular-regulated kinase 1,2 (ERK)(Sears et al., 2000) stabilises the c-Myc protein and has also been reported to play a role in determining its target genes(Benassi et al., 2006). However, this also primes c-Myc for subsequent phosphorylation at T58 by glycogen synthase kinase 3 beta (GSK-3β) and targeting c-Myc for proteasomal degradation(Gregory, Qi, & Hann, 2003).

When phosphorylated at both residues, PIN-1 isomerises c-Myc, causing a conformational change that allows PP2A to recognise and dephosphorylate c-Myc pS62(Yeh et al., 2004). Polyubiquitination of c-Myc pT58 then allows proteasomal degradation of c-Myc.

It is interesting to note the upstream role of RAS that can regulate the activity of ERK and GSK-3β; RAS activates ERK and inhibits GSK-3β, thus the balance of c-Myc is in favour of its more stabilised form, c-Myc pS62. As discussed in **Section 1.14.2**, the direct association of CIP2A with c-Myc also acts to inhibit PP2A's dephosphorylation of c-Myc pS62 and thereby protect endogenous c-Myc from degradation. (Junttila & Westermarck, 2008)

Figure 1.9. Normal mechanism of c-Myc degradation. c-Myc phosphorylation at serine 62 by ERK stabilises c-Myc. Subsequent threonine 58 phosphorylation by GSK-3β and isomerisation by PIN-1 prime c-Myc for proteasomal degradation, following c-Myc pS62 dephosphorylation by PP2A. Poly-ubiquitination of c-Myc leads to its degradation(Junttila & Westermarck, 2008).

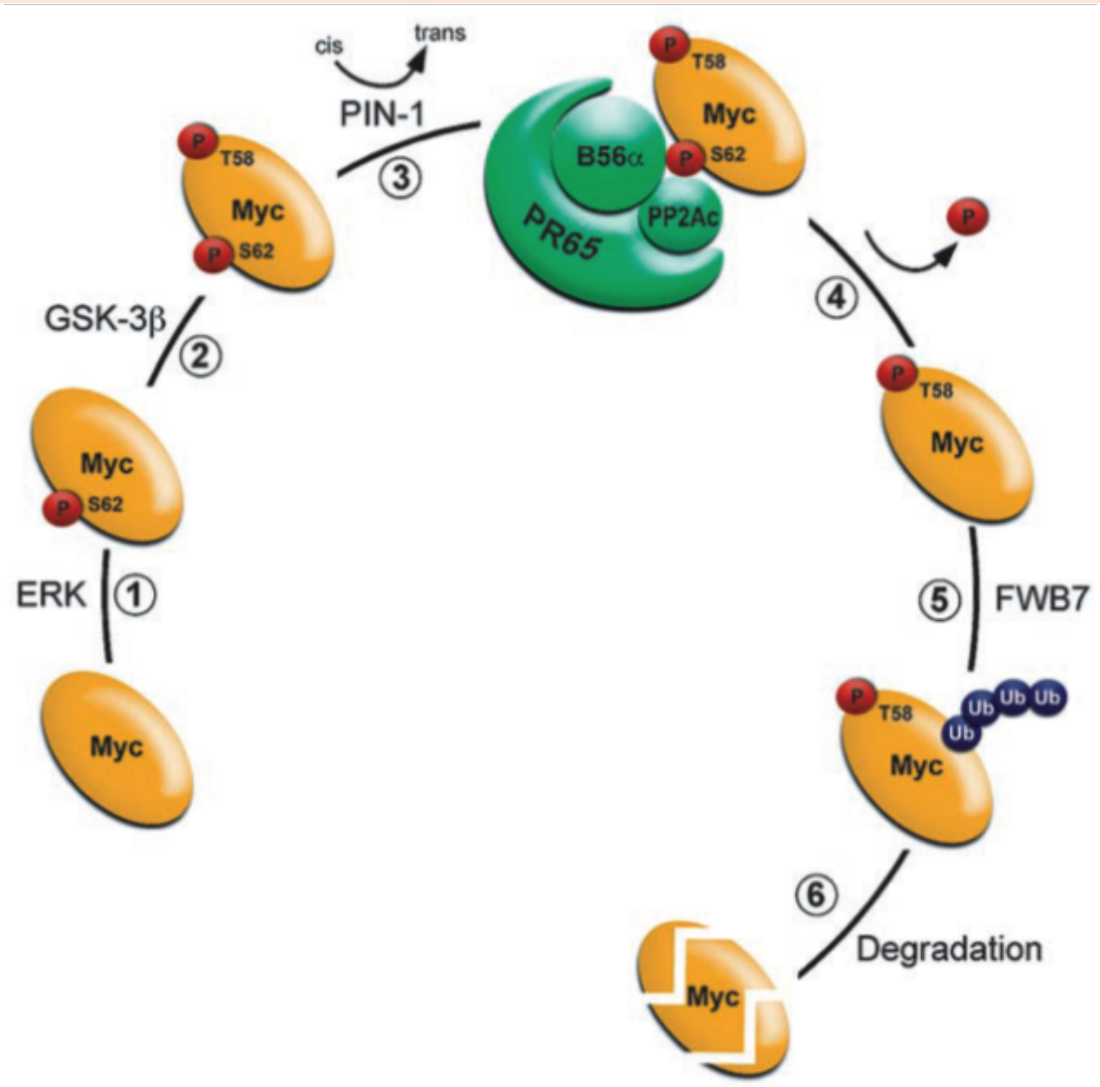

1.14. CIP2A Overview

*CIP2A*gene overexpression and increased cellular protein levels are reported in a variety of human malignancies and are shown to correlate with poor prognosis and aggressiveness of disease. In breast cancer, *CIP2A* not only correlated with an unfavourable patient outcome and tumour size and histological grade, but with proliferation markers and p53, *BRCA1* and *BRCA2* mutations(Come et al., 2009; Yu, Liu, Dong, & Jin, 2013). To date, a prognostic role for *CIP2A* has been published in: breast(Come et al., 2009), gastrointestinal(Teng et al., 2012; Wiegering et al., 2013), melanoma(Shi, Ding, Ju, Wu, & Cao, 2014), lung(Dong et al., 2011; Xu, Xu, Huang, Zhang, & Zhang, 2012), osteosarcoma(Zhai, Cong, Han, & Tu, 2013), pancreatic(Lei Wang et al., 2013), astrocytoma(Fuxin, Weimin, Weixian, Jinyang, & Wenbin, 2013), hepatocellular(He, Wu, Li, Cao, & Liu, 2012; Yua et al., 2013), ovarian(Bockelman, Lassus, et al., 2011; Fang, Li, Wang, & Zhang, 2012), bladder(L. P. Huang et al., 2012; Xue et al., 2012), renal(Ren et al., 2011), tongue(Bockelman, Hagstrom, et al., 2011), head and neck cancers(Basile & Czerninski, 2010), prostate(Vaarala, Väisänen, & Ristimäki, 2010) and cervical(J. Liu et al., 2011) solid tumours. Importantly, it has been firmly established in numerous malignancies that unlike CIP2A positive tumour cells, their tumour-adjacent normal tissues do not overexpress CIP2A. (Huang, Adelson, Mordechai, & Trama, 2011; J. Liu et al., 2011; X. Liu et al., 2014; Ma et al., 2011; Qu et al., 2012; Zhai et al., 2013)

In haematological malignancies, CIP2A has also been shown to be a biomarker of poor prognosis and an indicator of adverse responses to treatment; in AML, *CIP2A* overexpression is reported in newly diagnosed and relapsed patients. (J. Wang et al., 2011)

CML: The first publishing of CIP2A in CML showed it to be a possible prognostic indicator for blast crisis in imatinib-treated CML. The study showed diagnostic CIP2A protein levels to be significantly higher in patients destined to progress into blast crisis compared to those who do not, irrespective of whether they respond to imatinib treatment. The actuarial probability of progression into blast crisis after 2 years was shown to be 100% in patients who present with high CIP2A protein levels (MFI>7), compared to those with low CIP2A levels who remained progression-free after 30 months. This implies that CIP2A not only may be a possible biomarker for CML, but also a potential therapeutic target. (C. M. Lucas et al., 2011)

However, this study involved only patients treated with imatinib as first line therapy and currently no published works have shown this in patients treated with a second or third (2G/3G) generation TKI. This is a major gap in our knowledge as drug development moves forward with 3G TKIs in clinical trials and prescribing 2G therapies becoming more common practice.

1.14.1. CIP2A Structure

1.14.1.1. Predicted Protein Structure of CIP2A

Nothing is known of the tertiary structure of the CIP2A protein by primary experimentation; however it is possible to make predictions from the known 905 amino acid sequence. This proto-oncogene is predicted by computer programs to include a transmembrane and coiled coil domain(Coenen et al., 2010). It has two known phosphorylation sites (threonine 761 and serine 904) and is localised within the cytoplasm or perinuclear region.

Figure 1.10. CIP2A predicted protein structure. Taken from www.atlasgeneticsoncology.com.

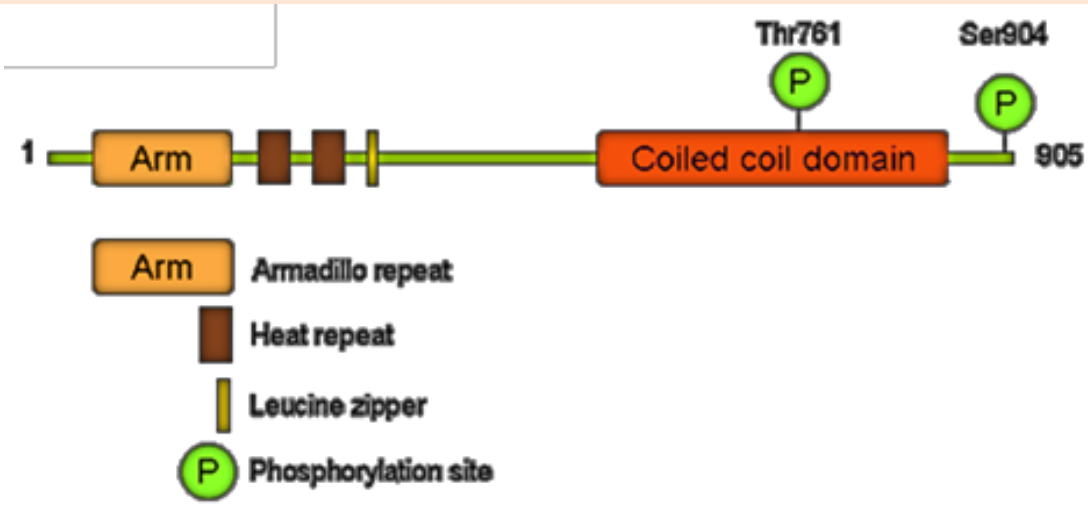

1.14.1.2. Structure of the *CIP2A* Gene

The *CIP2A* gene (also known as KIAA1524) is located at 3q13.13, consists of 21 exons and is well conserved across various mammals. Though much is known of the expression levels of the *CIP2A* gene, little is known of its different splice variants. To date, six alternative *CIP2A* transcripts have been reported and are shown in **Table 1.4**. (Data taken from *Ensembl gene database*) There are currently no publications that specify a certain *CIP2A* transcript expression in relation to any malignancy.

Table 1.4. Alternative splice variants of *CIP2A*.

	LENGTH (bp)	LENGTH (aa)	BIOTYPE
1 (*CIP2A-1a*)*	4075	905	Protein Coding
2 (*CIP2A-1b*)*	3877	746	Protein Coding
3	2764	121	Nonsense-mediated decay
4	654	48	Nonsense-mediated decay
5	2014	-	Processed Transcript
6	11	-	Retained intron

*Transcript variant investigated in **Chapter 6**.

1.14.2. CIP2A Protein Interactions

The functional activity of CIP2A was first published in July 2007 as an endogenous oncoprotein acting to inhibit the tumour suppressor activity of PP2A towards phosphorylated (serine 62) c-Myc. Also described was an interaction between CIP2A and the oncogenic transcription factor, c-Myc and also with PP2A. As CIP2A's direct interaction with PP2A is via the A subunit, it is important to consider the possibility that this may impact on the ability of PP2A to form the necessary PP2A trimers in certain malignancies and may be one method of CIP2A function. Additionally, CIP2A and RAS together were shown to induce malignant cell transformation. (Junttila et al., 2007)

MYC: Several human malignancies have reported on the relationship between CIP2A and c-Myc, with recent findings suggesting a positive feedback between the two oncoproteins(Khanna et al., 2009). Overexpression of CIP2A encourages c-Myc phosphorylation at serine 62, leading to enhanced c-Myc oncogenic activity and facilitating disease progression. In malignant cells, the direct interaction of CIP2A with c-Myc pS62 shields c-Myc from the dephosphorylation by PP2A that is essential for c-Myc turnover within normal cells. (Junttila & Westermarck, 2008)

Figure 1.11. CIP2A-mediated stabilisation of c-Myc. In normal cells, dephosphorylation of c-Myc pS62 by PP2A facilitates c-Myc degradation. In malignant cells, CIP2A binds to c-Myc, shielding the phosphorylated serine from PP2A-mediated c-Myc degradation(Junttila & Westermarck, 2008).

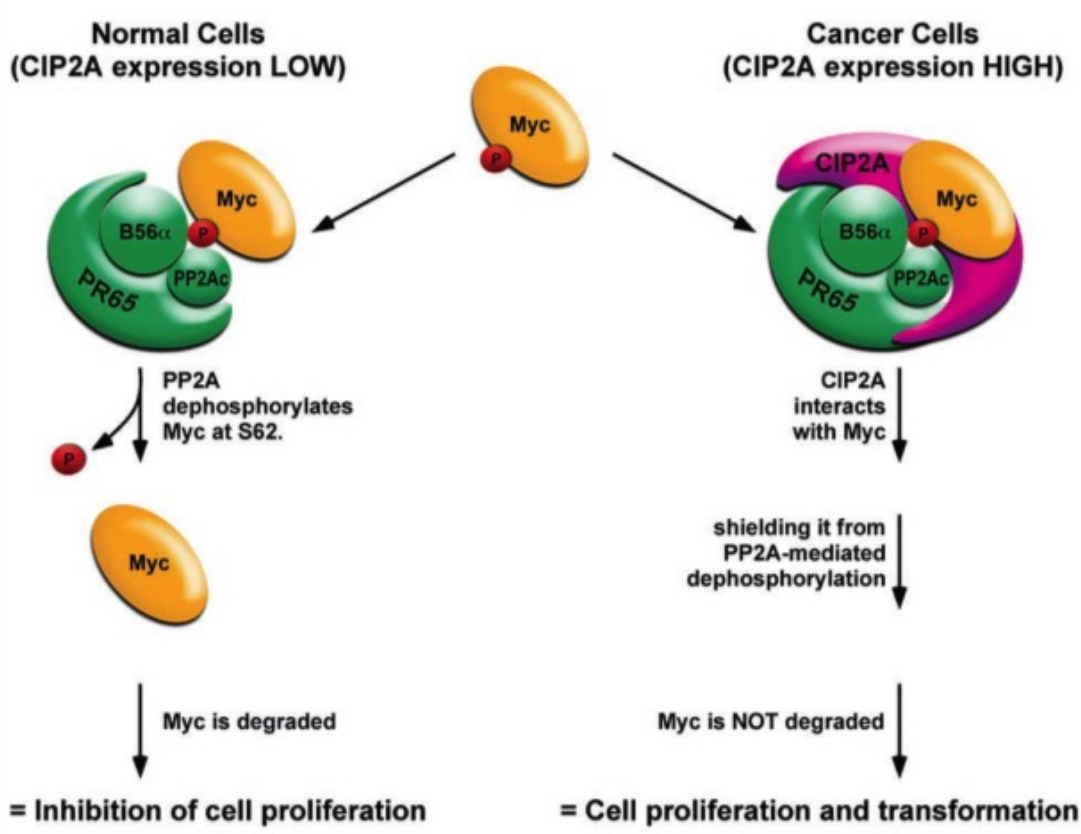

The action of CIP2A upon c-Myc appears to be post-translational and may explain why in many tumours, *c-Myc* mRNA expression is low though the protein levels are elevated.

E2F1: Like c-Myc, E2F1 is an oncogenic transcription factor, shown to be overexpressed in various cancers. Its activation can be regulated by phosphorylation at serine 364, which has been shown to be a target for PP2A. Strong evidence suggests the effects of CIP2A on E2F1 are mediated through PP2A inhibition. Increasing CIP2A levels rescued E2F1 pS364 expression via the inhibition of PP2A serine/threonine phosphatase activity. Interestingly, a specific PP2A holoenzyme assembly may be involved in E2F1 phosphorylation; B55αinhibition caused increased levels of E2F1 pS364, yet inhibition of B56β caused no such effect. This may suggest that CIP2A can interact with and inhibit specific PP2A holoenzymes depending upon their subunit make-up, in order to cause different effects within a cell, and is an interesting area for future research. Additionally, a positive feedback loop between E2F1 and CIP2A has been recently established; stable expression of CIP2A prevented downregulation of E2F1 protein, as well as E2F1 binding to the *CIP2A* promoter. (Khanna, Pimanda, & Westermarck, 2013; Laine et al., 2013)

1.14.3. *CIP2A*: Genetic and Epigenetic Regulation

***CIP2A* Transcription Factors:** As already discussed, E2F1 can induce the expression of *CIP2A*. The involvement of other oncogenic transcription factors in *CIP2A* induction is also emerging. *JNK2* has recently been reported to act via the transcription factor *ATF2* to regulate *CIP2A* transcription. (Mathiasen et al., 2012; Yongxun Zhao et al., 2014)

Increased kinase activity of the MEK/ERK1 MAPK pathway has been reported in many cancers. The ETS1 and ELK1 transcription factors are a target of this signalling pathway. ETS1 has recently been shown to be the transcription factor responsible for mediating the EGFR-MEK dependent regulation of *CIP2A* expression. An additional study in female urogenital cancers identified the cooperative roles of ETS1 and ELK1 in promoting *CIP2A* transcription. However, in gastric and prostate cancers, ETS1 alone can regulate CIP2A expression, suggesting that the transcriptional regulation of *CIP2A* may vary between malignancies and any future treatments developed to target CIP2A transcription factors should take this into careful consideration. (Khanna et al., 2011; Pallai, Bhaskar, Sodi, & Rice, 2012)

***CIP2A* Methylation:** The first functional analysis of the *CIP2A* promoter region was recently reported. Interestingly, a large CpG island was identified within this region that is conserved in several other species. In this study, gastric (AGS) and cervical (HELA) cancer cell lines, along with normal cells, were analysed for any methylation within this GC rich area. No methylation was

reported, however this is a very limited study and no methylation analysis of *CIP2A* has been undertaken in any other cancer cells. As *CIP2A* expression has been found to vary between patients in numerous cancer types, and methylation has been reported to cause gene silencing, this area may be of interest in other malignancies and certainly warrants further investigation. (Khanna et al., 2011)

1.15. The CIP2A/PP2A Pathway in CML

The inhibition of PP2A's phosphatase activity towards c-Myc pS62 by CIP2A has been reported in a variety of cancers since its discovery in 2007(Junttila et al., 2007). CIP2A overexpression in many diseases has been correlated with impaired PP2A activity and the oncogenic activity of CIP2A has been proved necessary in cell transformation. CIP2Adirectly interacts with c-Myc pS62(Junttila & Westermarck, 2008), preventing PP2A/c-Myc binding and subsequent dephosphorylation of c-Myc pS62. This allows c-Myc to remain stabilised and evade proteolytic degradation.

The involvement of the CIP2A/PP2A pathway in CML was reported by Lucas *et al*(C. M. Lucas et al., 2011)and showed an overexpression of CIP2A protein to be indicative of disease progression in imatinib-treated CML. In line with other literature, high CIP2A levels correlated with high levels of inactive PP2A and c-Myc pS62. PP2A inhibition via JAK2/SET has also been reported in CML, more specifically the BCR-ABL1 dependent induction of SET overexpression. **Figure 1.12** shows the CIP2A/PP2A pathway as it has been currently reported in CML.

This thesis focuses on the relationships between CIP2A, PP2A and c-Myc in CML and the effects of TKIs on these within the CIP2A/PP2A pathway.

Figure 1.12. The CIP2A/PP2A Pathway in CML(C. M. Lucas et al., 2011).

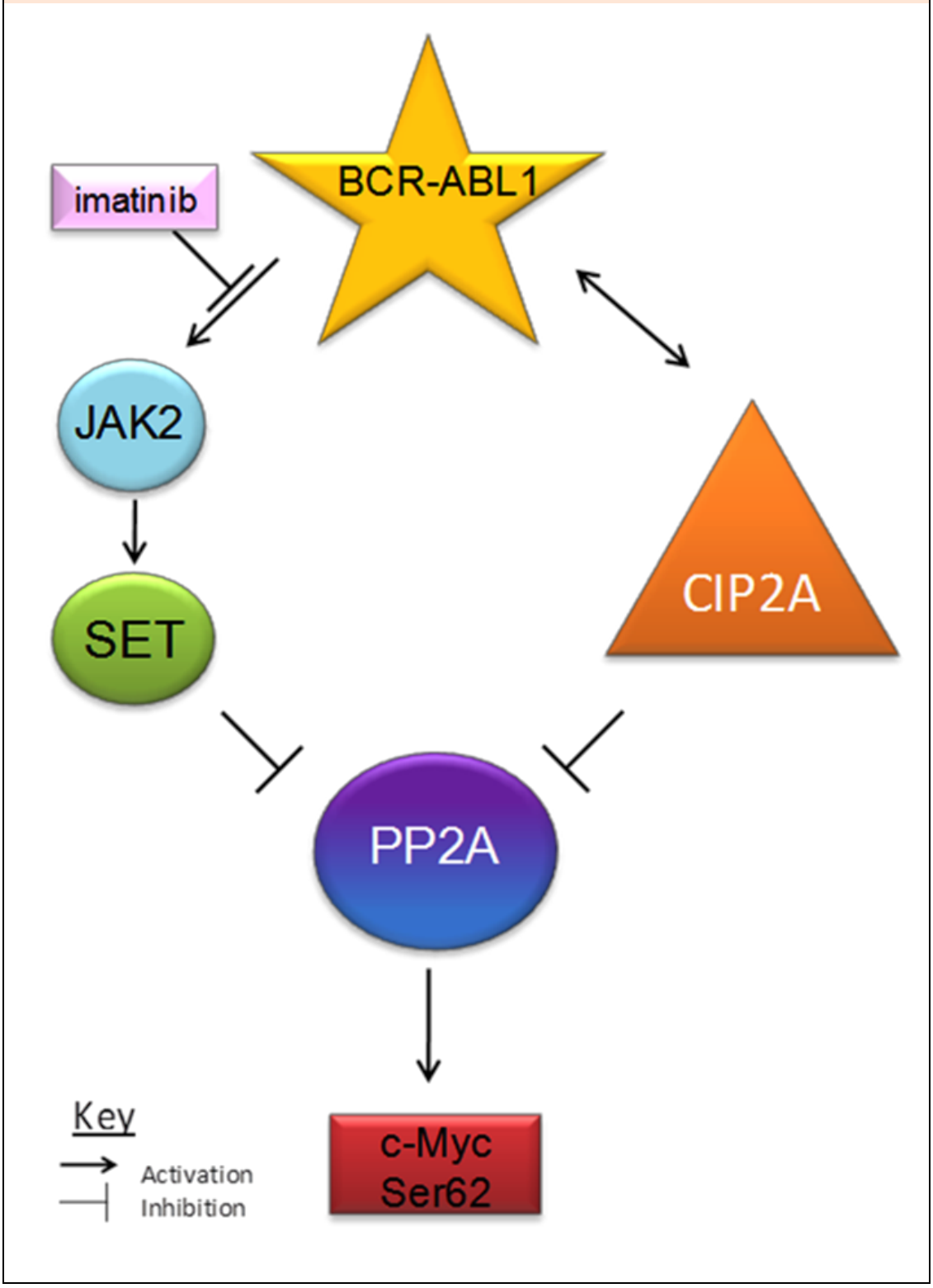

Thesis Aims

This thesis was inspired by the previous work of Dr Lucas on CIP2A's involvement within imatinib-treated CML. Her investigations identified CIP2A as a potential biomarker of blast crisis in patients treated with imatinib. However CIP2A involvement in CML treated with second and third generation TKIs is not known; will a patient with a high basal level of CIP2A protein still progress to blast crisis if they were treated with a second generation TKI from initial diagnosis? This initial question led to a more in depth investigation of CIP2A's role within the CIP2A/PP2A pathway as well as studying its genetic variants and epigenetic regulation. My aims were as follows:

1. **CIP2A protein in CML:**
    a. ***Chapter 3:****Biomarker status of CIP2A:*
        i. First I aimed to classify my patient cohorts according to high/low CIP2A protein level at diagnosis, using flow cytometry.
        ii. Correlations between basal CIP2A protein and clinical outcomes were investigated and compared to previous work on imatinib-treated CML. The aim was to study the potential biomarker role of CIP2A in second generation TKI treated CML.
    b. ***Chapter 4:****Comparative effects of TKIs on the CIP2A/PP2A pathway:*
        i. Using patient follow-up samples, I investigated the effects of long-term *in vivo* TKI therapy on various parts of the CIP2A/PP2A pathway.
        ii. After designing a short-term *in vitro* TKI culture, I investigated short-term effects of treatments upon various parts of the

CIP2A/PP2A pathway. Comparisons could then be made of the different TKIs and their effectiveness in targeting the oncogenic proteins within the pathway.

c. ***Chapter 5:****Effects of direct CIP2A and PP2A manipulation:*
    i. This section of work aimed to manipulate the CIP2A/PP2A pathway by directly targeting *CIP2A* using siRNA and *CIP2A* transient transfection. Changes in pathway proteins' expressions were examined following these manipulations. PP2A was also deliberately increased/decreased and the effects monitored.

2. ***Chapter 6: CIP2A transcript variants:***
    a. First I aimed to identify, using scientific literature, the potential presence of different *CIP2A* isoforms and design primers to target (via qRT-PCR) any protein coding transcript variants.
    b. Next the aim was to investigate whether all isoforms are present in CML, using BCR-ABL1 positive cell lines and CML patient samples.
    c. Finally, correlation between high/low CIP2A protein and the transcript variant were examined, as well as any link between *CIP2A* transcript variants and clinical outcome.

3. ***Chapter 7: Epigenetic regulation of CIP2A:***
    a. I aimed to identify any areas of potential methylation within the *CIP2A* promoter region, design primers to span these areas and use PCR pyrosequencing to measure the presence or absence of methylation in this promoter area. From this, suggestions could be made of *CIP2A* epigenetic regulation via methylation in CML.

Chapter 2: Materials and Methods

2.1. Patient Samples Declaration

All CML patients included in this research were 18 or older at diagnosis and were *BCR-ABL1* positive by metaphase cytogenetic analysis. Minimum patient follow-up was 12 months. Healthy volunteers were all fit and well at the time of donation and were 21 or more years of age. Each patient and healthy volunteer within this study was given a unique patient number (UPN) by which he/she is identified. Each section of work includes specific information of the samples used. A comprehensive table of all patient samples used in this thesis can be found in the Appendix.

This work was approved by the Liverpool Central Committee of the UK National Research Ethics Service. All healthy volunteer and patient samples included in this study were given with informed consent in accordance with the declaration of Helsinki.

2.2. Introduction

General methods used throughout this work are cell culture, flow cytometry, western blotting, enzyme-linked immunosorbence assay (ELISA), white blood cell (WBC) separation, RNA extraction, cDNA synthesis, manual polymerase chain reaction (PCR), quantitative reverse transcriptase PCR (qRT-PCR), PCR pyrosequencing, cell transfection and confocal microscopy. Cell lines, normal peripheral blood mononuclear cells (PBMCs) and patient samples were used.

2.3. Sample Collection and Preparation

2.3.1 Total leukocytes for RNA Extraction

To prepare patient and normal healthy volunteer blood cells for RNA extraction, approximately 6ml of venous blood was mixed with 40ml of red cell lysis buffer (0.1M ammonium chloride, 10mM sodium bicarbonate and 1.3mM ethylenediaminetetraacetic acid (EDTA) (Sigma-Aldrich, Gillingham, Dorset, UK)) and incubated for 5 minutes at room temperature. Samples were then centrifuged at 770 x g for 5 minutes, washed in phosphate buffered saline (PBS) and centrifuged for a further 5 minutes. Finally the pellet was reconstituted in 600µl of RNeasy Lysis Buffer (RLT) buffer (Qiagen, Manchester, Lancashire, UK) supplemented with 1% β-mercaptoethanol (Sigma-Aldrich) and stored at either -20°C short term or -80°C long-term.

2.3.2 MNC preparation for Protein Analysis

MNC were prepared from approximately 25ml of peripheral blood collected into EDTA and layered onto 10ml of lymphoprep (Axis-Shield, Cambridge, Cambridgeshire, UK). MNC were separated by density-dependent centrifugation and resuspended in 4°C Roswell Park Memorial Institute 1640 (RPMI-1640) containing 10% dimethyl sulphoxide (DMSO) (Sigma-Aldrich) and 10% foetal calf serum (FCS: BioSera, Uckfield, East Sussex, UK). Cells were cryopreserved in liquid nitrogen until required. Freshly extracted MNC from normal healthy volunteers were prepared and used immediately.

2.4. Cell Culture

2.4.1. Maintenance of Cell Lines

BCR-ABL1 positive cell lines used in this study were K562, KCL22 and LAMA84 (donated by Prof Junia Melo, LRF Leukaemia Unit, Hammersmith Hospital, London, UK). The *BCR-ABL1* negative cell lines HL60 (promyelocytic leukaemia-derived) and AGS (gastric adenocarcinoma-derived) were also used. All cell lines were maintained with standard 'culture medium' of RPMI-1640 supplemented with 1% L-glutamine, 1% Penicillin/streptomycin (Invitrogen, Paisley, Renfrewshire, UK) and 10% foetal calf serum, with the exception of the adherent AGS cell line for which Dulbecco's Modified Eagle Medium (DMEM: Sigma-Aldrich) supplemented with 1% L-glutamine, 1% penicillin/streptomycin, 10% foetal calf serum and 2% non-essential amino acid solution (Sigma-Aldrich) was used.

Cell lines were suspended in standard culture medium at an approximate starting density of $3x10^5$ cells per ml and re-seeded in fresh media every 3/4 days. Cells were resuspended in fresh culture medium 24 hours prior to any experimental use to ensure optimal exponential growth. Standard tissue culture conditions were observed (37˚C, 5% CO_2 in air, 100% humidity).

For the AGS cell line, trypsin EDTA was used to lift adherent cells from their surface when they reached 100% confluence or following a 24 hour *in vitro*

culture. Non-adherent cells were maintained at 2 x 10^6 per ml and HL60 cells at a maximum of 1 x 10^6 per ml.

Additionally, genomic DNA from U937 (leukaemic monocyte lymphoma-derived), HEK293 (human embryonic kidney-derived) and KYO-1 cell lines were used for methylation analysis (**Chapter 7**). These samples were given by Dr Lakis Liloglou, Molecular and Clinical Cancer Medicine, University of Liverpool.

2.4.2. Patient Cells

When required, patient samples were retrieved from liquid nitrogen cryopreservation and thawed rapidly at 37°C with agitation. Cells were then diluted dropwise over 30 minutes in pre-warmed (37°C) RPMI-1640 supplemented thawing medium (RPMI-1640/10% Heparin Sodium (1,000 IU/ml from Wockhardt UK Ltd, Wrexham, Wrexham County Borough, UK)) to dilute the DMSO. Cells were then washed and resuspended in standard culture medium and left to recover at 2 x 10^6 cells per ml at 37°C for 24 hours.

2.4.3. *In vitro* Cultures

This work used both cell lines and patient samples for *in vitro* studies. Cells were seeded into 6-well tissue culture plates (Becton Dickinson (BD) Biosciences, Oxford, Oxfordshire, UK), in standard culture medium at 2 x 10^6

cells per ml at 37°C for 24 hours with relevant treatments (**Table 2.1**). For patient samples, this was following a 24 hour recovery. Cell lines had been re-seeded in fresh culture medium 24 hours prior to *in vitro* treatments.

Protein levels were subsequently analysed using a variety of methods; flow cytometry (**Section 2.5**), western blotting (**Section 2.6**) and ELISA (**Section 2.7**).

Table 2.1. Drug concentrations used for *in vitro* cultures.

Drug / Reagent	Final Concentration	Manufacturing Company
Imatinib	5μM	Novartis (Basel, Switzerland)
Dasatinib	150nM	Bristol-Myers Squibb (New York, NY USA)
Nilotinib	5μM	Novartis
Ponatinib	130nM	ARIAD (Cambridge, MA, USA)
FTY720	2.5μM	Millipore (Billerica, MA, USA)
Forskolin	40μM	Sigma-Aldrich
Okadaic Acid	6nM	Sigma-Aldrich

2.5. Flow Cytometry

The cell lines used had been through a minimum of 5 passages prior to use; each passage entailed the cells being washed in PBS and replacing used medium with fresh following a 3-4 day growth period. Patient samples had been thawed and left to recover (**Section 2.4.2**). A minimum of 5 x 10^5 cells were used per flow cytometry tube.

2.5.1. Protein Staining and Flow Cytometry Analysis

Cells were washed in PBS, resuspended in 500µl of 2% paraformaldehyde (Van Waters and Rogers (VWR), Radnor, Pennsylvania, USA) and fixed for 10 minutes at 37°C. Then cells were centrifuged for 3 minutes at 500 x g and the supernatant discarded. The cells were then incubated on ice in 500µl of 90% methanol for 30 minutes to permeabilise the membranes. Cells were washed in a PBS buffer containing 0.5% bovine serum albumin (BSA), resuspended in 25µl of PBS/BSA buffer and incubated with the primary antibody (**Table 2.2**) at room temperature with rocking for 1 hour. Cells were washed in PBS/BSA buffer and resuspended in 50µl of the appropriate conjugated secondary antibody (**Table 2.2**) at a concentration of 20µg/ml. Finally, cells were incubated for 30 minutes at room temperature in the dark with rocking and washed in PBS/BSA buffer. Analysis used a FACSCalibur machine (BD Biosciences) with CellQuest Pro 3.3 software.

To analyse the protein level of a sample, events were gated on the live cell population, determined by forward and side scatter light properties. Antibody fluorescence was measured for cells falling within this gate. Protein level was defined as the geometric mean fluorescence intensity (MFI) of the protein, minus the control sample MFI.

Table 2.2.Antibody concentrations used in flow cytometry.

Primary Antibody	Final Concentration	Control Antibody	Secondary Antibody
CIP2A (Santa Cruz Biotechnology (SCBT), Dallas, TX, USA)	16µg/ml	Mouse IgG_1	Alexa Fluor 488 Mouse
PP2A (Millipore)	100µg/ml	Mouse IgG_1	Alexa Fluor 488 Mouse
pY307-PP2A (Abcam, Cambridge, Cambridgeshire, UK)	9µg/ml	Rabbit IgG	Alexa Fluor 488 Rabbit
SET (I2PP2A) (SCBT)	20µg/ml	Rabbit IgG	Alexa Fluor 488 Rabbit
SETBP1 (SCBT)	20µg/ml	Rabbit IgG	Alexa Fluor 488 Rabbit
JAK2 (SCBT)	20µg/ml	Rabbit IgG	Alexa Fluor 488 Rabbit
CrKL (SCBT)	10µg/ml	Rabbit IgG	Alexa Fluor 488 Rabbit
pY207-CrKL (Cell Signalling Technology (CST), Danvers, MA, USA)	10µg/ml	Rabbit IgG	Alexa Fluor 488 Rabbit
c-Myc (CST)	20µg/ml	Rabbit IgG	Alexa Fluor 488 Rabbit
c-Myc pS62 (Abcam)	10µg/ml	Rabbit IgG	Alexa Fluor 488 Rabbit

Mouse IgG_1 (BD Biosciences; #349040)

Rabbit IgG (Research & Development (R&D) Systems, Abingdon, Oxfordshire, UK; AB-105-C)

Alexa Fluor 488 Goat Anti-Mouse IgG (H+L) (Life Technologies, Paisley, Renfrewshire, UK; A-11001)

Alexa Fluor 488 Goat Anti-Rabbit IgG (H+L) (Life Technologies; A-11001)

2.5.2. CD34+ Staining of Patient Samples

For diagnostic patient samples, the protein expression of CD34+ expressing cells was also analysed. A CD34+ conjugated antibody (BD Biosciences) was used. Standard flow cytometry protocol was followed and the CD34+ antibody added to the cell suspension at the same point as the secondary antibodies previously described. The CD34+ antibody was added at a concentration of 0.1mg/ml.

To analyse the protein expression of the CD34+ expressing cells, a gating method was used. For example, the CD34+ cell population was gated. CIP2A expression of this gated cell population was analysed as previously described, therefore giving the CIP2A expression in CD34+ cells.

2.5.3. Cell Viability by Propidium Iodide Staining

Prior to beginning each flow cytometry experiment, 50µl (approximately 2 x 10^5 cells) were taken from each sample and placed in a flow cytometry tube. To these, 50µl of propidium iodide (PI) was added and tubes incubated on ice for 30 minutes.

During analysis, the percentage of PI positive cells was measured; PI positive cells were classified as dead cells and the PI negative as alive. Cell death was analysed using flow cytometry (FACSCalibur, BD Biosciences) and CellQuest Pro 3.3 software for data analysis.

2.6. Western Blotting

2.6.1. Lysate Preparation

A total of 1 x 10^7 cells were first washed in PBS, then resuspended in 100µl of Radioimmunoprecipitation assay (RIPA) buffer (25mM $NaPO_4$ (pH7.5), 25mM NaF, 25mM β-glycerol phosphate, 100mM NaCl, 5mM ethylene glycol tetraacetic acid (EGTA), 0.5% deoxycholate, 0.5% Igepal, 0.1% sodium dodecyl sulphate (SDS), 0.01% sodium azide) containing phosphatase and protease inhibitors (Roche, Basel, Switzerland). Cells were sonicated five times (30 seconds on/30 seconds off), spun for 5 minutes at 4°C at 500 x g and the supernatant collected for subsequent protein determination.

2.6.2. Protein Concentration Determination

Protein determination was performed according to manufacturer's recommendations (Bio-Rad, Hemel Hempstead, Hertfordshire, UK) and protein standards (**Table 2.3**) were made using a 10µg/ml BSA stock and RIPA buffer described in **Section 2.6.1**.

The Bio-Rad manufacturer's kit comprised several lettered reagents. A working reagent (A*) was prepared by adding 20µl of reagent S to each 1ml of reagent A. 25µl of A* was then added to each well of a 96 well flat-bottomed plate, followed by 5µl of standard or sample in the appropriate wells. 200µl of reagent B was then added, the plate incubated for 15 minutes and then read on

a spectrophotometer at 630nM. The protein concentration of each lysate was then determined from a standard curve.

Table 2.3. Concentration of Protein Standards

Final Concentration (µg/ml)	BSA Stock (10µg/ml)	RIPA Buffer
0	(1000µl ddH_2O)	
0.5	50µl	950µl
1	100µl	900µl
1.5	150µl	850µl
2	200µl	800µl
2.5	250µl	750µl
3	300µl	700µl

2.6.3. Gel Electrophoresis

Prior to loading, samples were diluted to 20µg/ml in double strength SDS buffer (DSSB) and heated at 95°C for 5 minutes. A 12% polyacrylamide gel (4ml resolving gel buffer, 8ml acrylamide, 4ml H_2O, 75µl of 10% ammonium persulphate (APS), 15µl tetramethylethylenediamine (TEMED; Sigma-Aldrich)) was assembled between two glass plates and left until polymerisation occurred (gel has set). A 5% polyacrylamide stacking gel was then assembled on top (1.5ml stacking buffer, 1ml acrylamide, 3.5ml H_2O, 50µl of 10% APS, 15µl TEMED), with a 10-well comb used to create sample wells. Protein samples were loaded alongside a pre-stained protein ladder (Bio-Rad), and then the samples were run at 35mA per gel for approximately 90 minutes.

2.6.4. PVDF Membrane Transfer

A polyvinylidene difluoride (PVDF) membrane (GE Healthcare, Little Chalfont, Buckinghamshire, UK) was first soaked in 100% methanol for 5 minutes. The polyacrylamide gel was carefully removed from between the glass plates and the stacking gel section cut away and discarded. A transfer cassette was assembled according to manufacturer guidelines (Bio-Rad) as shown in **Figure 2.1**. The cassette was placed in a transfer tank alongside an ice pack and submerged in transfer buffer (Tris 25mM, Glycine 0.2M (SCBT, USA). This transfer was performed at 400mA for 60 minutes. After the transfer was complete the protein ladder was marked on the membrane with a pencil.

Figure 2.1. Assembly of Western Blot Cassette.

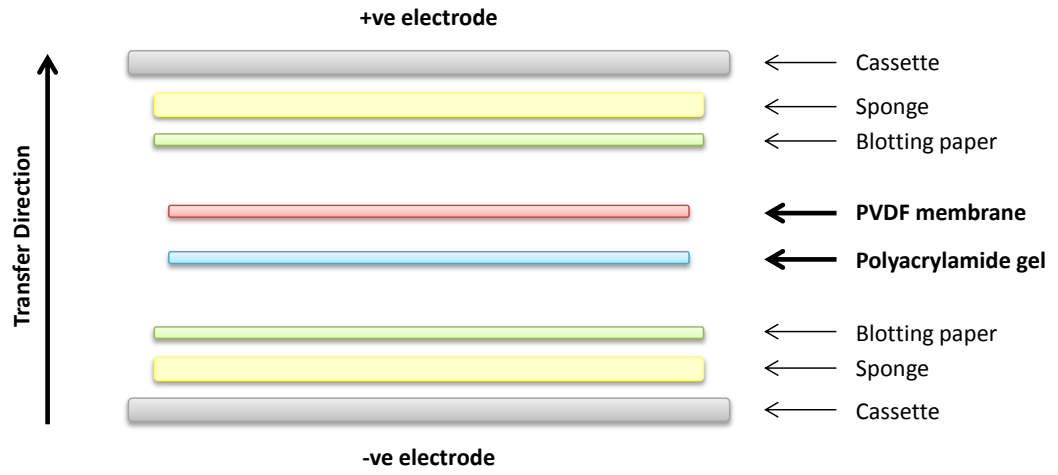

2.6.5. Membrane Blocking and Antibody Incubation

The membrane was blocked in 3% enhanced chemiluminescence (ECL) prime blocking milk (GE Healthcare) in Tris-buffered saline-Tween20 (TBS-T) (Tris 20mM, NaCl 150mM, Tween20 (0.1%), pH7.5) for 60 minutes at room temperature with rocking. The antibodies were added directly to the milk in the appropriate concentration and incubated at room temperature with rocking overnight. Following this, the membrane was then washed in TBS-T every 15 minutes for an hour, at room temperature with rocking. Appropriate secondary antibodies (0.4µg/ml in 3% ECL Prime blocking milk in TBS-T) were then added and left for 30-60 minutes. Another hour of washing with TBS-T followed, before the membrane was ready for analysis. Antibody concentrations are shown in **Table 2.4**.

ECL advance (GE Healthcare) was applied to the membrane for 1 minute, before membrane exposure and band visualisation using UNITEC Alliance 2.7 software.

2.6.6. Membrane Stripping and Re-probing

To strip the antibodies from the membrane, it was first washed in TBS-T every 15 minutes for an hour. The membrane was then incubated for 10 minutes in a 55°C water bath in a sealed film bag, with 10ml of stripping buffer (1M Tris, 2% SDS) containing 70µl β-mercaptoethanol. The membrane was then washed every 10 minutes in TBS-T for 30 minutes, ready to re-probe. To re-probe the

membrane, blocking and antibody incubation was as previously described, though primary antibody incubation need only be for 1-2 hours.

Table 2.4. Antibody Concentrations used in Western Blotting.

Primary Antibody	Final Concentration	Secondary Antibody
CIP2A (SCBT)	80ng/ml	Mouse IgG
PP2A (Millipore, USA)	0.3µg/ml	Mouse IgG
pY307-PP2A (Abcam)	40ng/ml	Rabbit IgG
SET (I2PP2A) (SCBT)	80ng/ml	Rabbit IgG
SETBP1 (SCBT)	80ng/ml	Rabbit IgG
JAK2 (SCBT)	80ng/ml	Rabbit IgG
pY207-CrKL (CST)	40ng/ml	Rabbit IgG
c-Myc (CST)	120ng/ml	Rabbit IgG
c-Myc pS62 (Abcam)	120ng/ml	Rabbit IgG

Anti-mouse IgG, HRP-linked Antibody (CST; #7076)

Anti-rabbit IgG, HRP-linked Antibody (CST; #7074)

2.7. ELISA

Patient samples were thawed as described (**Section 2.4.2**) and left to recover overnight. Lysates were prepared as described (**Section 2.6.1**), but lysed in PP2A Lysis Buffer 8 (50mM HEPES, 0.10.1mM EGTA, 0.1mM EDTA 120mM NaCl, 0.5% nonyl phenoxypolyethoxylethanol (NP-40), 25µg/ml leupeptin (Sigma-Aldrich), 25µg/ml pepstatin (Sigma-Aldrich), 2µg/ml aprotinin (Sigma-Aldrich) (1ul 44 per 100ul), 1mM PMSF) at 100µl buffer per 1 x 10^7 cells. Following protein determination (2.5.2), cell lysates were diluted; 20µg of protein in 100µl of carbonate-bicarbonate coating buffer (Sigma-Aldrich). 100µl of sample was added to a 96 well ELISA plate (Microplate Immulon 4HBX 96 well flat bottom polystyrene irradiated clear DIS-950-090L) and incubated at 4°C overnight with rocking. Each sample was performed in triplicate and a mean taken of the three results.

The plate was next washed four times with 200µl of TBS-T and then 200µl blocking buffer (5% BSA and 1% rabbit serum (Sigma-Aldrich) in TBS-T) added and incubated for 2 hours at room temperature, with rocking. Following a further four washes in 200µl of TBS-T, 100µl of either c-Myc or c-Myc pS62 antibodies (40ng/ml, 100ng/ml respectively) in 5% BSA and 1% rabbit serum in TBS-T was added. In addition, control wells contained 100µl (1:500) rabbit anti–glyceraldehyde 3-phosphate dehydrogenase (GAPDH) in 5% BSA in TBS-T. The plate was then incubated for 3 hours at room temperature with rocking.

A further four washes in 200µl TBS-T followed and the plate was then incubated at room temperature for one hour (with rocking) with 100µl (1:1000) anti-rabbit IgG–horseradish in 5% BSA in TBS-T. The plate was again washed and 100µl of tetramethylbenzidine added for a 20 minute incubation at room temperature with rocking, in the dark. Finally, 50µl of 2M HCl was added to stop the reaction and the absorbance read at 450nm immediately.

2.8. Confocal Microscopy

Samples for confocal microscopy analysis were first prepared as discussed in **Section 2.4**. Approximately 2 x 10^6 cells per ml were used per sample slide.

Slide preparation: Slides were submerged in 10% Poly-L Lysine (Sigma-Aldrich) for 5-10 minutes, then allowed to dry at 37°C for 60 minutes. An area of approximately 3cm^2 was marked on the slide using a hydrophobic liquid blocker pen and allowed to dry for 30 minutes at 37°C. The slides were then ready for cells to be added.

Cell preparation: Cells were spun at 500 x g for 3 minutes, washed in PBS and resuspended in 4% paraformaldehyde for 15 minutes at room temperature. Following another wash in PBS, cells were permeabilised with 0.2% Triton-X-100 (Sigma-Aldrich) for 5 minutes at room temperature and washed in PBS. Cells were then blocked for 30 minutes at room temperature in 150µl of PBS with 10% BSA and 0.1% sodium azide. Next, the cells were stained with primary antibodies (**Table 2.5**) in blocking buffer for 60 minutes at room temperature, washed in PBS and stained with secondary antibodies (20µg/ml in PBS) for 30 minutes at room temperature. Again, cells were washed in PBS then incubated for 15 minutes at room temperature with the nuclear stain TO-PRO-3 (Life Technologies) at a concentration of 3.3µg/ml. After a final wash in PBS, cells were resuspended in 100µl of PBS and mounted on the appropriate slide.

Slides were left at 4°C in the dark overnight to allow cells to adhere to the slide surface. 10µl of CyGel (BioStatus Limited, Shepshed, Leicestershire, UK) was pipetted onto a cover slip, which was pressed firmly onto the cell slide ready to be analysed.

Table 2.5. Antibody Concentrations used in Confocal Microscopy.

Primary Antibody	Final Concentration	Secondary Antibody
CIP2A (SCBT)	1µg/ml	Alexa Fluor 488 Mouse
PP2A (Millipore)	100µg/ml	Alexa Fluor 488 Mouse
pY307-PP2A (Abcam)	11.2µg/ml	Alexa Fluor 488 Rabbit
c-Myc (CST)	2µg/ml	Alexa Fluor 488 Rabbit
c-Myc pS62 (Abcam)	100µg/ml	Alexa Fluor 488 Rabbit

Alexa Fluor 488 Goat Anti-Mouse IgG (H+L) (Life Technologies; A-11001)

Alexa Fluor 488 Goat Anti-Rabbit IgG (H+L) (Life Technologies; A-11001)

2.9. Polymerase Chain Reaction (PCR)

In this thesis, 3 PCR methods were used; quantitative real-time PCR (qRT-PCR), standard manual PCR and Pre-pyrosequencing manual PCR.

Sample preparation for qRT-PCR and standard manual PCR was the same: total leukocytes previously separated (**Section 2.3.1**) were used for RNA extraction and cDNA synthesis. In **Chapter 4**, patient mRNA samples were analysed by qRT-PCR, using pre-designed TaqMan real time PCR assays.

Table 2.6. Pre-Designed Taqman Real-Time Assay Primers used for PCR

Assay Primers	Product Code	Company
CIP2A	Hs00405413_m1	Life Technologies
PP2A (catalytic subunit)	Hs00427259_m1	Life Technologies
c-Myc	Hs00153408_m1	Life Technologies
SET	Hs00853870_g1	Life Technologies
JAK2	Hs01078136_m1	Life Technologies
GAPDH	Hs99999905_m1	Life Technologies

Chapter 6 also uses qRT-PCR to analyse patient samples, though assays used were purposefully designed to identify two different *CIP2A* variants. Additionally, **Chapter 6** uses standard manual PCR to detect the presence/absence of these *CIP2A* variants in CML cell lines.

Sample preparation for pre-pyrosequencing manual PCR differed from other PCR methods: genomic DNA was used following a bisulphite conversion. This PCR method was used to indicate the suitable amplification of the product to be analysed by pyrosequencing, for potential methylation (**Chapter 7).**

CIP2A primers were designed using PyroMark Assay Design 2.0 for the detection of a long (*CIP2A-1a*) and short (*CIP2A-1b*) transcript; **Chapter 6** discusses the design and results of these primers. *CIP2A* methylation primers were also designed; **Chapter 7** discusses the design and results of these.

Table 2.7. Primer Sequences for *CIP2A* transcript variants and *CIP2A* Methylation

Target	Assay Primer	Primer Sequence
CIP2A-1a	*CIP2A-1a* Forward primer	ACTCCACTGCCTGCTTGA
	CIP2A-1a Reverse primer	TGTCCAGAAATTACCTCCAAGT
	CIP2A-1b probe	CGCAAAAGCTGAGTGGCGTTC
CIP2A-1b	*CIP2A-1b* Forward primer	TCCTCCCTCAAAGTAATTTCTG
	CIP2A-1b Reverse primer	TGGGGTCTTCAAGTAGCTCTA
	CIP2A-1b probe	CAAGGCAACTCAAGCATTCACT TGTTA
***CIP2A* methylation**	*CIP2A* meth-Forward (biotinylated)	TTTAGGGTGTTTAGGGATT
	CIP2A meth-Reverse	CACAATAAAATCCATTACACC
	CIP2A meth-Sequence	CACAATAAAATCCATTA

2.9.1. RNA Extraction

RNA extraction was performed according to the RNeasy mini kit (Qiagen) and RNase-Free DNase Set. Prepared samples (**Section 2.3.1**) were transferred to a QIA shredder column within a 2ml collection tube, centrifuged at 14000 x g for 2 minutes and 600µl of ethanol (70%) added to the flow through. The sample was mixed well and spun in a mini spin column within a 2ml collection tube at 14000 x g, for 5 minutes. The flow through was discarded, 700µl of RNeasy Wash buffer (RW1) added and incubated for 5 minutes at room temperature, centrifuged at 14000 x g for 5 minutes and the flow through again discarded. The spin column (within a new 2ml collection tube) was twice washed with 500µl RNeasy Wash buffer 2 (RPE), spun for 15 seconds at 14000 x g and 40µl of RNA/DNA free water added to the spin tube membrane. This was incubated for 5 minutes at room temperature, centrifuged for 2 minutes at 14000 x g and the eluted RNA was either immediately converted to cDNA or gDNA, or stored long term at -70°C.

2.9.2. cDNA synthesis

RNA (28µL) was aliquoted into DNase/RNase free tubes and incubated at 70°C for 10 minutes with 2µl (500ng/µl) of random hexamers (Promega, Southampton, Hampshire, UK). Tubes were immediately cooled on ice for 3 minutes. A reaction mix containing 16µl of 5 x reaction buffer (RT buffer), 8µl of 0.1M DL-dithiothreitol (DTT), and 4µl of 10mM deoxyribonucleotide triphosphate (dNTP) was added to the samples and tubes were incubated at

25°C for 5 minutes. Superscript II reverse transcriptase kit (200µg/µl) (Invitrogen) was added and tubes incubated sequentially, at 25°C for 10 minutes, 42°C for 60 minutes then finally 70°C for 15 minutes to stop the reaction. The acquired cDNA could be used immediately, or stored long-term at -20°C.

2.9.3. Quantitative Real-Time PCR

Pre-designed TaqMan real time PCR assays were used in a 96 well assay plate. Each assay consisted of a forward and reverse primer at a final concentration of 900nM and a 6-FAM dye-labelled TaqMan MGB probe at a final concentration of 250nM.

The amount of cDNA was determined using the Nanodrop2000; 100ng of cDNA was used per 20ul reaction consisting of 20x TaqMan gene expression assay and 2x TaqMan gene expression master mix (pre-made, Life Technologies). Each sample was run in triplicate. After loading the reaction mixture, the plate was sealed with appropriate cover and spun briefly to ensure all of the samples were at the bottom of their well. The real time PCR amplifications were undertaken using an ABI Prism 7900HT system (ThermoFisher Scientific, Altrincham, Cheshire, UK) with the following conditions as specified by the manufacturer: 50°C for 2min, 10min at 95°C followed by 40 cycles of denaturation at 95°C for 15secs and annealing/extension at 60°C for 1min.

The relative expression level of a particular gene of a given sample was calculated by the comparative Ct method(Livak & Schmittgen, 2001). The comparative Ct method uses the $2^{-\Delta\Delta Ct}$ formula to achieve results for relative quantification, where ΔΔCt is the normalised signal level in a sample relative to the normalised signal level in the calibrator sample. In this study a pool of cDNA from 7 normal individuals was used as calibrator and all the samples were normalised to *GAPDH* endogenous control.

2.9.4. Manual PCR

Forward and reverse primers (**Table 2.7**) were diluted in ddH_2O to give a primer mix containing 4µM concentration of each. Into each necessary well of a 96 well PCR plate was added: 10µl expression mix (Life technologies), 1µl primer mix and 4µl ddH_2O. cDNA from samples and controls (5µl) was added in triplicate, the plate sealed tightly with a film cover and placed in the PCR block.

After optimisation of a range of temperatures, PCR conditions were set as:

- 95°C – 5 min
- 40 cycles;
    - 95°C – 15 sec (denaturation of double stranded DNA)
    - 56°C – 20 sec (annealing of primers)
    - 60°C – 45 sec (extension by DNA polymerase)
- 72°C – 10 min

The plate was then left at 4-8°C until the samples were run on a 2% agarose gel (agarose and Safeview Nucleic Acid Stain (Novel Biological Solutions (NBS), Huntingdon, Cambridgeshire, UK) in 135ml TBE (0.1M Tris/0.1M Borate/2mM EDTA)). Agarose and TBE were heated in a microwave and mixed until the agarose was completely dissolved, then the nucleic stain added. The gel was poured into a mould with a comb and left to set for 30-60 minutes at room temperature. The gel was placed in a running tank, submerged in TBE and the amplified samples (diluted 1:1 in running buffer (Life Technologies)) loaded alongside a 50bp ladder. Finally the gel was run for approximately 30 minutes at 100V and photographed.

2.10. PCR Pyrosequencing (Methylation Analysis)

For this method, genomic DNA was used. This was available within the lab and had been previously extracted according to the Qiagen DNA extraction kit protocol.

2.10.1. Bisulphite Conversion

Only samples with the optimum DNA concentration of 200-500ng/µl were used for the methylation analysis. For the bisulphite conversion the EZ DNA Methylation-Gold Kit (Zymo Research, Irvine, California, USA) was used. The method described is for the conversion of 10 samples. N.B. Solutions described in this method are not detailed within the manufacturer's protocol and are therefore merely named as the company states in their protocol.

First, the CT Conversion Reagent was prepared by adding 900µl ddH_2O, 300µl M-Dilution Buffer and 50µl M-Dissolving Buffer. Then the M-Wash Buffer was prepared by adding 24ml of 100% ethanol per 6ml of M-Wash Buffer concentrate. The CT Conversion Reagent (130µl) was added to 20µl of DNA sample in a PCR tube, the tubes sealed, spun briefly and then placed into a thermal cycler. The following steps were then performed:

- 98°C – 10 min
- 64°C – 150 min

The samples could then be stored overnight if necessary at 4-8°C.

The samples were then transferred to a Zymo-Spin IC Column inside a Collection Tube, along with 600µl of M-Binding Buffer and centrifuged at 10000 x g for 30 seconds and the flow-through discarded. Samples were then washed with 100µl M-Wash Buffer and the flow-through again discarded. 200µl of M-Desulphonation Buffer was added to each column and incubated at room temperature for 15-20 minutes before being spun and the flow-through discarded. Next, the samples were washed twice with M-Wash Buffer and then Zymo-Spin IC Columns transferred into 1.5ml microcentrifuge tubes. Pre-warmed M-Elution buffer (30µl) was added directly to the column membrane and centrifuged to elute the newly bisulphite converted DNA.

Samples could be immediately analysed (via pre-pyrosequencing manual PCR (**Section 2.10.2**), and then run through the pyrosequencer for methylation analysis (**Section 1.10.3**)) or stored long term at -20°C.

2.10.2. Pre-Pyrosequencing PCR

Forward and reverse primers (**Table 2.7**) were diluted in ddH_2O and mixed to give a 150nM forward primer (5'-Biotinylated) and 300nM reverse primer concentration. Into each necessary well of a 96 well PCR plate was added: 19.5µl ddH_2O, 3µl buffer, 1.25µl dNTPs, 1.25µl primer mix, 1.2µl $MgCl_2$ and 0.15µl Hot-Start Taq DNA polymerase (New England Biolabs (NEB), Hitchin, Hertfordshire, UK). cDNA (4µl) from each sample and control was then added in triplicate, the plate sealed and placed in the PCR block.

After optimisation with a range of temperatures, PCR conditions were set as:

- 95°C – 5 min
- 20 cycles
    - 94°C – 20 sec (denaturation of DNA)
    - 54°C – 40 sec (annealing of primers)
    - 72°C – 30 sec (extension by DNA polymerase)
- 20 cycles
    - 94°C – 30 sec (denaturation of DNA)
    - 54°C – 30 sec (annealing of primers)
    - 72°C – 35 sec (extension by DNA polymerase)
- 72°C – 15 min

Again, the plate could be left at 4-8°C overnight if necessary, before the samples were run on a 2% agarose gel (**Section 2.9.4**) and analysed to ensure the product was suitably amplified prior to methylation analysis on the pyrosequencer.

2.10.3. Methylation Analysis

Following manual PCR analysis to check adequate DNA amplification, approximately 25µl of sample was loaded into a round-bottomed 96 well plate and mixed with 75µl of binding premix (50µl binding buffer, 2µl streptavidin sepharose beads, 25µl ddH_2O per sample). The plate was then sealed and mixed with constant agitation for a minimum of 10 minutes to allow the amplified DNA sequence to bind to the beads. Annealing mix was then prepared, consisting of 43.5µl annealing buffer and 1.5µl of sequence primer (10µM) per sample and transferred to a soft, flat-bottomed 96 well plate.

The bench-top pyrosequencer unit was washed in ddH_2O and placed in the 96 well plate containing the samples. It was then used to agitate the solution within each well to ensure the beads were suspended, before the unit was switched on and the solution 'sucked up', leaving the beads stuck to the prongs. This was repeated first in 70% ethanol to wash, then in 0.2M NaOH to ensure the sequences were single stranded and finally, sodium acetate to neutralise. Lastly the samples were transferred to the 96 well plate containing the prepared annealing mix and incubated at 80°C for 2 minutes.

The samples were then ready to be placed in the PSQ 96MA Qiagen pyrosequencer machine. The assay sequence was entered into the software, the reagent cartridge filled with appropriate amounts of substrate, enzyme and nucleotides (A/C/T/G) according to machine guidelines, and the sequence analysed for methylation sites within the sequence.

2.11. Gene Silencing (siRNA)

siRNA was performed using Cell Line Nucleofector(TM) Kit V (Lonza/Amaxa Biosystems, Basel, Switzerland). For each reaction, 1 x 10^6 cells were used. Firstly, the kit reagents were prepared; *CIP2A* siRNA (SCBT) and scrambled control siRNA (SCBT) were diluted in RNase-free water to 10µM.

Cells were washed 3 times in PBS and resuspended in 100µl of nucleofector solution in a 1.5ml Eppendorf. The siRNAs were added to their appropriate Eppendorf containing cells at a concentration of 100nM and the cells transferred to an Amaxa cuvette. Electroporesis was used and finally the cells were immediately transferred to 500µl of pre-warmed supplemented RPMI-1640 medium (1% L-glutamine, 1% penicillin/streptomycin, 10% foetal calf serum). Cells were then incubated for 72 hours at 37°C before analysis.

Table 2.8. siRNA used

siRNA	Catalogue Number	Company
CIP2A	sc-77964	SCBT
Scrambled Control	sc-37007	SCBT

2.12. Gene Transfection

2.12.1. Bacterial Transformation

One 50µl vial of One Shot cells (Life Technologies) were thawed on ice and 1µl of plasmid added directly to the vial. These were mixed by gently tapping the vial before 30 minutes incubation on ice. Next, the competent cells were incubated for exactly 30 seconds in a 42°C water bath and immediately placed on ice. Pre-warmed super optimal broth with catabolite repression (SOC) medium (250µl) (Sigma-Aldrich) was added using sterile technique and the vial secured with tape in a microcentrifuge (the vial was well aerated and placed at an angle). Shaking was applied for 1 hour at 37°C, before 50µl of cells were spread on a pre-warmed lysogeny broth (LB) agar plate (Sigma-Aldrich) containing 100µg/ml ampicillin and incubated overnight at 37°C.

2.12.2. Maxiprep

For this, an EndoFree Plasmid Maxi Kit (Qiagen) was used. N.B. Details of buffers used in this protocol are not given by the manufacturer and thus are merely named as the company does within its guidelines.

A single colony was picked and incubated at 37°C with shaking at for 8 hours in 5ml of LB medium (100µg/ml ampicillin). This culture was then diluted 1/500 with fresh LB medium and incubated in the same conditions for a further 12-16 hours. Bacterial cells were isolated via a centrifugation at 6000 x g for 15

minutes at 4°C and the pellet resuspended in 10ml of buffer P1 and 10ml P2 in a sealed tube. The bacteria were vigorously mixed and incubated for 5 minutes at room temperature. Next, 10ml of chilled Buffer P3 was added, vigorously mixed and then the mixture transferred to a QIA filter Cartridge and incubated at room temperature for 10 minutes before filtering the lysate into a fresh 50ml tube. Buffer ER (2.5ml) was added to the filtered substrate and mixed by inversion and incubated for 30 minutes on ice.

A Qiagen-tip 500 was equilibrated using 10ml of Buffer QBT and the lysate added. Finally, the tip was washed twice with 30ml of Buffer QC and the DNA eluted with 15ml of Buffer QN. To precipitate the DNA, 10.5ml of room temperature isopropanol was added to the eluted DNA, mixed and centrifuged at 15000 x g for 30 minutes at 4°C. The DNA pellet was washed with endotoxin free 70% ethanol at room temperature and centrifuged at 15000 x g for 10 minutes. Finally, the DNA pellet was allowed to air-dry and then dissolved in endotoxin-free Buffer TE. The concentration of the plasmid was determined using a NanoDrop system before use.

2.12.3. Cell Transfection

Transfection was performed using the Cell Line Nucleofector(TM) Kit V (Lonza/Amaxa Biosystems, Switzerland). For each reaction 2 x 10^6 cells were used. Kit reagents were prepared before use. The plasmids used were purchased ready-made from Origene (Rockville, MD, USA) and are discussed more thoroughly in **Chapter 5**. Cells were washed 3 times in PBS and resuspended in 100µl room-temp nucleofector solution. *CIP2A-GFP* tagged and *GFP* plasmids (5µg/ml) were added to the appropriate Eppendorf. Cells were transferred to an Amaxa cuvette and electroporation used. Cells were then immediately transferred to 500µl of pre-warmed supplemented RPMI-1640 culture medium. Cells were incubated for 48 hours at 37°C before analysis.

Figure 2.2. Design of the *CIP2A-GFP* tagged Transfection Plasmid; A Schematic of the Cloning Sites.

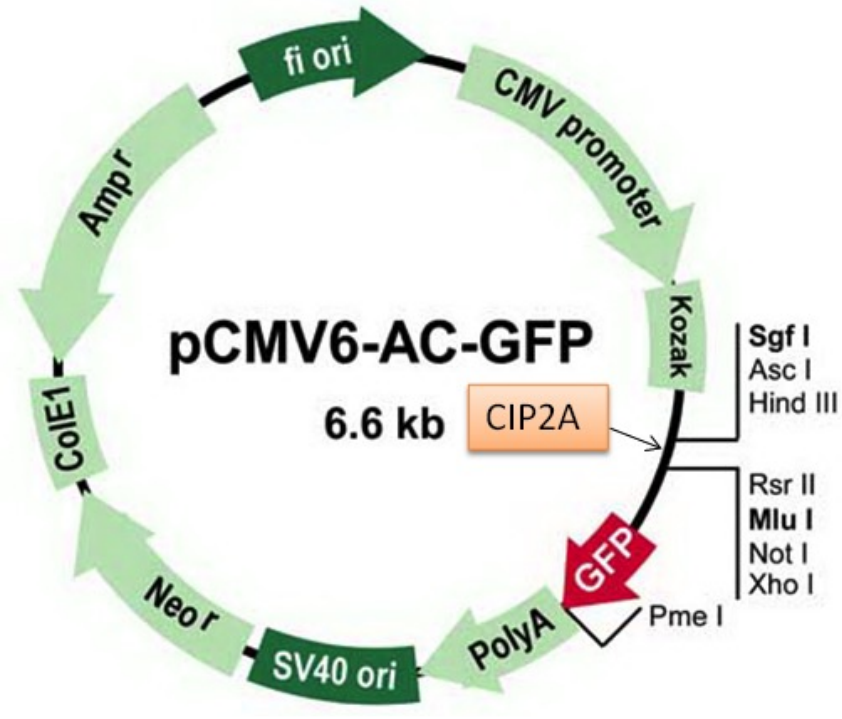

Chapter 3: CIP2A as a CML Biomarker

3.1. Introduction

The dawn of the imatinib era revolutionised CML treatment and improved clinical outcome dramatically, though resistance to this drug is still a major concern in almost 50% of patients(C. M. Lucas et al., 2011). Second (dasatinib and nilotinib) and third (ponatinib) generation TKIs have been developed in an effort to provide alternative treatment options for patients resistant or intolerant to imatinib. The ability to recognise at diagnosis which patients will fail to achieve and maintain a response on imatinib, yet fare better on the newer, more potent TKIs would be of immense value to CML treatment.

CIP2A has recently emerged as a biomarker for poor prognosis in many cancers(Bockelman, Lassus, et al., 2011; Dong et al., 2011; He et al., 2012; P. Huang et al., 2012; Khanna et al., 2009; Ren et al., 2011; Teng et al., 2012; Vaarala et al., 2010; Xue et al., 2012; Yu et al., 2013); in CML, high CIP2A protein levels predict blast crisis in imatinib treated patients(C. M. Lucas et al., 2011). However, its prognostic role in CML treated with second and third generation TKIs is entirely unknown. With the increasing use of these newer TKIs clinically, there is a need for information on their effects on the molecular mechanisms of CML.

3.2. Aims

This thesis focuses on the component parts of the CIP2A/PP2A pathway. Here I begin by investigating the role of CIP2A as a CML biomarker in patients treated with 2G TKIs. This chapter examines the correlation between CIP2A protein expression and clinical outcome of CML treated with a 2G TKI compared to imatinib.

3.3. Methods

In this chapter 69 treatment-naive CP-CML patient PBMC samples were analysed using flow cytometry (**Section 2.5**). Clinical characteristics of patients within this cohort are shown in the **Appendix**. Two statistical analysis methods were used within this chapter: receiver operating characteristics (ROC) to distinguish between high and low CIP2A cohorts (**Section 3.4.1**) and Mann-Whitney tests to perform comparative analysis between patient cohorts (**Section 3.4.3**).

3.4. Results

3.4.1. Determining High/Low CIP2A Protein Levels

This work was inspired by data published previously in our lab by Lucas *et al*(C. M. Lucas et al., 2011) . The identification of CIP2A protein as a potential biomarker for blast crisis in imatinib treated CML was of scientific value that has since been supported by many publications in various other malignancies. Lucas' data identified a clear difference in CIP2A protein level at diagnosis between those CML patients destined to progress to blast crisis and those who were not. This was the first identification of CIP2A as an early indicator of blast crisis in CML and is shown in **Figure 3.1** (**Figure 3B** in (C. M. Lucas et al., 2011)).

Throughout this work patients are stratified according to diagnostic CIP2A protein level; high or low, as measured by flow cytometry (mean fluorescence intensity (MFI)) and described in **Section 2.5**. The range was 0-52, the median was 2.85and the mean was 6.5. From the original publication it is clear no overlap occurs between diagnostic cohorts of interest; a cut-off of MFI = 6-8 could be used to separate these. Using receiver operating characteristics (ROC) curve analysis(Hajian-Tilaki, 2013) for the prediction of BC based on basal CIP2A protein, a cut-off value of 7.3 was determined; high (MFI>7.3) or low (MFI<7.3).

Figure 3.1. Determining High/Low CIP2A Protein by flow cytometry. Data taken from Lucas *et al(C. M. Lucas et al., 2011)*. The previous publication measured the CIP2A protein level of 36 patients, using flow cytometry; all samples shown were treatment-naïve CP-CML of known clinical outcome. Patients were stratified according to future clinical outcome; CCR, no CCR and subsequent BC at any time. These were the standard clinical outcomes used at the time of publication; CCR and BC were as described in **Section 1.7.1** and **1.5**, respectively. The 'no CCR' response was defined as patients who had achieved CHR but not CCR by 12 months, but had not progressed.

The red line indicates MFI = 7.3, the chosen boundary for determining high/low CIP2A protein in diagnostic CML patient samples, as described in the text. The mean CIP2A protein level of 10 normal healthy volunteers is shown; 0.4 (range, 0.17-0.63).

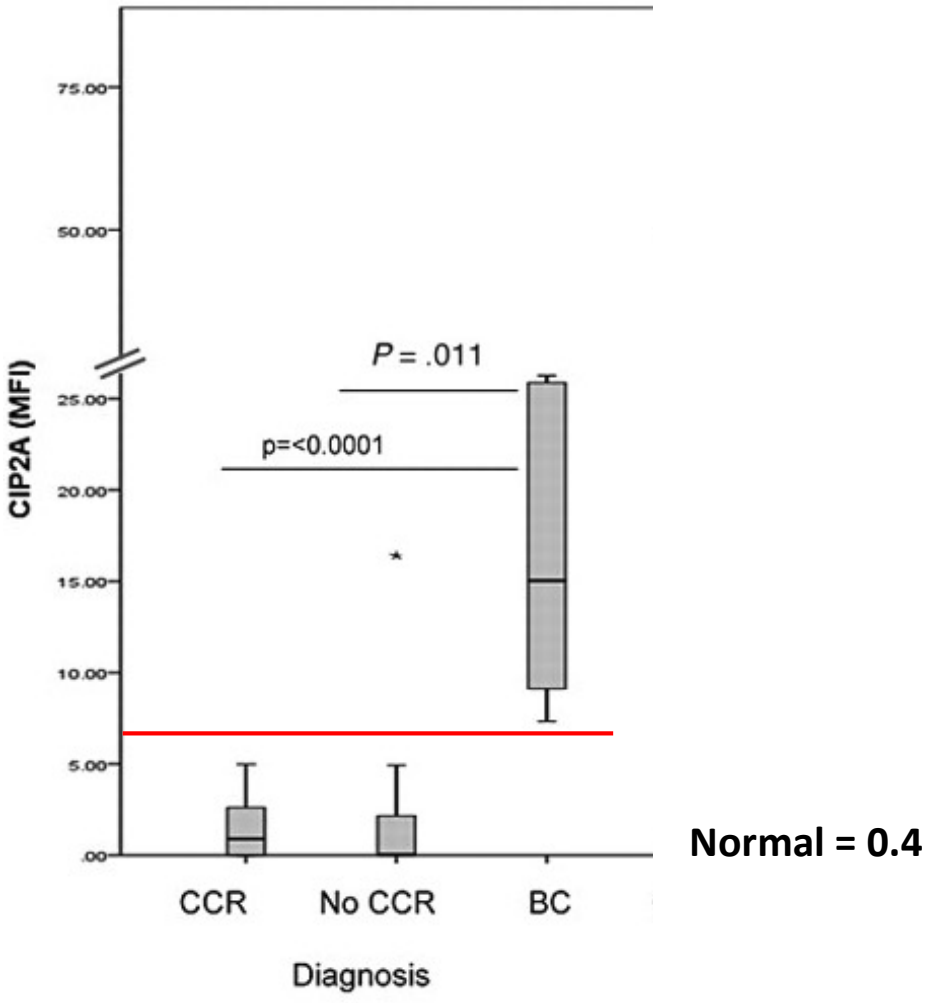

3.4.2. Measuring CIP2A Protein Levels

The flow cytometry method was previously optimised within our lab to measure CIP2A in both patient samples and cell lines; methods used in this thesis were as described by Lucas *et al*(C. M. Lucas et al., 2011)in previous publications. The ability to use flow cytometry even on samples with minimal amounts of cells means it is an extremely advantageous technique for this work.

The initial step was to measure the levels of diagnostic CIP2A protein in CML patients of known clinical outcome. Patients were then split into the two cohorts (high/low CIP2A level) for comparative analysis.

Figure 3.2 shows representative flow cytometry plots for a high and low CIP2A patient. The top dot plots for each sample show the cell clouds; live (right) clouds are gated as shown. The CIP2A and IgG control antibodies used fluoresce on the FL3 wavelength, thus the gated cells were then analysed to identify the level of CIP2A (or control) present in each sample. The CIP2A value for each sample was then calculated manually (CIP2A (geometric mean) MFI minus control sample (geometric mean) MFI).

Figure 3.2. Representative Flow Cytometry Plots of CML Patients. A. Representative low CIP2A patient; UPN 001. B. Representative high CIP2A patient; UPN 031. Plots (i) and (ii) show cell clouds; live cells are gated. Plot (iii) represents the level of CIP2A present in the sample cells. Plot (iv) is a statistical table analysing the data from (iii); the geometric mean CIP2A level is used for sample analysis.

A. Low CIP2A patient example

(i) (ii)

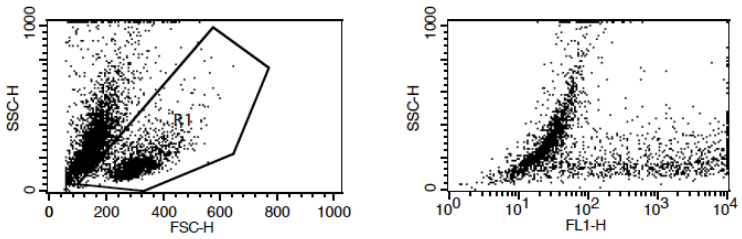

(iii)

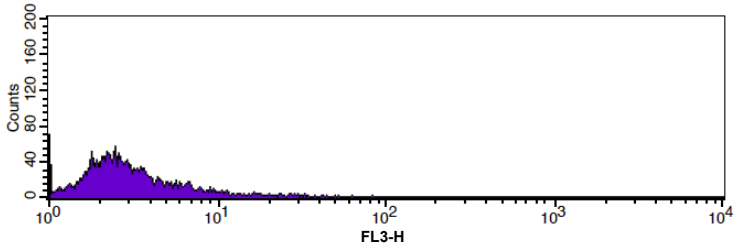

(iv)

Marker	Left, Right	Events	% Gated	% Total	Mean	Geo Mean	CV	Median	Peak Ch
All	1, 9910	3170	100.00	31.70	2772.75	553.44	128.71	873.79	9910

B. High CIP2A patient example

(i) (ii)

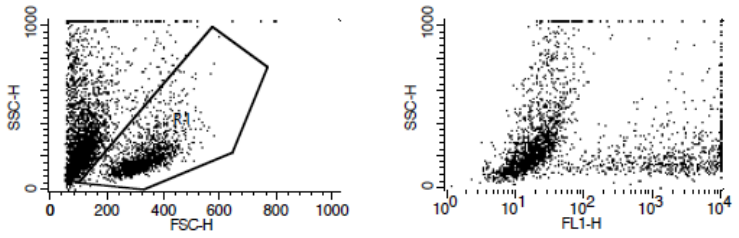

(iii)

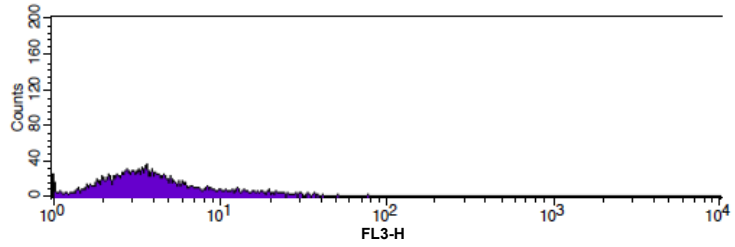

(iv)

Marker	Left, Right	Events	% Gated	% Total	Mean	Geo Mean	CV	Median	Peak Ch
All	1, 9910	2841	100.00	28.41	3854.28	1254.00	98.62	2226.67	9910

3.4.3. Clinical Relevance of CIP2A in CML Patients

The CIP2A protein levels of 28 CP-CML patients treated with either dasatinib or nilotinib as a first line therapy were analysed by flow cytometry and compared to 41 CP-CML patients treated with imatinib as a first line therapy. Thirty one of these 41 imatinib recipients were originally reported by Lucas *et al*; I have added a further 10 and updated the follow-up on all 41. The 28 recipients of 2G TKIs have not been previously reported. Patients used were UPN001-069 as detailed in the **Appendix**, which also gives the CIP2A level (high/low) for each patient, calculated as shown previously. Clinical characteristics for all 69 patients are summarised below in **Table 3.1**.

Table 3.1. Summary of clinical characteristics.

	Total	Imatinib treated	2G TKI treated
No. of patients	69	41	28
Average age (range)	50 (19-75)	48 (19-74)	54 (24-75)
Sex M/F	34/35	23/18	11/17
HIGH CIP2A	22	12	10
LOW CIP2A	47	29	18

It should be noted that the high rate of blast crisis patients within my samples is due to deliberate selection. It is therefore not possible from these data to comment on the incidence of high CIP2A in a general CML population.

Figure 3.3 shows the overall survival (OS), progression free survival (PFS) and event free survival (EFS), stratified according to diagnostic CIP2A level.

Imatinib recipients with low CIP2A level and 2G TKI recipients irrespective of CIP2A level had excellent OS (**Figure 3.3 A**) and PFS (**Figure 3.3 B**); 100% and 96% (27/28) of patients (respectively) were alive and progression free with a maximum follow-up of 36 months. In sharp contrast, imatinib recipients with high diagnostic CIP2A had poor OS, because of progression to blast crisis; in fact, only 2 such patients have not progressed, and these were switched to a 2G TKI at approximately 18 and 23 months respectively, because of poor molecular response on imatinib.

EFS (**Figure 3.3 C**), which includes switching TKI for whatever reason as an event, even if still in CP, also shows a similar significantly inferior outcome for imatinib recipients with high diagnostic CIP2A level.

Figure 3.3 Overall survival, progression free survival and event free survival of chronic phase CML patients; stratified according to diagnostic CIP2A protein level.

All patients are either imatinib treated or 2G TKI (dasatinib or nilotinib) treated.

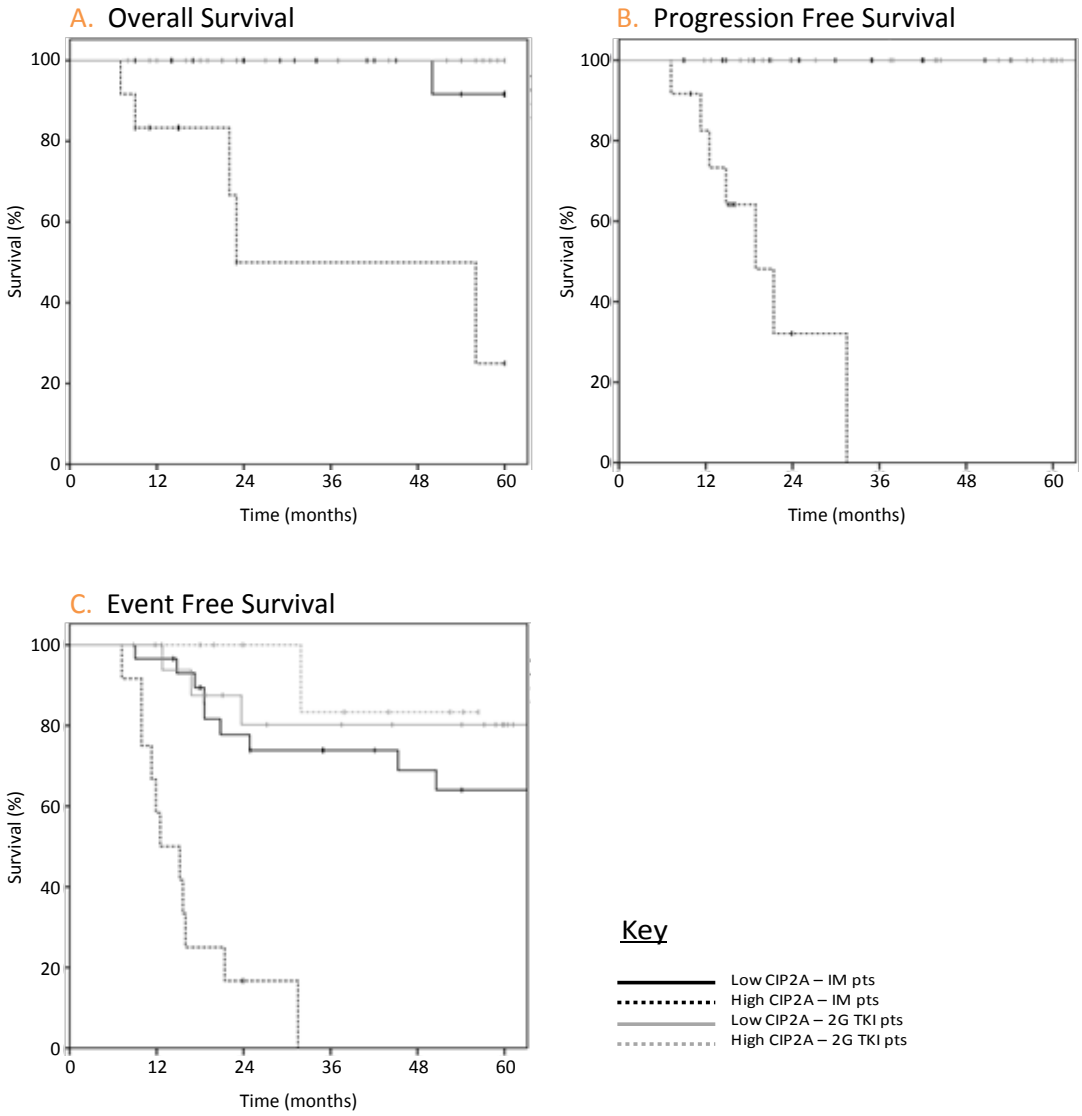

The rates of cytogenetic and molecular response were then investigated to determine if CIP2A played a role in determining the depth of patient response to treatment and the time taken to achieve it. The time taken to achieve three clinical milestones was assessed; complete cytogenetic response (CCR), major molecular response (MMR) and molecular response at the 4-log level (MR4) as defined in **Section 1.7.1** and illustrated in **Figure 1.4**.

Imatinib recipients with a low CIP2A level and 2G TKI recipients irrespective of CIP2A level had excellent rates of CCR and MMR; approximately 80% of all three of these cohorts had achieved CCR (**Figure 3.4 A**) and MMR (**Figure 3.4 B**) by 24 months. Imatinib recipients with a high CIP2A level showed a striking dissimilarity to these results; no patient in this cohort had achieved a CCR or MMR, with a maximum follow-up of 57 months.

The deeper response of MR4 was also examined (**Figure 3.4 C**). MR4 was not achieved by any imatinib recipients with high CIP2A level. The time taken to achieve MR4 was more rapid in 2G TKI recipients irrespective of CIP2A level, compared to imatinib recipients with low CIP2A. 2G TKI recipients irrespective of CIP2A level had a good rate of MR4; approximately 50% had achieved MR4 by 24 months and this had risen to 80% by 30 months. Imatinib recipients with low CIP2A level had a lesser proportion of patients achieving MR4 and a slower rate of response; only by 40 months had 50% of patients achieved MR4 and by 24 months only 20% had achieved this response.

Figure 3.4 Time to achieve CCR, MMR and MMR4 of chronic phase CML patients; stratified according to diagnostic CIP2A protein level.

All patients are either imatinib treated or 2G TKI (dasatinib and nilotinib) treated.

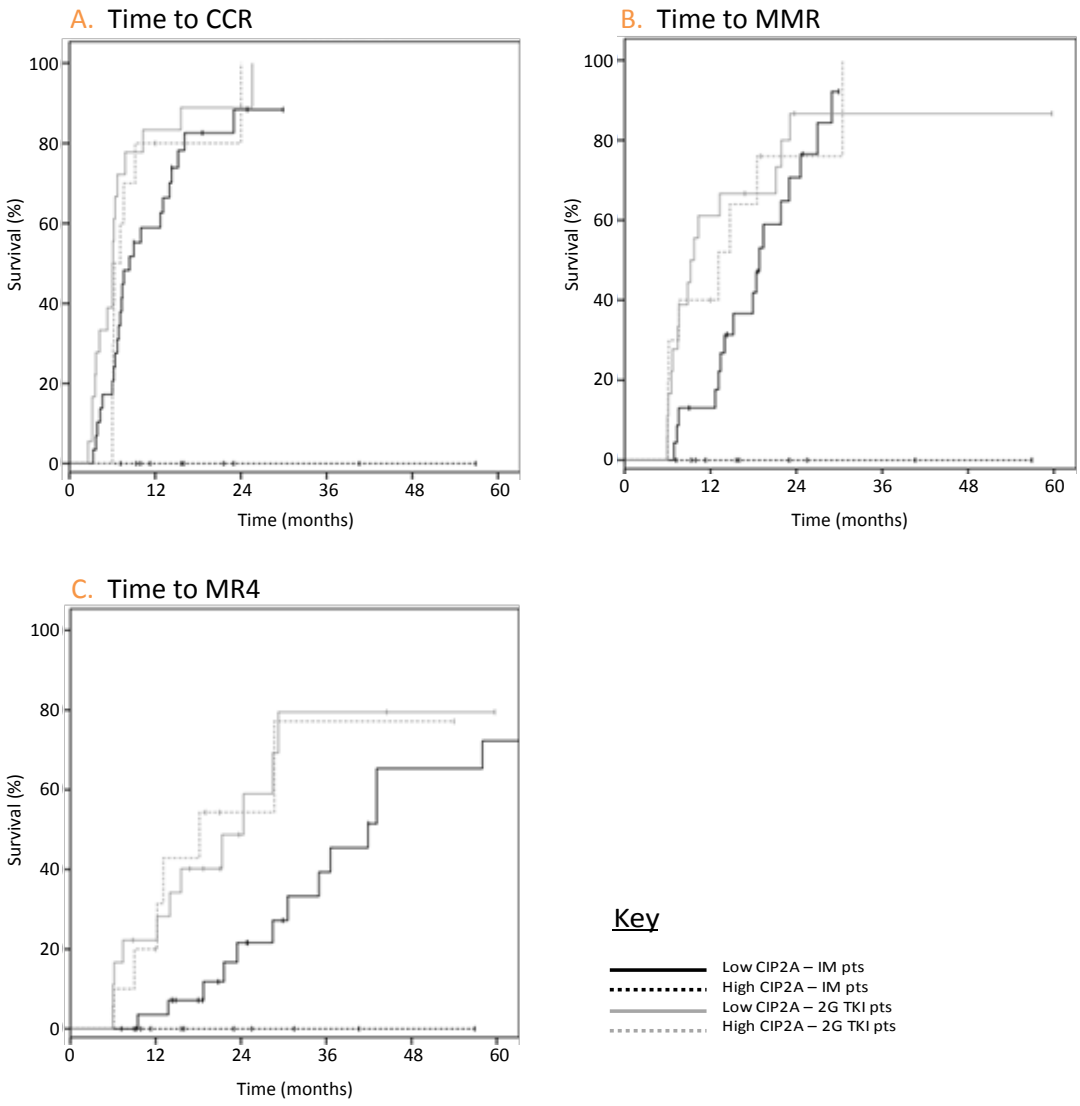

3.5 Discussion

With modern medicine rapidly becoming more personalised in terms of patient treatment, it is necessary to acquire as much scientific information as possible about the variety of treatment options available for each specific disorder. Armed with this knowledge, medical professionals will have the best possible chance of managing individual clinical idiosyncrasies and preventing disease progression.

In CML, clinicians have a range of extremely effective therapies at their disposal. The introduction of imatinib as first-line therapy revolutionised CML treatment and patient prognosis improved dramatically. However, imatinib is not curative and resistance and failure remain a regular occurrence in at least one third of patients(Francis et al., 2013).

At the time of starting this work, both nilotinib and dasatinib were newly approved for treatment-naïve CP-CML (FDA approval in June and October 2010, respectively). However, it remained unclear how to distinguish the patients who would most benefit from the use of these 2G TKIs as first- line therapy. It is plausible that clinical decisions about these CML treatment plans could benefit from monitoring clinical biomarkers in individual patients.

CIP2A had been previously investigated within our department and shown to be a biomarker for progression to blast crisis in imatinib-treated CML, with

100% actuarial probability(C. M. Lucas et al., 2011). It was not known however, whether this observation would hold true for dasatinib- and nilotinib-treated CML.

All patient samples investigated here are taken from newly diagnosed and treatment-naïve CP-CML. This study focussed on the effects of TKIs on long-term clinical outcome, dependent upon their diagnostic CIP2A protein level.

Results from this chapter show a clear difference in the clinical outcomes of patients treated with imatinib compared with 2G TKIs. All patients who received dasatinib or nilotinib as their initial therapy survived, with the exception of one CML-unrelated death. Additionally, none of these patients progressed to blast crisis and approximately 80% remained event-free at the time of their latest clinical follow-up. This was true for both high and low CIP2A patient cohorts. With regards to imatinib-treated CML, all but two patients (who were switched to a 2G TKI) with high CIP2A protein at diagnosis had progressed to blast crisis within two years and 80% had died; none of the low CIP2A cohort had progressed at latest follow-up. As the poor results seen in high CIP2A imatinib-treated CML are not mirrored by 2G TKI-treated CML, it can be stated that the blast crisis biomarker status of CIP2A is not upheld in patients treated with dasatinib or nilotinib. The fact that patients have a positive response to 2G TKIs, regardless of initial CIP2A level, indicates a superior effect of dasatinib and nilotinib over imatinib when combatting the oncogenic effects of CIP2A.

To further evaluate the different clinical outcomes achieved on 2G TKIs in comparison to their first generation predecessor, the depth of molecular response and the time taken to achieve them were evaluated. Independent studies have suggested that patients with suboptimal or no response to treatment within the first 3-6 months have less favourable long-term outcomes than those achieving a rapid response to treatment(Savona & Saglio, 2013). Importantly, studies also show that patients treated second line with dasatinib or nilotinib following imatinib therapy were less likely to achieve a CCR and more likely to progress had they a suboptimal or failure response to imatinib, when compared to those with better than suboptimal responses(Savona & Saglio, 2013). These studies suggest that in improving the proportion of early clinical responses in CML, we may decrease the AP/BC progression rate and thus improve CML prognosis. Identifying the correct TKI for each patient to achieve an early response is therefore paramount.

These data again show no differences between high/low CIP2A patient cohorts in the time taken to achieve a CCR, MMR or MR4 if patients were treated with dasatinib or nilotinib. The majority of these patients (>80%) achieve a CCR by 24 months and approximately 80% will have achieved the deepest response of MR4 by 30 months. Though low CIP2A imatinib-treated patients had similar results in the time taken to achieve a CCR and MMR, there was a trend suggesting a delay in the time taken to achieve an MR4 in comparison to patients treated with newer TKIs. However, approximately 70% of low CIP2A patients will have achieved an MR4.0 if treated for 5 years with imatinib. In

stark contrast, no patient treated with imatinib achieved a CCR or deeper molecular response if they had a high CIP2A level at diagnosis. The poor overall survival and progression to blast crisis shown earlier are therefore not due to a loss of response, but a failure of imatinib to manage the CML from initial diagnosis.

The initial observation of this chapter suggests a benefit in measuring diagnostic CIP2A protein of CML patients to use as an indicator of suitable TKI treatment; patients with high CIP2A should *not* be prescribed imatinib as a first line therapy, but offered dasatinib or nilotinib as an alternative treatment. This novel identification of the 2G TKI's effectiveness in the face of high CIP2A expression may be of importance in avoiding poor clinical outcomes due to a delay in prescribing a suitable therapy; patient prognosis is more favourable if an appropriate treatment is prescribed earlier(Savona & Saglio, 2013). Therefore, this finding may suggest CIP2A level as an immediate indicator of the most effective treatment plan.

In this chapter, the more rapid deeper molecular responses to 2G TKIs in comparison to imatinib indicate a significant role of CIP2A within CML. The different TKI mechanisms of action that may lead to the apparent dampening of the CIP2A oncogene's effects warrants further investigation. In understanding the nature of CIP2A's role in CML and the way in which it is targeted by the various TKIs, future CML treatment may be more suited to an individual patient's need, thus improving the overall prognosis of CML.

Chapter 4: Effects of Second and Third Generation TKIs on the CIP2A/PP2A Pathway

4.1. Introduction

The finding of the previous chapter, showing superior clinical outcomes achieved by 2G TKI treated patients, was an interesting observation requiring further investigation. The clinical data suggest an action by dasatinib and nilotinib that overcomes the high levels of CIP2A. This action is not mirrored by imatinib and led to the further consideration of how these TKIs impart their desired effects.

Figure 4.1. A Proposed Model for the Action of CIP2A in CML cells. Figure taken from Lucas et al(C. M. Lucas et al., 2011). An inhibitory action of imatinib is also indicated.

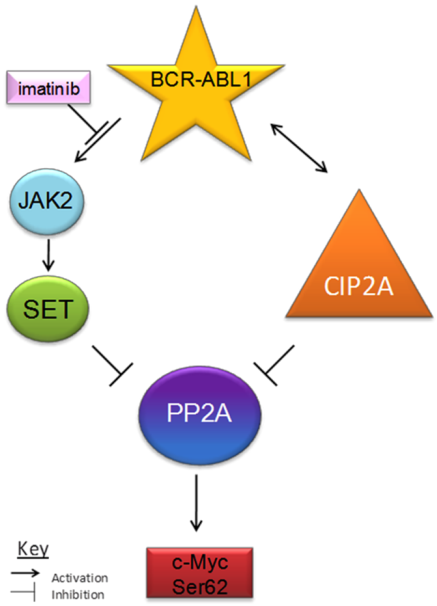

CIP2A works alongside c-Myc to inhibit the tumour suppressor activity of PP2A, and thus allows the continued action of BCR-ABL1. This part of the illustrated pathway had before been shown to be unaffected by imatinib treatment; imatinib's inhibitory activity was shown to be via the JAK2/SET part of this molecular signalling cascade.

4.2. Aims

Though Lucas *et al*(C. M. Lucas et al., 2011)identified CIP2A in CML as able to avoid inhibition by imatinib (**Figure 4.1**), this work did not take into consideration the newer TKIs that are now more readily available. No study has examined the effects of dasatinib, nilotinib or ponatinib specifically on the CIP2A/PP2A pathway that is prominent in CML. This work therefore aimed to investigate the CIP2A/PP2A pathway following newer treatments, both in long-term settings by looking at patient follow-up samples, and using short-term *in vitro* TKI cultures. More specifically it aimed to:

- Investigate the effects of long-term *in vivo* TKI therapy on the CIP2A/PP2A pathway
- Investigate the effects of short-term *in vitro* TKI treatments on the CIP2A/PP2A pathway
- Compare the effects of imatinib to 2G and 3G TKIs on the CIP2A/PP2A pathway and consider any differences as a possible reason for more favourable outcomes for CML patients treated with the latter TKIs.

4.3. Methods

In this chapter, cell lines and diagnostic and 12 month follow-up patient PBMC samples were analysed using standard cell culture (**Section 2.4**), *in vitro* TKI cultures (**Section 2.4.3**), flow cytometry (**Section 2.5**), qRT-PCR (**Section 2.9.3**), and ELISA (**Section 2.7**). Clinical characteristics of patients used for long-term 2G TKI *in vivo* studies are shown in the **Appendix** (UPN001-069) and those used for short-term 2G and 3G TKI *in vitro* studies shown in **Table 4.1**. Clinical characteristics of ponatinib patients are shown in **Table 4.2**. Student t-tests were used for statistical analysis.

4.4. Results

4.4.1. Effects of long-term immunotherapy with 2G TKIs on the CIP2A/PP2A pathway

The clinical significance of CIP2A shown thus far led me to investigate the rest of the CIP2A/PP2A pathway (**Figure 4.1**) for any altering levels between diagnosis and 12 months follow-up, as well as any variations between treatment cohorts. The patients analysed were the same as in the previous chapter and are shown in the **Appendix**.

As previous lab work (C. M. Lucas et al., 2011)had shown the significance of CIP2A in CML to be at the protein level, patient MNC samples were initially analysed. As described (**Section 3.4.1**), patients were split according to diagnostic levels of CIP2A protein from MNCs (**Figure 4.2 A**; p=0.001). A significant increase in CIP2A level following 12 months of treatment can be seen in the low CIP2A cohort of patients (p=0.001). No significant change in CIP2A protein level is seen in the high CIP2A cohort.

Diagnostic levels of the other proteins examined appear to follow a similar trend; low CIP2A patients also have low levels of PP2A, inactive PP2A (assessed by Tyrosine 307 phosphorylation (pY307-PP2A)), SET and JAK2, while high CIP2A patients have higher levels of these proteins, though this does not reach statistical significance (**Figure 4.2 B-E**). Interestingly, JAK2 levels increase

significantly after 12 months of TKI treatment in the low CIP2A cohort (**Figure 4.2 E**; p=0.011).

Figure 4.2. Protein levels from MNCs of 2G TKI CML patients; stratified according to diagnostic CIP2A protein level. 28 patients were analysed at diagnosis and after 12 months of 2G TKI therapy; 11 high CIP2A and 17 low CIP2A.

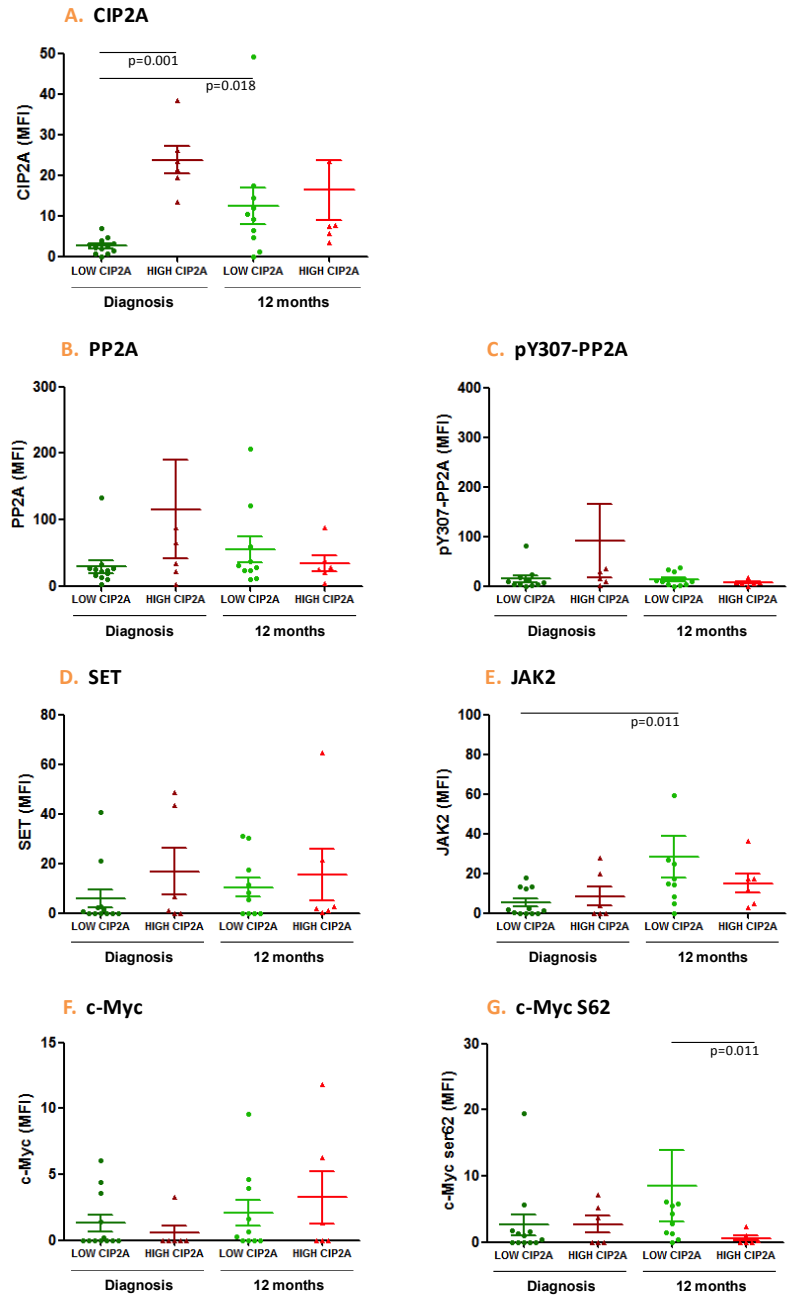

In addition to the MNC protein levels, the more primitive CD34+ cell population was also investigated. In post-treatment CML blood samples, the majority of the leukaemic cell population has been replaced by normal circulating blood cells; therefore only diagnostic CD34+ levels were measured.

As in the MNC samples, the CD34+ cells from high CIP2A patients also had significantly higher CIP2A protein in their early progenitor cells (**Figure 4.3 A**; p=0.035). Again similar to the MNC data, the high CIP2A patient cohort also had a trend for higher levels of all proteins compared to the low CIP2A patients; PP2A, pY307-PP2A, SET and JAK2 (**Figure. 4.3 B-E**).

As expected, all protein levels were considerably higher in the CD34+ cells compared to the MFI values of the MNCs.

Levels of c-Myc and c-Myc pS62 protein in both MNC and CD34+ cells were also measured by flow cytometry in these patient samples (**Figures 4.2 F-G** and **4.3 F-G**). Little of either protein was identified and no significant difference could be seen between cohorts. However, published work had used the ELISA method for measuring this protein(C. M. Lucas et al., 2011). Unfortunately, due to the large amount of cells necessary for ELISAs and the limited amount of precious patient samples available, this work could not be repeated for these patients. Any further c-Myc and c-Myc pS62 measurement was performed by

the ELISA technique as described by Lucas *et al(C. M. Lucas et al., 2011)*, in samples with an abundance of cells available.

Figure 4.3. Protein levels from CD34+ cells of 2G TKI patients; stratified according to diagnostic CIP2A protein level. Diagnostic samples of 28 patients were analysed; 11 high CIP2A and 17 low CIP2A.

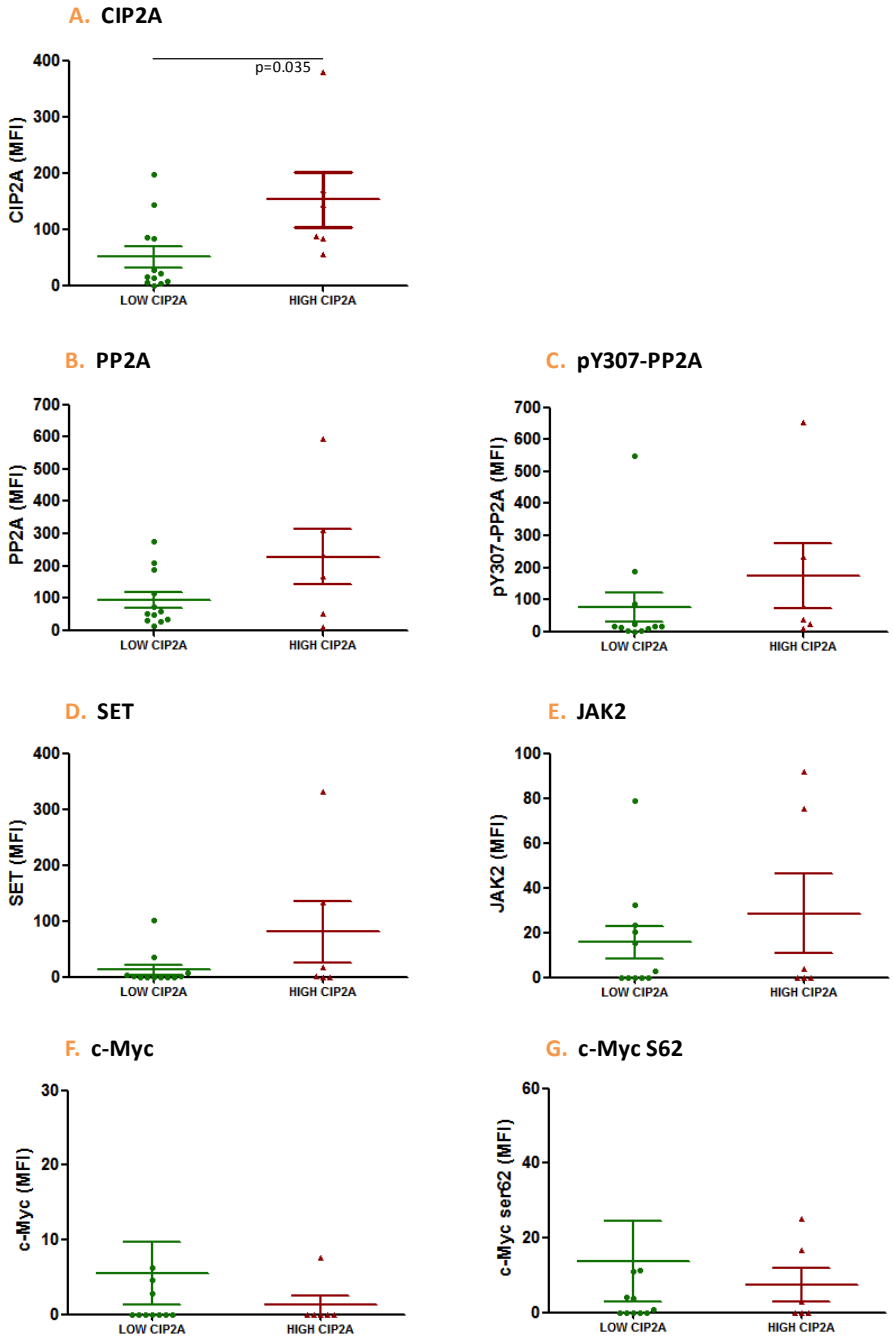

Gene expression was also examined in these patient samples to identify any changes that may have occurred at the transcriptional level following long-term *in vivo* dasatinib and nilotinib treatment. **Figure 4.4** shows mRNA levels for the same patients as in **Figures 4.2** and **4.3**, again stratified according to diagnostic CIP2A MNC protein levels.

In accordance with published data(C. M. Lucas et al., 2011)*CIP2A* mRNA levels did not alter between high/low CIP2A cohorts at diagnosis (**Figure 4.4 A**) (though interestingly, a trend is seen for an inverse relationship). A small difference can be observed after 12 months of therapy; low CIP2A patients' levels decrease at 12 months follow-up whereas high CIP2A patients' levels increase, however this trend is not statistically significant. **Figures 4.4 B-D** show similar results; low CIP2A patients' levels of *PP2A*, *SET* and *JAK2* all decrease significantly following 12 months dasatinib/nilotinib treatment ($p=0.009$, $p=0.027$, $p<0.0001$, respectively); the same trend is seen in the high CIP2A patients (**Figure 4.4 B**; $p=0.015$, **Figure 4.4 D**; $p=0.004$, no statistical significance in *SET* level decrease).

All patients have elevated *c-Myc* levels at diagnosis compared to their follow-up levels, as would be expected in light of the published literature. However, the high CIP2A patient cohort also had significantly higher *c-Myc* mRNA when compared to the low CIP2A cohort at diagnosis. In both cohorts, *c-Myc* mRNA expression decreased following 12 months of dasatinib/nilotinib treatment

(**Figure 4.4 E**; p=0.015 high CIP2A, no statistical significance in low CIP2A cohort *c-Myc* level decrease).

Figure 4.4. mRNA levels of 2G TKI CML patients; stratified according to diagnostic CIP2A protein level. 28 patients were analysed at diagnosis and 12 months follow-up; 11 high CIP2A and 17 low CIP2A.

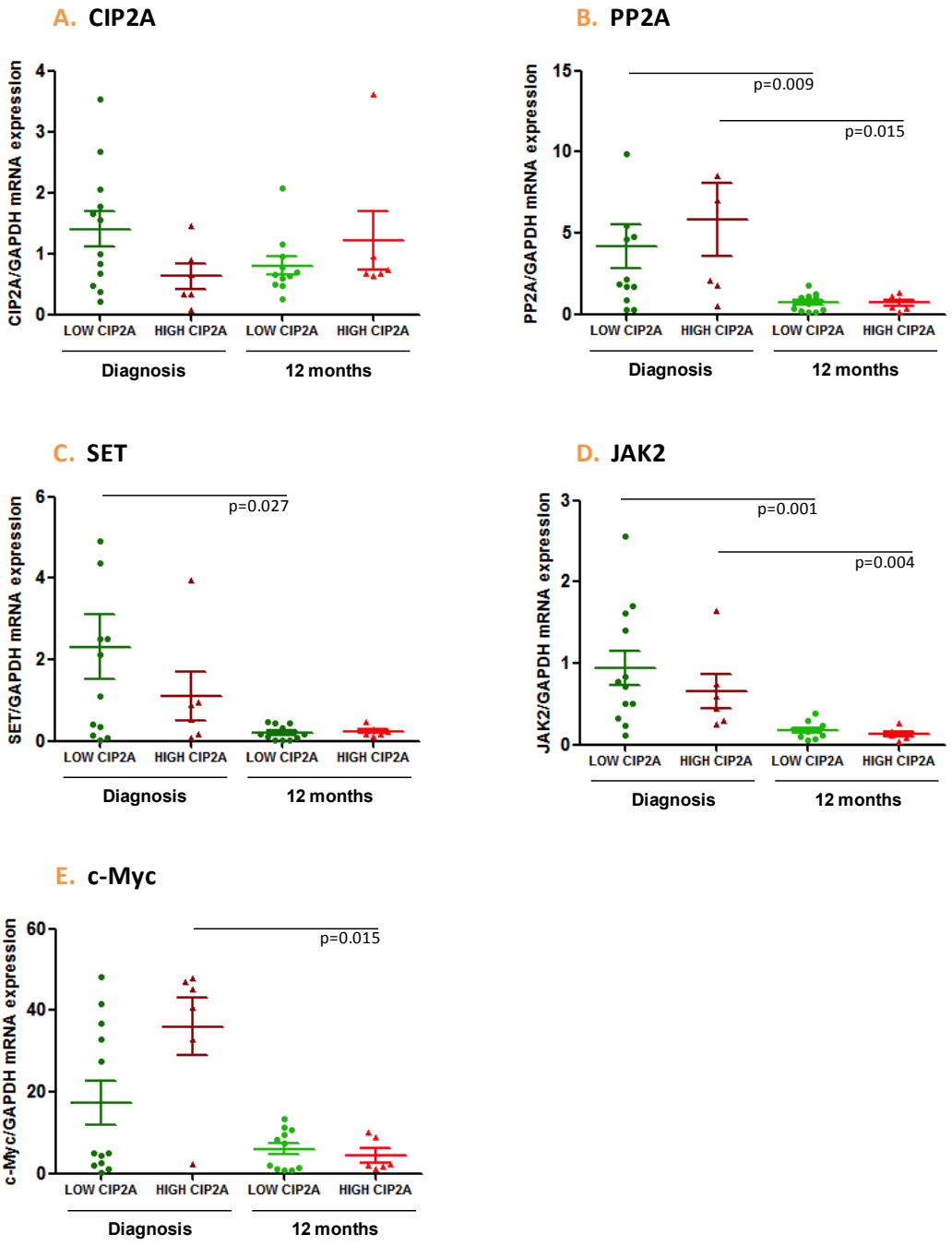

4.4.2. Effects of short-term 2G TKI treatment on the CIP2A/PP2A pathway

Long-term analysis of MNC, CD34+ cells and mRNA expression of CML patients has thus far not given an explanation for the exciting observations shown in **Chapter 3**. The clinical results suggested a mechanism of overcoming the negative effects of the CIP2A oncogene using dasatinib or nilotinib. As this explanation had not arisen, it was theorised that the initial methodology may be the cause.

Comparing diagnostic and 12 month patient follow-up samples has its limitations due to the largely different populations of cells they contain. Following long-term TKI treatment the majority of CML patients (especially those remaining in CP) have a low leukaemic cell population within their blood; the majority of the initial leukaemic cells have been replaced by their normal counterparts. It is therefore prudent to investigate the effects of the different TKIs on the proteins afore-mentioned, in a short-term culture. Exploring the effects of imatinib, dasatinib and nilotinib upon treatment naïve CML samples may lead to a better understanding of the way in which these drugs act on the CIP2A/PP2A pathway at the molecular level.

Due to limited availability of patient samples and reagents, this work was performed in a smaller subset of patients. Thirteen CP-CML patient samples were suitable for this *in vitro* TKI culture; a large cell count was necessary, which was not met in many samples. **Table 4.1** describes the characteristics of those patients investigated.

Table 4.1. Patient characteristics table for samples studied by *in vitro* TKI

UPN	M/F	AGE AT DIAGNOSIS	CIP2A LEVEL (Low=0, High=1)
070	F	73	Low
071	F	54	Low
072	F	68	Low
073	M	69	Low
074	M	55	Low
075	M	54	Low
076	M	34	Low
077	F	35	High
078	F	27	High
079	F	62	High
080	F	52	High
081	M	29	High
082	M	69	High

Diagnostic cell samples were cultured for 24 hours with 5μM imatinib, 150nM dasatinib and 5μM nilotinib and CIP2A/PP2A pathway proteins measured to scrutinise the changes post-treatment. The untreated CP-CML CIP2A levels were used to separate samples into high/low CIP2A cohorts as before and the results shown in **Figure 4.5**.

As with previous publications, the percentage of phosphorylated CrKL was used as a measure of BCR-ABL1 activity, as CrKL is directly phosphorylated by BCR-ABL1. As expected, all three TKIs inhibited BCR-ABL1 activity (**Figure 4.5 B(i)** and **B(ii)**), regardless of CIP2A level. However, this was not the case with their effects on CIP2A. In the low CIP2A patient cohort, CIP2A level remained unaltered following all TKI treatment (**Figure 4.5 A(ii)**). Interestingly however, in the high CIP2A patient samples, only 2G TKIs caused a significant decrease in CIP2A protein level (**Figure 4.5 A(i)**; p=0.012 (dasatinib), p=0.005 (nilotinib)); no significant drop is seen in cells treated with imatinib.

This trend is mirrored in inactive PP2A levels (**Figure 4.5 F(i)**; p=0.039 (dasatinib), p=0.042 (nilotinib)). A similar trend is shown in both c-Myc (**Figure 4.5 C**) and c-Myc pS62 (**Figure 4.5 D**) samples following treatment, though imatinib (p=0.009, p=0.001), dasatinib (p<0.001, p=001) and nilotinib (p<0.001, p=0.001) all significantly decrease the levels of these proteins. Of note, in the low CIP2A patient cohort no change is observed in pY307-PP2A, c-Myc and c-Myc S62 following TKI treatment and no pattern in SET protein level is seen in either patient cohort.

Figure 4.5. Protein levels of treatment naïve CP-CML patients following 24 hour *in vitro* TKI culture; stratified according to diagnostic CIP2A protein level. (i) 6 high CIP2A and (ii) 7 low CIP2A patients were investigated.

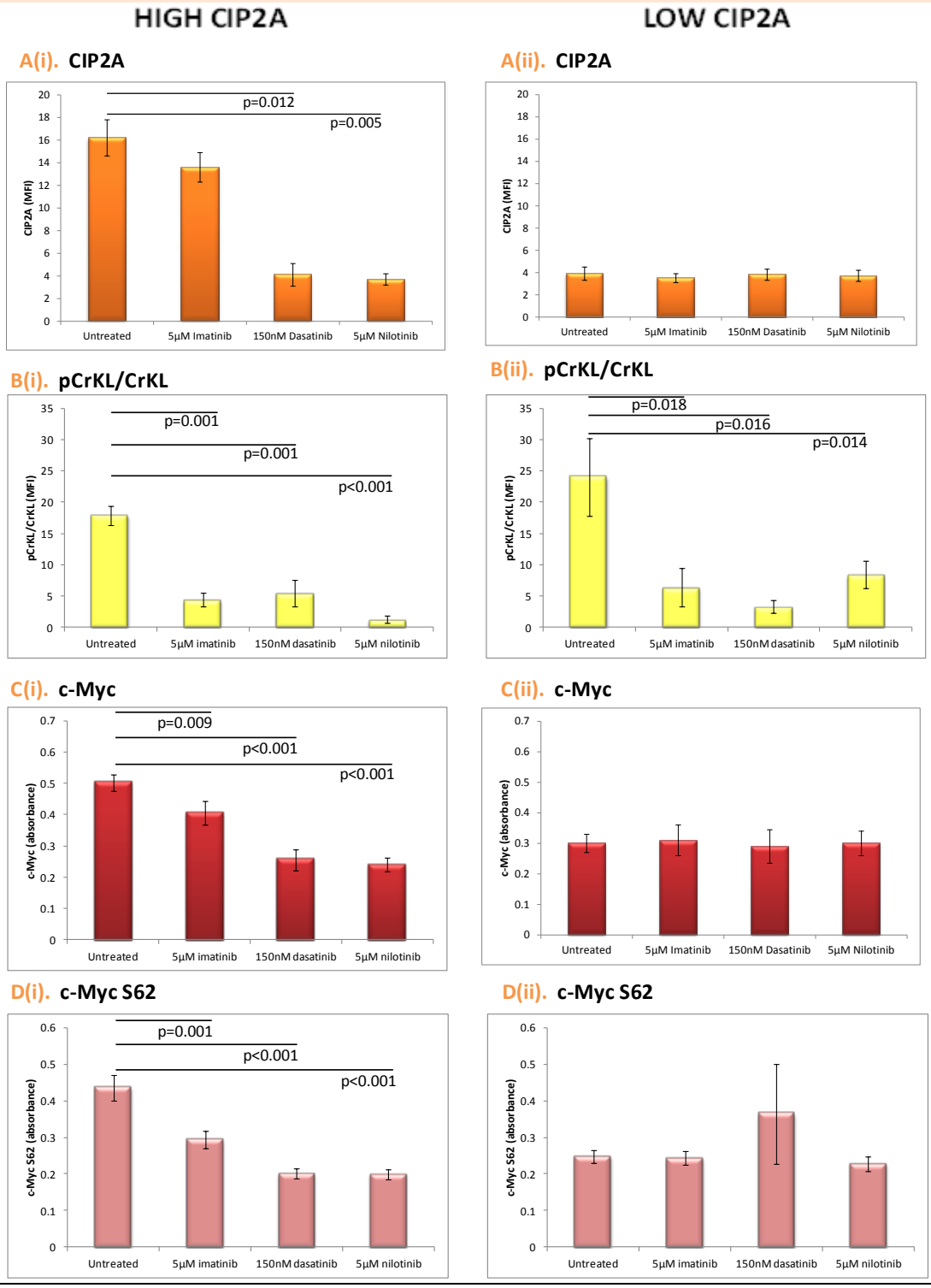

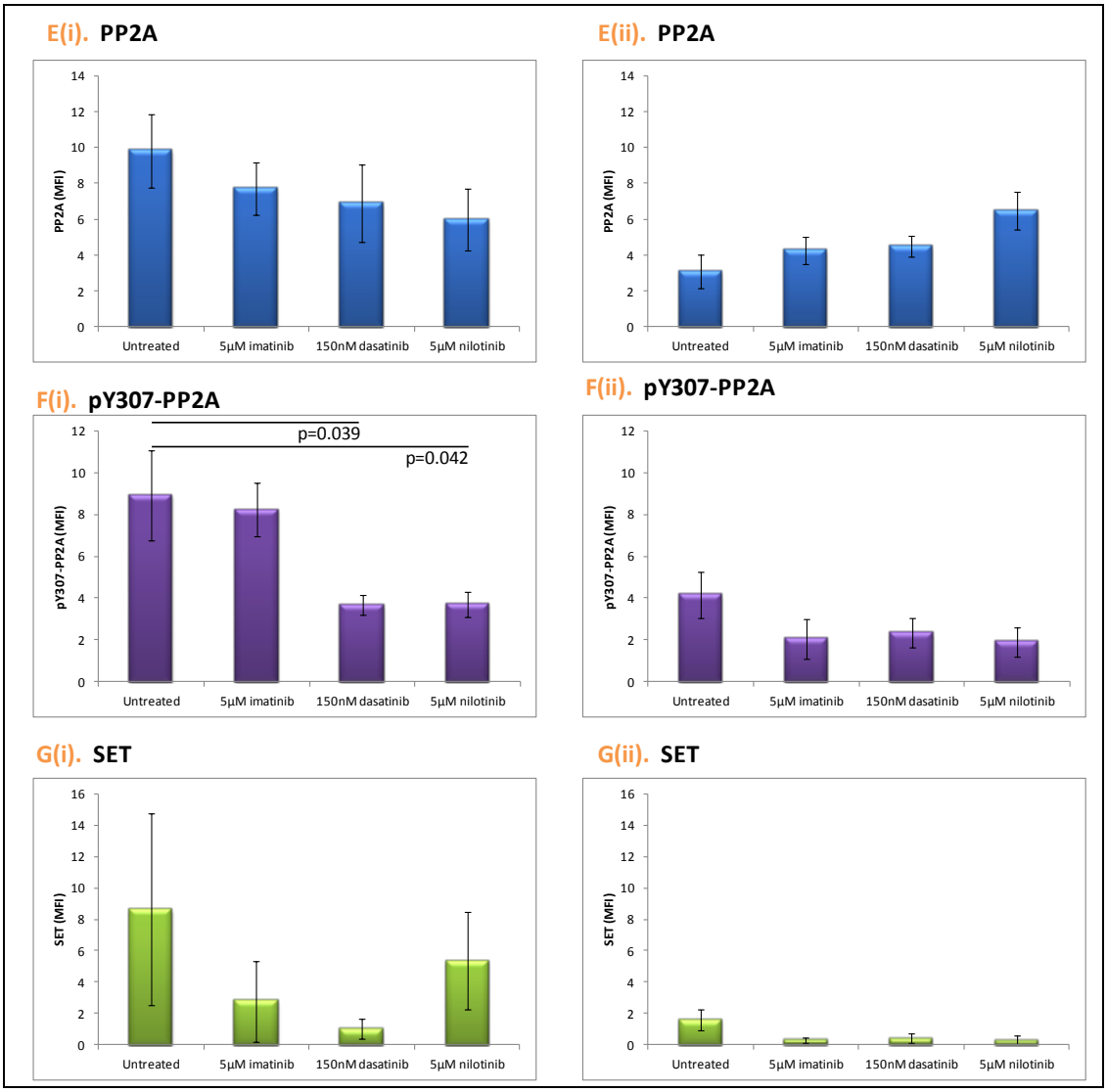

4.4.2.1. Results Summary: short-term 2G TKI treatment

Second generation TKIs have a superior effect on overcoming high CIP2A levels, in comparison to imatinib treatment. All three TKIs significantly decrease BCR-ABL1 activity irrespective of basal CIP2A level. In stark contrast, high CIP2A levels are only significantly decreased by dasatinib and nilotinib, and not by imatinib, therefore the ability of 2G TKIs to overcome CIP2A may be a mechanism for the superior clinical outcomes of 2G TKI-treated CML that is discussed in **Chapter 3**.

4.4.3. Ponatinib Treatment in CML

The third generation TKI ponatinib was originally hailed as a wonder-drug of CML after it was specifically designed to overcome the thus far untreatable T315I 'gatekeeper' mutation. Its long and flexible design allows it to fit into the active site of BCR-ABL1, despite the awkward structural changes the tyrosine kinase molecule undergoes following the T315I mutation.

Early clinical results were extremely promising, with almost 90% of T315I patients achieving a CCR(T O'Hare et al., 2009) and ponatinib was pushed forwards into phase III patient trials. Unfortunately, a number of serious cardiovascular complications occurred, causing the phase III trial of first line ponatinib to be permanently halted in October 2013.

This study gained preliminary results prior to the unsuccessful turn of events causing the trial to be halted(Lipton et al., 2015). Though ponatinib is now available for those patients who have exhausted all other treatment options, this thesis did not examine the effects of *in vivo* ponatinib on CIP2A and its related proteins. First line ponatinib patient samples are not available (all Liverpool patients in the first line ponatinib trial actually received imatinib) and those local patients who received second, third or fourth line ponatinib have too diverse clinical histories.

Here, the immediate molecular effects of ponatinib on the CIP2A/PP2A pathway are investigated in treatment-naïve CML samples and a small study of six patients treated with ponatinib following other TKI failures are individually analysed.

4.4.3.1. Optimisation of ponatinib *in vitro*

The appropriate dose and incubation time of ponatinib had not yet been optimised for studies of this nature, thus it was necessary to begin by identifying such parameters. K562 and KCL22 cell lines were treated with varying levels of ponatinib, with the current clinical Cmax of 130nM used as an initial guide. Levels of pCrKL/CrKL (analysed by flow cytometry) were used as an indicator of ponatinib efficacy in inhibiting BCR-ABL1 activity (n=3).

Figure 4.6. Dose Optimisation of Ponatinib. A. Cell viability and B. pCrKL/CrKL ratio were analysed using flow cytometry in (i) K562 (high CIP2A) and (ii) KCL22 (low CIP2A) cell lines.

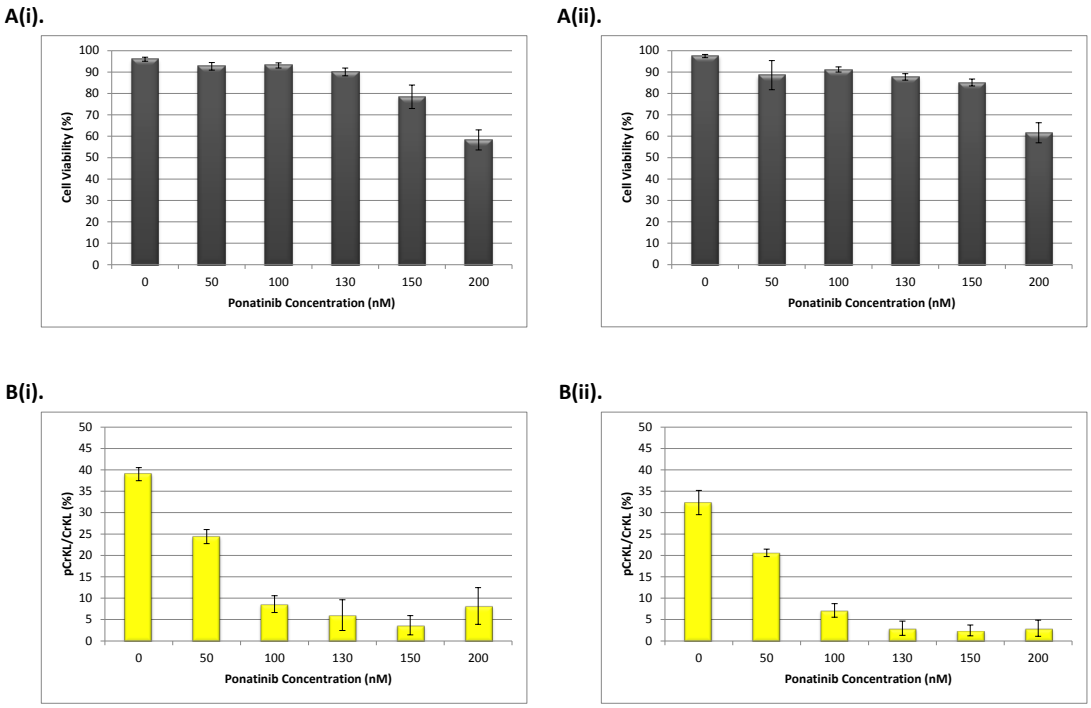

It was necessary to also identify the optimal incubation period for ponatinib treatment in this *in vitro* TKI study and thus a time course assay was conducted. Again using K562 and KCL22 cell lines, cells were cultured for 4, 24 and 48 hours with the clinically achievable concentration of 130nM. Cell viability and pCrKL/CrKL ratio were analysed using flow cytometry and the experiment performed in triplicate.

Figure 4.7. Optimisation of ponatinib treatment incubation period. A. Cell viability and B. pCrKL/CrKL ratio were analysed using flow cytometry in (i) K562 (high CIP2A) and (ii) KCL22 (low CIP2A) cell lines following a variety of treatment incubation lengths; 0, 4, 24 and 48 hours.

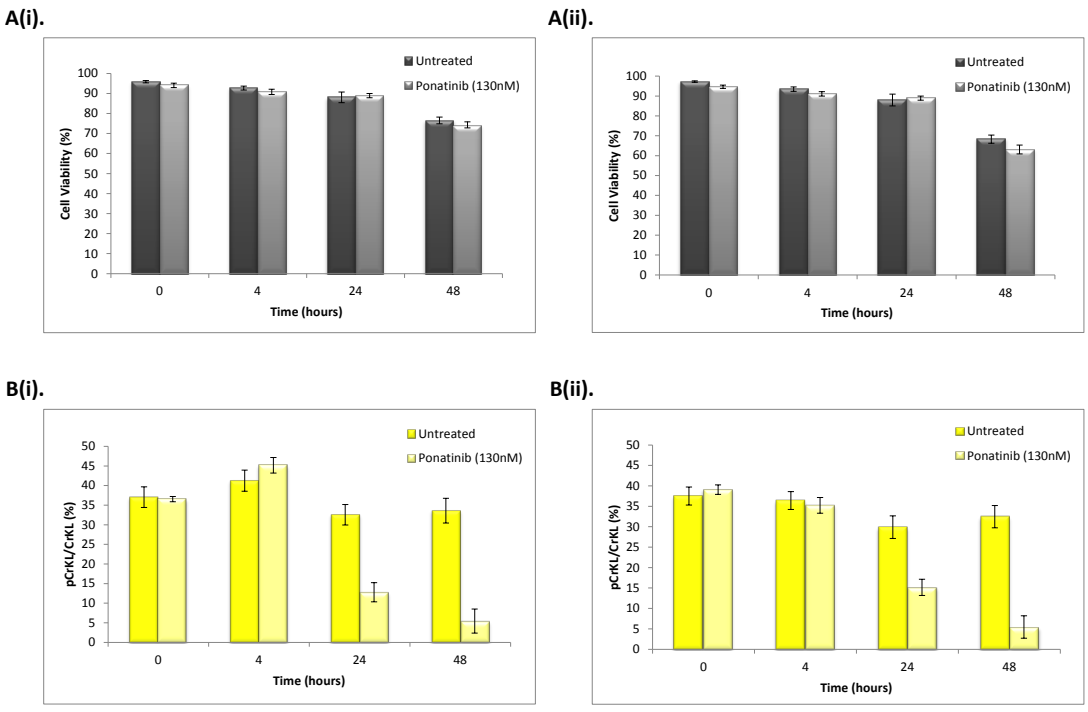

Figures 4.6 and **4.7** show ponatinib having little effect on cell viability, yet causing a clear decrease in BCR-ABL1 activity, as expected. A significant reduction in pCrKL/CrKL protein is seen in both cell types with 100nM ponatinib, but the largest decrease is seen at the clinically relevant concentration; 130nM. This clinical concentration was chosen for future investigations as it induced the larger decrease in pCrKL/CrKL and also to allow for the data to be more easily comparable to ponatinib concentrations achievable *in vivo*.

With regards to the length of incubation time, little effect is seen after only 4 hours of ponatinib treatment, yet both cell lines display clear reductions in pCrKL/CrKL levels from 24 hours onwards. However, elevated levels of cell death were observed in the K562 cell line after a 48 hour incubation period. First and second generation TKI studies within the department have used a 24 hour treatment incubation; this, coupled with the reduced cell viability at 48 hours, led to the conclusion that 24 hours incubation with 130nM ponatinib were the optimal conditions for *in vitro* TKI study.

4.4.3.2. Effects of Short-term Ponatinib Treatment on the CIP2A/PP2A Pathway

An *in vitro* TKI ponatinib culture was performed in both cell lines (**Figure 4.8**) and patient samples (**Figure 4.9**). Both CIP2A high (K562) and CIP2A low (KCL22) cell lines were treated. The thirteen treatment-naïve CP-CML patient samples shown previously (**Table 4.1**) were also used for this ponatinib study. Samples were cultured for 24 hours with 130nM ponatinib and CIP2A/PP2A pathway proteins were analysed by flow cytometry.

The results of the ponatinib *in vitro* TKI assays showed strong inhibition of the CIP2A/PP2A pathway, following the trends seen in 2G TKI *in vitro* assays, yet to an even greater extent.

The effectiveness of ponatinib's inhibition of BCR-ABL1 activity can be seen in the significant decrease of pCrKL/CrKL following TKI treatment; K562, KCL22 and high and low CIP2A patients all show a significant drop (**Figure 4.8 B(i)**, p=0.014; **Figure 4.8 B(ii)**, p=0.035; **Figure 4.9 B(i)**, p=0.007; **Figure 4.9 B(ii)**, p=0.001; respectively).

Levels of c-Myc and its stabilised form c-Myc pS62 are also decreased by ponatinib treatment. The K562 cells have a higher basal level of total c-Myc (as expected due to a greater level of CIP2A and according to previously published work) and c-Myc pS62 (**Figure 4.8 C(i)** and **D(i)**) and both decrease

significantly following exposure to 130nM ponatinib (p=0.080 and p=0.010, respectively). The lower CIP2A cell line, KCL22, shows a slight fall in c-Myc and c-Myc pS62, though neither result is statistically significant (**Figure 4.8 C(ii)** and **D(ii)**). CML patient samples show similar results to those observed in cell lines, however both c-Myc and c-Myc pS62 show significantly decreased levels in both high and low CIP2A patient cohorts (**Figure 4.9 C(i)**, p=0.002, **Figure 4.9 D(i)**, p=0.012, **Figure 4.9 C(ii)**, p=0.006, **Figure 4.9 D(ii)**, p=004; respectively).

Interestingly, the effects of ponatinib on CIP2A level differ between cell lines and patient samples. In cell lines, ponatinib reduces the level of CIP2A regardless of the original level (**Figure 4.8 A(i)** and **(ii)**). However, in low CIP2A patients, the levels of CIP2A are not decreased any further than their average level of approximately MFI=2, following ponatinib exposure. Patients with high CIP2A see their levels drop to approximately MFI=2 upon ponatinib treatment. In both cell lines and patient samples, though CIP2A levels may decrease, the levels tend to remain around MFI=1-2 at their minimum. The fact that CIP2A is not entirely extinguished following treatment with this extremely potent TKI suggest a baseline level of CIP2A may be necessary for an alternative physiological function within the leukaemic cell.

Additionally, inactive PP2A decreases following ponatinib treatment; the trend is apparent in all cell lines and cohorts, though only K562 cells and high CIP2A patients show a statistically significant decrease (**Figure 4.8 F(i)**, p=0.021;

Figure 4.9 F(i), p=0.026). SET levels are unaffected by ponatinib treatment in patient samples (**Figure 4.9 G(i)** and **(ii)**), though a significant drop can be seen in KCL22 SET level following ponatinib treatment (**Figure 4.8 G(ii)**).

Figure 4.8. Ponatinib *in vitro* TKI culture; observed effects in (i) K562 and (ii) KCL22 cells. Protein levels were measured by (A, B, E-G) flow cytometry or (C, D) ELISA following 24 hour incubation with 130nM ponatinib and in untreated controls (n=3). A. CIP2A, B. pCrKL/CrKL, C. c-Myc, D. c-Myc pS62, E. PP2A, F. pY307-PP2A, G. SET.

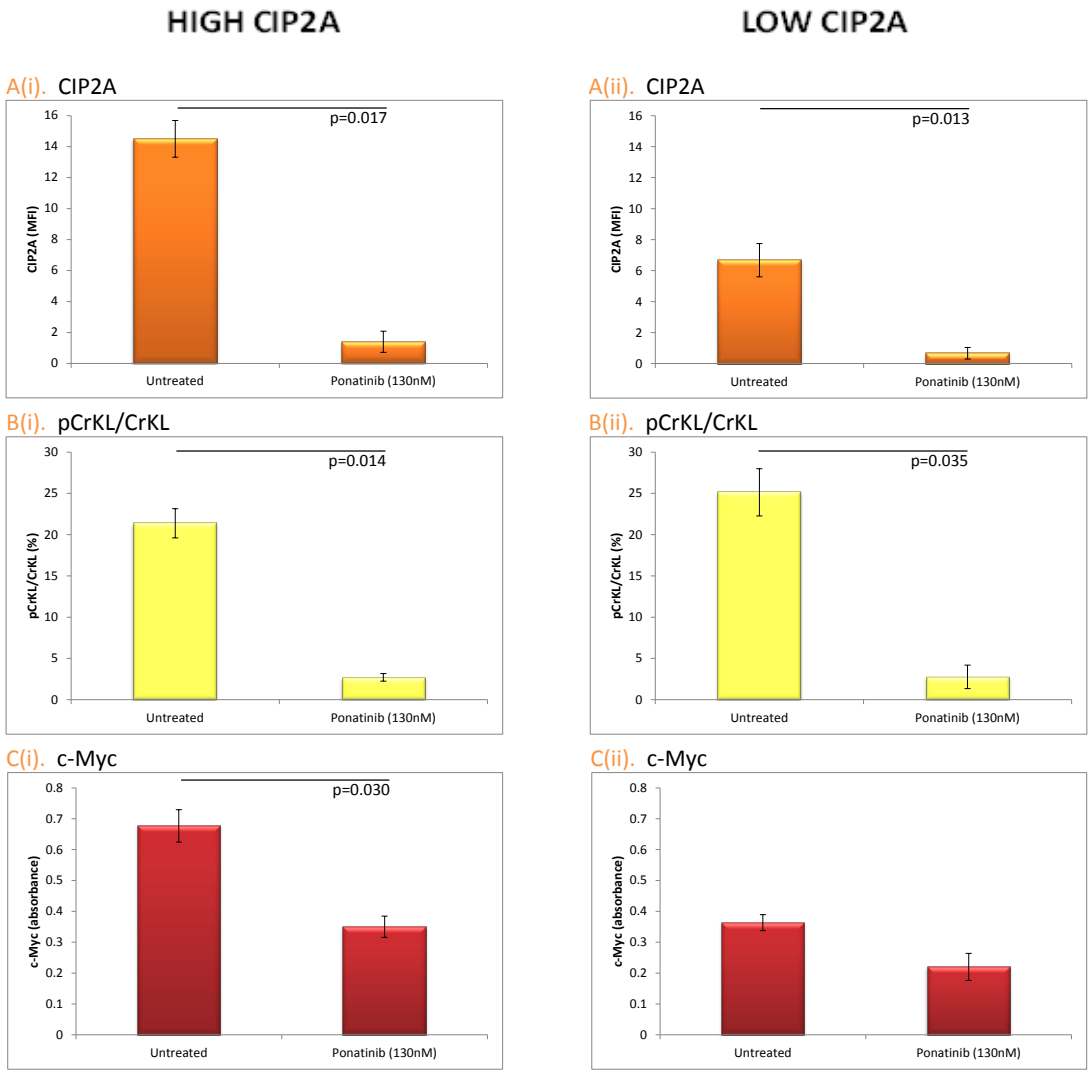

D(i). c-Myc pS62

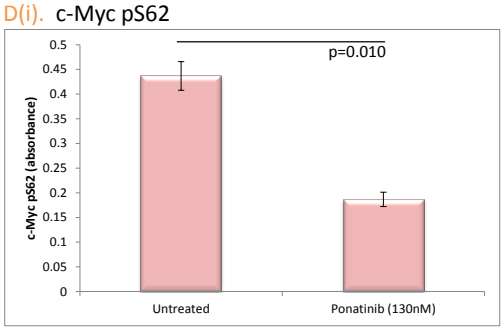

D(ii). c-Myc pS62

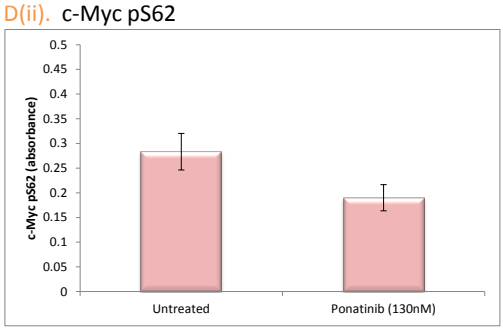

E(i). PP2A

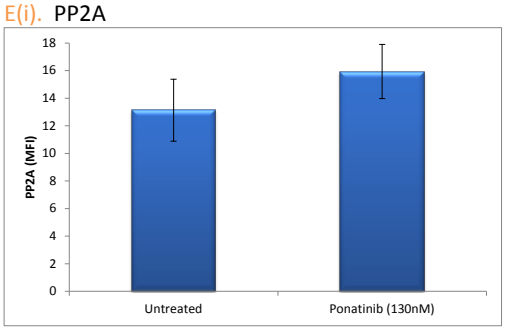

E(ii). PP2A

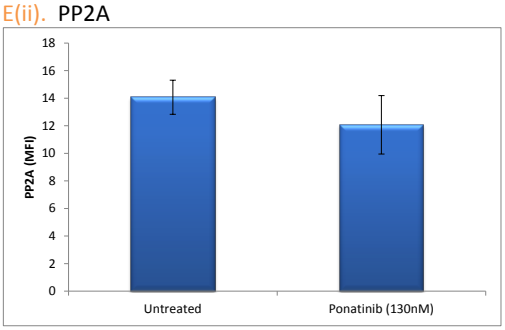

F(i). pY307-PP2A

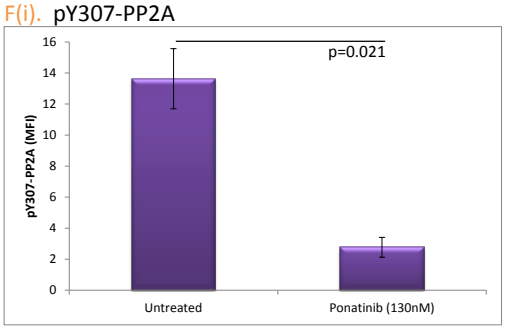

F(ii). pY307-PP2A

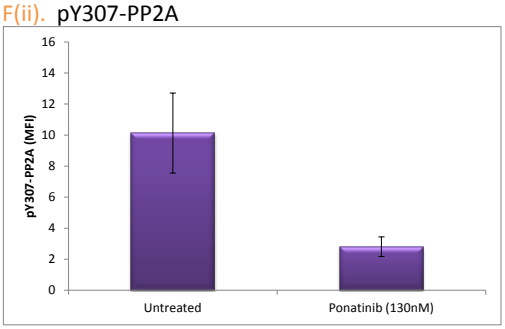

G(i). SET

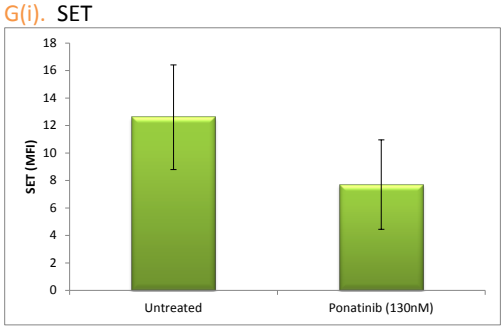

G(ii). SET

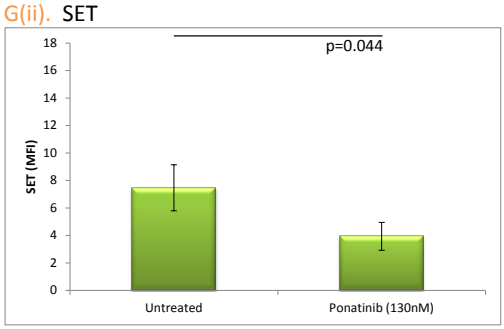

Figure 4.9. Ponatinib in vitro TKI culture; observed effects in treatment-naïve CP-CML samples. Protein levels were measured by (A, B, E-G) flow cytometry or (C, D) ELISA following 24 hour incubation with 130nMponatinib. Patients were stratified according to diagnostic CIP2A protein level; (i) high (n=6) or (ii) low (n=7). A. CIP2A, B. pCrKL/CrKL, C. c-Myc, D. c-Myc pS62, E. PP2A, F. pY307-PP2A, G. SET.

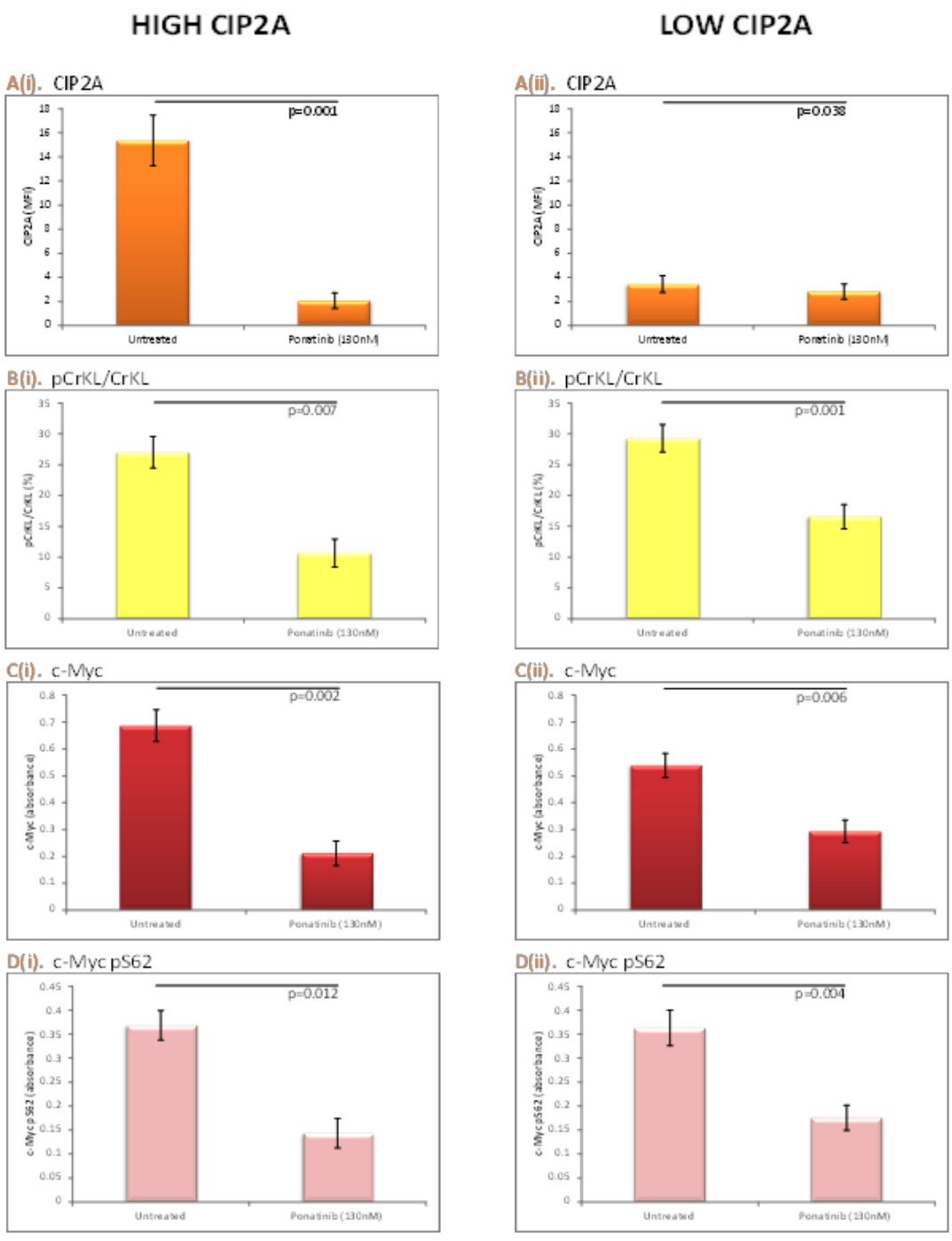

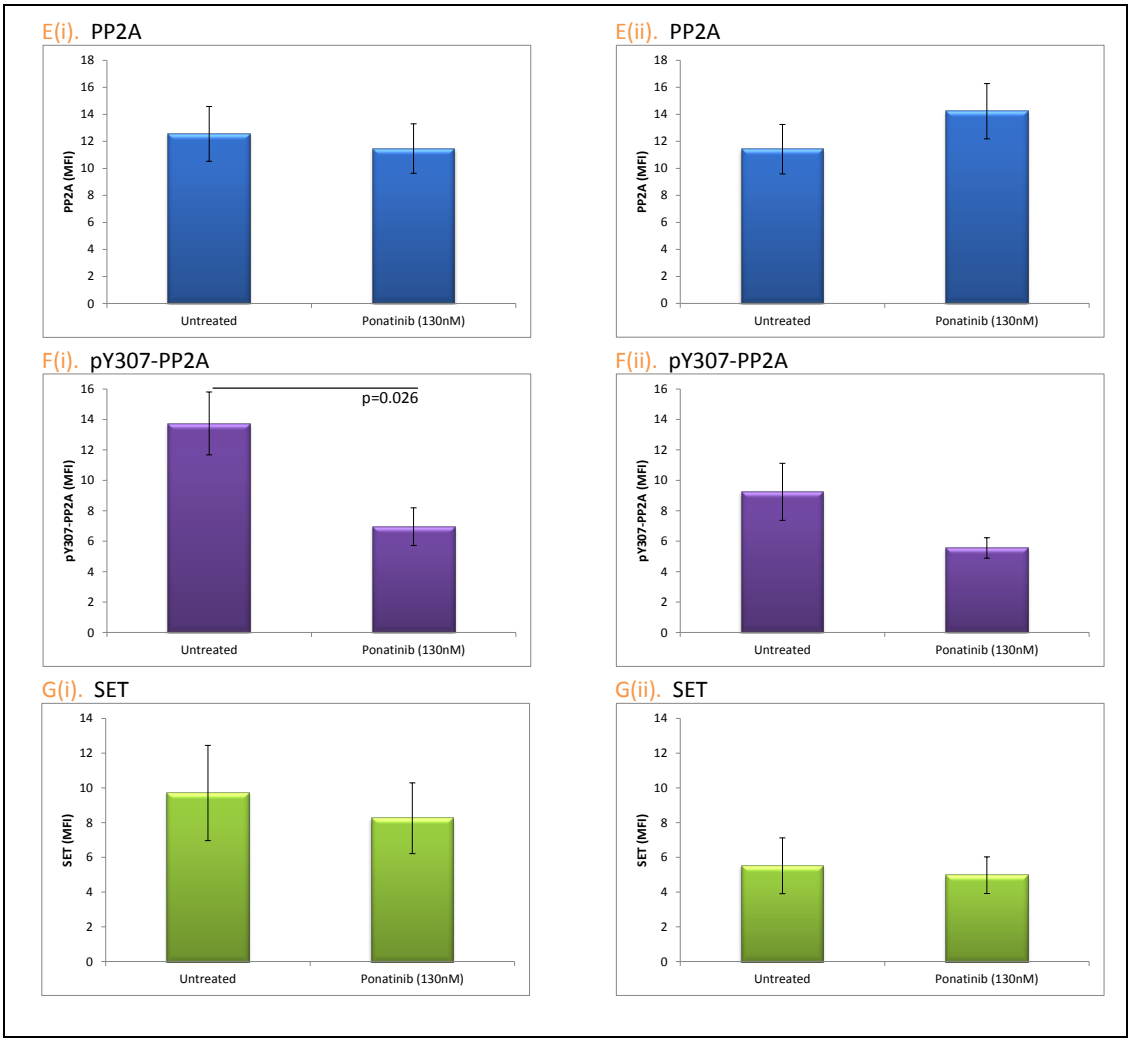

4.4.3.2.1. Results Summary: short-term ponatinib treatment

Similarly to 2G TKIs, ponatinib significantly decreases BCR-ABL1 activity irrespective of basal CIP2A protein; this decrease is apparent in both CML cell lines and treatment naïve CP-CML. Ponatinib also overcomes high CIP2A, leading to its decrease, along with other of the CIP2A/PP2A pathway proteins. Interestingly, ponatinib is the only TKI that affects this pathway in low CIP2A expressing cells, suggesting a more potent inhibition of CIP2A that is effective even at lower levels.

4.4.3.3. Long-term Ponatinib Treatment

The ponatinib trial PACE recruited CML patients that had failed previous treatments, including second generation TKIs. The CIP2A levels of six enrolled patients were measured. These data were collected from patient samples taken at trial entry point and thus are ponatinib-naïve samples. Unfortunately, no follow-up samples were available for comparison. Here, the clinical outcomes of the six patients are discussed and their patient information summarised in **Table 4.2**.

Table 4.2. Patient characteristics of ponatinib-treated CML.

UPN	SEX (M/F)	AGE	GENETIC MUTATION (Y/N)	CIP2A LEVEL (H/L)	CLINICAL OUTCOME/TIME (months)
083	F	63	Y (abl1 KD)	Low	CCR / 19
084	F	74	N	High	CCR / 2
085	M	76	Y (abl1 KD)	High	NO RESPONSE
086	M	61	Y (T315I)	Low	NO RESPONSE
087	F	69	Y (abl1 KD)	Low	DIED / 6
088	M	60	N	High	DIED / 1

Six CML patients that had failed to respond to previous TKIs and thus were prescribed ponatinib were studied. Two achieved a CCR, two died and two had achieved no response. All patients were over 60 years of age. Of these patients, three had a high CIP2A level and three had a low CIP2A level at the time of beginning ponatinib treatment (diagnostic samples were unavailable for analysis).

High CIP2A patients

UPN084: This patient had a high CIP2A level (MFI=17.75) at the start of ponatinib treatment, but achieved a CCR after only two months on ponatinib. It can be hypothesised that the high levels of CIP2A were depleted by ponatinib, as in the *in vitro* TKI assay, supporting **Figure 4.9**.

UPN085: This patient had the highest CIP2A level (MFI=90.32) and a*BCR-ABL1* KD mutation. At the time of treatment discontinuation after 18 months of therapy, no response had been achieved though no disease progression had been recorded. It is prudent to highlight, however, that patient UPN083 took longer than this to achieve CCR.

UPN088: This patient had a high CIP2A level (MFI=27.39), but no *BCR-ABL1*KD mutation. As this patient died after only a single month of ponatinib it is possible that this patient had progressed too far for ponatinib to be effective.

Low CIP2A patients

UPN083: This patient had developed a *BCR-ABL1* KD mutation by commencement of ponatinib, yet achieved CCR after 19 months.

UPN086: This patient was positive for the T315I mutation. The patient had a low CIP2A level, though regardless of this, T315I renders imatinib and all 2G TKI treatments unsuccessful and the patient would only have minimal treatment options; including ponatinib if available. The patient did not achieve a response on ponatinib, but actually only received ponatinib for a period of two months. It is possible that a response may have been reached if ponatinib had continued.

UPN087: This patient had a low CIP2A level. She also had a *BCR-ABL1* KD mutation, which can affect the efficacy of TKI treatment. Additionally, the time taken to swap to ponatinib therapy may have been too long to rescue the disease and halt its advancement.

Though various assumptions can be made when analysing individual cases, these six patients are so varied in their clinical outcomes, their treatment histories and their length of treatment exposure and are therefore impossible to analyse collectively. Analysis of a larger cohort would be necessary to thoroughly investigate the implications of the CIP2A/PP2A pathway in ponatinib-treated CML long term.

4.5. Discussion

Due to the impressive results of the IRIS trial and the 'expanded access' follow-up studies, many CML patients are initially treated with imatinib, though resistance still persists in at least one third of patients(Francis et al., 2013; C. Lucas et al., 2008). This resistance is often attributed to a variety of *BCR-ABL1* mutations, against which imatinib is not effective. Newer TKIs, including dasatinib, nilotinib and ponatinib were designed to combat these mutations in addition to being more potent BCR-ABL1 inhibitors.

The second generation TKI trials DASISION and ENESTnd showed superior response rates of dasatinib and nilotinib over imatinib as a first line therapy; MMR rates at 2 years follow-up were 64/46% (dasatinib/imatinib) and 71/67/44% (nilotinib 300mg/nilotinib 400mg/imatinib) respectively(H. M. Kantarjian et al., 2011; H. M. Kantarjian et al., 2012). However, there is still no direct indication that the poor prognosis of patients given second generation TKIs after imatinib failure can be rescued by these newer treatments. Therefore, it becomes imperative, to identify whether a patient should be prescribed the newer TKIs initially to avoid these circumstances.

This chapter builds on the observation in Chapter 3, of a superior clinical response in high CIP2A patients treated initially with dasatinib or nilotinib in comparison to imatinib.

The initial experimental design did not take into account the varying cell populations within a patient sample at different points throughout treatment. Untreated CML will have an abundance of malignant cells circulating within the peripheral blood. However, the effectiveness of TKIs in targeting the circulating leukaemic cell populations and reducing the tumour burden, leads to the malignant cells being depleted and replaced by their normal counterparts. Thus, in comparing diagnostic and long term follow-up samples it is impossible to quantify the differences in oncogenic protein levels that are abnormal in only the leukaemic cell populations (**Figures 4.2**-**4.4**). Therefore, a short-term in vitro TKI assay was designed that investigated the effects of imatinib, dasatinib and nilotinib on molecular levels of the CIP2A/PP2A pathway proteins in diagnostic patient samples (**Figure 4.5**).

The main finding of this chapter is shown in **Figure 4.5 A(i)**; *2G TKIs but not imatinib will suppress CIP2A protein expression, despite all three TKIs having broadly equivalent effects on BCR-ABL1 activity (assessed by pCrKL/CrKL).* Similar basal levels of BCR-ABL1 activity can be seen in both cohorts, regardless of CIP2A protein level and a significant reduction in kinase activity, irrespective of TKI treatment type (**Figure 4.5 B(i)** and **(ii)**). However, additional effects of dasatinib and nilotinib upon other parts of the CIP2A/PP2A pathway that are not apparent in imatinib treated cells can also be seen in **Figure 4.5**. Total c-Myc and stabilised c-Myc pS62 are both decreased by all three TKIs in high CIP2A cohorts (**Figure 4.5 C(i)** and **D(i)**), but only 2G TKI treatment causes the levels of inactive PP2A (pY307-PP2A) to fall in these patients (**Figure 4.5 F(i)**).

This chapter strongly suggests that the reason for superior response rates seen in dasatinib/nilotinib treated CML (**Chapter 3**) is due to additional molecular targeting of the CIP2A/PP2A pathway. **Figure 4.5** suggests that nilotinib and dasatinib, but not imatinib, also target CIP2A, causing CIP2A protein levels to decrease. This in turn alleviates the inhibitory action of CIP2A over PP2A, and thus inactive PP2A levels also fall. However, it is important to note that dasatinib and nilotinib may act either directly or indirectly upon CIP2A to produce the results seen in this chapter and that other proteins not investigated in this thesis may also be involved.

The latter part of this chapter looked briefly at the 3G TKI ponatinib and its effects upon the CIP2A/PP2A pathway.

Despite the availability of several licenced TKIs, treatment resistance in CML remains a problem. A delayed response to TKI treatment can increase the risk of transformation to accelerated phase or blast crisis; increase probability of a later loss of response and the risk of developing further genetic mutations. Emerging evidence is supporting this thesis's biological data that initial treatment with more potent (2G and 3G) TKIs may improve long term CML outcomes(H. Kantarjian et al., 2010; H. M. Kantarjian et al., 2011; H. M. Kantarjian et al., 2012; Saglio et al., 2010; Savona & Saglio, 2013). Newer TKIs have a broader spectrum of molecular targets and greater mutational coverage, therefore the likelihood of emerging resistance and subsequent disease progression is significantly lowered. However, of the newer TKIs, ponatinib is the only treatment that has shown efficacy against all mutations, including the 'gatekeeper' mutation, T315I.

Treatment of cell lines and patient cells (**Figure 4.8 B** and **Figure 4.9 B**) with ponatinib showed a subsequent depletion of pCrKL/CrKL. This decrease in BCR-ABL1 activity following ponatinib exposure was mirrored by a significant decrease of CIP2A, c-Myc, c-Myc pS62 and pY307-PP2A in high CIP2A expressing cells. Though these data are similar to the 2G TKI experiments, it is interesting to note that low CIP2A levels are further diminished with ponatinib treatment, which was not observed with dasatinib or nilotinib.

The ponatinib-induced reduction in CIP2A was observed in both cell lines and patient samples. CIP2A is known to stabilise c-Myc by maintaining its phosphorylated form, and also prevents the de-phosphorylation of PP2A, at its Y307 residue, thus deactivating it. As a result, the visible reduction in pY307-PP2A seen in high CIP2A expressing cells, coincides with the significant decrease in CIP2A and c-Myc pS62 protein levels. However, again caution must be used in interpreting the results of this experiment as the TKI-induced decrease of CIP2A levels may be either direct or indirect and cannot be fully deciphered here.

The observed reduction in CIP2A levels is very promising when considered clinically. Ponatinib is already proving effective in the combat of *BCR-ABL1*, T315I and other *BCR-ABL1* mutants; these results would tentatively indicate its potential use as an additional treatment option for patients deemed to have high diagnostic CIP2A protein levels. However, clinical trials had a significant proportion of patients with serious cardiovascular events. Though these preliminary results indicate a positive molecular effect upon the CIP2A/PP2A pathway, the risks associated with prescribing this drug may far out-weigh the potential benefits except in advanced disease or possibly late chronic phase refractory to all other TKIs. While those patients with the T315I mutation have no other TKI options at the moment, it would be wise to limit the use of ponatinib in other circumstances.

Chapter 5: Manipulating the CIP2A/PP2A Pathway

5.1. Introduction

All tyrosine kinase inhibitors are shown to successfully inhibit BCR-ABL1 activity in both CML cell lines and patient samples, yet their actions upon the CIP2A/PP2A pathway differ. This thesis has so far shown an inhibition of CIP2A and reactivation of PP2A by dasatinib, nilotinib and ponatinib that is not mirrored by imatinib treatment.

Manipulation of the CIP2A/PP2A pathway may lead to a better understanding of CML molecular pathophysiology. Observing any potential knock-on effects to genetic and post-translational alterations may even add to a better comprehension of how or where to target this pathway with future therapies.

5.2. Aims

Previous chapters have looked at the effects of TKIs upon the CIP2A/PP2A pathway. This chapter focuses on the manipulation of this pathway by specific alteration of the level of CIP2A within BCR-ABL1-positive cells. Additionally, experiments to inhibit and reactivate PP2A were carried out. The more specific aims of this chapter were to:

- Use siRNA to knock down *CIP2A* levels in high and low CIP2A cell lines and observe the effects upon proteins within the CIP2A/PP2A pathway
- Optimise *CIP2A* transient transfection in low and high CIP2A cell lines
- Investigate the effects of successful *CIP2A* transfection upon proteins within the CIP2A/PP2A pathway
- To inhibit/activate PP2A and observe the effects upon proteins within the CIP2A/PP2A pathway

5.3. Methods

In this chapter, K562 (high CIP2A) and KCL22 (low CIP2A) cell lines were analysed using standard cell culture (**Section 2.4**), *in vitro* TKI cultures (**Section 2.4.3**), flow cytometry (**Section 2.5**), qRT-PCR (**Section 2.9.3**), ELISA (**Section 2.7**), confocal microscopy (**Section 2.8**), siRNA (**Section 2.11**) and gene transfection (**Section 2.12**). Student t-tests were used for statistical analysis.

5.4. Results

It is known that varying levels of CIP2A expression are found in many cancers; these differing CIP2A levels correspond with changes in PP2A activity. In work shown thus far, CIP2A levels show an inverse correlation with the level of PP2A activity. To investigate this relationship further, the expression of CIP2A was directly targeted to be decreased using siRNA or increased by transient transfection.

5.4.1. siRNA of CIP2A

CIP2A knock down experiments were performed to show the effects of decreasing CIP2A on proteins within the CIP2A/PP2A pathway. The knock down of *CIP2A* was successful in both high and low CIP2A cell lines (**Figure 5.1 A(i)**; p<0.005 and **(ii)**; p=0.005). Following this, BCR-ABL1 activity, measured by pCrKL/CrKL ratio, decreased significantly (**Figure 5.1 B(i)**; p=040 and **(ii)**; p=0.042) suggesting a feedback mechanism between CIP2A and BCR-ABL1. Additionally, depleting *CIP2A* via siRNA led to the decrease of both c-Myc (**Figure 5.1 C(i)**; p=0.014 and **(ii)**; p=0.033) and its stabilised phosphorylated form, c-Myc pS62 (**Figure 5.1 D(i)**; p=0.009 and **(ii)**; p=0.006). SET protein decreased in both high and low CIP2A cell lines, though neither fall in SET protein was significant (**Figure 5.1 G(i)** and **(ii)**).

The level of inactive PP2A, measured by its phosphorylation at tyrosine 307, decreased significantly (**Figure 5.1 F(i)**; p=0.039 and **(ii)**; p=0.043) following

CIP2A knock down, though total PP2A protein did not alter (**Figure 5.1 E(i)** and **(ii)**). This shows an increase in the proportion of active PP2A within the cells following a fall in CIP2A level.

Figure 5.1. Effects of CIP2A siRNA upon the CIP2A/PP2A pathway, shown in BCR-ABL1 positive cell lines. Two BCR-ABL1 positive cell lines of differing basal CIP2A protein concentrations were used; (i) K562 (high CIP2A) and (ii) KCL22 (low CIP2A). For each protein analysed, the control siRNA and *CIP2A* siRNA results are shown. A. CIP2A, B. pCrKL/CrKL, C. c-Myc, D. c-Myc pS62, E. PP2A, F. pY307-PP2A, G. SET.

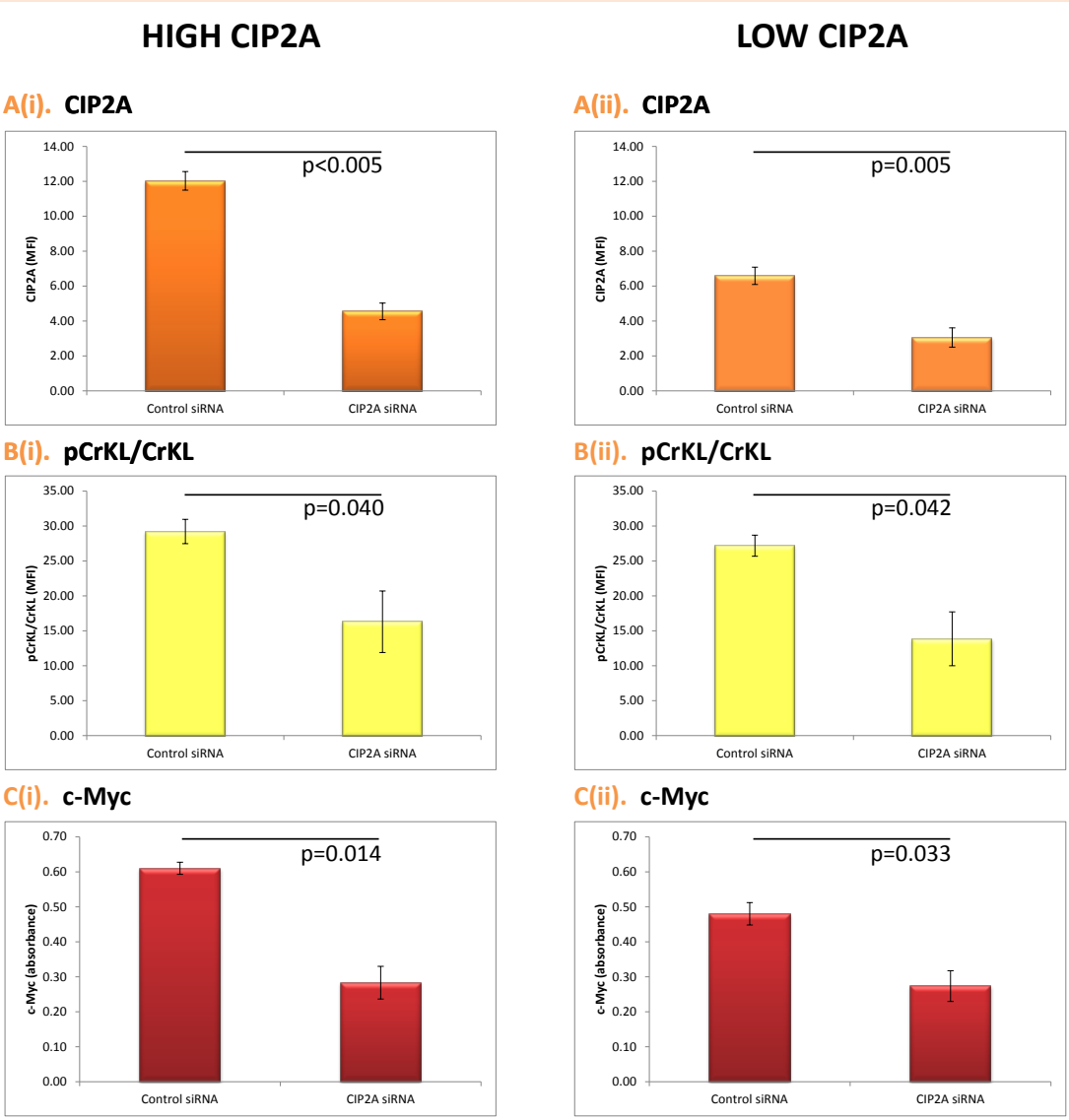

D(i). c-Myc pS62

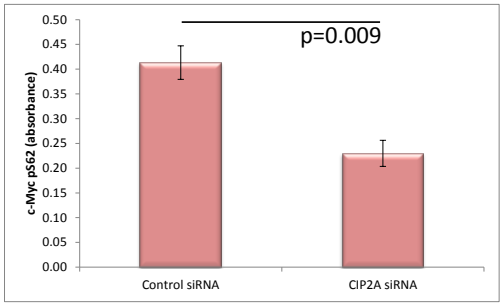

D(ii). c-Myc pS62

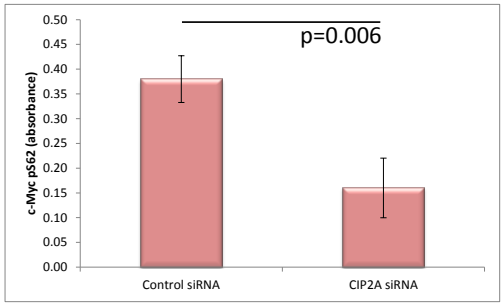

E(i). PP2A

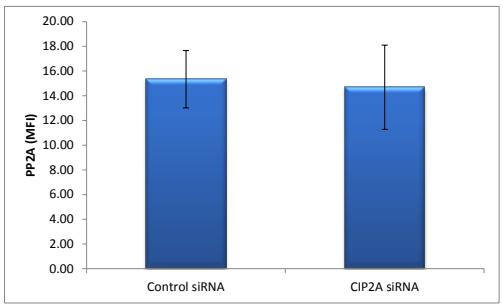

E(ii). PP2A

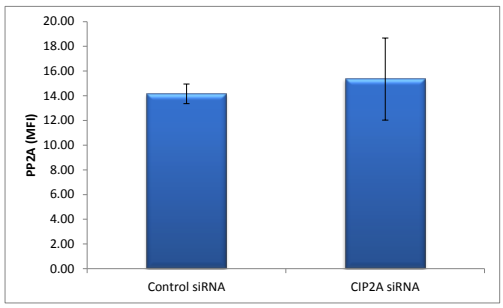

F(i). pY307-PP2A

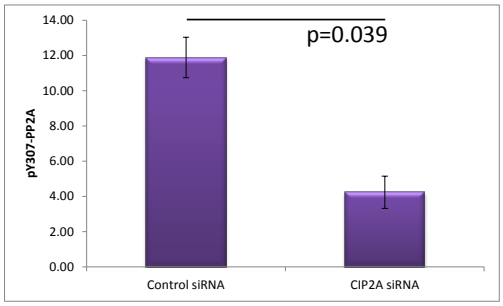

F(ii). pY307-PP2A

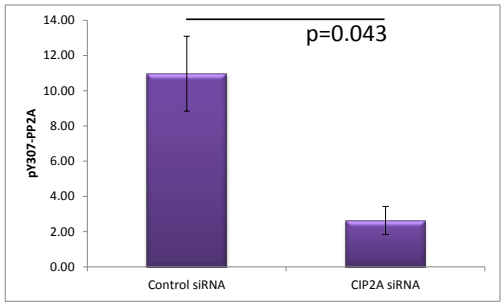

G(i). SET

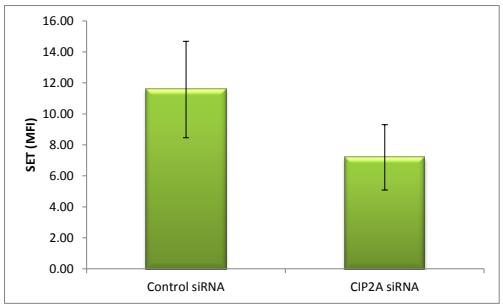

G(ii). SET

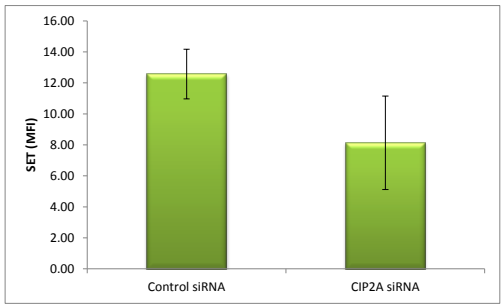

5.4.2. Transient Transfection of *CIP2A*

Next, the effects of directly increasing CIP2A protein levels were investigated using transient transfection of *CIP2A* into the BCR-ABL1 positive cell lines K562 and KCL22. The pCMV6-AC-GFP vector used included a GFP-tagged *CIP2A* gene to more easily observe the increased expression of CIP2A. **Figure 5.2** shows the design of this 6.6kb plasmid, designed and bought from Origene (**Section 2.12.3**). A mock transfection plasmid, tagged only with GFP was used as a control throughout this work. This was available within our lab, given by Dr John Allen, Department of Molecular and Clinical Pharmacology, University of Liverpool.

Figure 5.2. Design of GFP-tagged *CIP2A* plasmid. The vector was designed for rapid expression of bright fluorescence in mammalian cells, with a C-terminal GFP tag. The image highlights the location of the inserted *CIP2A* gene within the vector and the restriction enzymes (Sgf I and Mlu I) used to create it.

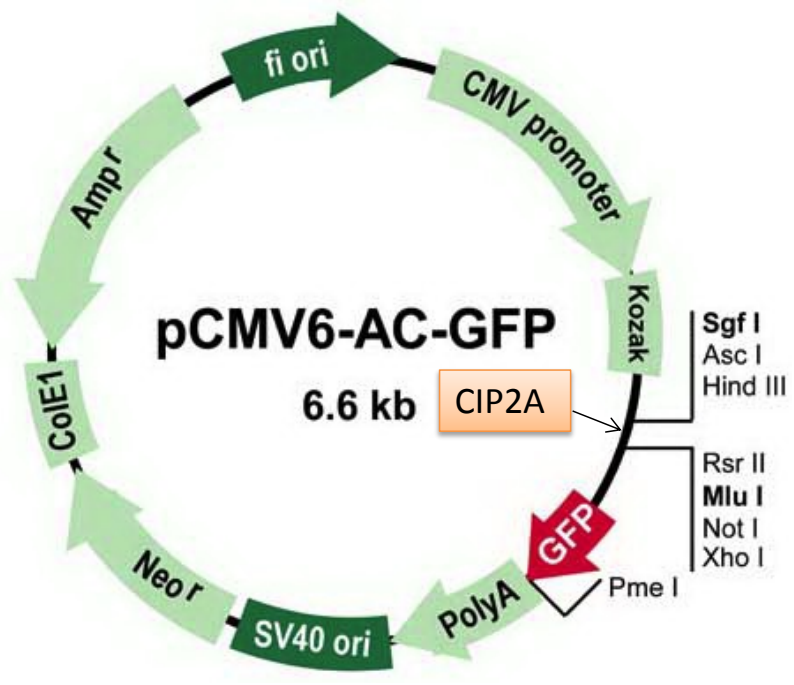

5.4.2.1. Analysing *CIP2A* Transient Transfection

Analysis of the transient transfection was performed using flow cytometry and cell microscopy to confirm a positive transfection. As the *CIP2A* plasmid included a GFP tag, fluorescence at this wavelength corresponded to positive expression of the transfected *CIP2A*.

Transfection Efficiency

To analyse the efficiency of each transfection, the difference in GFP fluorescence (FL1) of a transfected and untransfected sample was measured. The percentage of cells from within the transfected sample that express more GFP than the untransfected cells, gives the transfection efficiency (i.e. 'CIP2A % gated' in **Figures 5.4** and **5.5**).

Intracellular Protein Expression

Measuring the levels of intracellular protein expression in transiently transfected cells proved more complex. **Figure 5.3** shows an example of intracellular protein analysis in K562 cells. Firstly, samples were gated to include only live cells (**Figure 5.3 A(i)**, **B(i)** and **C(i)**). These live cells were then gated according to their GFP fluorescence on FL-1 (**Figure 5.3 A(ii)**, **B(ii)** and **C(ii)**). This gate was set according to the untransfected cells; untransfected cells would not express GFP. Therefore, when using this gate for GFP and GFP-*CIP2A* transfected cells, this gate should encompass purely the transfected K562 cells within the sample.

Finally, the intracellular protein concentration (i.e. CIP2A, PP2A etc.) of the GFP positive (gated) cells was analysed on FL-2 as previously described according to the geometric mean. Of note, the number of events (cells) detected in each sample was taken into consideration; any sample with less than 50 gated cells (vi) was disregarded.

Figure 5.3. An example of protein level analysis of transiently transfected BCR-ABL1 positive cells. Protein levels were analysed by flow cytometry. This example shows CIP2A protein level analysis of K562 cells following the transient transfection of *CIP2A*. For each sample, A. untransfected, B. mock transfected and C. *CIP2A* transfected cells were analysed. 10000 events were measured per sample.

For A-C, (i) Events measured; live cells are gated, (ii) GFP fluorescence of live cells; high GFP fluorescing cells are gated, (iii) CIP2A protein of GFP fluorescing cells, (iv) logarithmic plot of panel (iii). Sample statistics are also shown (v).

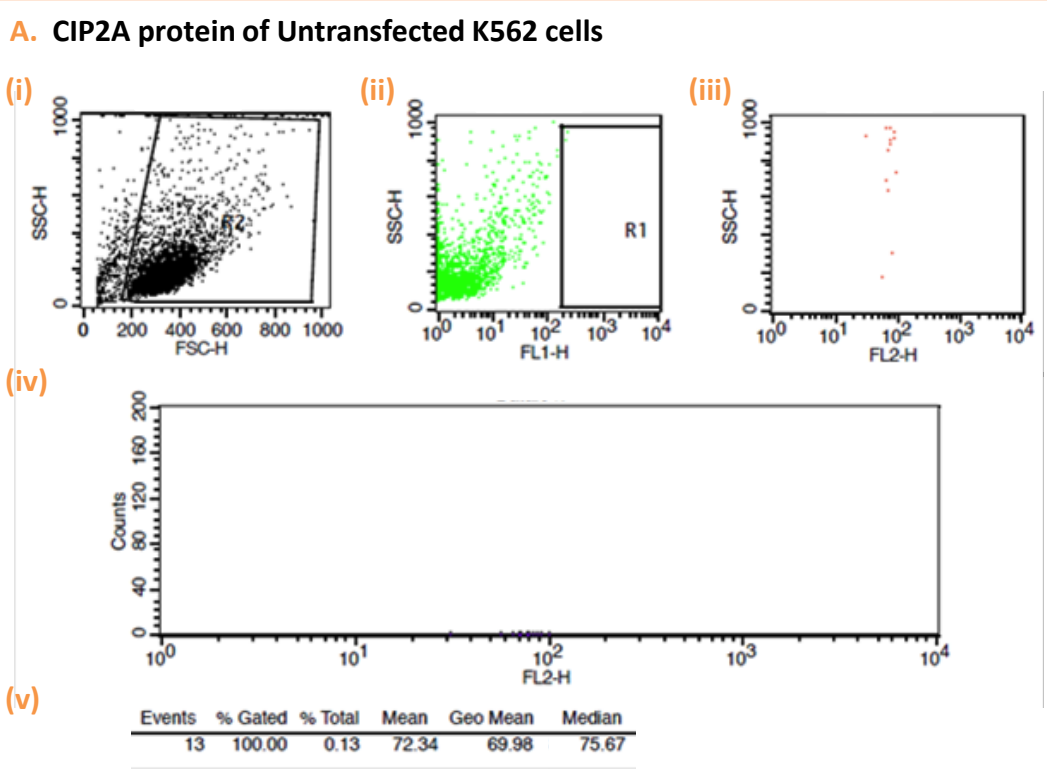

B. CIP2A protein of MOCK Transfected K562 cells

(i) (ii) (iii)

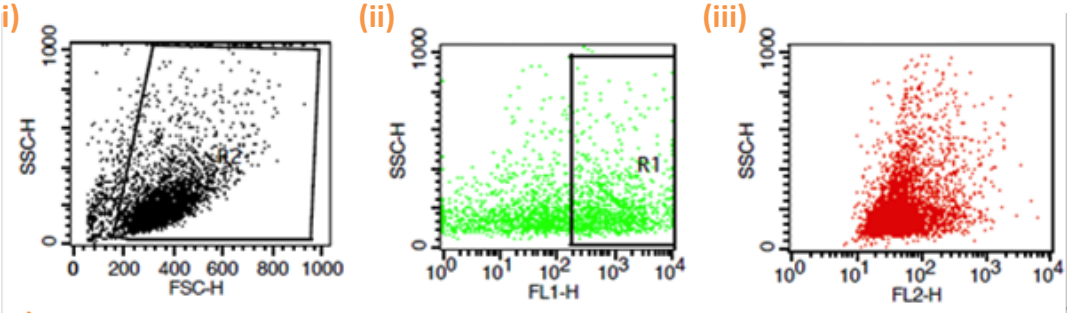

(iv)

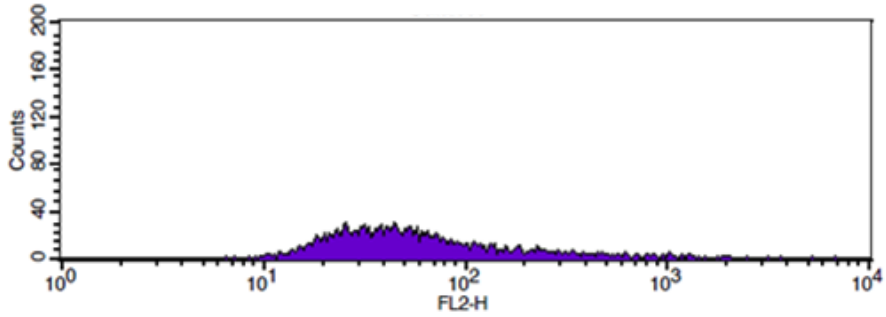

(v)

Events	% Gated	% Total	Mean	Geo Mean	Median
4310	100.00	43.10	91.50	52.24	44.51

C. CIP2A protein of CIP2A Transfected K562 cells

(i) (ii) (iii)

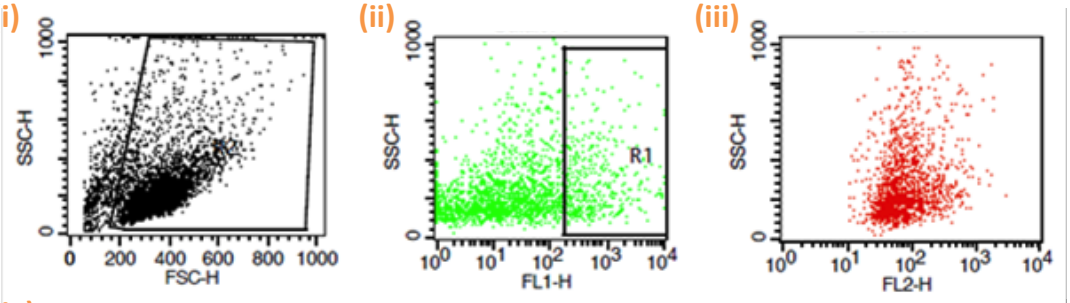

(iv)

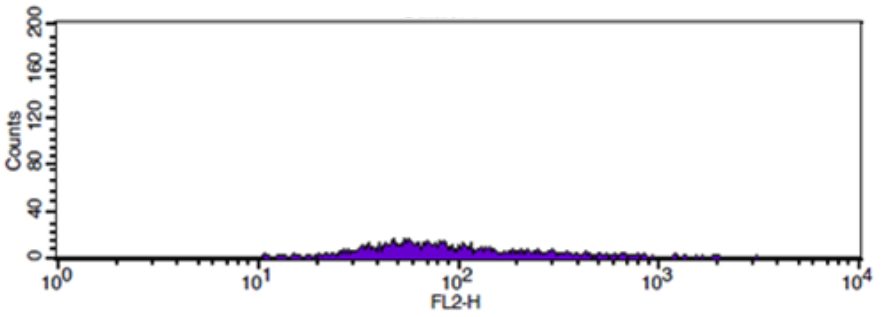

(v)

Events	% Gated	% Total	Mean	Geo Mean	Median
1667	100.00	16.67	122.64	80.80	70.41

5.4.2.2. Optimising *CIP2A* Transient Transfection

To optimise the transient transfection of *CIP2A*, the concentration of *CIP2A* plasmid used was varied and analysed to see which gave optimum transfection efficiency. Additionally, both low (KCL22) and high (K562) CIP2A-expressing cell lines were used.

Initially, 2µg/ml of *CIP2A* plasmid was transfected into both cell lines and analysed using flow cytometry after a 24 hour incubation (**Figure 5.4**). A transfection efficiency of only 31.88% in K562 cells was measured, which was not sufficient integration of the plasmid to use for further work. An increase to 5µg/ml was next chosen (**Figure 5.5**), which yielded a much more efficient 73.03% in the K562 cell line. Though a high efficiency of 71.04% was seen in KCL22 cells at 2µg/ml, this increased to 82.56% with a 5µg/ml plasmid concentration and thus this higher concentration was used for further work. Of note, the *CIP2A* transfection efficiency was also analysed using microscopy to ensure 5µg/ml was sufficient (**Figure 5.5 B** and **C**).

Figure 5.4. Optimisation of *CIP2A* Transient Transfection; initial transfection. Transfection efficiency analysis of KCL22 and K562 cells using an initial *CIP2A* plasmid concentration of 2µg/ml. Analysis was performed using flow cytometry. Two BCR-ABL1 positive cell lines of varying initial CIP2A protein concentrations were transfected; (i) KCL22 (low CIP2A) and (ii) K562 (high CIP2A).

A(i). KCL22 cells

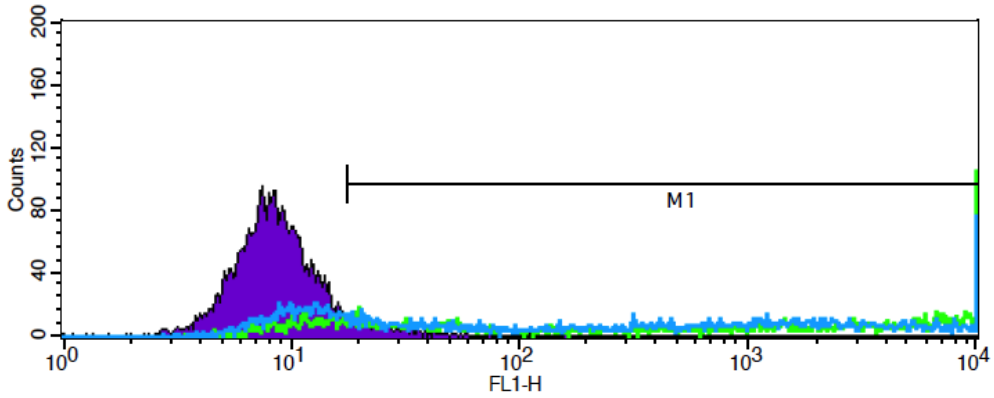

	Events	% Gated	% Total
Untransfected:	4390	100.00	43.90
Mock transfected:	3689	84.03	36.89
CIP2A transfected:	3466	71.04	34.66

:Untransfected
:GFP control plasmid
:CIP2A 5µg plasmid

A(ii). K562 cells

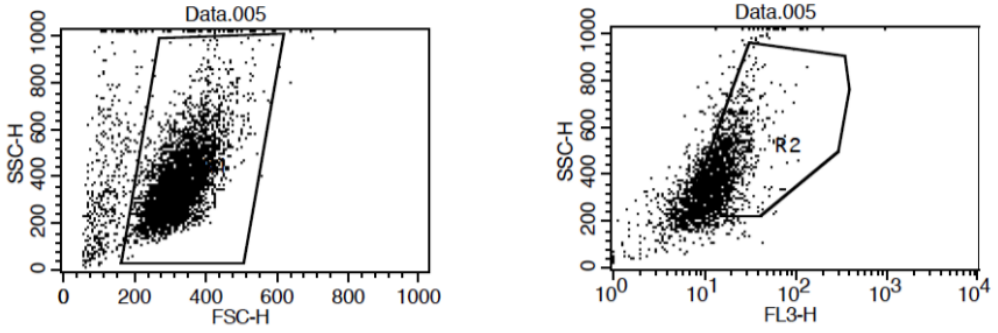

Untransfected:
Mock transfected:
CIP2A transfected:

:Untransfected
:GFP control plasmid
:CIP2A 5µg plasmid

Figure 5.5. Amended *CIP2A* Transient Transfection. Transfection efficiency analysis of KCL22 and K562 cells using the higher concentration of 5µg/ml. Two BCR-ABL1 positive cell lines of varying initial CIP2A protein concentrations were transfected; (i) KCL22 (low CIP2A) and (ii) K562 (high CIP2A). Transfection efficiency was confirmed using both flow cytometry (A) and microscopy (B and C). Microscopy magnification: 1cm: 200µm.

A(i). KCL22 cells

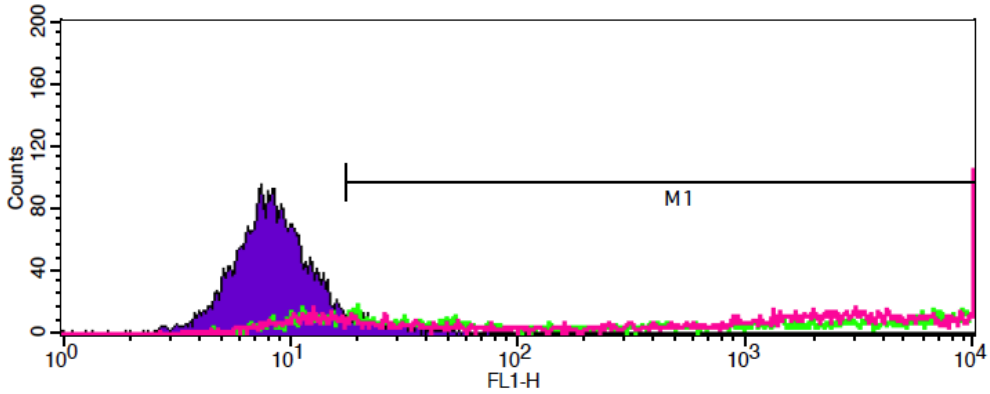

	Events	% Gated	% Total
Untransfected:	4390	100.00	43.90
Mock transfected:	3689	84.03	36.89
CIP2A transfected:	3433	82.56	34.33

:Untransfected
:GFP control plasmid
:CIP2A 5µg plasmid

A(ii). K562 cells

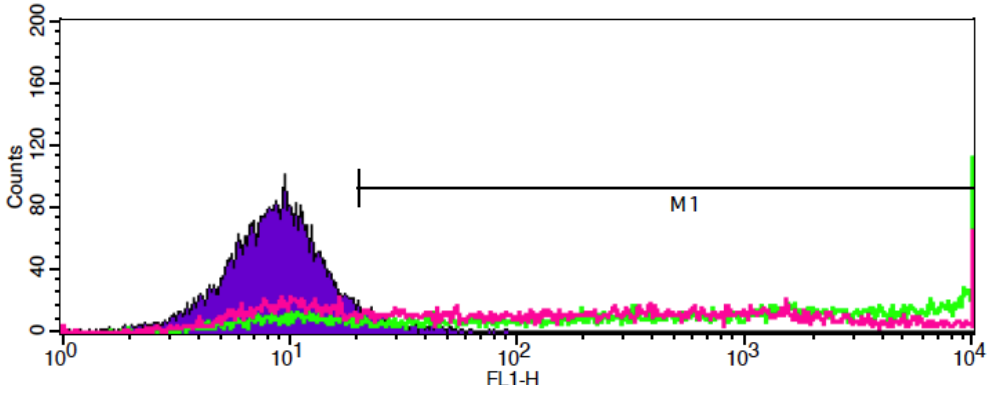

	Events	% Gated	% Total
Untransfected:	8160	100.00	81.60
Mock transfected:	7197	88.20	71.97
CIP2A transfected:	5367	73.03	53.67

:Untransfected
:GFP control plasmid
:CIP2A 5µg plasmid

B(i). **KCL22: Untransfected**

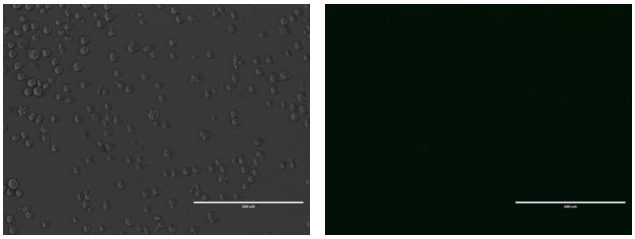

B(ii). **KCL22: Mock Transfected**

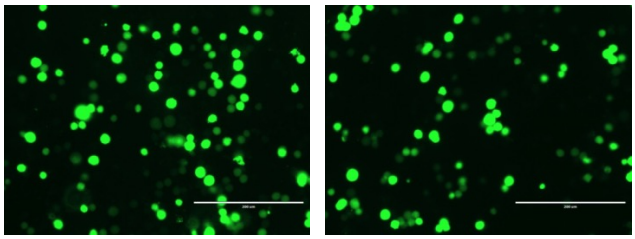

B(iii). **KCL22: CIP2A Transfected**

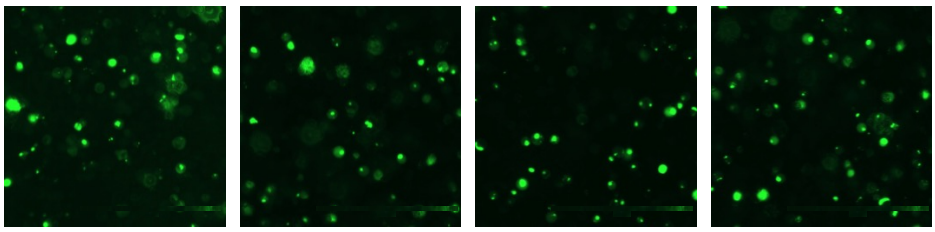

C(i). **K562: Untransfected**

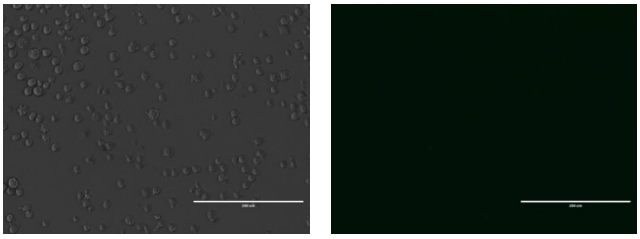

C(ii). **KC562: Mock Transfected**

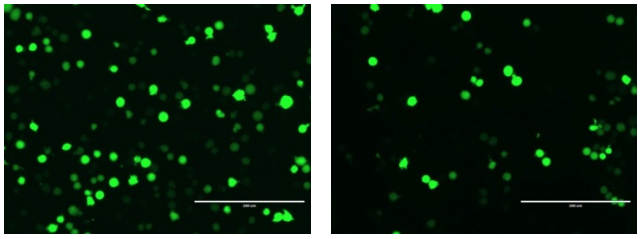

C(iii). **K562: CIP2A Transfected**

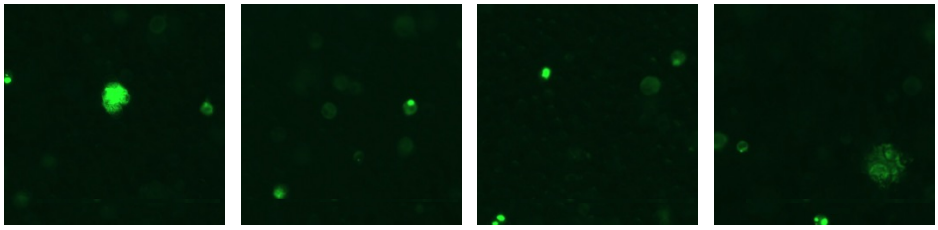

5.4.2.3. *CIP2A* Transient Transfection Results

Following the successful transient transfection of *CIP2A* into KCL22 and K562 cells, flow cytometry was used to analyse the effects on other CIP2A/PP2A pathway proteins.

The CIP2A protein level is shown to increase following successful transient transfection in both K562 and KCL22 cells (**Figure 5.6 A(i)**; p=0.002 and **(ii)**; p=0.029). Subsequent increases in stabilised c-Myc pS62 protein (**Figure 5.6 D(i)**; p=0.017 and **(ii)**; p=0.020) are also apparent. BCR-ABL1 activity (**Figure 5.6 B(i)** and **(ii)**; p=0.001) and pY307-PP2A (**Figure 5.6 F(i)** and **(ii)**; p=0.037) also increase in both K562 and KCL22 cells, though a significant rise is only observed in the low CIP2A cell line.

No significant change is observed in total c-Myc (**Figure 5.6 C**), PP2A (**Figure 5.6 E**) or SET (**Figure 5.6 G**) levels following the rise in CIP2A.

Figure 5.6. Protein Levels of BCR-ABL1 positive cells transiently transfected with *CIP2A*. Two BCR-ABL1 positive cell lines of varying initial CIP2A protein concentrations were transfected; (i) KCL22 (low CIP2A) and (ii) K562 (high CIP2A). For each protein analysed, untransfected, GFP-transfected and *CIP2A*-GFP transfected results are shown. A. CIP2A, B. pCrKL/CrKL, C. c-Myc, D. c-Myc pS62, E. PP2A, F. pY307-PP2A, G. SET.

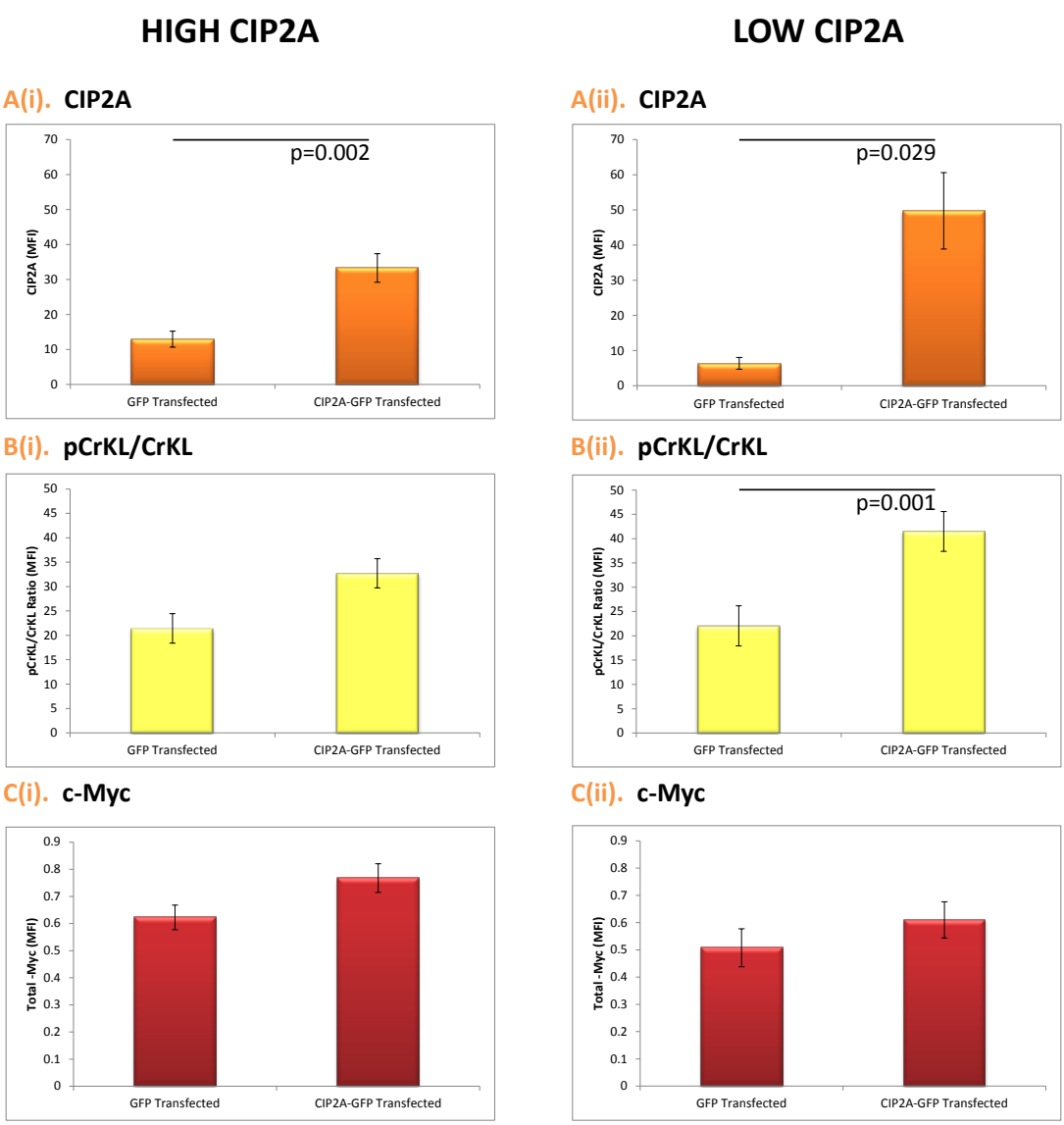

D(i). c-Myc pS62

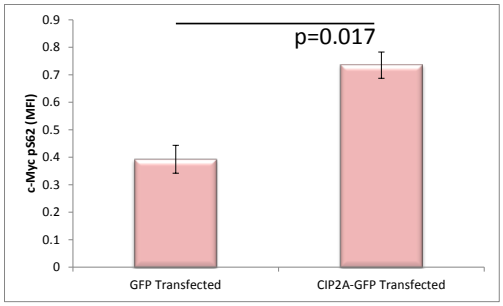

D(ii). c-Myc pS62

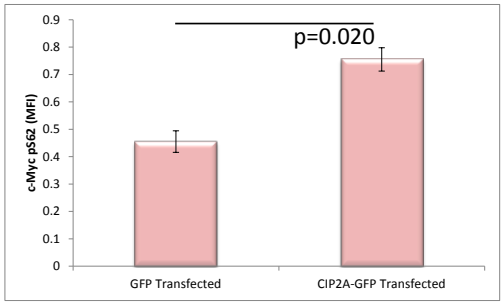

E(i). PP2A

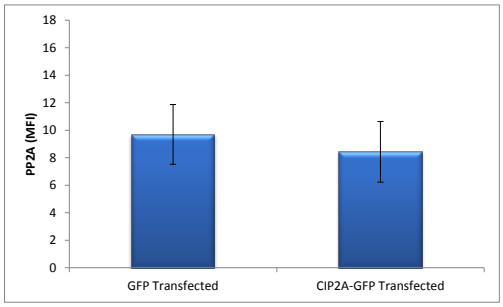

E(ii). PP2A

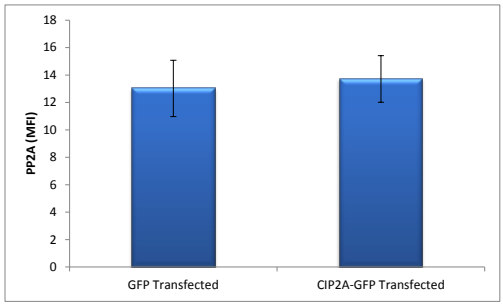

F(i). pY307-PP2A

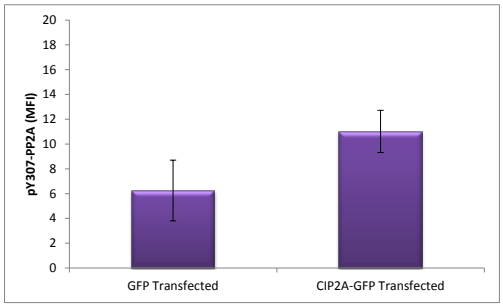

F(ii). pY307-PP2A

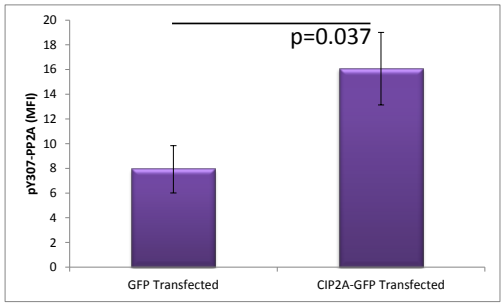

G(i). SET

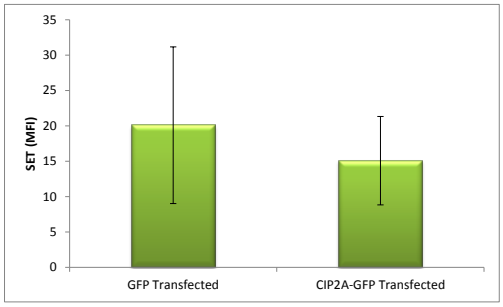

G(ii). SET

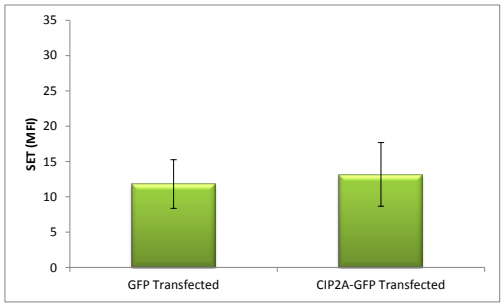

5.4.3. Manipulation of PP2A

It has been suggested that a feedback mechanism may occur upon BCR-ABL1 by PP2A. The data shown in **Chapter 4** suggest an additional role of 2G TKIs in suppressing CIP2A that is not seen with imatinib, despite a similar decrease in BCR-ABL1 activity following both imatinib and 2G TKI treatment. Whether this 2G TKI-specific effect on CIP2A is direct or indirect is not known. It was hypothesised that the more potent inhibition of PP2A (**Figure 3.6 E-F**) may play a role in the results that had been uncovered.

K562 cells were treated for 24 hours with PP2A activators FTY720 and forskolin, and also by the PP2A inhibitor okadaic acid. Protein levels were subsequently analysed by FACS, and the results are shown in **Figure 5.7**. Forskolin and FTY720 treatment not only increased PP2A levels, but showed an extreme drop in the levels of CIP2A. Conversely, okadaic acid treatment led to an increase in BCR-ABL1 activity, CIP2A levels and c-Myc stabilisation.

Figure 5.7. Effects of PP2A Activation/Inhibition on the CIP2A/PP2A Pathway. K562 cells were treated with forskolin, FTY720 and okadaic acid for 24 hours and then protein levels analysed using flow cytometry.

A(i). **PP2A**

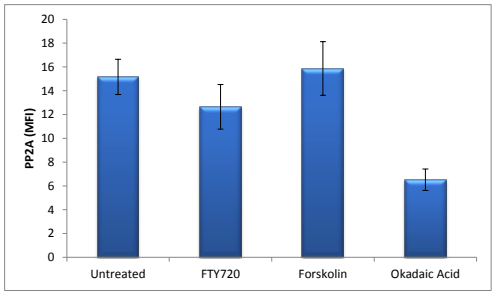

B(i). **pY307-PP2A**

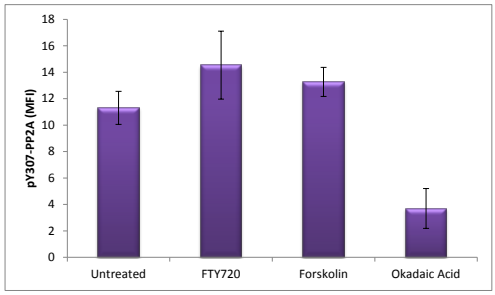

C(i). **CIP2A**

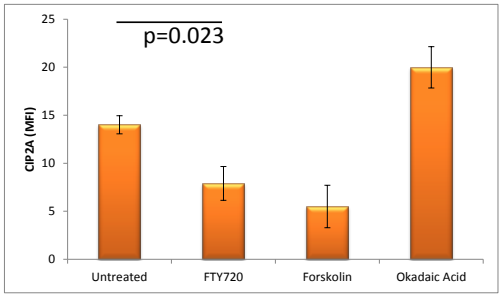

D(i). **pCrKL/CrKL**

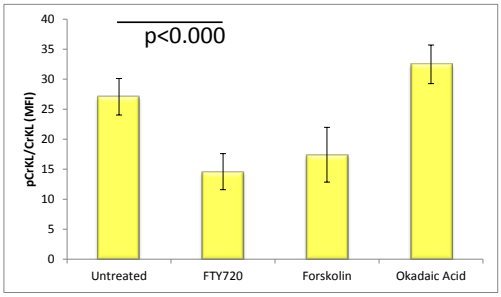

E(i). **c-Myc**

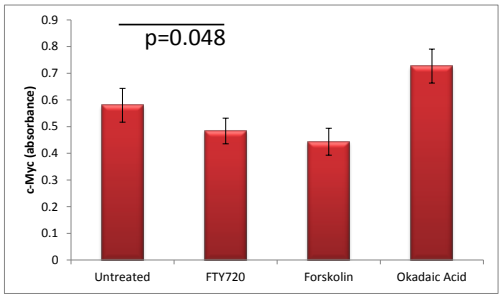

F(i). **c-Myc pS62**

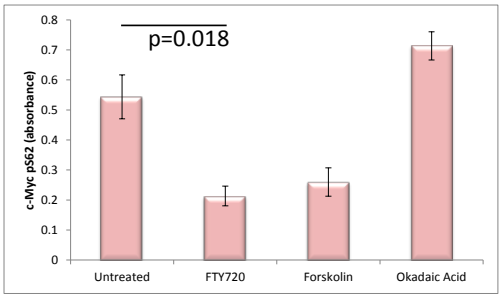

G(i). **SET**

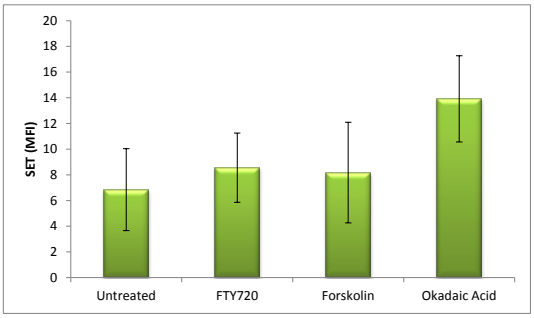

5.5. Discussion

Understanding the molecular pathophysiology of CML is key to developing more effective ways of treating this disease in the future. In **Chapters 3** and **4** I showed a variation in TKI effectiveness of targeting CIP2A. Unravelling the complex relationships between the components of the CIP2A/PP2A pathway may help us understand the reason behind these different effects.

Accordingly, *CIP2A* was directly targeted via siRNA and transient transfection, in order to observe the consequences of decreasing or elevating CIP2A. Decreasing *CIP2A* by siRNA caused a significant decrease in c-Myc, the stable c-Myc pS62 and inactive PP2A protein. On the other hand, *CIP2A* elevation by transfection leads to increased levels of these proteins. These data are in support of the published role of CIP2A; CIP2A inhibits the tumour suppressor activity of PP2A upon c-Myc(Junttila et al., 2007; Khanna et al., 2013). They also show that by removing this inhibition upon PP2A activity via *CIP2A* siRNA, the effects are reversed and PP2A inhibitory action upon c-Myc is restored.

Interestingly, specifically altering the expression of CIP2A also influences the level of BCR-ABL1 activity, as measured the by pCrKL/CrKL ratio. When *CIP2A* is knocked down by siRNA, BCR-ABL1 activity also falls, and increasing the CIP2A level leads to a rise in BCR-ABL1 activity. In **Chapter 4** it was shown that although imatinib inhibits BCR-ABL1 activity, it does not have a significant effect upon CIP2A level, which it is assumed continues to function

independently of BCR-ABL1. The data in this chapter are compatible with the view that a feedback mechanism may exist with CIP2A acting either directly or indirectly through PP2A, upon BCR-ABL1(C. M. Lucas et al., 2011; Juandong Wang et al., 2014).

To add to my information on this complex pathway, the PP2A activators FTY720 and forskolin and the PP2A inhibitor okadaic acid were used to treat K562 cells. Inhibition of PP2A activity increased CIP2A, stable c-Myc pS62 and BCR-ABL1 activity, and the inverse was apparent when treated with forskolin and FTY720. Though these data support the various findings of this pathway and suggest yet another feedback mechanism, this time involving PP2A and BCR-ABL1, it is not entirely known how the PP2A activators work upon their target. Without ensuring the direct targeting of PP2A, it cannot be clear whether forskolin or FTY720 are causing these results via off target effects, perhaps upon CIP2A or BCR-ABL1 themselves.

Chapters 3, **4** and **5** highlight the importance of CIP2A in the pathogenesis of CML. The initial promising observations of its use as a potential CML biomarker led to investigating its complex involvement within the CIP2A/PP2A pathway that is shown in this chapter. As I have shown that altering the levels of CIP2A consequently increases/decreases BCR-ABL1 activity, targeting CIP2A itself in future CML therapies may be an interesting avenue to pursue. Excitingly, the combination of a purposefully designed CIP2A inhibitor used alongside a TKI

may lead to an even greater inhibition of BCR-ABL1 and an improvement in clinical outcome, especially in CML patients partially refractory to TKIs.

Chapter 6: *CIP2A* Transcripts

6.1 Introduction

Splice variants of numerous genes have been shown to play different roles and have altered interacting partners. A single gene can encode many different protein isoforms, the expressions of which are tightly regulated by cells via different promoters and alternative splicing. In cancers, isoform expressions can vary to favour disease progression and treatment resistance. One well-studied example of this is the aberrant expression of human p53 isoforms, which actively favours cancer formation(Surget, Khoury, & Bourdon, 2013).

Alternative gene isoforms may have implications in CML progression and TKI resistance. With regards to the *CIP2A* oncogene, previous investigations into its role within CML have thus far focussed on protein expression and the involvement of this protein in post-translational modifications(C. M. Lucas et al., 2011). However, regulation occurring at a transcriptional level is yet to be explored in this malignancy.

This chapter presents novel information on the relative expression of two *CIP2A* transcripts previously unreported in any malignancy.

CIP2A is so far reported to have six different isoforms, of which only two are protein coding. No *CIP2A* splice variant has been investigated in any malignancy and thus the potential variation between patient expression and isoform involvement in treatment resistance is still entirely unknown.

Figure 6.1. Reported *CIP2A* isoforms. Data taken from *ensemble* gene database.

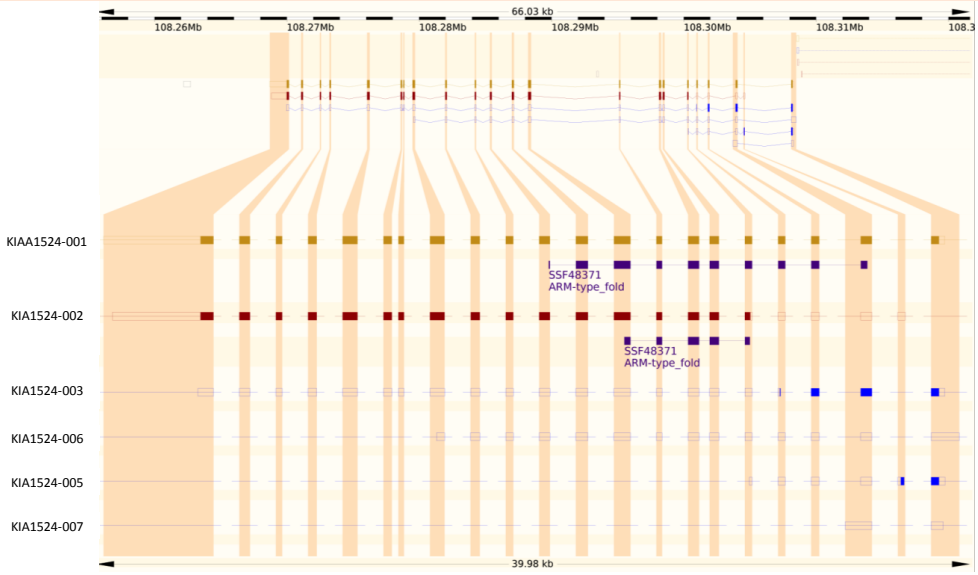

Name	Length (bp)	Length (aa)	Biotype
KIAA1524-001	4075	905	Protein coding
KIAA1524-002	3877	746	Protein coding
KIAA1524-003	2764	121	Nonsense mediated decay
KIAA1524-006	654	48	Nonsense mediated decay
KIAA1524-005	2014	-	Processed transcript
KIAA1524-007	511	-	Retained intron

Key

Boxes = exons

Lines = introns

Filled boxes = coding sequences (gold or red)

Unfilled boxes = untranslated regions (UTR)

Protein motifs and domains = purple

6.2. Chapter Aims

This chapter focuses on two reported *CIP2A* variants, aiming to investigate their possible presence and subsequent expression levels in CML. The main aims were to:

- Design primers to target two protein coding *CIP2A* variants.
- Investigate whether these *CIP2A* transcripts are present in BCR-ABL1 positive cell lines.
- Investigate whether these *CIP2A* transcripts are present, and at what levels, in CML patient samples taken at varying stages of the disease and of differing clinical outcomes.

6.3. Methods

In this chapter cell lines and patient and normal healthy volunteer PBMC samples were analysed using standard cell culture (**Section 2.4**), cell viability by PI (**Section 2.5.3**), RNA extraction (**Section 2.9.1**), cDNA synthesis (**Section 2.9.2**), manual PCR (**Section 2.9.4**), qRT-PCR (**Section 2.9.3**) and western blotting (**Section 2.6**). Clinical characteristics of patients used within this chapter are shown in **Table 6.1**. Student t-tests were used for statistical analysis.

6.4. Results

6.4.1. Designing *CIP2A* transcript primers

An initial search into the possible *CIP2A* variants(Database) identified two protein coding isoforms. The first isoform is the full length transcript, which spans 905 amino acids and the second a shorter isoform of only 746 amino acids. Full length *CIP2A* encompasses 21 exons in total. The shorter transcript has an alternative promoter situated within the intron between exons 1 and 2 as opposed to the 'normal' promoter site before exon 1. For clarity, the 'normal' exon 1 of the longer variant will be referred to as exon 1a and the alternative promoter of the shorter variant referred to as exon 1b. Similarly, the long and short isoforms are named *CIP2A-1a* and *CIP2A-1b*, respectively. Using the 'PyroMark Assay Design 2.0' software, optimal primer sites were identified to distinguish between *CIP2A-1a* and *CIP2A-1b* (**Figure 6.2**). (N.B. To confirm primer specificity the PCR products were sequenced, results checked using a BLAST search and confirmed to be identifying *CIP2A-1a* and *CIP2A-1b*.)

Figure 6.2. Summary of *CIP2A-1a* and *CIP2A-1b* primer positions. The *CIP2A-1a* reverse primer spans the exon1a/exon2 boundary; this does not exist within *CIP2A-1b*. The *CIP2A-1b* forward primer spans the exon1b/exon2 boundary; this does not exist within *CIP2A-1a*. Therefore, the primer sets specifically target their respective *CIP2A* variants.

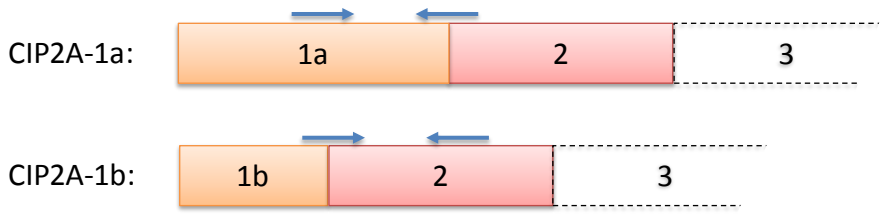

In addition to the alternative promoter of *CIP2A-1b*, this truncated variant's start site (ATG) is situated further downstream within exon 5, while the *CIP2A-1a* start site is within exon 1a.

Figure 6.3. Comparison of *CIP2A-1a* and *CIP2A-1b* gene sequences. Three separate sections are shown: exon 1a, exon 1b and exon 5. Primers and probes are also highlighted.

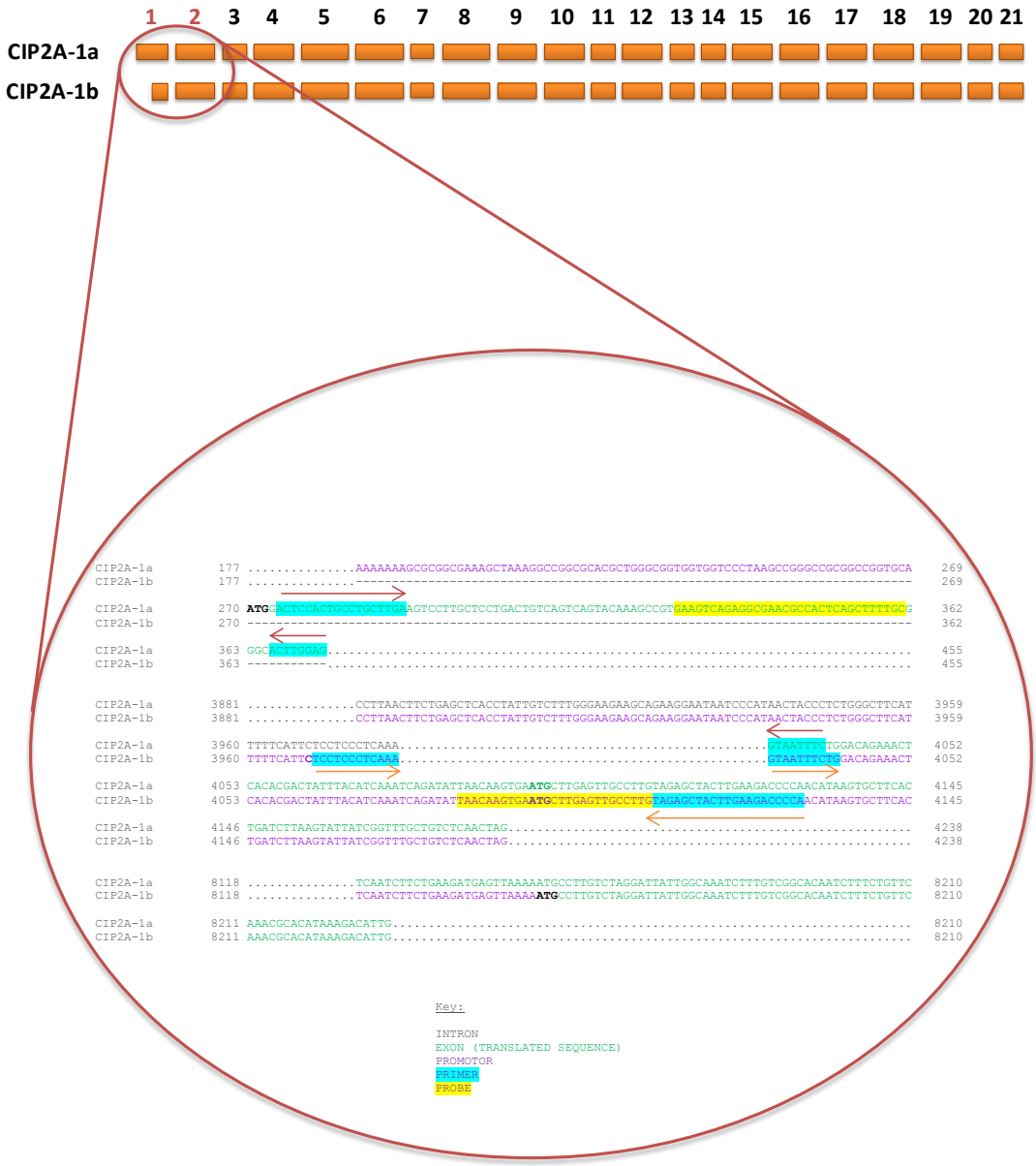

6.4.2. Optimisation of *CIP2A-1a* and *CIP2A-1b* PCR Conditions

To ensure the optimum PCR conditions for the primers so as to accurately detect the two *CIP2A* isoforms, a variety of conditions were optimised including primer mix ratios, PCR running conditions and annealing temperatures (**Figure 6.4**). Both high (K562) and low CIP2A (KCL22 and LAMA84) cell lines were used in addition to a negative control (no cDNA).

The primer mix was as follows:

- 4µl ddH_2O
- 1µ primer mix (4µM forward and reverse primer)
- 1µl expression mastermix
- 5µl cDNA sample

The PCR running conditions were as follows:

- 95°C – 5 minutes
- 40 cycles of:
    - 95°C – 15 seconds
    - 53-58°C – 20 seconds
    - 60°C – 45 seconds
- 72°C – 10 minutes
- 6°C – until used

Figure 6.4. Optimisation of PCR conditions for *CIP2A-1a* and *CIP2A-1b* Primers. A. *CIP2A-1a* primer optimisation. B. *CIP2A-1b* primer optimisation. A range of temperatures were used; 53-58°C. Optimisation was performed in three BCR-ABL1 positive cell lines; K562, KCL22 and LAMA84 and included a negative control.

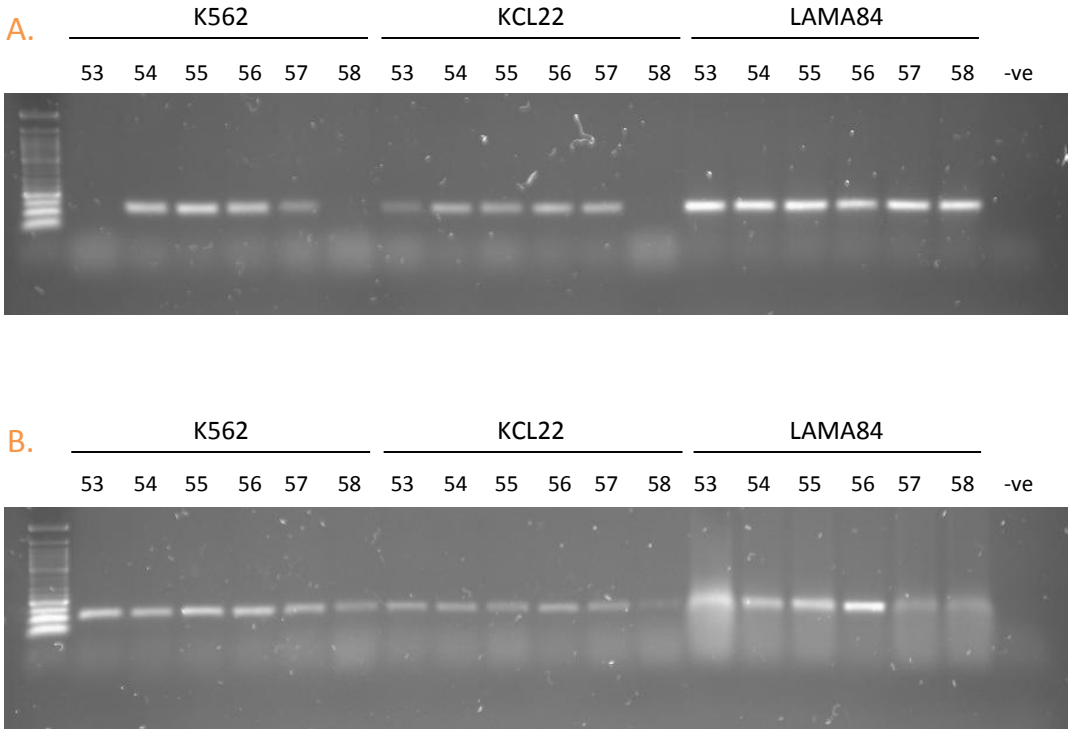

The annealing temperature of 56°C was chosen following the optimisation. This also confirmed the presence of both *CIP2A* transcripts in all BCR-ABL1 positive cell lines, giving a positive indication of the possible presence of both in CML patients.

6.4.3. Quantification of *CIP2A-1a* and *CIP2A-1b* Isoforms in CML

CIP2A primers used previously within this thesis and within our lab identify both of the *CIP2A* isoforms studied here, if not more as yet undiscovered variants. In work done here and by others in our lab, no statistically significant correlations were shown between mRNA levels of *CIP2A* and clinical outcome in CML patients, despite the strong differences seen at the protein level(C. M. Lucas et al., 2011)In contrast, publications of other malignancies have shown strong correlations between high *CIP2A* mRNA and aggressiveness of the tumour(Come et al., 2009; Dong et al., 2011; He et al., 2012; X. Liu et al., 2014; Ren et al., 2011; Teng et al., 2012). It was hypothesised that the presence of these two separate *CIP2A* isoforms in varying ratios may give rise to the seeming lack of correlation between gene and protein expression in CML.

Additionally, there was the possibility of alternative isoforms being expressed by different cohorts of patients. The potential for a patient with a poorer outcome to be expressing a variant more readily translated into protein and/or stabilised at the protein level was an exciting theory to be explored.

Here, the diagnostic levels of *CIP2A-1a* and *CIP2A-1b* mRNA were analysed in 28 CML samples by qRT-PCR; 17 of low CIP2A protein level and 11 of high CIP2A protein. The levels of both variants were assessed according to patient CIP2A protein levels and correlated with patient outcome. **Table 6.1** summarises the patient samples used.

Table 6.1. Characteristics of patients studied for their *CIP2A* transcript variants. Clinical grading is in accordance with the ELN guidelines, as explained in **Section 1.7.1**. The CIP2A protein level is as categorised as low or high, using the methodology of **Chapters 3** and **4**, as explained in **Section 3.4.1**.

UPN	SEX	High/Low CIP2A Protein Level	Clinical Outcome
025	M	LOW	Optimal
065	M	LOW	Optimal
011	F	LOW	Optimal
012	F	LOW	Optimal
066	M	LOW	Optimal
001	F	LOW	Optimal
028	M	LOW	Failure
062	F	LOW	Optimal
007	F	LOW	Optimal
018	M	LOW	Sub-Optimal
017	M	LOW	Optimal
051	M	LOW	Optimal
061	F	LOW	Optimal
014	F	LOW	Optimal
045	F	LOW	Optimal
029	M	LOW	Optimal
043	F	LOW	Sub-Optimal
059	M	HIGH	Optimal
068	F	HIGH	Optimal

053	F	HIGH	Optimal
031	F	HIGH	Sub-Optimal
056	F	HIGH	Optimal
055	F	HIGH	Optimal
032	F	HIGH	Failure
041	M	HIGH	Optimal
033	M	HIGH	Blast Crisis
057	M	HIGH	Optimal
058	M	HIGH	Optimal

Similarly to the three BCR-ABL1 cell lines tested (**Figure 6.4**), both of the *CIP2A* isoforms appear to be present in CML patient samples, as shown in **Figure 6.5**. Though the mRNA levels indicated here appear relatively low, this is consistent with results from previous chapters when using alternative primers that would identify both isoforms without discriminating between the two.

CIP2A-1b mRNA levels do not differ between patients with high or low CIP2A protein at diagnosis; no significant difference is observed between the two cohorts (**Figure 6.5 B**; p=0.8141 not shown). However, when comparing the expression of *CIP2A-1a* between high and low CIP2A protein cohorts, a significant inverse relationship is observed; patients with low CIP2A protein have significantly higher levels of *CIP2A-1a* mRNA than patients with high CIP2A protein (**Figure 6.5 A**; p=0.0035).

This interesting observation may be due to alternative levels of stability between *CIP2A-1a* and *CIP2A-1b*, with one isoform being degraded more readily than the other and/or a failure for one isoform to be translated into CIP2A protein. In order to investigate this, the half-life of these two isoforms was analysed.

Figure 6.5. Patient mRNA levels of A. *CIP2A-1a* and B. *CIP2A-1b*, as assessed by qRT-PCR. A total of 28 patient diagnostic samples were analysed; 17 with low CIP2A protein and 11 with high CIP2A protein levels.

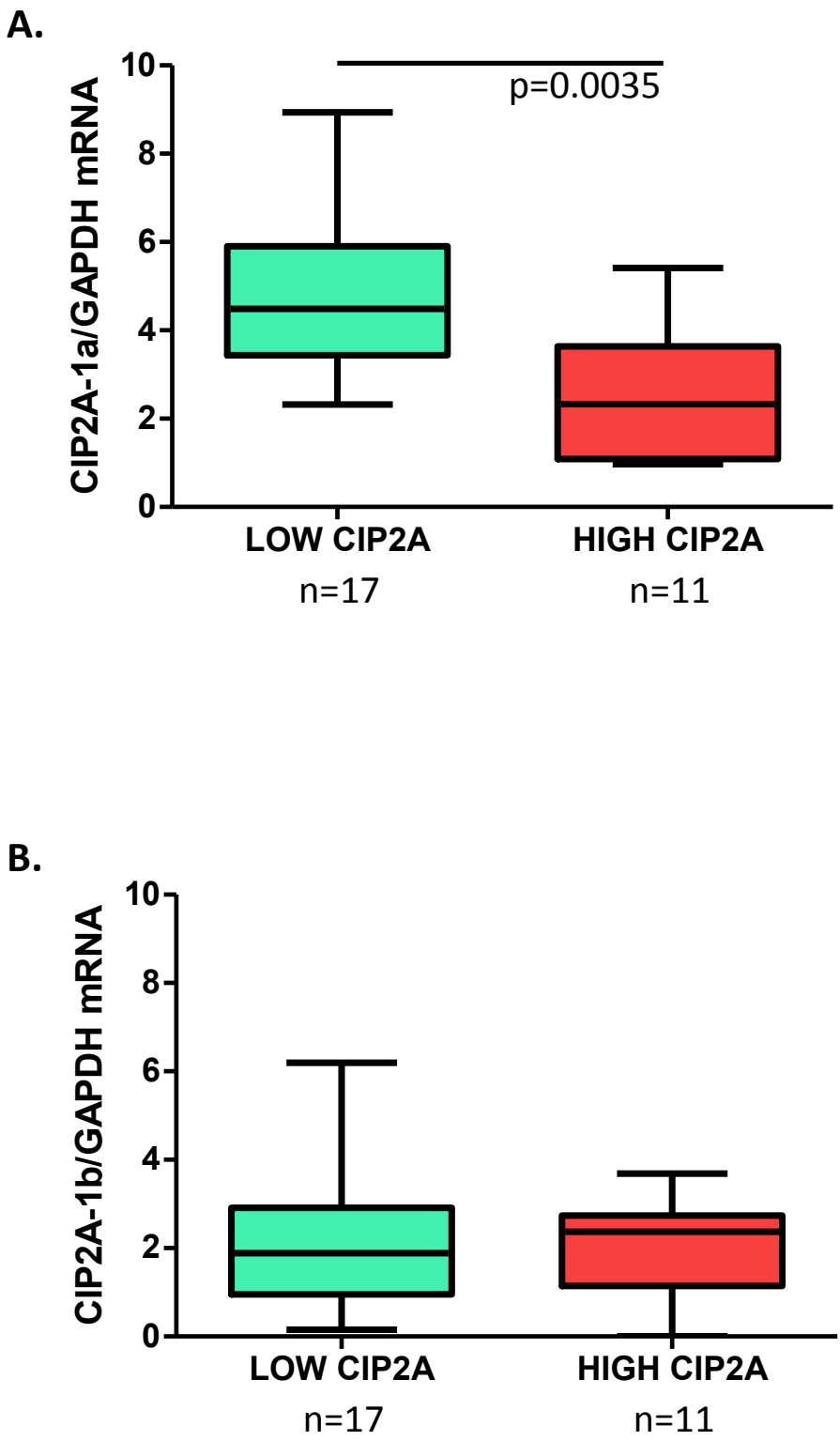

6.4.4. CIP2A Isoform Stability

Cycloheximide exerts its protein synthesis inhibition via the blockage of the translocation step, thus halting the conversion of mRNA into its corresponding protein. The rapid and (if desired) reversible effects of this compound make it of excellent use in *in vitro* studies. **Figure 6.6** shows the effects of 10µg/ml cycloheximide treatment on the level of CIP2A present in K562 cells.

Figure 6.6 B shows cell viability across a period of 96 hours, with and without cycloheximide treatment; cell viability has dropped to approximately 60% in this time, regardless of treatment and shows that any alterations seen in protein or gene levels are not due to cell death.

In accordance with the literature(Tseng et al., 2012), CIP2A half-life is here shown to be around 60 hours, as a sharp drop in CIP2A protein is seen at this time point in the treated cells, yet not in the untreated control. Interestingly, cycloheximide treatment has different effects on the *CIP2A-1a* and *CIP2A-1b* mRNA levels; treatment causes no alteration in the shorter isoform, *CIP2A-1b* (**Figure 6.6 D**) yet causes a sharp rise in the mRNA expression of the full length variant, *CIP2A-1a* (**Figure 6.6 C**).

Figure 6.6. Half-life of CIP2A Protein and *CIP2A-1a/1b* Isoform mRNA in K562 cells. A. CIP2A protein levels measured by flow cytometry (n=3) following treatment with 10µg/ml cycloheximide. B. Cell viability of untreated and cycloheximide (10µg/ml) treated K562 cells. C. *CIP2A-1a* mRNA levels following cycloheximide treatment (10µg/ml). D. *CIP2A-1b* mRNA levels following cycloheximide treatment (10µg/ml).

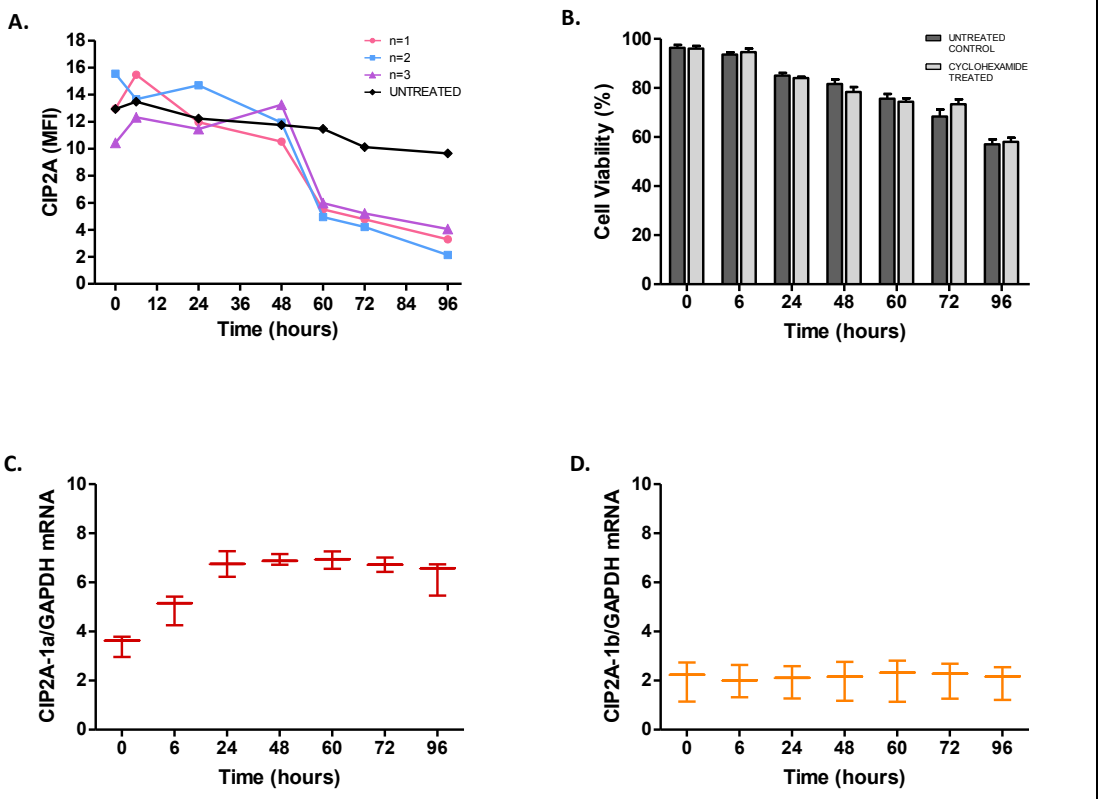

As no compensatory effect was seen in the already low levels of *CIP2A-1b*, following the suppression of protein synthesis, it may follow that this truncated gene is not in fact translated into protein. **Figure 6.7** shows the identification of CIP2A protein in K562 and KCL22 cells, using two alternative CIP2A antibodies (SCBT: 1; CIP2A (4A9-1A2), 2; CIP2A (HL1925)). As both antibodies give a single, clear band appearing at 90kDa, it appears that the smaller CIP2A variant, CIP2A-1b, is not detectable at the protein level in CML. As it is present at the mRNA level, this suggests an inability for the truncated protein to be properly translated or an instability at the gene level that leads to rapid degradation of the mRNA before it can be translated. Though this appears to be the case in CML-positive cells, it is important to stress that CIP2A behaviour, translation and stability may vary from malignancy to malignancy and should be an area for further investigation in a wide array of tumours in future.

Figure 6.7. CIP2A protein expression. A. Western blot of CIP2A in K562 (high CIP2A) and KCL22 (low CIP2A) cells, using antibody 1. B. Western blot of CIP2A in K562 (high CIP2A) and KCL22 (low CIP2A) cells, using antibody 2.

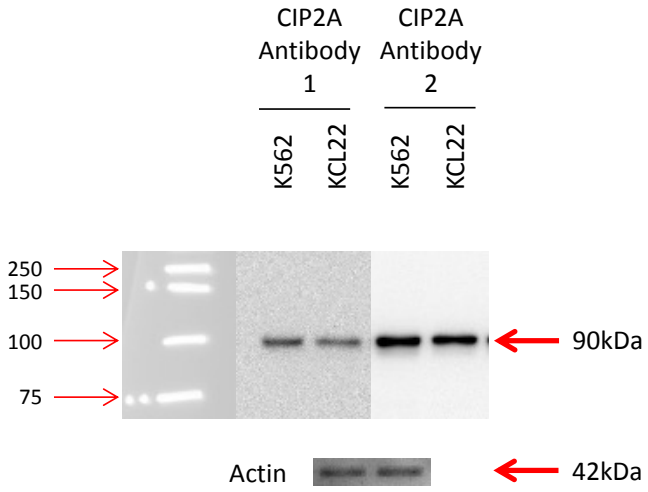

6.5. Discussion

Previous work in this thesis showed an interesting observation; similar *CIP2A* mRNA levels across all CML patients, regardless of high/low CIP2A protein levels. This chapter focussed on the possibility that varying ratios of *CIP2A* isoforms may exist between patients. It was hypothesised that the segregation of CML patients into high/low CIP2A protein may in fact correlate with either a specific *CIP2A* isoform or the ratio of these isoforms to one another.

Throughout cancer literature, transcript variants have been shown to play a role in the development and progression of the malignancy(Adamia, Pilarski, Bar-Natan, Stone, & Griffin, 2013; Dehm, 2013; Naro & Sette, 2013; Pagliarini, Naro, & Sette, 2015). Alternative genetic isoforms can have drastically different roles within the cell; deregulated isoform expression has been shown to favour the expansion of several malignancies.

As a relatively new oncogene of interest, little is reported of alternative *CIP2A* isoforms. Genetic analysis using the 'ensemble' database identified six different *CIP2A* isoforms at the time of starting this work; of these only two were reported to be protein coding. This chapter showed the design of two sets of *CIP2A* primers specifically targeting these *CIP2A* variants. Here it is shown that both the short (*CIP2A-1b*) and long (*CIP2A-1a*) isoforms are present in three different BCR-ABL1 positive cell lines and also in treatment-naïve CML patients (**Figures 6.4** and **6.5**). This is the first reported identification of a specific

CIP2A isoform in any malignancy, and thus represents novel information about this oncogene.

When stratified according to CIP2A protein levels it is apparent that an inverse correlation occurs between *CIP2A-1a* mRNA and CIP2A protein (**Figure 6.4 A**). Additionally, following cycloheximide treatment *CIP2A-1a* mRNA expression was upregulated, suggesting a compensation mechanism by the cell as CIP2A protein synthesis is compromised. The fact that high CIP2A protein correlates with low *CIP2A-1a* mRNA and vice versa, hints at a difference in the level of CIP2A protein stability between the patient cohorts. If the cell compensates when CIP2A protein levels are compromised, one could hypothesise that this is occurring in the low CIP2A patients, leading to an increased level of *CIP2A-1a* mRNA due to a possible instability and/or degradation of the CIP2A protein. A greater protein stability and/or lack of CIP2A degradation may therefore explain the apparent lower *CIP2A-1a* mRNA expression.

Interestingly, *CIP2A-1b* expression was consistently low amongst all patients and did not alter at all following cycloheximide treatment. This evidence suggests that while *CIP2A-1b* mRNA may indeed be present in patient samples it is not a vital *CIP2A* variant to the malignant cell. The lack of a CIP2A band present at 74kDa further supports this theory and may even suggest that *CIP2A-1b* fails to be translated into protein, though this is not confirmed; it is possible that structural alterations in CIP2A-1b prevent antibody binding and thereby its detection by western blot. Nothing is known of CIP2A crystallography structure

by direct observation at present and hopefully future studies will shed more light on this area of interest.

This chapter suggests a need to consider alternative isoforms of *CIP2A* in future research. The apparent similarity of all patient *CIP2A* mRNA levels in earlier chapters and previously published data(C. M. Lucas et al., 2011) did not examine isoform specificity. Using primers that identify all *CIP2A* variants may mask a difference between *CIP2A-1a* levels in different CML patient cohorts. Identifying this difference in *CIP2A-1a* mRNA level and the important inverse correlation between this isoform and its protein counterpart asks many questions of CIP2A regulation and stability. Unfortunately, time constraints did not allow for further work in this area, though future work to investigate CIP2A stability and its impact on the CIP2A/PP2A pathway in CML will be of great interest.

Chapter 7: Epigenetic Regulation of *CIP2A*

7.1 Introduction

Epigenetic regulation is defined as "heritable changes in gene activity and expression that occur without alteration in gene sequence" (Aaron, Goldberg, Allis, & Bernstein, 2007; Bird, 2007)and is generally understood to encompass DNA methylation, histone modifications and miRNAs. Aberrant epigenetic regulation of genes involved in CML is one possible underlying mechanism of disease pathogenesis and treatment resistance. This chapter focuses specifically on DNA methylation of the *CIP2A* gene promoter.

The methylation of CpG islands has been reported to play a vital role in both solid tumours and haematological malignancies(Constanze & Cockerill, 2011). In CML, the methylation of a number of genes has been reported to vary between disease phase and some to show clinical correlations with patient response to treatment(Dunwell et al., 2010). Most notable is the potential significance of *ABL1* methylation in CML. *ABL1* promoter methylation was reported in CP-CML bone marrow at diagnosis yet no methylation was observed in normal bone marrow. *ABL1* methylation has therefore been suggested as a possible early indicator of CML in bone marrow(Sun et al., 2001). (Polakova, Koblihova, & Stopka, 2013)

The fast-expanding investigative area of gene methylation highlights the importance of this method of regulation. Though many studies are beginning to focus on this area within cancer research, the field is still somewhat limited. With regards to *CIP2A*, very little is known of its methylation. When analysing a 1.8kb region downstream of the predicted *CIP2A* start site, Khanna *et al* (2011) discovered a highly conserved CpG island within the gene promoter (**Figure 7.1**). (Khanna et al., 2011)

Figure 7.1. Bioinformatic analysis of the *CIP2A* promoter methylation status. Data are taken from Khanna *et al(Khanna et al., 2011)*. A. Identification of putative CpG Island from −150 bp to +400 bp (blue shaded area) on the *CIP2A* promoter using MethPrimer software. B. Sequencing results of the extracted genomic DNA from normal human blood. CpG sites are represented by black rectangular blocks and all are shown to be unmethylated.

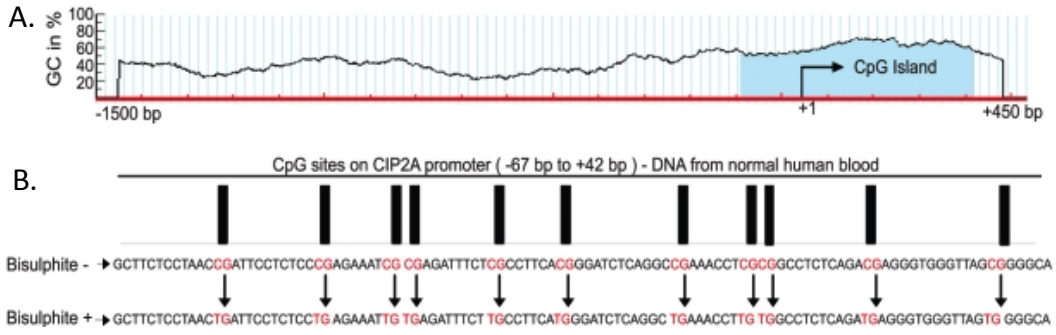

Khanna *et al* reported no methylation of this region in normal human blood samples or cultured fibroblasts, AGS and HELA cell lines(Khanna et al., 2011). However, the methylation of *CIP2A* in non-adherent cell lines, specifically BCR-ABL1 positive, has never been investigated. Additionally, *CIP2A* methylation in any cancerous patient samples has not been reported.

7.2. Chapter Aims

This chapter investigates the possible methylation of *CIP2A* as a means for its genetic regulation in CML. The main aims were to:

- Design primers to target the CpG island of the *CIP2A* promoter.
- Investigate the presence of *CIP2A* methylation in normal samples.
- Investigate the presence of *CIP2A* methylation in both BCR-ABL1 positive and negative cell lines.
- Investigate the presence of *CIP2A* methylation in CML patient samples taken from patients at varying stages of the disease and of differing clinical outcomes.

7.3. Methods

In this chapter cell lines and patient and normal healthy volunteer genomic DNA samples were analysed using manual PCR (**Section 2.9.4**), bisulphite conversion (**Section 2.10.1**) and PCR pyrosequencing (**Section 2.10**) to detect *CIP2A* methylation. Clinical characteristics of patients used in this chapter are shown in **Table 7.1**.

7.4. Results

7.4.1. An Overview of the Pyrosequencing Method

The recently identified CpG island located at the *CIP2A-1a* promoter represents an interesting area to investigate. To detect the presence of any methylation within the CpG island, the pyrosequencing technique was used. The basic principle of pyrosequencing is founded on the application of DNA polymerase to sequence a complementary strand of DNA to the strand designed by the investigator. The initial step in the pyrosequencing methodology is to design primers that encompass the desired GC rich area to be explored. Following this, the genomic DNA of the chosen samples undergoes a bisulphite conversion (**Figure 7.2**). Methylation refers to the addition of a methyl group to the carbon-5 position of the cytosine within a CpG (CG/GC) di-nucleotide. During the bisulphite conversion, the bisulphite ion acts to preferentially deaminate unmethylated cytosines, thereby converting them to uracil residues. For methylated cytosines this does not occur. Therefore, any remaining cytosines detected are sites of methylation. (Darst, Pardo, Ai, Brown, & Kladde, 2010)

Figure 7.2. Basic Principle of Bisulphite Conversion.

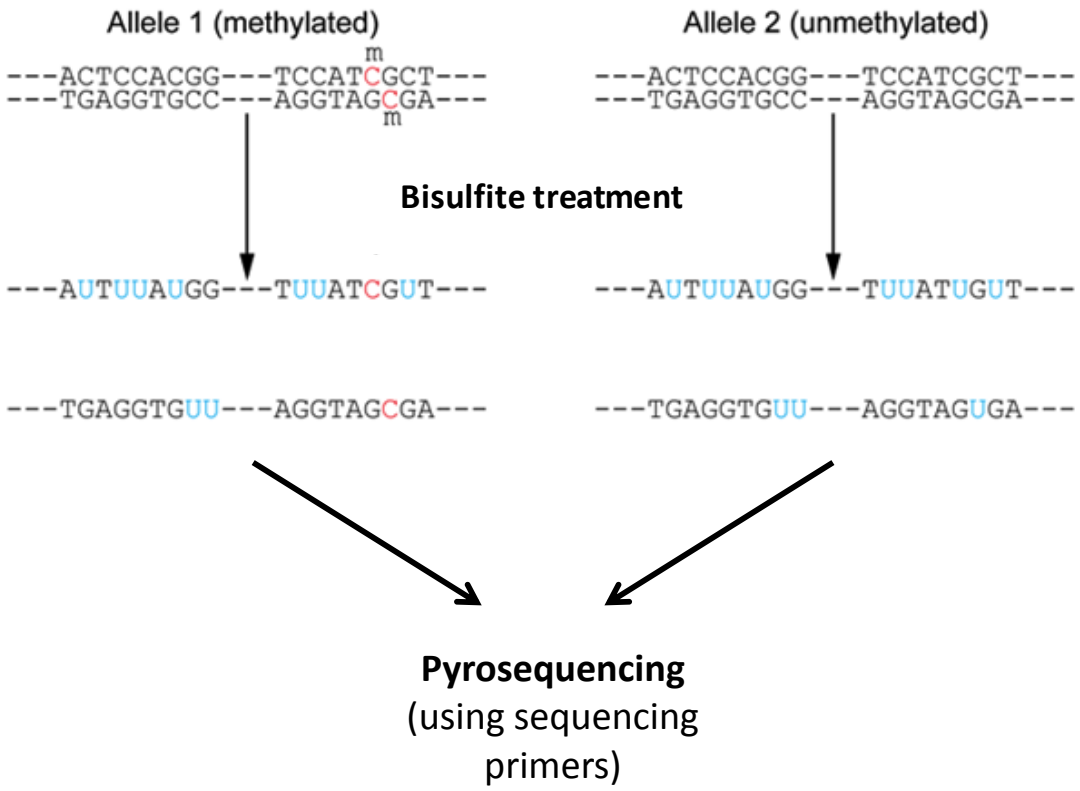

The final step in measuring the methylation of a gene within a sample is to run the converted samples through the pyrosequencing machinery. During pyrosequencing, it is the dispensation of a single type of nucleotide at a time and in a predetermined order, that is key. This predetermined order is complementary to the amplified strand of DNA for which the possible sites of methylation are to be analysed. With each set of nucleotide released there are two possibilities: either it is incorporated into the DNA strand by DNA polymerase and via a chain of reactions, causes light to be emitted *quantitatively* and recorded by the pyrograph, or; it does not match the complementary strand, is not incorporated into the DNA, no chain of reactions occurs and therefore no light is emitted.

With regards to detecting methylation, any pyrograph peak representative of a present cytosine shows there is methylation at this residue within the sample. **Figure 7.3** gives an explanation of how to aptly analyse example pyrographs.

Figure 7.3. Analysing a Methylation Pyrograph. B. A pyrograph of a tumour sample. A. An example of all pyrosequencing steps.

For each pyrograph: the x axis represents the dispensation order and the y axis the relative luminescence. Blue/grey areas indicate polymorphisms between T/C generated by bisulphite treatment; methylation at a dinucleotide is calculated by the ratio of T/C and shown as a percentage above. (N.B. yellow areas (not shown) indicate positions of internal controls of conversion at non-CpG sites.) Blue/yellow percentages indicate acceptable analysis; red boxes indicate a problem and manual verification of the sequence may be necessary.

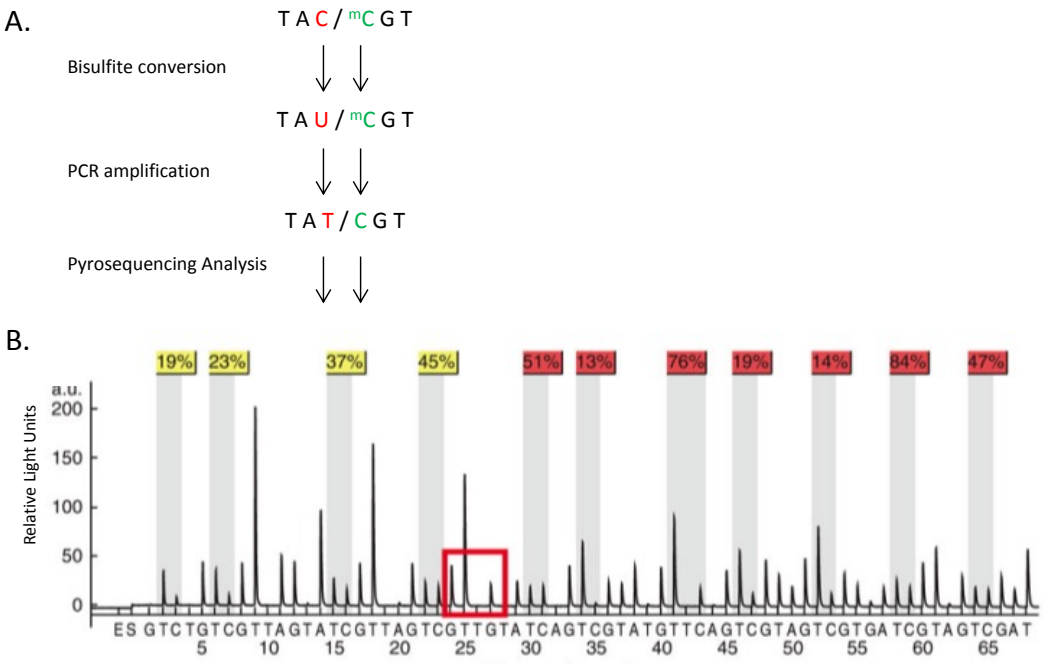

7.4.2. Designing Methylation Primers

Using the 'PyroMark Assay Design 2.0' software, methylation primers were designed as shown in **Figure 7.4**. The primers were designed to span the promoter and large portion of exon 1a. They encompass 11 possible methylation sites of the CpG island.

Figure 7.4. Design of the *CIP2A* methylation primers. Forward and reverse primers are shown as blue arrows and the pyrosequencing primer as a red arrow. Red vertical lines represent the encompassed sites of possible methylation to be investigated.

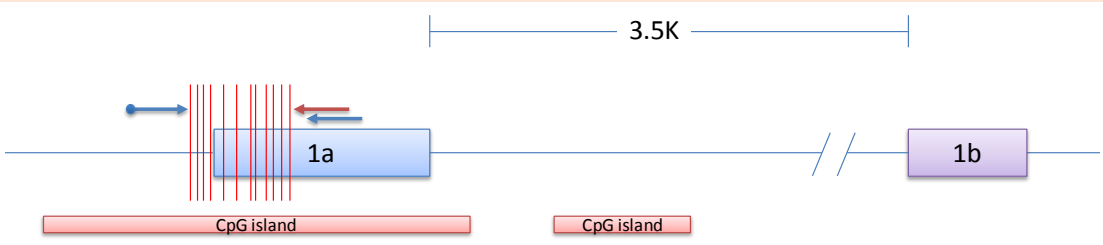

Though a lesser CpG island is also present further downstream, it is not proximal to any exon or promoter site, making it unlikely to be of interest in this particular case.

7.4.3. Bisulphite Conversion of Pyrosequencing Samples

Successful bisulphite conversion was performed on a total of 50 samples. These included four control samples; a 0% methylated control and three positive controls (10%, 20% and 95% methylated). These are DNA taken from the white blood cells of healthy individuals that had previously been *in vitro* methylated using Sssl methylase (NEB) as per supplier protocol. The methylated DNA was subsequently diluted with unmethylated WBC DNA to result in the desired dilution standards. Four BCR-ABL1 positive cell lines (K562 (high CIP2A), KCL22 (low CIP2A), LAMA84 and KYO-1) and two BCR-ABL1 negative cell lines (HEK293 and U937) were also used. Additionally, 8 normal healthy volunteer samples and 32 CML patient samples were analysed. Of the CML patients all except two were diagnostic samples; two samples were taken from patients in blast crisis. The diagnostic samples were categorised according to future patient response to treatment (optimal, sub-optimal, failure or blast crisis). **Table 7.1** summarises all samples that underwent successful bisulphite conversion and subsequent pyrosequencing analysis.

Table 7.1. Information of samples converted for Methylation Analysis.

METHYLATION SAMPLE NUMBER	UPN	Sample Type	SEX	Time of Sample	Clinical Outcome
1	N/A	Normal	F	N/A	N/A
2	N/A	Normal	F	N/A	N/A
3	N/A	Normal	F	N/A	N/A
4	N/A	Normal	F	N/A	N/A
5	N/A	Normal	M	N/A	N/A
6	N/A	Normal	M	N/A	N/A
7	N/A	Normal	M	N/A	N/A
8	N/A	Normal	M	N/A	N/A
9	N/A	Cell line (K562)	N/A	N/A	N/A
10	N/A	Cell line (KCL22)	N/A	N/A	N/A
11	N/A	Cell line (LAMA84)	N/A	N/A	N/A
12	N/A	Cell line (U937)	N/A	N/A	N/A
13	N/A	Cell line (HEK293)	N/A	N/A	N/A
14	N/A	Cell line (KY01)	N/A	N/A	N/A
15	022	Patient	M	Diagnosis	Optimal

16	001	Patient	F	Diagnosis	Optimal
17	003	Patient	F	Diagnosis	Optimal
18	006	Patient	F	Diagnosis	Optimal
19	024	Patient	M	Diagnosis	Optimal
20	021	Patient	M	Diagnosis	Optimal
21	012	Patient	F	Diagnosis	Optimal
22	020	Patient	M	Diagnosis	Optimal
23	013	Patient	F	Diagnosis	Optimal
24	009	Patient	F	Diagnosis	Optimal
25	043	Patient	F	Diagnosis	Sub-Optimal
26	018	Patient	M	Diagnosis	Sub-Optimal
27	031	Patient	F	Diagnosis	Sub-Optimal
28	089	Patient	M	Diagnosis	Sub-Optimal
29	090	Patient	M	Diagnosis	Sub-Optimal
30	091	Patient	M	Diagnosis	Sub-Optimal
31	032	Patient	F	Diagnosis	Failure
32	092	Patient	F	Diagnosis	Failure
33	093	Patient	F	Diagnosis	Failure
34	094	Patient	F	Diagnosis	Failure
35	095	Patient	M	Diagnosis	Failure

36	096	Patient	M	Diagnosis	Failure
37	097	Patient	M	Diagnosis	Failure
38	098	Patient	M	Diagnosis	Failure
39	099	Patient	M	Diagnosis	Failure
40	100	Patient	M	Diagnosis	Failure
41	030	Patient	F	Diagnosis	Blast Crisis
42	101	Patient	F	In BC	Blast Crisis
43	033	Patient	M	Diagnosis	Blast Crisis
44	034	Patient	M	Diagnosis	Blast Crisis
45	035	Patient	M	Diagnosis	Blast Crisis
46	102	Patient	M	In BC	Blast Crisis
(47)		Negative Control (0% methylated)			
(48)		Positive Control (10% methylated)			
(49)		Positive Control (40% methylated)			
(50)		Positive Control (95% methylated)			

7.4.4. Optimisation of the Pyrosequencing Technique

One limiting factor of the pyrosequencing method is the quality of the DNA sample. It is therefore imperative to optimise the appropriate amplification of DNA during the PCR reaction to validate the successful bisulphite conversion and ensure an adequate sample for pyrosequencing analysis. **Figure 7.5** shows the optimisation of the annealing temperature for the original PCR conditions.

The original primer mix was as follows:

- 16.875µl ddH_2O
- 2.5µl buffer
- 1µl dNTPs (5mM)
- 0.5µl $MgCl_2$ (25mM)
- 1µ primer mix (150nM forward (biotinylated) primer, 300nM reverse primer)
- 0.125µl Hot start Plus Taqman (Qiagen, UK)
- 3µl sample

The original PCR running conditions were as follows:

- 95°C – 5 minutes
- 40 cycles of:
    - 94°C – 30 seconds
    - 48-57°C – 30 seconds
    - 72°C – 30 seconds
- 72°C – 10 minutes
- 6°C – until used

As is visible from **Figure 7.5 A**, the initial annealing temperatures were too low and did not give a clear single band as is optimal. Higher temperatures were then used (**Figure 7.5 B**) and the clearest strong single band appeared at 54°C.

These conditions were then used for the bisulphite-converted samples previously mentioned (**Table 7.1**).

Figure 7.5. Optimisation of Pre-Pyrosequencing PCR. Known positive methylation samples (1% and 40%) were used. A. Temperatures 48-52°C; no clear single bands. B. Temperatures 53-57°C. Optimum temperature was 54°C; this shows the strongest single PCR band.

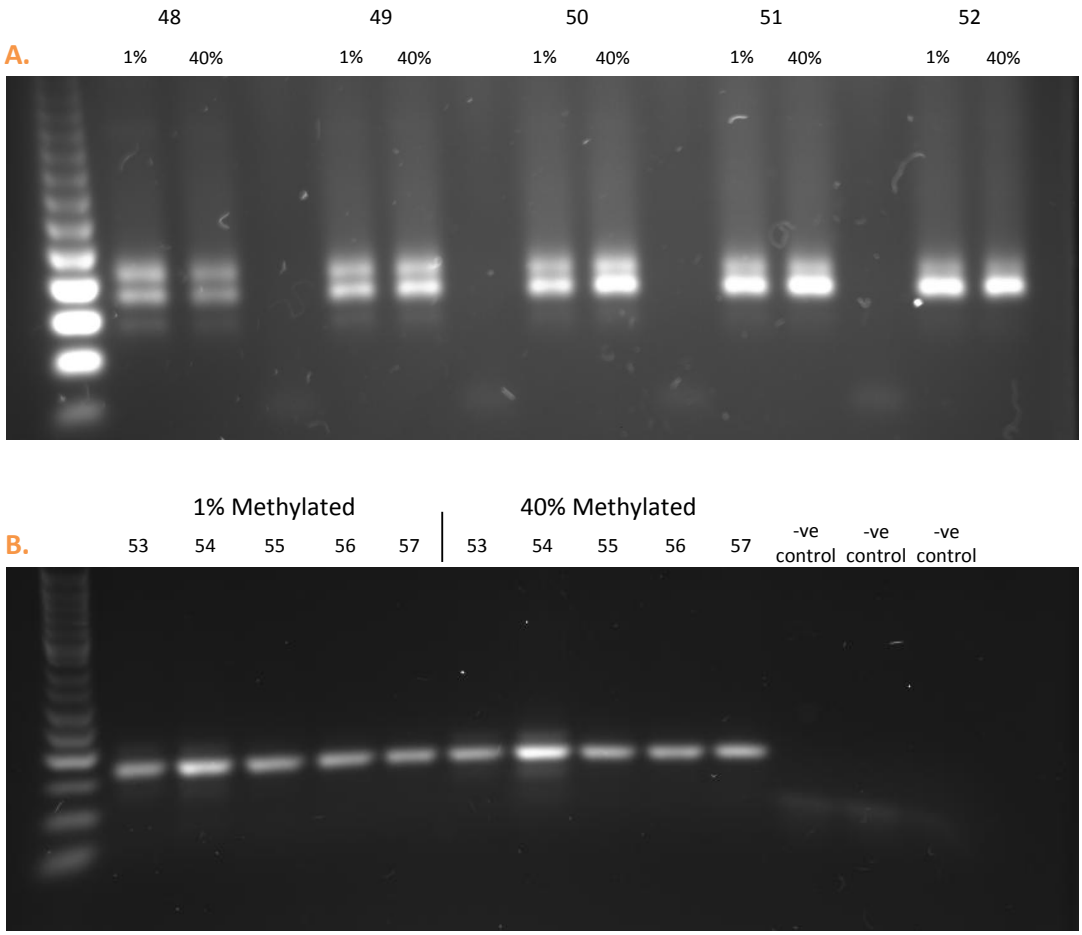

Figure 7.6 shows the results of the initial pre-pyrosequencing PCR of the samples, using the original conditions. Samples 6, 13, 23 and 24 were not used in the pyrosequencing analysis that followed, as they were not adequately amplified during the PCR. The bands for all samples are not strong and indicated that the PCR amplification was not optimal. This was confirmed by the subsequent pyrosequencing analysis (**Figure 7.7**), which shows representative results of the initial pyrosequencing analysis. All samples appeared to have extremely low peaks, indicating the sample quality was not good enough for pyrosequencing analysis. (Quality control checks performed by the software also highlight this by the red percentage boxes apparent in most samples.) **Figure 7.7 D** shows a sample that completely failed; the result shows only background noise. Some samples gave low methylation levels at certain positions. However, the low sample peaks make this hard to interpret; 'methylation' peaks may just be background noise or some methylation may be hidden by background noise.

This experiment needed repeating, with amended PCR conditions to increase amplification and quality of the sample and produce valid and interpretable results.

Figure 7.6. Initial Pre-Pyrosequencing Results. A-D. Electrophoresis gels of samples (**Table 7.1**) following bisulphite conversion.

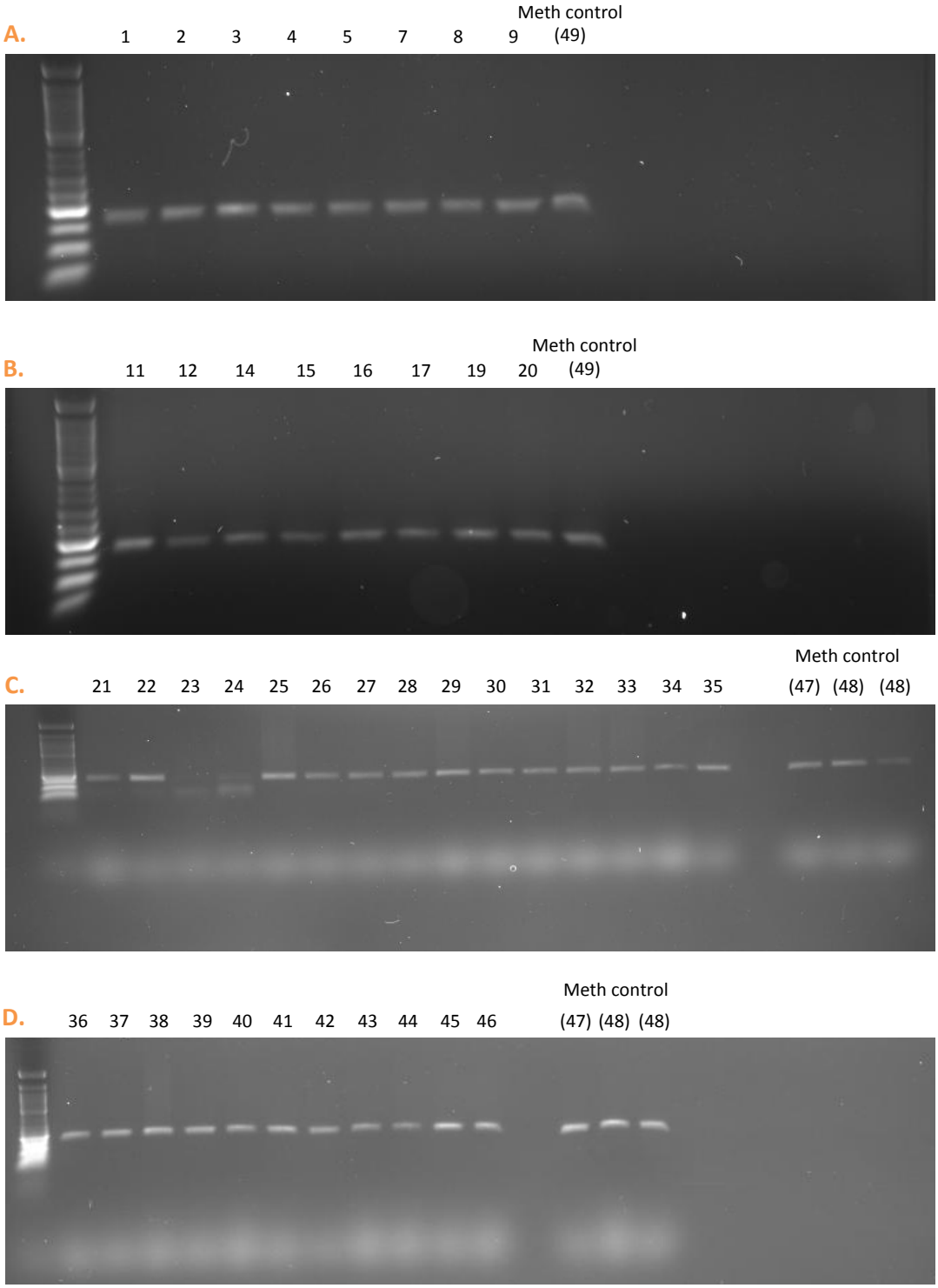

Figure 7.7. Representative Results of Initial Pyrosequencing Analysis. A. Normal healthy volunteer. B. Failure patient (diagnosis). C. Negative control (0% methylated). D. Positive control (95% methylated). All samples showed inadequate analysis.

A. Sample 5

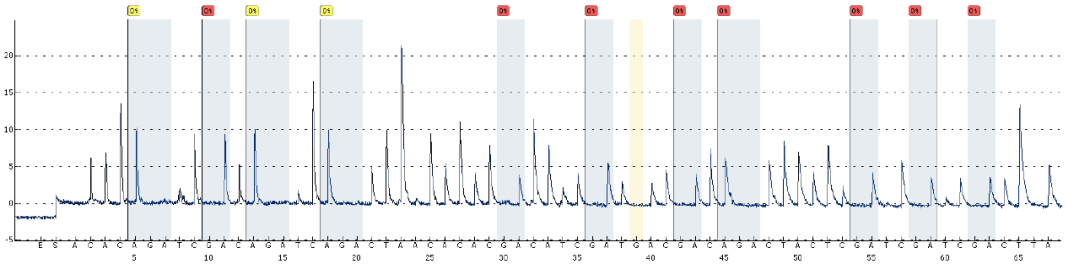

B. Sample 36

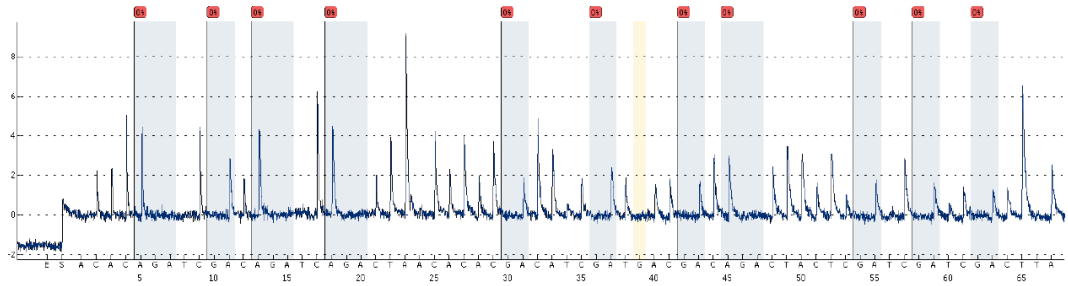

C. Sample (47)

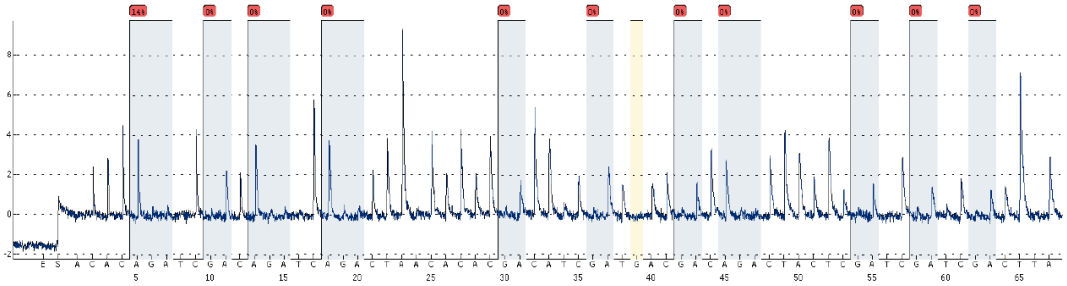

D. Sample (50)

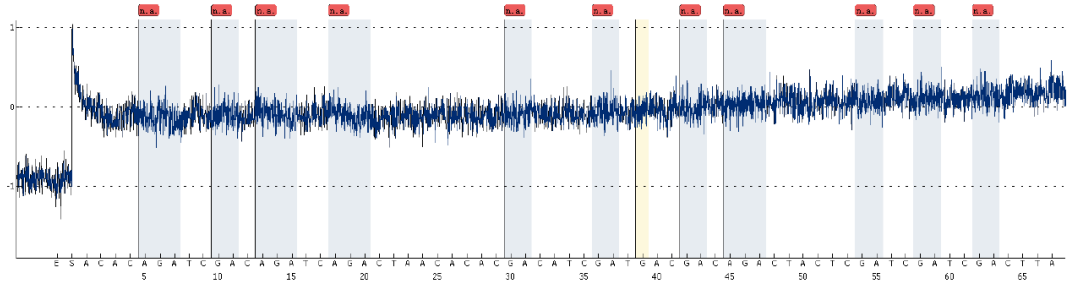

The following are the amended conditions for the PCR amplification. These changes gave valid results and were deemed the optimal conditions for the pyrosequencing analysis.

The amended primer mix was as follows:

- 19.15µl ddH_2O
- 3µl buffer
- 1.2µl $MgCl_2$ (25mM)
- 1.25µl dNTPs (5mM)
- 1.25µ primer mix (150nM forward (biotinylated) primer, 300nM reverse primer)
- 0.15µl Hot start Plus Taqman (Qiagen, UK)
- 4µl sample

The amended PCR running conditions were as follows:

- 95°C – 5 minutes
- 20 cycles:
    - 94°C – 20 seconds
    - 54°C – 40 seconds
    - 72°C – 30 seconds
- 20 cycles:
    - 94°C – 30 seconds
    - 54°C – 30 seconds
    - 72°C – 35 seconds
- 72°C – 15 minutes
- 6°C – until used

7.4.5. Pyrosequencing Analysis of *CIP2A* Methylation

Using the amended conditions, all bisulphite-converted samples were amplified by PCR (**Figure 7.8**). The bands are stronger than in the previous sample run (**Figure 7.6**), indicating superior amplification results. Peak heights for this pyrosequencing run (**Figure 7.9**) were much greater than previously, verifying the quality of the sample product following bisulphite conversion and PCR amplification. The yellow areas that are indicative of internal controls at non-CpG sites are all clear of any peaks, further confirming the bisulphite conversion reactions were successful. All three positive methylated controls gave correct methylation levels (approximately 10%, 20% and 95%) and importantly, the negative control sample had no methylation present.

Figure 7.8. Amended Method Pre-Pyrosequencing Results. A-B. Electrophoresis gels of samples (**Table 7.1**) following bisulphite conversion.

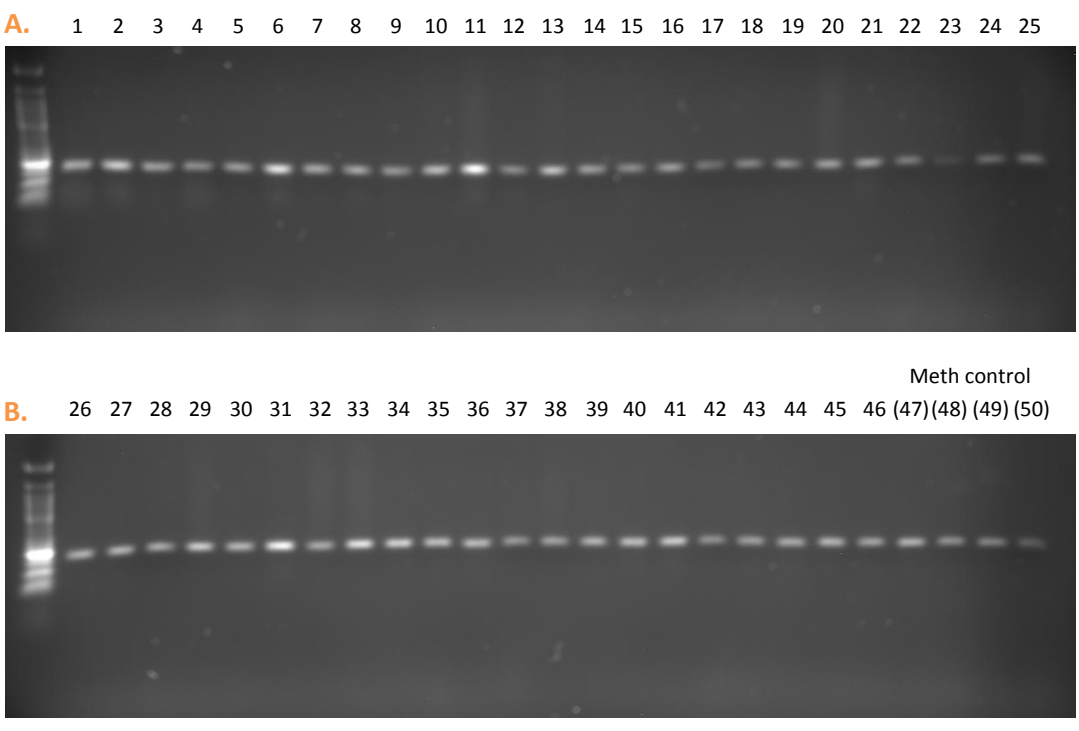

Figure 7.9. Representative Results of Pyrosequencing Analysis. A. Negative control; B.C.D. Positive controls (10%, 20%, 95% methylated); E. K562 (BCR-ABL1 positive, high CIP2A); F. KCL22 (BCR-ABL1 positive, low CIP2A); G. U937 (BCR-ABL1 negative); H.I.J.K. Diagnostic patient samples (Optimal, Sub-optimal, Failure, Blast Crisis); L. Blast Crisis patient (in blast crisis).

A. Sample (47) – negative control 0% methylated

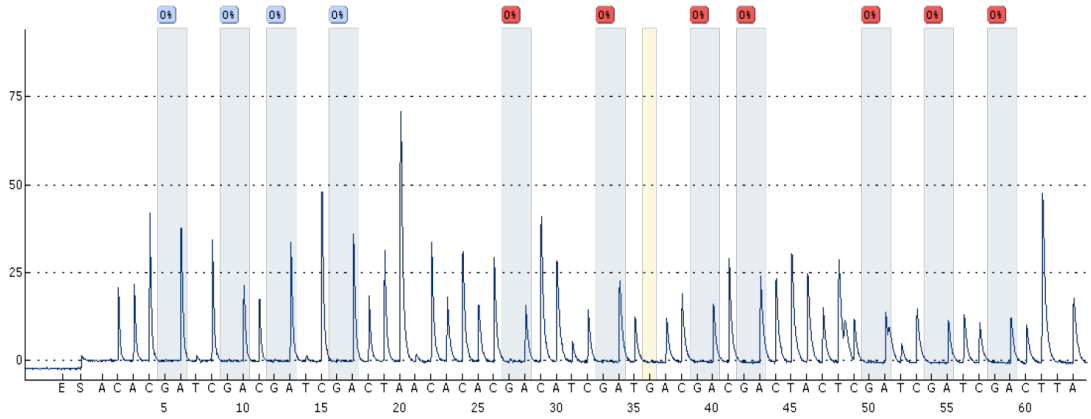

B. Sample (48) – positive control 10% methylated

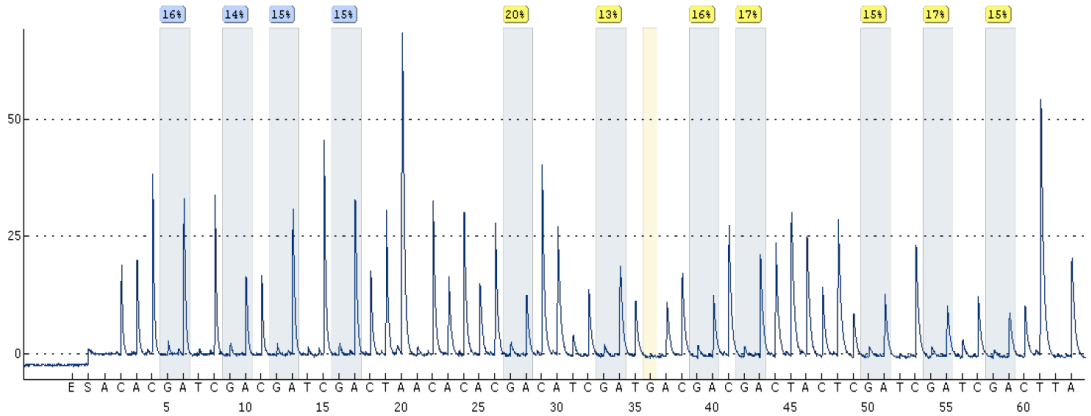

C. Sample (49) – positive control 40% methylated

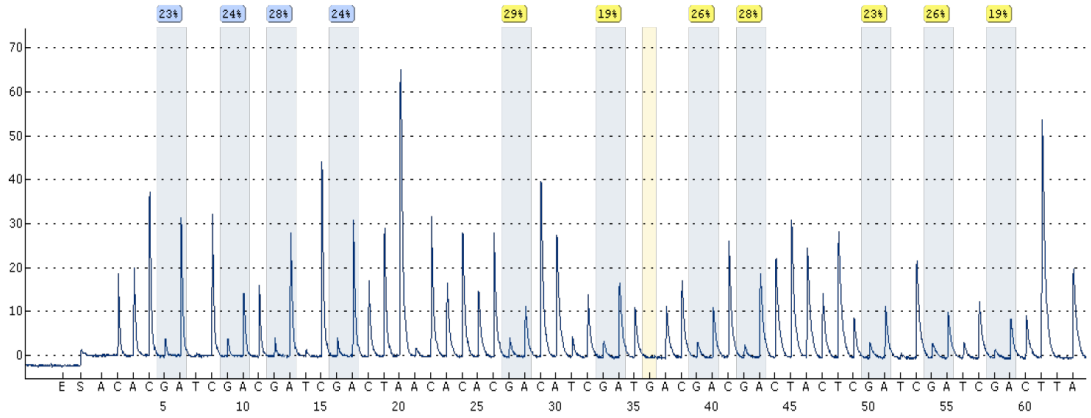

D. Sample (50) – positive control 95% methylated

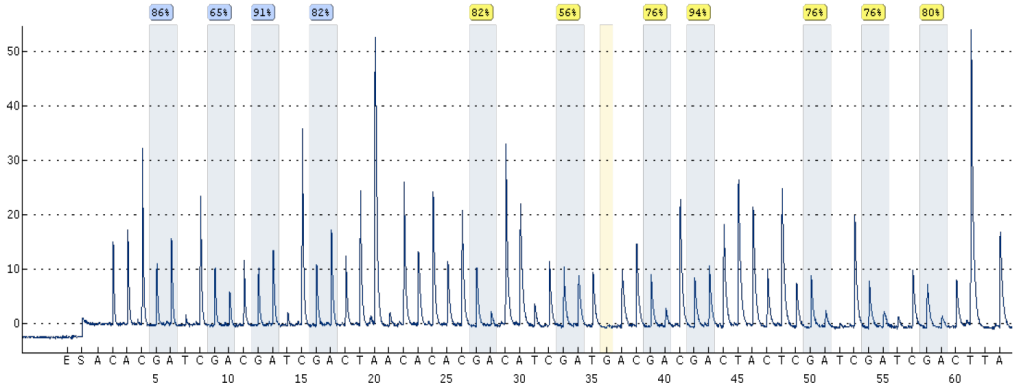

E. Sample 9 – K562

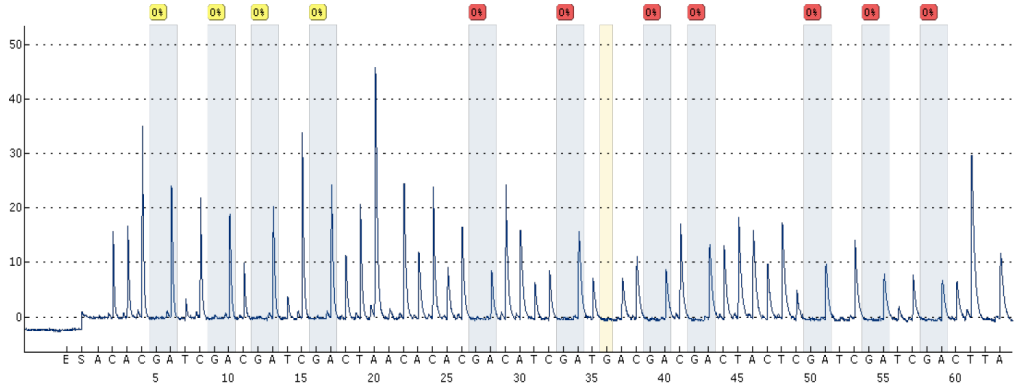

F. Sample 10 – KCL22

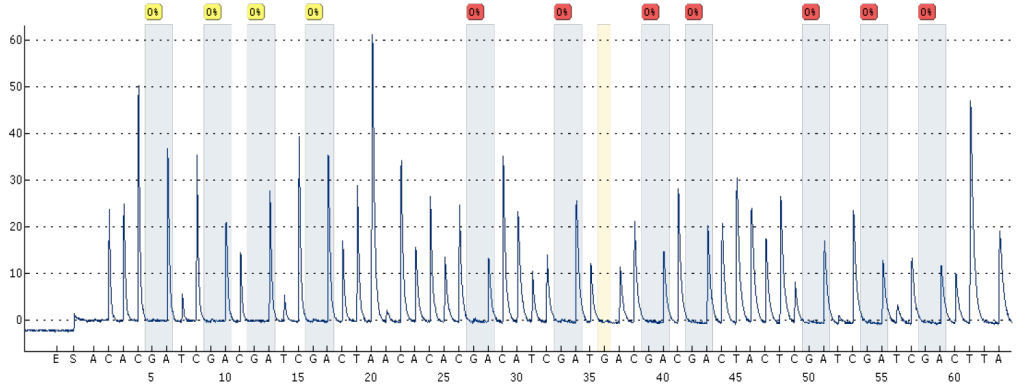

G. Sample 12 – U937

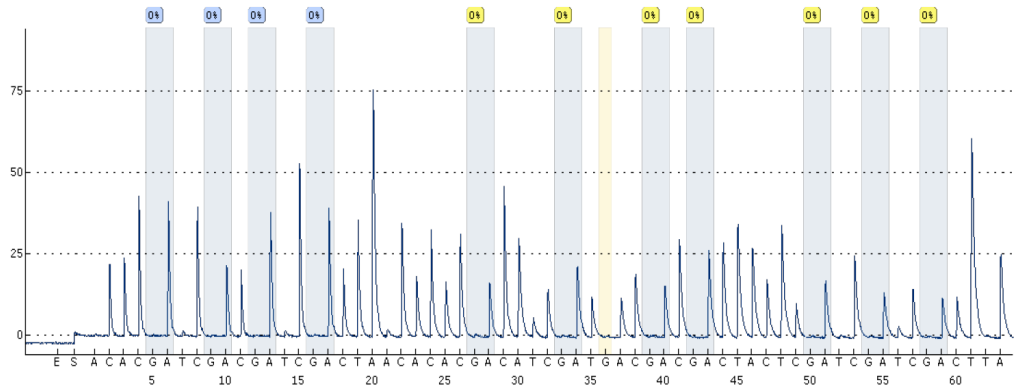

H. Sample 19 – Optimal in CP

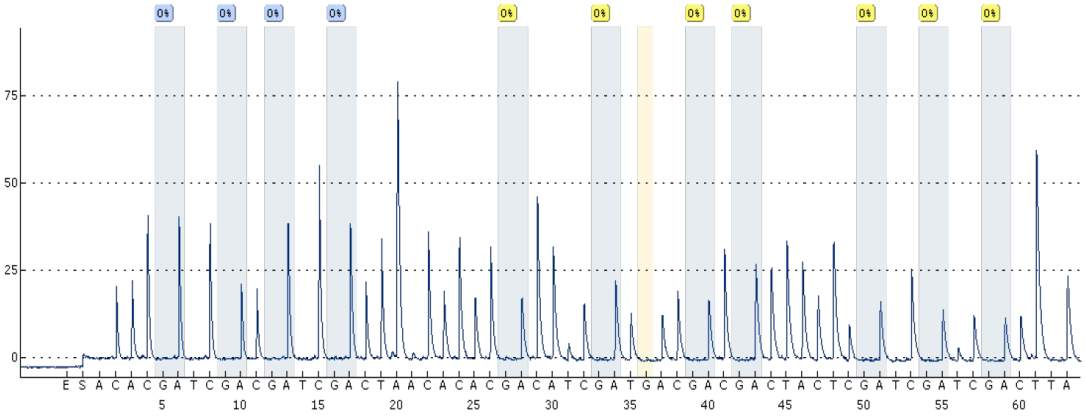

I. Sample 26 – Sub-Optimal in CP

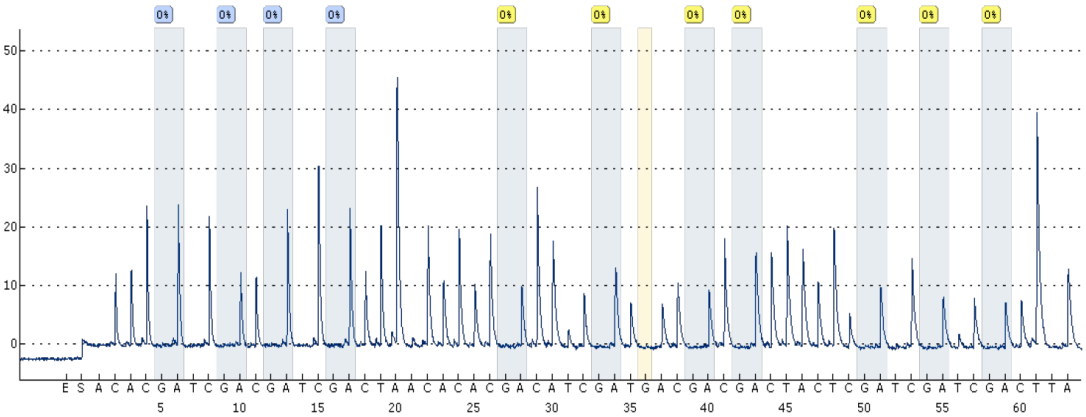

J. Sample 31 – Failure in CP

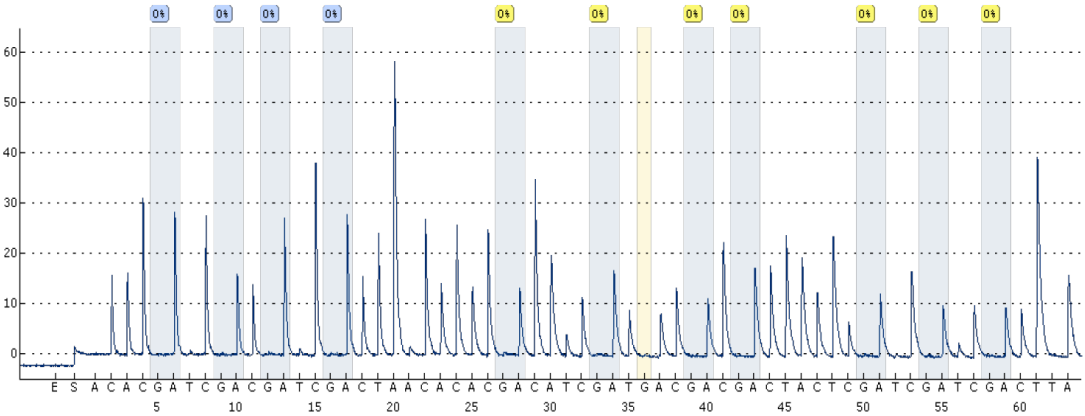

K. Sample 41 – BC in CP

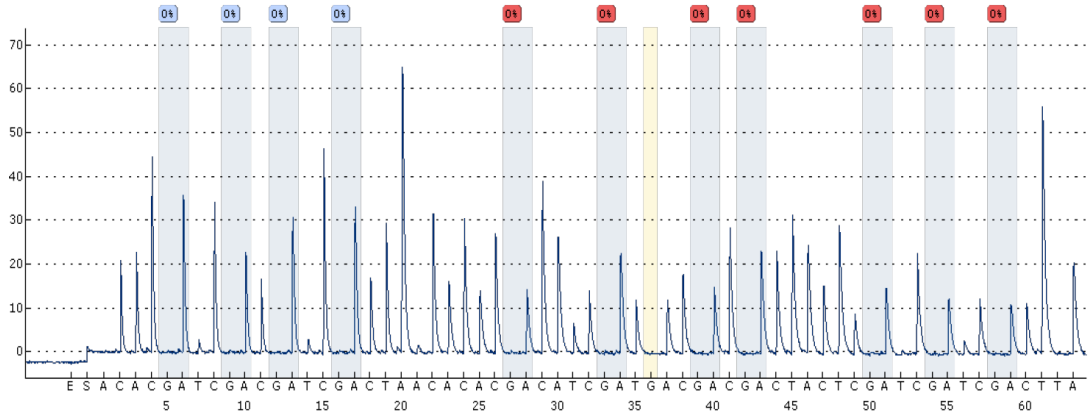

L. Sample 46 – BC in BC

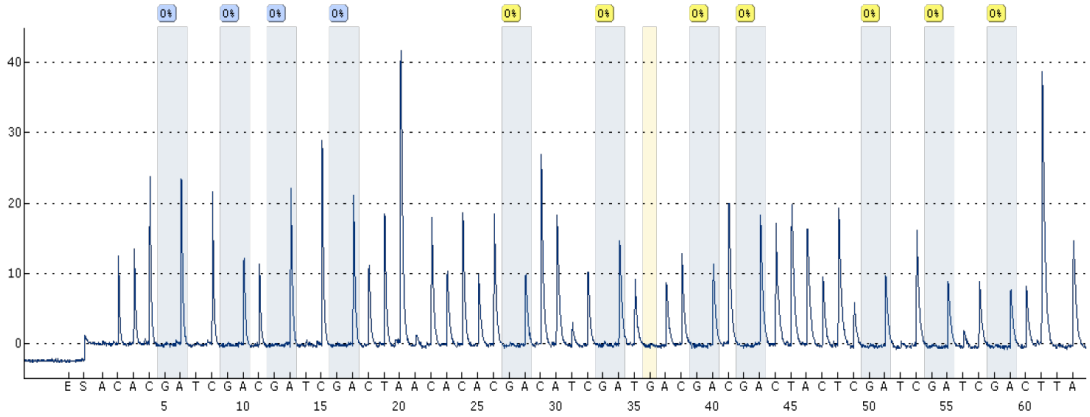

7.4.6. Results Summary

In this CpG island of *CIP2A*, no methylation was detected in any of the six cell lines, eight normal healthy volunteers or 32 patient samples within this experiment. Three positive controls, including one high methylated control sample, showed methylation; this verifies the pyrosequencing technique used here. This indicates that the *CIP2A* gene is not methylated in human white cells, irrespective of the presence of CML.

7.5. Discussion

CpG island methylation has been shown to be deregulated in both solid tumours and haematological malignancies. It is known that the hypermethylation of tumour suppressor genes and hypomethylation of a number of oncogenes plays an important role in haematological malignancies(Constanze & Cockerill, 2011). As stated, the hypomethylation of oncogenes has been shown in certain malignancies; e.g. c-Ha-ras is hypomethylated in colonic adenocarcinomas(P. M. Das & Singal, 2004; Feinberg & Cogelstein, 1983)In CML, a variety of genes have been shown to have an increased level of methylation that correlates with disease progression into advanced (AP/BC) stages of the malignancy; these include calcitonin(Nelkin, Przepiorka, Burke, Thomas, & Baylin, 1991), HIC1(J.-P. J. Issa, Zehnbauer, Kaufmann, Biel, & Baylin, 1997)ER(J.-P. J. Issa et al., 1996) and Abl1(Asimakopoulos, Shteper, Fibach, et al., 1999; Asimakopoulos, Shteper, Krichevsky, et al., 1999). Interestingly, the significance of *Abl1* promoter (Pa) methylation is highly disputed in CML research, with reported levels of CP-CML methylation varying from 26%(Ben-Yehuda et al., 1997) to 81%(Jelinek et al., 2011). However, as stated earlier, high levels of Pa methylation in CML bone marrow (BM) samples (both in CP and at diagnosis) compared to a complete absence of methylation in normal BM, suggest the possibility of Pa methylation as an early indicator of CML(Sun et al., 2001). (Boultwood & Wainscoat, 2007)

This chapter aimed to investigate the potential variation in methylation levels of the *CIP2A* promoter. However, gene methylation of the *CIP2A* oncogene in clinical samples is as yet completely unknown in any malignancy, thus this

chapter represents entirely novel information on *CIP2A* epigenetics. Despite the growing level of interest in CIP2A, only one paper has touched on the potential implications of its methylation(Khanna et al., 2011). In this paper they identified the CpG island of interest and measured the levels of *CIP2A* methylation in four normal blood samples and two adherent cancer cell lines (AGS and HeLa). Though they saw no methylation, this body of work investigated very few samples, with no non-adherent cell lines or patient samples included in their study. Given the apparent differences in the identified levels of *Abl1* methylation reported by different groups(Ben-Yehuda et al., 1997; J. Issa et al., 1999; Jelinek et al., 2011; Nguyen et al., 2000), investigating *CIP2A* methylation in a larger cohort that included a variety of samples is necessary.

In this study the methylation of the CpG island located at the *CIP2A* promoter was measured in a total of 50 samples; these included one negative and three positive controls, four BCR-ABL1 positive and two BCR-ABL1 negative cell lines, eight normal peripheral blood samples, and 32 diagnostic samples of CML patients with known clinical outcomes. The validation of the pyrosequencing technique is clearly seen by the positive and negative controls.

For every cell line, CML patient sample and normal PBMC sample, the bisulphite treatment of genomic DNA converted all cytosines to thymidines, indicating a completely negative methylation result at every CG dinucleotide investigated. This confirms that the variation in *CIP2A* expression between cancerous and non-cancerous samples is not due to its promoter methylation/de-methylation,

nor is the variation in CIP2A expression between patient cohorts. Additionally, this work validates the initial work by Khanna *et al(Khanna et al., 2011)* as the normal human blood samples within this thesis are also negative for *CIP2A* methylation.

This work clearly shows that the *CIP2A* oncogene is not regulated by methylation; however other epigenetic mechanisms cannot be ruled out. As yet, there is no information on acetylation of *CIP2A*, however a small number of papers have shown potential links between miRNAs and this gene's oncogenic activity(Jung et al., 2013). This will hopefully be a fruitful area of future research into CIP2A. Additionally, the effects of PP2Ac methylation have been highlighted in some publications(Jackson & Pallas, 2012; Seshacharyulu et al., 2013; Stanevich et al., 2014)Though this chapter may have ruled out the regulation of *CIP2A* by its direct methylation, the possibility of CIP2A involvement in promoting *PP2Ac* methylation (and thereby its repression) is a very interesting prospect for expanding our knowledge of the CIP2A/PP2A pathway in haematological malignancies.

Chapter 8: Conclusions

With the future of modern medicine likely to become more personalised, it is imperative that we know as much as possible about the treatment options at our disposal. In CML, treatment options have long favoured imatinib, the gold-standard tyrosine kinase treatment since its approval in 2001. The discovery of this TKI treatment accelerated CML therapy and drastically improved CML survival. However, imatinib is not a curative therapy and resistance or failure still occurs in at least one third of CML patients.

When this work began, dasatinib and nilotinib were newly approved as first line CML treatment and though clinicians now had a range of therapies at their disposal, it remained unclear how to distinguish an individual's best course of treatment. Understanding the complex pathophysiology of CML and identifying useful clinical biomarkers to monitor could help distinguish which patients would benefit most from 2G TKIs as first line treatment.

Knowledge and interest around the *CIP2A* oncogene has rapidly grown since it was discovered as an interacting partner for PP2A in 2002 and later as a potent oncogenic inhibitor of this tumour suppressor(Junttila et al., 2007). Its overexpression in a wide array of tumour types means its involvement in malignancies is likely crucial for tumour development and disease progression.

Overexpression of CIP2A protein in CP-CML and its use as a potential biomarker of blast crisis in imatinib treated CML was an intriguing previous observation(C. M. Lucas et al., 2011). The present work extends this by separating treatment naïve CP-CML into high/low CIP2A cohorts and observed a stark difference in clinical outcomes that was dependent upon future CML therapy. Survival and progression rates for all low CIP2A patients, irrespective of TKI treatment and high CIP2A patients treated with 2G TKIs, were excellent. However high CIP2A patients treated with imatinib had poor OS, PFS and EFS. Additionally, none of this poor outcome cohort achieved a CCR or better – a stark contrast to all other cohorts.

The inferior results of imatinib treatment upon high CIP2A are not seen in patients treated with 2G TKIs, therefore CIP2A's potential biomarker status was not upheld in 2G TKI treated CML. This indicated that dasatinib and nilotinib have an additional effect of suppressing the oncogenic activity of CIP2A in patients that would otherwise have fared poorly on imatinib. **Chapter 4** investigated this more thoroughly and showed a superior suppression of CIP2A protein level by dasatinib and nilotinib over imatinib. This, however, cannot be conclusively stated to be a direct molecular targeting of CIP2A.

This work then looked more closely at the molecular workings of the CIP2A/PP2A pathway (**Chapter 5**) and suggests complex feedback mechanisms between CIP2A, PP2A, BCR-ABL1 and c-Myc. Decreasing CIP2A level via siRNA

or increasing via transient transfection had a causal effect on c-Myc total level and stability, PP2A phosphatase activity and BCR-ABL1 tyrosine kinase activity.

Though this work shows CIP2A levels to inversely correlate with PP2A activity, as measured by tyrosine 307 phosphorylation, the direct interactions between these two molecules are not shown. The many PP2A holoenzymes that can be formed from the three subunits that make up this trimeric protein are varied in their subcellular localisations and binding partners(Haesen et al., 2014; Seshacharyulu et al., 2013). It is possible that CIP2A targets the effects of multiple PP2A molecules that vary between tumours. It is also possible that the binding of CIP2A to PP2A is disrupted by dasatinib and nilotinib and not by imatinib, hence the superior results. Individual patients may express varying proportions of PP2A complexes, some of which are unaffected by CIP2A, which remains at low levels. Investigating the different PP2A subunits and their interactions with CIP2A and c-Myc within a CML population would be an extremely interesting area of research. Unfortunately due to time restrictions and the vast amount of research this would entail, I was unable to take this idea further.

The relationship between CIP2A and c-Myc is also complex. CIP2A is reported to be localised to the cytoplasmic or perinuclear region across a range of malignancies, yet c-Myc is mainly nuclear. Thus, the direct association of these two proteins or the way in which they interact to give the correlating results shown in this thesis seems unclear. A recent study described a novel form of c-Myc that is phosphorylated by c-Abl1 directly, at tyrosine 74(Lobo et al., 2013).

c-Myc pY74 is otherwise not described within the literature. It was reported to amount to only a small fraction of the total cellular myc, though in CML cell lines its ablation correlated directly with a decrease in BCR-ABL1 activity; K562 cells were treated with imatinib; this showed no decrease in total c-Myc which was nuclear, though c-Myc pY74 decreased statistically. Additionally, c-Myc pY74 was not present in the BCR-ABL1 negative cell line HL60. It is possible that the newly described c-Myc pY74 may be the CIP2A-interacting form within the cytoplasm. The colocalisation of CIP2A and c-Myc pY74 and the effects of 2G TKIs upon this tyrosine phosphorylation was not investigated and may be an area of future interest in CML.

CIP2A is overexpressed in solid tumours, but not in normal adjacent cells and is more highly expressed in more aggressive tumours. Though CIP2A protein was stratified according to high/low levels in our CML patients, it had not previously been investigated as to why this varying level was observed. Many genes express different isoforms that can have stark alterations in translation, stability and protein-protein interactions(Surget et al., 2013). It was hypothesised that high/low CIP2A protein levels were due to different expressions of *CIP2A* isoforms in CML patients. I showed the presence of both long and truncated *CIP2A* transcripts in BCR-ABL1 positive cells. Interestingly, the shorter gene transcript was not detectable at the protein level, suggesting a defect in its protein translation or a rapid degradation that makes for its difficult detection at the protein level. Also, an inverse correlation between the full length *CIP2A* mRNA and CIP2A protein level was observed, suggesting a

compensation mechanism of the cell to produce more CIP2A when the level is minimal. It would be interesting to observe the proteasomal degradation of CIP2A in high/low CIP2A expressing cells as a more effective or rapid ubiquitination process may be responsible for the lower levels of CIP2A protein in patients with a more favourable clinical outcome.

Finally, the possibility of epigenetic regulation as an explanation for differing CIP2A levels was considered. Unregulated methylation of genes has been shown to play a role in cell transformation and disease progression in a variety of malignancies(Constanze & Cockerill, 2011; Khanna et al., 2011). Though this work had a stable technique for the detection of methylation, the *CIP2A* promoter was found to be unmethylated at the CpG island investigated. All residues included were unmethylated in both BCR-ABL1 positive and negative cells at all stages of the disease investigated and suggests this type of epigenetic regulation of CIP2A is not of importance in CML.

8.1. Summary

In summarising the aims of this work it can be concluded that the suppression or overexpression of CIP2A is causal in defining c-Myc stability, BCR-ABL1 tyrosine kinase activity and PP2A inactivity and the suppression of CIP2A in conjunction with TKI therapy would be a promising future of CML treatment. Different *CIP2A* transcript variants are present in BCR-ABL1 positive cells. The presence/absence of detectable CIP2A protein for each transcript variant may be due to differing stabilities and/or protein translation success. It is possible that more *CIP2A* isoforms will be discovered in the future and these should be investigated in relation to protein expression in CML. The *CIP2A* promoter is not methylated in my samples, irrespective of whether or not they are BCR-ABL1 positive and suggests this is not a mechanism of CIP2A regulation.

But the most critically relevant finding is that the potential biomarker status of CIP2A is not upheld in 2G TKI treated CML and that this is due to the superior suppression of CIP2A by dasatinib and nilotinib in comparison to imatinib treatment. This has the valuable implication that CIP2A assessment could be part of the diagnostic work-up of newly diagnosed CML, and that patients with high levels should receive a 2G TKI in preference to imatinib, whereas patients with low levels could safely receive either imatinib or a 2G TKI. However, caution is needed in extrapolating the present data as they derive from only 69 patients who were selected for cases with poor outcome. Validation of the present findings in an independent un-selected series is necessary.

Appendix

Patient Characteristics Table of all patients used within this thesis:

UPN	AGE	SEX	1ST-LINE TKI	Alive/Dead	Progression/ Time (months)	Event/ Time (months)	CLINICAL OUTCOME	CIP2A Level
001	59	F	IM	ALIVE	N/81.53	N/81.53	OPTIMAL	LOW
002	62	F	IM	ALIVE	N/24.85	Y/24.85	OPTIMAL	LOW
003	35	F	IM	ALIVE	N/103.1	Y/22.13	OPTIMAL	LOW
004	49	F	IM	ALIVE	N/41.92	Y/45.3	OPTIMAL	LOW
005	54	F	IM	ALIVE	N/18.58	Y/18.58	OPTIMAL	LOW
006	30	F	IM	ALIVE	N/84.99	N/84.99	OPTIMAL	LOW
007	18	F	IM	ALIVE	N/76.01	Y/22.39	OPTIMAL	LOW
008	68	F	IM	ALIVE	N/50.6	N/50.6	OPTIMAL	LOW
009	55	F	IM	ALIVE	N/66.94	N/66.94	OPTIMAL	LOW
010	23	F	IM	ALIVE	N/29.88	Y/18.61	OPTIMAL	LOW
011	43	F	IM	ALIVE	N/34.98	Y/34.98	OPTIMAL	LOW
012	45	F	IM	ALIVE	N/54.08	N/54.08	OPTIMAL	LOW

013	67	F	IM	ALIVE	N/34.95	N/34.95	OPTIMAL	LOW
014	40	F	IM	ALIVE	N/17.62	N/17.95	OPTIMAL	LOW
015	70	F	IM	ALIVE	N/11.54	N/14.27	OPTIMAL	LOW
016	73	M	IM	DEAD	N/92.98	N/92.98	N/A	LOW
017	59	M	IM	ALIVE	N/86.5	N/86.5	OPTIMAL	LOW
018	47	M	IM	ALIVE	N/14.3	Y/17.29	SUB-OPTIMAL	LOW
019	55	M	IM	ALIVE	N/86.37	N/86.37	OPTIMAL	LOW
020	48	M	IM	ALIVE	N/82.09	N/82.09	OPTIMAL	LOW
021	48	M	IM	ALIVE	N/24.92	N/24.92	OPTIMAL	LOW
022	39	M	IM	ALIVE	N/42.12	Y/25.78	OPTIMAL	LOW
023	72	M	IM	ALIVE	N/69.27	N/69.27	OPTIMAL	LOW
024	47	M	IM	ALIVE	N/66.44	Y/16.27	OPTIMAL	LOW
025	33	M	IM	ALIVE	N/68.42	N/68.42	OPTIMAL	LOW
026	28	M	IM	ALIVE	N/14.79	Y/14.79	OPTIMAL	LOW
027	24	M	IM	ALIVE	N/20.81	Y/20.81	OPTIMAL	LOW
028	58	M	IM	ALIVE	N/9.01	Y/9.04	FAILURE	LOW

029	59	M	IM	ALIVE	N/15.88	N/17.95	OPTIMAL	LOW
030	30	F	IM	ALIVE	Y/14.79	Y/9.34	BC	HIGH
031	28	F	IM	ALIVE	N/15.98	Y/15.98	SUB-OPTIMAL	HIGH
032	68	F	IM	ALIVE	N/9.9	Y/9.9	FAILURE	HIGH
033	58	M	IM	ALIVE	Y/7.17	Y/7.17	BC	HIGH
034	23	M	IM	ALIVE	Y/36.03	Y/11.87	BC	HIGH
035	33	M	IM	ALIVE	Y/12.53	Y/13.91	BC	HIGH
036	56	M	IM	ALIVE	Y/11.28	Y/11.28	BC	HIGH
037	24	M	IM	ALIVE	Y/21.44	Y/22.98	BC	HIGH
038	64	M	IM	ALIVE	Y/15.62	Y/15.62	BC	HIGH
039	60	M	IM	ALIVE	Y/31.53	N/31.53	BC	HIGH
040	32	M	IM	ALIVE	Y/15.19	Y/15.19	BC	HIGH
041	45	M	IM	ALIVE	Y/23.18	Y/23.18	BC	HIGH
042	69	F	DAS	ALIVE	N/54.12	N/54.12	OPTIMAL	LOW
043	30	F	DAS	ALIVE	N/16.77	Y/16.77	SUB-OPTIMAL	LOW

044	24	F	DAS	ALIVE	N/44.48	N/44.48	OPTIMAL	LOW
045	51	F	DAS	ALIVE	N/27.16	N/27.16	OPTIMAL	LOW
046	62	F	DAS	ALIVE	N/23.93	Y/12.79	OPTIMAL	LOW
047	58	F	DAS	ALIVE	N/12.66	N/12.66	OPTIMAL	LOW
048	54	M	DAS	ALIVE	N/59.67	N/59.67	OPTIMAL	LOW
049	43	M	DAS	ALIVE	N/23.7	N/23.7	OPTIMAL	LOW
050	48	M	DAS	ALIVE	N/37.55	N/37.55	OPTIMAL	LOW
051	48	M	DAS	ALIVE	N/21.14	N/21.14	OPTIMAL	LOW
052	66	M	DAS	ALIVE	N/18.67	N/18.67	OPTIMAL	LOW
053	54	F	DAS	ALIVE	N/44.02	N/44.02	OPTIMAL	HIGH
054	47	F	DAS	ALIVE	N/43.73	Y/31.89	OPTIMAL	HIGH
055	73	F	DAS	ALIVE	N/23.87	N/23.87	OPTIMAL	HIGH
056	53	F	DAS	ALIVE	N/17.98	N/17.98	OPTIMAL	HIGH
057	52	M	DAS	ALIVE	N/54.35	N/54.35	OPTIMAL	HIGH
058	62	M	DAS	ALIVE	N/52.47	N/52.47	OPTIMAL	HIGH
059	54	M	DAS	ALIVE	N/37.91	N/37.91	OPTIMAL	HIGH
060	49	F	NIL	ALIVE	N/64.67	N/64.67	OPTIMAL	LOW

061	63	F	NIL	ALIVE	N/61.18	N/61.18	OPTIMAL	LOW
062	53	F	NIL	ALIVE	N/60	N/60	OPTIMAL	LOW
063	67	F	NIL	ALIVE	N/60.49	N/60.49	OPTIMAL	LOW
064	46	M	NIL	ALIVE	N/58.82	N/58.82	OPTIMAL	LOW
065	45	M	NIL	ALIVE	N/57.21	N/57.21	OPTIMAL	LOW
066	64	M	NIL	ALIVE	N/8.81	N/8.81	OPTIMAL	LOW
067	57	F	NIL	ALIVE	N/56.45	N/56.45	OPTIMAL	HIGH
068	27	F	NIL	ALIVE	N/19.86	N/19.86	OPTIMAL	HIGH
069	74	F	NIL	ALIVE	N/11.77	N/11.77	OPTIMAL	HIGH
070	73	F	N/A	N/A	N/A	N/A	N/A	LOW
071	54	F	N/A	N/A	N/A	N/A	N/A	LOW
072	68	F	N/A	N/A	N/A	N/A	N/A	LOW
073	69	M	N/A	N/A	N/A	N/A	N/A	LOW
074	55	M	N/A	N/A	N/A	N/A	N/A	LOW
075	54	M	N/A	N/A	N/A	N/A	N/A	LOW
076	34	M	N/A	N/A	N/A	N/A	N/A	LOW
077	35	F	N/A	N/A	N/A	N/A	N/A	HIGH
078	27	F	N/A	N/A	N/A	N/A	N/A	HIGH

079	62	F	N/A	N/A	N/A	N/A	N/A	HIGH
080	52	F	N/A	N/A	N/A	N/A	N/A	HIGH
081	29	M	N/A	N/A	N/A	N/A	N/A	HIGH
082	69	M	N/A	N/A	N/A	N/A	N/A	HIGH
083	63	F	N/A	ALIVE	N/A	N/A	N/A	LOW
084	74	F	N/A	ALIVE	N/A	N/A	N/A	HIGH
085	76	M	N/A	ALIVE	N/A	N/A	N/A	HIGH
086	61	M	N/A	ALIVE	N/A	N/A	N/A	LOW
087	69	F	N/A	DEAD	N/A	N/A	N/A	LOW
088	60	M	N/A	DEAD	N/A	N/A	N/A	HIGH
089	55	M	N/A	ALIVE	N/A	N/A	SUB-OPTIMAL	LOW
090	24	M	N/A	ALIVE	N/A	N/A	SUB-OPTIMAL	HIGH
091	39	M	N/A	ALIVE	N/A	N/A	SUB-OPTIMAL	HIGH
092	45	F	N/A	ALIVE	N/A	N/A	FAILURE	LOW
093	68	F	N/A	ALIVE	N/A	N/A	FAILURE	LOW
094	69	F	N/A	ALIVE	N/A	N/A	FAILURE	HIGH
095	70	M	N/A	ALIVE	N/A	N/A	FAILURE	HIGH

096	58	M	N/A	ALIVE	N/A	N/A	FAILURE	HIGH
097	56	M	N/A	ALIVE	N/A	N/A	FAILURE	HIGH
098	49	M	N/A	ALIVE	N/A	N/A	FAILURE	HIGH
099	62	M	N/A	ALIVE	N/A	N/A	FAILURE	HIGH
100	63	M	N/A	ALIVE	N/A	N/A	FAILURE	HIGH
101	60	F	N/A	DEAD	N/A	N/A	BC	HIGH
102	51	M	N/A	DEAD	N/A	N/A	BC	HIGH

List of Abbreviations

ABBREVIATION	DEFINITION
2G/3G TKI	2nd generation/3rd generation TKI
ABC	ATP-binding cassette
ABCC3	ATP-binding cassette C3
ABL1	Abelson leukaemia
ADAGIO	Adherence assessment with Glivec: indicators and outcomes
AGP	α1-acid glycoprotein
AGS	Human Caucasian gastric adenocarcinoma
AKT (PKB)	Protein kinase B
ALL	Acute lymphoblastic leukaemia
AML	Acute myeloid leukaemia
AP	Accelerated phase
APML	Acute promyelocytic leukaemia
APS	Ammonium persulphate
ATF2	Activating transcription factor 2
ATP	Adenosine triphosphate
BC	Blast crisis
BCR	Breakpoint cluster region
BELA	Bosutinib efficacy and safety in newly diagnosed chronic myeloid leukaemia
BM	Bone marrow
BOS	Bosutinib
BRCA1/2	Breast cancer 1/2

BSA	Bovine serum albumin
CCR	Complete Cytogenetic Response
CHR	Complete haematological response
CIP2A	Cancerous inhibitor of PP2A
CIP2A-1a	*CIP2A* long transcript (905 amino acids)
CIP2A-1b	*CIP2A* short transcript (746 amino acids)
c-KIT	Cellular stem cell growth factor receptor
CML	Chronic myeloid leukaemia
c-Myc	v-myc myelocytomatosis viral oncogene homolog
CP	Chronic phase
CpG	Cytosine-phosphate-guanine
CrKL	V-Crk Avian Sarcoma Virus CT10 Oncogene Homolog-Like
DAS	Dasatinib
DASISION	Dasatinib versus imatinib study in treatment-naïve CML
DMEM	Dulbecco's modified eagle medium
DMSO	Dimethyl sulphoxide
DNA	Deoxyribonucleic acid
dNTP	Deoxyribonucleotide triphosphate
DSSB	Double strength SDS buffer
DTT	DL-dithiothreitol
E2F1	Eurkayote Transcription factor 2
ECL	Enhanced chemiluminescence
EDTA	Ethylene diamine tetraacetic acid
EFS	Event free survival
EGTA	Ethylene glycol tetraacetic acid
ELISA	Enzyme-linked immunosorbence assay
ELK1	ETS domain-containing protein Elk-1
ELN	European LeukemiaNet
ENESTnd	Evaluating nilotinib efficacy and safety in clinical trials newly diagnosed patients

EPIC	Phase III trial of ponatinib compared with imatinib in patients with newly diagnosed CP-CML
ER	Endoplasmic reticulum
ERK	Extracellular signal-regulated kinases
ETS1	V-Ets Avian Erythroblastosis Virus E26 Oncogene Homolog 1
FCS	Foetal calf serum
FDA	Food and drug administration
FO	Forskolin
FSC	Forward scatter
FTY720	Fingolimod
FWB7	F-box/WD repeat-containing protein 7
GAPDH	Glyceraldehyde 3 phosphate dehydrogenase
GFP	Green fluorescent protein
GRB2	Growth factor receptor-bound protein 2
GSK-3β	Glycogen synthase kinase 3 beta
HCl	Hydrogen chloride
HEAT	Huntingtin, elongation factor 3, PP2A, TOR1
HEK293	Human embryonic kidney-derived
HELA	Human epithelial cells
HEPES	4-(2-hydroxyethyl)-1-piperazineethanesulfonic acid
HIC1	Hypermethylated In Cancer 1
HL60	Human promyelocytic leukaemia cells
hOCT1	Human organic cation transporter 1
HSC	Haematopoietic stem cell
HSCT	Haematopoietic stem cell transplantation
IFN-α	Interferon-α
IGBP1	Immunoglobulin binding protein 1
IgG	Immunoglobulin G
IM	Imatinib
IRIS	International randomised study of interferon versus

	STI571
JAK2	Janus kinase 2
JNK2	c-Jun N-terminal kinase 2
KD	Kinase domain
L	Leucine
LAMA84	Human CML cell line
LB	Lysogeny broth
MAPK	Mitogen-activated protein kinases
M-/m-/μ-BCR	Major-/minor-/micro-breakpoint cluster region
MDR	Multi-drug resistant
MFI	Mean fluorescence intensity
$MgCl_2$	Magnesium chloride
MMR	Major molecular response
MNC	Mononuclear cell
MPN	Myeloproliferative neoplasms
MR4	Molecularly response at the 4 log level
NaCl	Sodium chloride
NaF	Sodium fluoride
NaOH	Sodium hydroxide
NIL	Nilotinib
NP-40	Nonyl phenoxypolyethoxylethanol
OA	Okadaic acid
Oral SCC	Oral squamous cell carcinoma
OS	Overall survival
p53	Tumour protein 53
PACE	Ponatinib Philadelphia-positive acute lymphoblastic leukaemia and CML evaluation
PBMC	Peripheral blood mononuclear cell
PBS	Phosphate buffered saline
PCR	Polymerase chain reaction
PDGFRα/β	Platelet-derived growth factor receptors

PFS	Progression free survival
Ph+	Philadelphia positive
PI	Propidium iodide
PI3K	Phosphoinositide 3-kinase
PIN-1	Peptidyl-prolyl cis-trans isomerase NIMA-interacting 1
PME-1	PP2A methyl esterase 1
PON	Ponatinib
PP2A	Protein phosphatase 2A
PP2A-A	PP2A-structural subunit
PP2A-B	PP2A-regulatory subunit
PP2A-C	PP2A-catalytic subunit
PR	Proline-rich
pS-	Phospho-serine-
pT-	Phospho-threonine-
PVDF	Polyvinylidene difluoride
pY-	Phospho-tyrosine-
qRT-PCR	Quantitative real-time polymerase chain reaction
RAS	Rat sarcoma
RIPA	Radioimmunoprecipitation assay
RLT	RNeasy lysis buffer
RNA	Ribonucleic acid
ROC	Receiver operating characteristics
RPE	RNeasy wash buffer 2
RPMI-1640	Roswell park memorial institute 1640
RW1	RNeasy wash buffer 1
SDS	Sodium dodecyl sulphate
SET	Nuclear proto-oncogene
SETBP1	SET binding protein 1
SFK	SRC family kinase

SH1/2/3	Src Homology domain 1/2/3
siRNA	Small interfering RNA
SNP	Single nucleotide polymorphism
SOC	Superoptimal broth with catabolite repression
SRC	Sarcoma
SSC	Side scatter
START-A/-B/-C/-L	SRC-ABL1 tyrosine kinase inhibition activity research trial-A/-B/-C/-L
STAT5	Signal transducer and activator of transcription 5
SV40	Simian virus 40
T315I	Tyrosine 315 isoleucine mutation
TBE	Tris/Borate/EDTA
TBS	Tris-buffered saline
TBS-T	Tris-buffered saline-Tween20
TEMED	Tetramethyl ethylene diamine
TK	Tyrosine kinase
TKI	Tyrosine kinase inhibitor
U937	Human leukemic monocyte lymphoma cell line
UPN	Unique patient number
WB	Western blotting
WBC	White blood cell

References

Aaron, D., Goldberg, C., Allis, D., & Bernstein, E. (2007). Epigenetics: A Landscape Takes Shape. *Cell, 128*(4), 4.

Abelson, H. T., & Rabstein, L. S. (1970). Lymphosarcoma: Virus-induced Thymic-independent Disease in Mice. *Cancer Research, 30*(8), 2213-2222.

Adamia, S., Pilarski, P. M., Bar-Natan, M., Stone, R. M., & Griffin, J. D. (2013). Alternative Splicing in Chronic Myeloid Leukemia (CML): A Novel Therapeutic Target? *Current Cancer Drug Targets, 13*(7), 14.

Advani, A. S., & Pendergast, A. M. (2002). Bcr–Abl variants: biological and clinical aspects. *Leukemia research, 26*(8), 713-720.

AK Samanta, SN Chakraborty, Y Wang, & H Kantarjian, X. S., 3 J Hood,4,6 D Perrotti,5 and RB Arlinghaus1. (2009). Jak2 inhibition deactivates Lyn kinase through the SET–PP2A–SHP1 pathway, causing apoptosis in drug-resistant cells from chronic myelogenous leukemia patients. *Oncogene, 28*(14), 12.

Armand, P. (2007). Novel Therapies for Acute Lymphoblastic Leukemia. *The Molecular Oncology Report, 1*(2).

Asimakopoulos, F., Shteper, P., Fibach, E., Rachmilewitz, E., Ben-Neriah, Y., & Ben-Yehuda, D. (1999). Prognostic Significance of c-ABL Methylation in Chronic Myelogenous Leukemia: Still an Open Question. *Blood, 94*(3), 1.

Asimakopoulos, F., Shteper, P., Krichevsky, S., Fibach, E., Polliack, A., Rachmilewitz, E., . . . Ben-Yehuda, D. (1999). ABL1 methylation is a distinct molecular event associated with clonal evolution of chronic myeloid leukemia. *Blood, 94*(7), 8.

Baccarani, M., Deininger, M. W., Rosti, G., Hochhaus, A., Soverini, S., Apperley, J. F., . . . Hehlmann, R. (2013). European LeukemiaNet recommendations for the management of chronic myeloid leukemia: 2013. *Blood, 122*(6), 872-884.

Baccarani, M., Saglio, G., Goldman, J., Hochhaus, A., Simonsson, B., Appelbaum, F., . . . Hehlmann, R. (2006). Evolving concepts in the management of chronic myeloid leukemia: recommendations from an expert panel on behalf of the European LeukemiaNet. *Blood, 108*(6), 1809-1820.

Basile, J., & Czerninski, R. (2010). The role of CIP2A in oral squamous cell carcinoma. *Cancer Biology & Therapy, 10*(7), 2.

Ben-Yehuda, D., Krichevsky, S., Rachmilewitz, E., Avraham, A., Palumbo, G., Frassoni, F., . . . Ben-Neriah, Y. (1997). Molecular Follow-Up of Disease Progression and Interferon Therapy in Chronic Myelocytic Leukemia. *Blood, 90*(12), 5.

Benassi, B., Fanciulli, M., Fiorentino, F., Porrello, A., Chiorino, G., Loda, M., . . . Biroccio, A. (2006). c-Myc Phosphorylation Is Required for Cellular Response to Oxidative Stress. *Molecular Cell, 21*(4), 509-519.

Bennet, J. H. (1845). Case of hypertrophy of the spleen and liver in which death took place from suppuration of the blood. *Edinburgh Medical and Surgical Journal*

64, 10.

Bennett, J. H. (1852). Leucocythaemia, or White Cell Blood in Relation to the Physiology and Pathology of the Lymphatic Glandular System. *Edinburgh Medical and Surgical Journal, 72*, 75.

Bird, A. (2007). Perceptions of Epigenetics. *Nature, 447*, 3.

Bockelman, C., Hagstrom, J., Makinen, L. K., Keski-Santti, H., Hayry, V., Lundin, J., . . . Haglund, C. (2011). High CIP2A immunoreactivity is an independent prognostic indicator in early-stage tongue cancer. *British Journal of Cancer, 104*(12), 5.

Bockelman, C., Lassus, H., Hemmes, A., Leminen, A., Westermarck, J., Haglund, C., . . . Ristimaki, A. (2011). Prognostic role of CIP2A expression in serous ovarian cance. *British Journal of Cancer, 105*(7), 6.

Boultwood, J., & Wainscoat, J. (2007). Gene silencing by DNA methylation in haematological malignancies. *British Journal of Haematology, 138*(1), 8.

Branford, S., Rudzki, Z., & Hughes, T. P. (2000). A novel BCR–ABL transcript (e8a2) with the insertion of an inverted sequence of ABL intron 1b in a patient with Philadelphia-positive chronic myeloid leukaemia. *British Journal of Haematology, 109*(3), 635-637.

Brasher, B., Roumiantsev, S., & Van Etten, R. (2001). Mutational analysis of the regulatory function of the c-Abl Src homology 3 domain. *Oncogene, 20*(53), 8.

Burmeister, T., & Reinhardt, R. (2008). A multiplex PCR for improved detection of typical and atypical BCR–ABL fusion transcripts. *Leukemia research, 32*(4), 579-585.

Chen, W., Arroyo, J. D., Timmons, J. C., Possemato, R., & Hahn, W. C. (2005). Cancer-Associated PP2A Aα Subunits Induce Functional Haploinsufficiency and Tumorigenicity. *Cancer Research, 65*(18), 8183-8192.

Cilloni, D., & Saglio, G. (2012). Molecular Pathways: BCR-ABL. *Clinical Cancer Research, 18*(4), 930-937.

Coenen, E. A., Zwaan, C. M., Meyer, C., Marschalek, R., Pieters, R., van der Veken, L. T., . . . van den Heuvel-Eibrink, M. M. (2010). KIAA1524: A novel MLL translocation partner in acute myeloid leukemia. *Leukemia research, 35*(1), 133-135.

Cohen, M. H., Williams, G., Johnson, J. R., Duan, J., Gobburu, J., Rahman, A., . . . Pazdur, R. (2002). Approval Summary for Imatinib Mesylate Capsules in

the Treatment of Chronic Myelogenous Leukemia. *Clinical Cancer Research, 8*(5), 935-942.

Colella, S., Ohgaki, H., Ruediger, R., Yang, F., Nakamura, M., Fujisawa, H., . . . Walter, G. (2001). Reduced expression of the Aα subunit of protein phosphatase 2A in human gliomas in the absence of mutations in the Aα and Aβ subunit genes. *International Journal of Cancer, 93*(6), 798-804.

Come, C., Laine, A., Chanrion, M., Edgren, H., Mattila, E., Liu, X., . . . Westermarck, J. (2009). CIP2A Is Associated with Human Breast Cancer Aggressivity. *Clinical Cancer Research, 15*.

Constanze, B., & Cockerill, P. (2011). Chromatin Mechanisms Regulating Gene Expression In Health And Disease. *Advanced Experimental Medical Biology, 7*(11), 13.

Cortes, J., Jones, D., & Kantarjian, H. (2010). Results of Dasatinib Therapy in Patients With Early Chronic-Phase Chronic Myeloid Leukemia. *Journal of Clinical Oncology, 29*(3), 6.

Cortes, J. E., Kantarjian, H. M., Brümmendorf, T. H., Kim, D.-W., Turkina, A. G., Shen, Z.-X., . . . Gambacorti-Passerini, C. (2011). Safety and efficacy of bosutinib (SKI-606) in chronic phase Philadelphia chromosome–positive chronic myeloid leukemia patients with resistance or intolerance to imatinib. *Blood, 118*(17), 4567-4576.

Cortes, J. E., Kim, D.-W., Kantarjian, H. M., Brümmendorf, T. H., Dyagil, I., Griskevicius, L., . . . Gambacorti-Passerini, C. (2012). Bosutinib Versus Imatinib in Newly Diagnosed Chronic-Phase Chronic Myeloid Leukemia: Results From the BELA Trial. *Journal of Clinical Oncology, 30*(28), 3486-3492.

Cortes, J. E., Kim, D.-W., Pinilla-Ibarz, J., le Coutre, P., Paquette, R., Chuah, C., . . . Kantarjian, H. (2013). A Phase 2 Trial of Ponatinib in Philadelphia Chromosome–Positive Leukemias. *New England Journal of Medicine, 369*(19), 1783-1796.

Cowan Doyle, A. (1882). Notes on a case of leucocythaemia. *Lancet*.

Darst, R., Pardo, C., Ai, L., Brown, K., & Kladde, M. (2010). Bisulfite Sequencing of DNA. *Cell & Molecular Biology*.

Das, J., Chen, P., Norris, D., Padmanabha, R., Lin, J., Moquin, R. V., . . . Barrish, J. C. (2006). 2-Aminothiazole as a Novel Kinase Inhibitor Template. Structure−Activity Relationship Studies toward the Discovery of N-(2-Chloro-6-methylphenyl)-2-[[6-[4-(2-hydroxyethyl)-1- piperazinyl)]-2-methyl-4-pyrimidinyl]amino)]-1,3-thiazole-5-carboxamide (Dasatinib, BMS-354825) as a Potent pan-Src Kinase Inhibitor. *Journal of Medicinal Chemistry, 49*(23), 6819-6832.

Das, P. M., & Singal, R. (2004). DNA Methylation and Cancer. *Journal of Clinical Oncology, 22*(22), 4632-4642. doi:10.1200/jco.2004.07.151

Database, e. E. Gene: KIAA1524.

Davies, A., Jordanides, N. E., Giannoudis, A., Lucas, C., Hatziieremia, S., Harris, R., . . . Mountford, J. (2009). Nilotinib concentration in cell lines and primary CD34+ chronic myeloid leukemia cells is not mediated by active uptake or efflux by major drug transporters. *Leukemia, 23*(11), 7.

De Braekeleer, E., Douet-Guilbert, N., Rowe, D., Bown, N., Morel, F., Berthou, C., . . . De Braekeleer, M. (2011). ABL1 fusion genes in hematological malignancies: a review. *European Journal of Haematology, 86*(5), 361-371.

Dehm, S. M. (2013). mRNA Splicing Variants: Exploiting Modularity to Outwit Cancer Therapy. *Cancer Research, 73*(17), 5309-5314.

Deininger, M. W. (2008a). Milestones and Monitoring in Patients with CML Treated with Imatinib. *ASH Education Program Book, 2008*(1), 419-426.

Deininger, M. W. (2008b). Nilotinib. *Clinical Cancer Research, 14*(13), 4027-4031.

Deininger, M. W. N., Goldman, J. M., & Melo, J. V. (2000). The molecular biology of chronic myeloid leukemia. *Blood, 96*(10), 3343-3356.

Dong, Q.-Z., Wang, Y., Dong, X.-J., Li, Z.-X., Tang, Z.-P., Cui, Q.-Z., & Wang, E.-H. (2011). CIP2A is Overexpressed in Non-Small Cell Lung Cancer and Correlates with Poor Prognosis. *Annals of Surgical Oncology, 18*(3), 857-865.

Druker, B. J., Talpaz, M., Resta, D. J., Peng, B., Buchdunger, E., Ford, J. M., . . . Sawyers, C. L. (2001). Efficacy and Safety of a Specific Inhibitor of the BCR-ABL Tyrosine Kinase in Chronic Myeloid Leukemia. *New England Journal of Medicine, 344*(14), 1031-1037.

Druker, B. J., Tamura, S., Buchdunger, E., Ohno, S., Segal, G. M., Fanning, S., . . . Lydon, N. B. (1996). Effects of a selective inhibitor of the Abl tyrosine kinase on the growth of Bcr–Abl positive cells. *Nature Medicine, 2*, 5.

Dunwell, T., Hesson, L., Rauch, T., Wang, L., Clark, R., Dallol, A., . . . Latif, F. (2010). A Genome-wide screen identifies frequently methylated genes in haematological and epithelial cancers. *Molecular Cancer, 9*(44).

Dupont, M., Jourdan, E., & Chiesa, J. (2000). Identification of E6A2 BCR-ABL fusion in a Philadelphia-positive CML. *Leukemia, 14*(11), 1.

Fang, Y., Li, Z., Wang, X., & Zhang, S. (2012). CIP2A is overexpressed in human ovarian cancer and regulates cell proliferation and apoptosis. *Tumor Biology, 33*(6), 2299-2306.

Fava, C., Kantarjian, H., & Cortes, J. (2012). Molecular Resistance: An Early Indicator for Treatment Change? *Clinical Lymphoma Myeloma and Leukemia, 12*(2), 79-87.

Feinberg, A., & Cogelstein, B. (1983). Hypomethylation of ras oncogenes in primary human cancers. *Biochemical and Biophysical Research Communications, 111*(1), 7.

Fernandez, P., Frank, S., Wang, L., Schroeder, M., Liu, S., Greene, J., . . . Amati, B. (2003). Genomic targets of the human c-Myc protein. *Genes and Development, 17*(9), 14.

Francis, S., Lucas, C., Lane, S., Wang, L., Watmough, S., Knight, K., . . . Clark, R. E. (2013). A population study showing that the advent of second generation tyrosine kinase inhibitors has improved progression-free survival in chronic myeloid leukaemia. *Leukemia research, 37*(7), 752-758.

Fuxin, Y., Weimin, N., Weixian, L., Jinyang, B., & Wenbin, L. (2013). Expression and biological role of CIP2A in human astrocytoma. *Molecular Medicine Reports, 7*(5), 4.

Gambacorti-Passerini, C., Barni, R., le Coutre, P., Zucchetti, M., Cabrita, G., Cleris, L., . . . D'Incalci, M. (2000). Role of α1 Acid Glycoprotein in the In Vivo Resistance of Human BCR-ABL+ Leukemic Cells to the Abl Inhibitor STI571. *Journal of the National Cancer Institute, 92*(20), 1641-1650.

Geary, C. G. (2000). The story of chronic myeloid leukaemia. *British Journal of Haematology, 110*(1), 9.

Giannoudis, A., Davies, A., Harris, R., Lucas, C., Pirmohamed, M., & Clark, R. (2014). The clinical significance of ABCC3 as an imatinib transporter in chronic myeloid leukaemia. *Leukemia*.

Giannoudis, A., Davies, A., Lucas, C. M., Harris, R. J., Pirmohamed, M., & Clark, R. E. (2008). Effective dasatinib uptake may occur without human organic cation transporter 1 (hOCT1): implications for the treatment of imatinib-resistant chronic myeloid leukemia. *Blood, 112*(8), 3348-3354.

Giannoudis, A., Wang, L., Jorgensen, A. L., Xinarianos, G., Davies, A., Pushpakom, S., . . . Clark, R. E. (2013). The hOCT1 SNPs M420del and M408V alter imatinib uptake and M420del modifies clinical outcome in imatinib-treated chronic myeloid leukemia. *Blood, 121*(4), 628-637.

Giles, F., Larson, R., Kantarjian, H., le Coutre, P., Palandri, F., Haque, A., . . . Ottmann, O. (2008). Nilotinib in patients with Philadelphia chromosome-positive chronic myelogenous leukemia in blast crisis (CML-BC) who are resistant or intolerant to imatinib. *Journal of Clinical Oncology, 26*(15).

Gorre, M. E., Mohammed, M., Ellwood, K., Hsu, N., Paquette, R., Rao, P. N., & Sawyers, C. L. (2001). Clinical Resistance to STI-571 Cancer Therapy Caused by BCR-ABL Gene Mutation or Amplification. *Science, 293*(5531), 876-880.

Gregory, M. A., Qi, Y., & Hann, S. R. (2003). Phosphorylation by Glycogen Synthase Kinase-3 Controls c-Myc Proteolysis and Subnuclear Localization. *Journal of Biological Chemistry, 278*(51), 51606-51612.

Group, C. T. C. (1997). Interferon Alfa Versus Chemotherapy for Chronic Myeloid Leukemia: A Meta-analysis of Seven Randomized Trials. *Journal of the National Cancer Institute, 89*(21), 1616-1620.

Haesen, D., Sents, W., Lemaire, K., Hoorne, Y., & Janssens, V. (2014). The Basic Biology of PP2A in Hematologic Cells and Malignancies. *Frontiers in Oncology, 4*, 347.

Hajian-Tilaki, K. (2013). Receiver Operating Characteristic (ROC) Curve Analysis for Medical Diagnostic Test Evaluation. *Caspian Journal of Internal Medicine, 4*(2), 8.

Hantschel, O., & Superti-Furga, G. (2004). Regulation of the c-Abl and Bcr-Abl tyrosine kinases. *Nat Rev Mol Cell Biol, 5*(1), 33-44.

Haškovec, C., Ponzetto, C., Polák, J., Maritano, D., Zemanová, Z., Serra, A., . . . Saglio, G. (1998). P230 BCR/ABL protein may be associated with an acute leukaemia phenotype. *British Journal of Haematology, 103*(4), 1104-1108.

Hassan, A. Q., Sharma, S. V., & Warmuth, M. (2010). Allosteric inhibition of BCR-ABL. *Cell Cycle, 9*(18), 4.

He, H., Wu, G., Li, W., Cao, Y., & Liu, Y. (2012). CIP2A Is Highly Expressed in Hepatocellular Carcinoma and Predicts Poor Prognosis. *Diagnostic Molecular Pathology, 21*(3), 143-149.

Helgason, G. V., Karvela, M., & Holyoake, T. L. (2011). Kill one bird with two stones: potential efficacy of BCR-ABL and autophagy inhibition in CML. *Blood, 118*(8), 2035-2043.

Hochhaus, A., & La Rosee, P. (2004). Imatinib therapy in chronic myelogenous leukemia: strategies to avoid and overcome resistance. *Leukemia, 18*(8), 10.

Hochhaus, A., Reiter, A., Skladny, H., Melo, J., Sick, C., Berger, U., . . . Cross, N. (1996). A novel BCR-ABL fusion gene (e6a2) in a patient with Philadelphia chromosome-negative chronic myelogenous leukemia. *Blood, 88*(6), 2236-2240.

Huang, L., Adelson, M., Mordechai, E., & Trama, J. (2011). CIP2A expression is elevated in cervical cancer. *Cancer Biomarkers, 8*(6), 8.

Huang, L. P., Savoly, D., Sidi, A. A., Adelson, M. E., Mordechai, E., & Trama, J. P. (2012). CIP2A protein expression in high-grade, high-stage bladder cancer. *Cancer Medicine, 1*(1), 5.

Huang, P., Qiu, J., You, J., Hong, J., Li, B., Zhou, K., . . . Zou, R. (2012). Expression and prognostic significance of CIP2A mRNA in hepatocellular carcinoma and nontumoral liver tissues. *Biomarkers, 17*(5), 7.

Hughes, T., Deininger, M., Hochhaus, A., Branford, S., Radich, J., Kaeda, J., . . . Goldman, J. M. (2006). Monitoring CML patients responding to treatment with tyrosine kinase inhibitors: review and recommendations for harmonizing current methodology for detecting BCR-ABL transcripts and kinase domain mutations and for expressing results. *Blood, 108*(1), 28-37.

Hughes, T., Kaeda, J., Branford, S., Rudzki, Z., Hochhaus, A., Hensley, M. L., . . . Group, I. R. S. o. I. v. S. I. S. (2003). Frequency of Major Molecular

Responses to Imatinib or Interferon Alfa plus Cytarabine in Newly Diagnosed Chronic Myeloid Leukemia. *New England Journal of Medicine, 349*(15), 9.

Hughes, T. P., Hochhaus, A., Branford, S., Müller, M. C., Kaeda, J. S., Foroni, L., . . . investigators, o. b. o. t. I. (2010). Long-term prognostic significance of early molecular response to imatinib in newly diagnosed chronic myeloid leukemia: an analysis from the International Randomized Study of Interferon and STI571 (IRIS). *Blood, 116*(19), 3758-3765.

Ichimaru, M., Tomonaga, M., Amenomori, T., & Matsuo, T. (1991). Atomic Bomb and Leukemia. *Journal of Radiation Research, 32*(Suppl 1), 162-167.

Issa, J.-P. J., Zehnbauer, B. A., Civin, C. I., Collector, M. I., Sharkis, S. J., Davidson, N. E., . . . Baylin, S. B. (1996). The Estrogen Receptor CpG Island Is Methylated in Most Hematopoietic Neoplasms. *Cancer Research, 56*(5), 973-977.

Issa, J.-P. J., Zehnbauer, B. A., Kaufmann, S. H., Biel, M. A., & Baylin, S. B. (1997). HIC1 Hypermethylation Is a Late Event in Hematopoietic Neoplasms. *Cancer Research, 57*(9), 1678-1681.

Issa, J., Kantarjian, H., Mohan, A., O'Brien, S., Cortes, J., Pierce, S., & Talpaz, M. (1999). Methylation of the ABL1 Promoter in Chronic Myelogenous Leukemia: Lack of Prognostic Significance. *Blood, 93*(6), 5.

Jabbour, E., Kantarjian, H. M., Saglio, G., Steegmann, J. L., Shah, N. P., Boqué, C., . . . Hochhaus, A. (2014). Early response with dasatinib or imatinib in chronic myeloid leukemia: 3-year follow-up from a randomized phase 3 trial (DASISION). *Blood, 123*(4), 494-500.

Jabbour, E. J., Kantarjian, H., Eliasson, L., Megan Cornelison, A., & Marin, D. (2012). Patient adherence to tyrosine kinase inhibitor therapy in chronic myeloid leukemia. *American Journal of Hematology, 87*(7), 687-691.

Jackson, J., & Pallas, D. (2012). Circumventing cellular control of PP2A by methylation promotes transformation in an Akt-dependent manner. *Neoplasia, 14*(7), 13.

Jelinek, J., Gharibyan, V., Estecio, M., Kondo, K., He, R., Chung, W., . . . Issa, J. (2011). Aberrant DNA methylation is associated with disease progression, resistance to imatinib and shortened survival in chronic myelogenous leukemia. *PLOS, 6*(7), e22110.

Jung, H., Patel, R., Phillips, B., Wang, H., Cohen, D., Reinhold, W., . . . Chan, E. (2013). Tumor suppressor miR-375 regulates MYC expression via repression of CIP2A coding sequence through multiple miRNA-mRNA interactions. *Molecular Biology of the Cell, 24*(11), 10.

Junttila, M. R., Puustinen, P., Niemelä, M., Ahola, R., Arnold, H., Böttzauw, T., . . . Westermarck, J. (2007). CIP2A Inhibits PP2A in Human Malignancies. *Cell, 130*(1), 51-62.

Junttila, M. R., & Westermarck, J. (2008). Mechanisms of MYC stabilization in human malignancies. *Cell Cycle, 7*(5), 592-596.

Kampen, K. R. (2012). The discovery and early understanding of leukemia. *Leukemia research, 36*(1), 7.

Kantarjian, H., Giles, F., Wunderle, L., Bhalla, K., O'Brien, S., Wassmann, B., . . . Ottmann, O. G. (2006). Nilotinib in Imatinib-Resistant CML and Philadelphia Chromosome–Positive ALL. *New England Journal of Medicine, 354*(24), 2542-2551.

Kantarjian, H., Shah, N. P., Hochhaus, A., Cortes, J., Shah, S., Ayala, M., . . . Baccarani, M. (2010). Dasatinib versus Imatinib in Newly Diagnosed Chronic-Phase Chronic Myeloid Leukemia. *New England Journal of Medicine, 362*(24), 2260-2270.

Kantarjian, H. M., Giles, F. J., Bhalla, K. N., Pinilla-Ibarz, J., Larson, R. A., Gattermann, N., . . . le Coutre, P. D. (2011). Nilotinib is effective in patients with chronic myeloid leukemia in chronic phase after imatinib resistance or intolerance: 24-month follow-up results. *Blood, 117*(4), 1141-1145.

Kantarjian, H. M., O'Brien, S., Cortes, J. E., Shan, J., Giles, F. J., Rios, M. B., . . . Talpaz, M. (2003). Complete cytogenetic and molecular responses to interferon-α-based therapy for chronic myelogenous leukemia are associated with excellent long-term prognosis. *Cancer, 97*(4), 1033-1041.

Kantarjian, H. M., Shah, N. P., Cortes, J. E., Baccarani, M., Agarwal, M. B., Undurraga, M. S., . . . Hochhaus, A. (2012). Dasatinib or imatinib in newly diagnosed chronic-phase chronic myeloid leukemia: 2-year follow-up from a randomized phase 3 trial (DASISION). *Blood, 119*(5), 1123-1129.

Kantarjian, H. M., Smith, T. L., O'Brien, S., Beran, M., Pierce, S., & Talpaz, M. (1995). Prolonged Survival in Chronic Myelogenous Leukemia after Cytogenetic Response to Interferon-α Therapy. *Annals of Internal Medicine, 122*(4), 254-261.

Khanna, A., Böckelman, C., Hemmes, A., Junttila, M. R., Wiksten, J.-P., Lundin, M., . . . Ristimäki, A. (2009). MYC-Dependent Regulation and Prognostic Role of CIP2A in Gastric Cancer. *Journal of the National Cancer Institute, 101*(11), 793-805.

Khanna, A., Okkeri, J., Bilgen, T., Tiirikka, T., Vihinen, M., Visakorpi, T., & Westermarck, J. (2011). ETS1 Mediates MEK1/2-Dependent Overexpression of Cancerous Inhibitor of Protein Phosphatase 2A (CIP2A) in Human Cancer Cells. *PLoS ONE, 6*(3), e17979.

Khanna, A., Pimanda, J. E., & Westermarck, J. (2013). Cancerous Inhibitor of Protein Phosphatase 2A, an Emerging Human Oncoprotein and a Potential Cancer Therapy Target. *Cancer Research, 73*(22), 6548-6553.

Kharas, M. G., & Fruman, D. A. (2005). ABL Oncogenes and Phosphoinositide 3-Kinase: Mechanism of Activation and Downstream Effectors. *Cancer Research, 65*(6), 2047-2053.

Khoury, H. J., Cortes, J. E., Kantarjian, H. M., Gambacorti-Passerini, C., Baccarani, M., Kim, D.-W., . . . Brümmendorf, T. H. (2012). Bosutinib is active in

chronic phase chronic myeloid leukemia after imatinib and dasatinib and/or nilotinib therapy failure. *Blood, 119*(15), 3403-3412.

Kwong, Y., & Cheng, G. (1993). Clonal nature of chronic neutrophilic leukemia [letter] [see comments]. *Blood, 82*(3), 1035-1036.

Laine, A., Sihto, H., Come, C., Rosenfeldt, M. T., Zwolinska, A., Niemelä, M., . . . Westermarck, J. (2013). Senescence Sensitivity of Breast Cancer Cells Is Defined by Positive Feedback Loop between CIP2A and E2F1. *Cancer Discovery, 3*(2), 182-197.

Larson, R., Hochhaus, A., Hughes, T., Clark, R., Etienne, G., Kim, D.-W., . . . Kantarjian, H. (2012). Nilotinib vs imatinib in patients with newly diagnosed Philadelphia chromosome-positive chronic myeloid leukemia in chronic phase: ENESTnd 3-year follow-up. *Leukemia, 26*(10), 6.

le Coutre, P., Giles, F., Hochhaus, A., Apperley, J., Ossenkoppele, G., Blakesley, R., . . . Kantarjian, H. (2012). Nilotinib in patients with Ph+ chronic myeloid leukemia in accelerated phase following imatinib resistance or intolerance: 24-month follow-up results. *Leukemia, 26*, 5.

le Coutre, P., Tassi, E., Varella-Garcia, M., Barni, R., Mologni, L., Cabrita, G., . . . Gambacorti-Passerini, C. (2000). Induction of resistance to the Abelson inhibitor STI571 in human leukemic cells through gene amplification. *Blood, 95*(5), 1758-1766.

Li, M., Makkinje, A., & Damuni, Z. (1996). The Myeloid Leukemia-associated Protein SET Is a Potent Inhibitor of Protein Phosphatase 2A. *Journal of Biological Chemistry, 271*(19), 11059-11062.

Lipton, J. H., Brydon, P., Sidhu, M. K., Huang, H., McGarry, L. J., Lustgarten, S., . . . Hawkins, N. (2015). Comparative efficacy of tyrosine kinase inhibitor treatments in the third-line setting, for chronic-phase chronic myelogenous leukemia after failure of second-generation tyrosine kinase inhibitors. *Leukemia research, 39*(1), 6.

Liu, J., Wang, X., Zhou, G., Wang, H., Xiang, L., Cheng, Y., . . . Zhao, W. (2011). Cancerous inhibitor of protein phosphatase 2A is overexpressed in cervical cancer and upregulated by human papillomavirus 16 E7 oncoprotein. *Gynecologic Oncology, 122*(2), 430-436.

Liu, L.-G., Tanaka, H., Ito, K., Kyo, T., Ito, T., & Kimura, A. (2003). Chronic myelogenous leukemia with e13a3 (b2a3) type of BCR-ABL transcript having a DNA breakpoint between ABL exons a2 and a3. *American Journal of Hematology, 74*(4), 268-272.

Liu, X., Chai, Y., Li, J., Ren, P., Liu, M., Dai, L., . . . Zhang, J.-Y. (2014). Autoantibody response to a novel tumor-associated antigen p90/CIP2A in breast cancer immunodiagnosis. *Tumor Biology*, 1-7.

Livak, K. J., & Schmittgen, T. D. (2001). Analysis of Relative Gene Expression Data Using Real-Time Quantitative PCR and the 2−ΔΔCT Method. *Methods, 25*(4), 6.

Lobo, S., Doni, M., Verrecchia, A., Sanulli, S., Fagà, G., Piontini, A., . . . Amati, B. (2013). Dual regulation of Myc by Abl. *Oncogene, 32*(45), 10.

Lucas, C., Wang, L., Austin, G., Knight, K., Watmough, S., Shwe, K., . . . Clark, R. (2008). A population study of imatinib in chronic myeloid leukaemia demonstrates lower efficacy than in clinical trials. *Leukemia, 22*(10), 3.

Lucas, C. M., Harris, R. J., Giannoudis, A., Copland, M., Slupsky, J. R., & Clark, R. E. (2011). Cancerous inhibitor of PP2A (CIP2A) at diagnosis of chronic myeloid leukemia is a critical determinant of disease progression. *Blood, 117*(24), 6660-6668.

Ma, L., Wen, Z., Liu, Z., Hu, Z., Ma, J., Chen, X., . . . Zhou, G. (2011). Overexpression and small molecule-triggered downregulation of CIP2A in lung cancer. *PLOS, 6*(5), 7.

Marin, D., Bazeos, A., Mahon, F.-X., Eliasson, L., Milojkovic, D., Bua, M., . . . Khorashad, J. S. (2010). Adherence Is the Critical Factor for Achieving Molecular Responses in Patients With Chronic Myeloid Leukemia Who Achieve Complete Cytogenetic Responses on Imatinib. *Journal of Clinical Oncology, 28*(14), 2381-2388.

Mathe, G., Amiel, J., Schwarzenberg, L., Cattan, A., & Schneider, M. (1963). Haematopoietic Chimera in Man After Allogenic (Homologous) Bone-marrow Transplantation. *British Medical Journal, 2*(5373), 3.

Mathiasen, D. P., Egebjerg, C., Andersen, S. H., Rafn, B., Puustinen, P., Khanna, A., . . . Kallunki, T. (2012). Identification of a c-Jun N-terminal kinase-2-dependent signal amplification cascade that regulates c-Myc levels in ras transformation. *Oncogene, 31*(3), 11.

McCubrey, J. A., Steelman, L. S., Abrams, S. L., Bertrand, F. E., Ludwig, D. E., Basecke, J., . . . Martelli, A. M. (2008). Targeting survival cascades induced by activation of Ras/Raf/MEK/ERK, PI3K/PTEN/Akt/mTOR and Jak/STAT pathways for effective leukemia therapy. *Leukemia, 22*, 14.

McCubrey, J. A., Steelman, L. S., Chappell, W. H., Abrams, S. L., Wong, E. W. T., Chang, F., . . . Franklin, R. A. (2007). Roles of the Raf/MEK/ERK pathway in cell growth, malignant transformation and drug resistance. *Molecular Cell Research, 1773*(8), 21.

McNally, R. J. Q., Rowland, D., Roman, E., & Cartwright, R. A. (1997). Age and sex distributions of hematological malignancies in the U.K. *Hematological Oncology, 15*(4), 173-189.

Melo, J. (1996). The diversity of BCR-ABL fusion proteins and their relationship to leukemia phenotype [editorial; comment]. *Blood, 88*(7), 2375-2384.

Naro, C., & Sette, C. (2013). Phosphorylation-Mediated Regulation of Alternative Splicing in Cancer. *International Journal of Cell Biology, 2013*, 15.

Nelkin, B., Przepiorka, D., Burke, P., Thomas, E., & Baylin, S. (1991). *Abnormal methylation of the calcitonin gene marks progression of chronic myelogenous leukemia* (Vol. 77).

Neumann, E. (1869). Ueber die bedeutung des knochenmarkes fur die blutbildung. Ein beitrag zur entwicklungsgeschichte der blutkorperchen. *Archives Heilkunde, 10*, 34.

Neumann, E. (1870). Ein fall von leukamie mit erkrankungen des knochenmarkes. *Archives Heilkunde*.

Neumann, E. (1878). Uber myelogene leukamie. *Berliner Klinische Wochenschrift, 15*, 1.

Neviani, P., Harb, J., Oaks, J., Santhanam, R., Walker, C., Ellis, J., . . . Perrotti, D. (2013). PP2A-activating drugs selectively eradicate TKI-resistant chronic myeloid leukemic stem cells. *Journal of Clinical Investigation, 123*(10), 13.

Neviani, P., Santhanam, R., Trotta, R., Notari, M., Blaser, B. W., Liu, S., . . . Perrotti, D. (2005). The tumor suppressor PP2A is functionally inactivated in blast crisis CML through the inhibitory activity of the BCR/ABL-regulated SET protein. *Cancer Cell, 8*(5), 355-368.

Nguyen, T., Mohrbacher, A., Tsai, Y., Groffen, J., Heisterkamp, N., Nichols, P., . . . Jones, P. (2000). Quantitative measure of c-abl and p15 methylation in chronic myelogenous leukemia: biological implications. *Blood, 95*(5), 2.

Noens, L., van Lierde, M.-A., De Bock, R., Verhoef, G., Zachée, P., Berneman, Z., . . . Abraham, I. (2009). Prevalence, determinants, and outcomes of nonadherence to imatinib therapy in patients with chronic myeloid leukemia: the ADAGIO study. *Blood, 113*(22), 5401-5411.

Nowell, P. C., & Hungerford, D. A. (1960). A minute chromosome in human granulocytic leukaemia. *Science, 132*(1497).

O'Brien, S. G., Guilhot, F., Larson, R. A., Gathmann, I., Baccarani, M., Cervantes, F., . . . Druker, B. J. (2003). Imatinib Compared with Interferon and Low-Dose Cytarabine for Newly Diagnosed Chronic-Phase Chronic Myeloid Leukemia. *New England Journal of Medicine, 348*(11), 994-1004.

O'Hare, T., Shakespeare, W., Zhu, X., Eide, C., Rivera, V., Wang, F., . . . Clackson, T. (2009). AP24534, a Pan-BCR-ABL Inhibitor for Chronic Myeloid Leukemia, Potently Inhibits the T315I Mutant and Overcomes Mutation-Based Resistance. *Cancer Cell, 16*(5), 12.

O'Hare, T., Walters, D. K., Stoffregen, E. P., Jia, T., Manley, P. W., Mestan, J., . . . Druker, B. J. (2005). In vitro Activity of Bcr-Abl Inhibitors AMN107 and BMS-354825 against Clinically Relevant Imatinib-Resistant Abl Kinase Domain Mutants. *Cancer Research, 65*(11), 4500-4505.

Pagliarini, V., Naro, C., & Sette, C. (2015). Splicing Regulation: A Molecular Device to Enhance Cancer Cell Adaptation. *BioMed Research International, 2015*, 13.

Pallai, R., Bhaskar, A., Sodi, V., & Rice, L. (2012). Ets1 and Elk1 transcription factors regulate cancerous inhibitor of protein phosphatase 2A expression in cervical and endometrial carcinoma cells. *Transcription, 3*(6), 12.

Pane, F., Frigeri, F., Sindona, M., Luciano, L., Ferrara, F., Cimino, R., . . . Rotoli, B. (1996). Neutrophilic-chronic myeloid leukemia: a distinct disease with a specific molecular marker (BCR/ABL with C3/A2 junction) [see comments]. *Blood, 88*(7), 2410-2414.

Park, I. J., Lim, Y. A., Lee, W. G., Park, J. S., Kim, H. C., Lee, H.-J., & Cho, S. R. (2008). A case of chronic myelogenous leukemia with e8a2 fusion transcript. *Cancer genetics and cytogenetics, 185*(2), 106-108.

Perrotti, D., & Neviani, P. (2006). ReSETting PP2A tumour suppressor activity in blast crisis and imatinib-resistant chronic myelogenous leukaemia. *British Journal of Cancer, 95*(7), 6.

Phekoo, K., Richards, M., Moller, H., & Schey, S. (2006). The incidence and outcome of myeloid malignancies in 2,112 adult patients in southeast England. *Haematologica, 91*(10), 1400-1404.

Piazza, R., Valletta, S., Winkelmann, N., Redaelli, S., Spinelli, R., Pirola, A., . . . Gambacorti-Passerini, C. (2013). Recurrent SETBP1 mutations in atypical chronic myeloid leukemia. *Nature Genetics, 45*(1), 6.

Piller, G. J. (2001). Leukaemia - a brief historical review from ancient times to 1950. *British Journal of Haematology, 112*(2), 10.

Polakova, K., Koblihova, J., & Stopka, T. (2013). Role of Epigenetics in Chronic Myeoloid Leukemia. *Current Hematologic Malignancy Reports, 8*(1), 8.

Qu, W., Li, W., Wei, L., Xing, L., Wang, X., & Yu, J. (2012). CIP2A is overexpressed in esophageal squamous cell carcinoma. *Medical Oncology, 29*(1), 113-118.

Quintás-Cardama, A., & Cortes, J. (2009). Molecular biology of bcr-abl1–positive chronic myeloid leukemia. *Blood, 113*(8), 1619-1630.

Ren, J., Li, W., Yan, L., Jiao, W., Tian, S., Li, D., . . . Xu, Z. (2011). Expression of CIP2A in renal cell carcinomas correlates with tumour invasion, metastasis and patients' survival. *British Journal of Cancer, 105*, 6.

Rohrbacher, M., & Hasford, J. (2009). Epidemiology of chronic myeloid leukaemia (CML). *Best Practice & Research Clinical Haematology, 22*(3), 295-302.

Rowley, J., Golomb, H., Vardiman, J. W., Fukuhara, S., Dougherty, C., & Potter, D. (1977). Further evidence for a non-random chromosomal abnormality in acute promyelocytic leukemia. *International Journal of Cancer, 20*(6), 3.

Rowley, J. D. (1973). A New Consistent Chromosomal Abnormality in Chronic Myelogenous Leukaemia identified by Quinacrine Fluorescence and Giemsa Staining. *Nature, 243*(5405), 290-293.

Ruediger, R., Ruiz, J., & Walter, G. (2011). Human Cancer-Associated Mutations in the Aα Subunit of Protein Phosphatase 2A Increase Lung Cancer Incidence in Aα Knock-In and Knockout Mice. *Molecular and Cell Biology, 31*(18), 12.

Sablina, A. A., & Hahn, W. C. (2007). The Role of PP2A A Subunits in Tumor Suppression. *Cell Adhesion & Migration, 1*(3), 140-141.

Saglio, G., Kim, D.-W., Issaragrisil, S., le Coutre, P., Etienne, G., Lobo, C., . . . Kantarjian, H. M. (2010). Nilotinib versus Imatinib for Newly Diagnosed Chronic Myeloid Leukemia. *New England Journal of Medicine, 362*(24), 2251-2259.

Santos, F., Kantarjian, H., Quintás-Cardama, A., & Cortes, J. (2011). Evolution of Therapies for Chronic Myelogenous Leukemia. *Cancer Journal, 17*(6), 11.

Savona, M. R., & Saglio, G. (2013). Identifying the Time to Change BCR-ABL Inhibitor Therapy in Patients with Chronic Myeloid Leukemia. *Acta Haematologica, 130*(4), 268-278.

Sawyers, C. L., Hochhaus, A., Feldman, E., Goldman, J. M., Miller, C. B., Ottmann, O. G., . . . Druker, B. J. (2002). Imatinib induces hematologic and cytogenetic responses in patients with chronic myelogenous leukemia in myeloid blast crisis: results of a phase II study. *Presented in part at the 43rd Annual Meeting of The American Society of Hematology, Orlando, FL, December 11, 2001., 99*(10), 3530-3539.

Schultheis, B., Wang, L., Clark, R., & Melo, J. (2003). BCR-ABL with an e6a2 fusion in a CML patient diagnosed in blast crisis. *Leukemia, 17*(10), 1.

Sears, R., Nuckolls, F., Haura, E., Taya, Y., Tamai, K., & Nevins, J. (2000). Multiple Ras-dependent phosphorylation pathways regulate Myc protein stability. *Genes and Development, 14*(19), 13.

Seshacharyulu, P., Pandey, P., Datta, K., & Batra, S. K. (2013). Phosphatase: PP2A structural importance, regulation and its aberrant expression in cancer. *Cancer Letters, 335*(1), 9-18.

Shet, A. S., Jahagirdar, B. N., & Verfaillie, C. M. (2002). Chronic myelogenous leukaemia: mechanisms underlying disease progression. *Leukemia, 16*(8), 9.

Shi, F., Ding, Y., Ju, S., Wu, X., & Cao, S. (2014). Expression and prognostic significance of CIP2A in cutaneous malignant melanoma. *Biomarkers, 19*(1), 70-76.

Sinclair, A., Latif, A. L., & Holyoake, T. L. (2013). Targeting survival pathways in chronic myeloid leukaemia stem cells. *British Journal of Pharmacology, 169*(8), 1693-1707.

Slupe, A. M., Merrill, R. A., & Strack, S. (2011). Determinants for Substrate Specificity of Protein Phosphatase 2A. *Enzyme Research, 2011*, 8.

Stanevich, V., Zheng, A., Guo, F., Jiang, L., Wlodarchak, N., & Xing, Y. (2014). Mechanisms of the Scaffold Subunit in Facilitating Protein Phosphatase 2A Methylation. *PLOS, 9*(1), e86955.

Steelman, L. S., Pohnert, S. C., Shelton, J. G., Franklin, R. A., Bertrand, F. E., & McCubrey, J. A. (2000). JAK//STAT, Raf//MEK//ERK, PI3K//Akt and BCR-ABL in cell cycle progression and leukemogenesis. *Leukemia, 18*(2), 189-218.

Stuppia, L., Calabrese, G., Peila, R., Guanciali-Franchi, P., Morizio, E., Spadano, A., & Palka, G. (1977). p53 loss and point mutations are associated with suppression of apoptosis and progression of CML into myeloid blastic crisis. *Cancer Genetics, 98*(1), 28-35.

Sun, B., Jiang, G., Zaydan, M., La Russa, V., Safah, H., & Ehrlich, M. (2001). ABL1 Promoter Methylation Can Exist Independently of BCR-ABL

Transcription in Chronic Myeloid Leukemia Hematopoietic Progenitors. *Cancer Research, 61*(18), 6.

Surget, S., Khoury, M., & Bourdon, J. (2013). Uncovering the role of p53 splice variants in human malignancy: a clinical perspective. *OncoTargets and Therapy, 7*, 11.

Talpaz, M., Shah, N. P., Kantarjian, H., Donato, N., Nicoll, J., Paquette, R., . . . Sawyers, C. L. (2006). Dasatinib in Imatinib-Resistant Philadelphia Chromosome–Positive Leukemias. *New England Journal of Medicine, 354*(24), 2531-2541.

Talpaz, M., Silver, R. T., Druker, B. J., Goldman, J. M., Gambacorti-Passerini, C., Guilhot, F., . . . Sawyers, C. L. (2002). Imatinib induces durable hematologic and cytogenetic responses in patients with accelerated phase chronic myeloid leukemia: results of a phase 2 study. *Blood, 99*(6), 1928-1937.

Teng, H.-W., Yang, S.-H., Lin, J.-K., Chen, W.-S., Lin, T.-C., Jiang, J.-K., . . . Chen, K.-F. (2012). CIP2A Is a Predictor of Poor Prognosis in Colon Cancer. *Journal of Gastrointestinal Surgery, 16*(5), 1037-1047.

Tokarski, J. S., Newitt, J. A., Chang, C. Y. J., Cheng, J. D., Wittekind, M., Kiefer, S. E., . . . Klei, H. E. (2006). The Structure of Dasatinib (BMS-354825) Bound to Activated ABL Kinase Domain Elucidates Its Inhibitory Activity against Imatinib-Resistant ABL Mutants. *Cancer Research, 66*(11), 5790-5797.

Tseng, L.-M., Liu, C.-Y., Chang, K.-C., Chu, P.-Y., Shiau, C.-W., & Chen, K.-F. (2012). CIP2A is a target of bortezomib in human triple negative breast cancer cells. *Breast Cancer Research, 14*(2), 68-68.

Vaarala, M., Väisänen, M., & Ristimäki, A. (2010). CIP2A expression is increased in prostate cancer. *Journal of Experimental and Clinical Cancer Research, 29*(1).

Van Hoof, C., & Goris, J. (2004). PP2A fulfills its promises as tumor suppressor: Which subunits are important? *Cancer Cell, 5*(2), 105-106.

Virchow, R. (1845). Weisses Blut. *Froriep's Notizen, 36*, 5.

Virchow, R. (1847). Weisses Blut und Milztumoren. *Medicale Zeitung, 16*, 6.

Virchow, R. (1849). Zur pathologishen Physiologie des Blutes; Farblose, pigmentierte und geschwantze nicht spezifische zellen im blut. *Archives of Pathology, Anatomy and Physiology, 2*, 12.

Virchow, R. (1856). Die Leukamie. *Gesammelte abhandlungen zur wissenschaftlihen medizin*, 21.

Wada, H., Mizutani, S., Nishimura, J., Usuki, Y., Kohsaki, M., Komai, M., . . . Kakishita, E. (1995). Establishment and Molecular Characterization of a Novel Leukemic Cell Line with Philadelphia Chromosome Expressing p230 BCR/ABL Fusion Protein. *Cancer Research, 55*(14), 3192-3196.

Walz, C., & Sattler, M. (2006). Novel targeted therapies to overcome imatinib mesylate resistance in chronic myeloid leukemia (CML). *Critical reviews in oncology/hematology, 57*(2), 145-164.

Wang, J., Huang, T., Sun, J., Yu, Y., Liu, Z., Li, W., . . . Chen, C. (2014). CIP2A is overexpressed and involved in the pathogenesis of chronic myelocytic leukemia by interacting with breakpoint cluster region-Abelson leukemia virus. *Medical Oncology, 31*(8), 1-7.

Wang, J., Li, W., Li, L., Yu, X., Jia, J., & Chen, C. (2011). CIP2A is over-expressed in acute myeloid leukaemia and associated with HL60 cells proliferation and differentiation. *International Journal of Laboratory Hematology, 33*(3), 290-298.

Wang, L., Giannoudis, A., Lane, S., Williamson, P., Pirmohamed, M., & Clark, R. (2008). Expression of the Uptake Drug Transporter hOCT1 is an Important Clinical Determinant of the Response to Imatinib in Chronic Myeloid Leukemia. *Clinical Pharmacology and Therapeutics, 83*(2), 6.

Wang, L., Gu, F., Ma, N., Zhang, L., Bian, J.-M., & Cao, H.-Y. (2013). CIP2A expression is associated with altered expression of epithelial–mesenchymal transition markers and predictive of poor prognosis in pancreatic ductal adenocarcinoma. *Tumor Biology, 34*(4), 2309-2313.

Weerkamp, F., Dekking, E., Ng, Y. Y., van der Velden, V. H. J., Wai, H., Bottcher, S., . . . van Dongen, J. J. M. (2009). Oncogenes, Fusion Genes and Tumor Suppressor Genes. Flow cytometric immunobead assay for the detection of BCR–ABL fusion proteins in leukemia patients. *Leukemia, 23*, 11.

Weisberg, E., & Griffin, J. D. (2000). Mechanism of resistance to the ABL tyrosine kinase inhibitor STI571 in BCR/ABL–transformed hematopoietic cell lines. *Blood, 95*(11), 3498-3505.

Weisberg, E., Manley, P., Mestan, J., Cowan-Jacob, S., Ray, A., & Griffin, J. (2006). AMN107 (nilotinib): a novel and selective inhibitor of BCR-ABL. *British Journal of Cancer, 94*(12), 4.

Weisberg, E., Manley, P. W., Cowan-Jacob, S. W., Hochhaus, A., & Griffin, J. D. (2007). Second generation inhibitors of BCR-ABL for the treatment of imatinib-resistant chronic myeloid leukaemia. *Nat Rev Cancer, 7*(5), 345-356.

Wiegering, A., Pfann, C., Uthe, F. W., Otto, C., Rycak, L., Mäder, U., . . . Germer, C.-T. (2013). CIP2A Influences Survival in Colon Cancer and Is Critical for Maintaining Myc Expression. *PLOS, 8*(10).

Xu, P., Xu, X.-L., Huang, Q., Zhang, Z.-H., & Zhang, Y.-B. (2012). CIP2A with survivin protein expressions in human non-small-cell lung cancer correlates with prognosis. *Medical Oncology, 29*(3), 1643-1647.

Xue, Y., Wu, G., Wang, X., Zou, X., Zhang, G., Xiao, R., . . . Liu, M. (2012). CIP2A is a predictor of survival and a novel therapeutic target in bladder urothelial cell carcinoma. *Medical Oncology, 30*(1), 1-11.

Yeh, E., Cunningham, M., Arnold, H., Chasse, D., Monteith, T., Ivaldi, G., . . . Sears, R. (2004). A signalling pathway controlling c-Myc degradation that impacts oncogenic transformation of human cells. *Nat Cell Biol, 6*(4), 308-318.

Yongxun Zhao, Yumin Li, Jian Han, Tao Liu, Quanlin Guan, Peng Zhao, . . . He, D. (2014). Helicobacter pylori enhances CIP2A expression and cell proliferation via JNK2/ATF2 signaling in human gastric cancer cells. *international Journal of Molecular Medicine, 33*(3), 7.

Yu, G., Liu, G., Dong, J., & Jin, Y. (2013). Clinical implications of CIP2A protein expression in breast cancer. *Medical Oncology, 30*(2), 1-6.

Yua, H.-C., Chena, H.-J., Changa, Y.-L., Liud, C.-Y., Shiaue, C.-W., Cheng, A.-L., & Chena, K.-F. (2013). Inhibition of CIP2A determines erlotinib-induced apoptosis in hepatocellular carcinoma. *Biochemical Pharmacology, 85*(3), 10.

Zhai, M., Cong, L., Han, Y., & Tu, G. (2013). CIP2A is overexpressed in osteosarcoma and regulates cell proliferation and invasion. *Tumor Biology*, 1-6.

Zhao, X., Ghaffari, S., Lodish, H., Malashkevich, V. N., & Kim, P. S. (2002). Structure of the Bcr-Abl oncoprotein oligomerization domain. *Nature Structural and Molecular Biology, 9*(2), 3.

Zirong Li, Sara Van Calcar, Chunxu Qu, Webster K. Cavenee, Michael Q. Zhang, & Ren, B. (2003). A global transcriptional regulatory role for c-Myc in Burkitt's lymphoma cells. *PNAS, 100*(14), 5.